INVESTIGATIONS INTO THE ROLE OF ZINC IN NORMAL AND ALLERGIC RESPIRATORY EPITHELIAL CELLS AND TISSUES

Table of Contents

7

ABSTRACT

ABSTRACT

This thesis describes an investigation of the physiological role of Zn within the airway epithelium. Zn is an essential biometal required for the healthy functioning of the body. Damage and shedding of airway epithelial cells (AEC) is a distinct feature of asthma hence, protection of this tissue is likely to have beneficial implications for the management of this disease. Several studies report a hypozincaemia in asthmatic patients, suggesting that decreased Zn levels may contribute to increased oxidative stress, chronic inflammation and decreased protection of the airway epithelium.

The distribution of labile intracellular Zn in the respiratory epithelium was measured by Zinquin, a novel Zn specific fluorophore. The pseudostratified ciliated epithelium was found to be continuously lined at the luminal surface by an intense region of Zinquin fluorescence, extending from the trachea to the bronchioles, but fluorescence was lower in the alveolar tissue. The positioning of intracellular Zn at a region which is most exposed to oxyradicals and other cytotoxins would allow Zn to act as a cytoprotectant in these cells.

Zn was found to be essential for respiratory epithelial cell (REC) survival since a decrease in intracellular Zn levels, mediated by the Zn chelator TPEN, resulted in the activation of caspase-3 activity and enhanced cell susceptibility to oxyradical-induced apoptosis. Increased intracellular Zn levels, via the Zn ionophore sodium pyrithione (NaPYR) and exogenous $ZnSO_4$, inhibited caspase-3 activation and apoptosis.

A murine model of allergic airway inflammation using BALB/c mice treated with ovalbumin (OVA) was established and used to determine the effects of mild nutritional Zn deficiency on airway inflammation and airway hyper-responsiveness (AHR). Mice were given Zn normal (ZN) or Zn limited (ZL) diets before and during induction of inflammation. ZL mice had increased systemic and local eosinophilia, mucus cell hyperplasia and AHR compared to the ZN mice. Eosinophilia was pronounced in the allergic ZL mice suggesting that Zn deprivation negatively influenced the pathogenesis of allergic airway inflammation. Increased levels of AHR in the ZL mice were reversed by 14 days of Zn repletion.

Airway inflammation significantly decreased Zinquin fluorescence and increased pro-caspase-3 protein in AEC of OVA-treated mice. These mice also had increased levels of apoptosis as detected by enhanced levels of active caspase-3 (AC3) and increased cleavage of cytokeratin 18 (CK18), a specific substrate of caspase-3. Interestingly, ZL OVA-treated mice had a more pronounced increase in AC3 protein, cleavage of CK18 and the presence of apoptotic bodies within the airway epithelium.

This thesis provides new data on the role of Zn in the respiratory system which should lead to a greater understanding of the association between Zn deficiency and airway disease. Clinical implications of these studies suggest the monitoring of Zn levels in subjects with varying severity of atopy and asthma and the potential for Zn supplementation as a possible therapeutic in the treatment of allergic airways disease.

DECLARATION

This work contains no material which has been accepted for the award of any other degree or diploma in any university or other tertiary institution and, to the best of my knowledge and belief, contains no material previously published or written by another person, except where due reference has been made in the text.

I give consent to this copy of my thesis, when deposited in the University Library, being available for loan and photocopying.

Signed..

Date... 30|7|02

Ai Q. Truong-Tran

x

ACKNOWLEDGEMENTS

I would like to take this opportunity to acknowledge the people who have made this Ph.D. candidature such a wonderful experience.

Firstly, this thesis would not have been possible without the support, love and encouragement from my family. As such, this thesis is dedicated to mother Van, dad Lam, my brother Hung and my sister Kim.

I would also like to thank the staff and students in the Basil Hetzel Institute for their support and encouragements. Many thanks to Alex, Adrian, Anne, Andrea, Ashley, Bec, Betty, Damian, Evelyn, Fiona, Gary, Geradine, Gwenda, Henry, Jim, Joanne, Jenny H, Kate, Lefta, Lor Wai, Michael, Madelyn, Natalie, Nathaniel, Ravi, Ray, Rachel, Richard, Randall, Olympia, Peter, Samantha, Sally, Tanya, Tina and Terry. Thank you for your friendship and the support you have given me.

I would like to especially thank:

- *Dr Jenny Kennedy* for her support during the last few months. I have really appreciated your help and I wish you all the best as postgraduate co-ordinator.

- *Mrs Ermioni Mourtizos* for EVERYTHING! Thank you Ermioni for always coming up with solutions when I needed them most. But most of all, I want to especially thank you for being a great friend to me during the past 4 years. I have learnt so much from you and I will miss you a great deal.

- *Miss Lien Ho and Miss Sarah Appleton* for making my time here very memorable indeed. I just don't know what to say, except you both have taught me so much about life and I wish you the very best in your futures. To Lien,

Most of all, I wish to thank Chris for being such a supportive and loving boyfriend. Thank you for standing by me, believing in me, encouraging me and understanding me. But most of all, thank you so much for letting me be a part-time girlfriend. The past few years haven't been easy and I want you to know that I wouldn't have wanted to experience it with anyone else but you. Good luck also with your thesis.

Finally, I must acknowledge my two supervisors, *Dr. Peter Zalewksi* and *Professor Richard Ruffin*. Without your constant support, encouragement and friendship I would not have been able to get this far. I want to thank you for the many opportunities you have given me but most importantly, for your faith in me, and with this has come the most amazing amount of freedom any student can ask for in her research! It has been wonderful having two brilliant mentors whom have guided me and stood by me constantly and I am very lucky to be a part of such a wonderful team. I look forward to maintaining collaborations with you as you are two of the fairest, honorable and dedicated people in science. Good luck with everything and I will certainly miss you!

Finally, I dedicate this quote to all those people who have helped me to climb my mountain.

"Live your life each day as you would climb a mountain:

An occasional glance toward the summit keeps the goal

in mind, but many beautiful scenes are to be observed from each new

vantage point. Climb slowly, steadily, enjoying each passing moment;

and the view from the summit will serve as a fitting climax for the

journey." - Harold V. Melchert –

"Just A Thought"

"If we could actually see the explosion of miraculous events that get triggered inside our bodies by every breath we take, we would be left speechless, marvelling at the beauty and magnificence of the gift that is every moment of our lives. Everything else that we suffer or worry about would melt away. But the miracles are hidden from our naked eye, and therefore we just accept their occurrence at a very superficial and intellectual level, and largely take them all for granted (when we're healthy). Our brains are designed and programmed to be on the lookout for 'what's wrong' that might threaten our physical existence in the present moment, while doing nothing to insure our actual experience of the miracle of that same moment as it's passing. The 'existence' of human life is up to our brains to protect, but the 'gift' of life is up to our souls to unwrap and savor. Take a moment to step outside your mind's survival machinations to see the incredible miracle that is you, ... and celebrate." Anonymous.

ABBREVIATIONS USED IN THIS THESIS

AAS	Atomic Absorption Spectroscopy
AC3	Active Caspase-3
Apaf-1	Activating Factor-1 Protein
AEC	Airway Epithelial Cells
AHR	Airway Hyperreactivity
AMG	Autometallography
BAL	Bronchoalveolar Lavage
BALF	Bronchoalveolar Lavage Fluid
BSA	Bovine Serum Albumin
BM	Basement Membrane
Ca	Calcium
CAD	Caspase Activated DNase
CARD	Caspase Recruitment Domain
CK18	Cytokeratin 18
CRIP	Cysteine Rich Intestinal Protein
Cu	Copper
Cu-Zn SOD	Copper Zn Superoxide Dismutase
°C	Degrees Celcius
DCT-1/DMT-1	Divalent Cation (Metal) Transporter-1
DED	Death Effector Domain
DMSO	Dimethylsulfoxide
EM	Electron Microscopy
EP	Epithelium
Fe	Iron

FITC	Fluoroscein Isothiocyanate
g	Force in Gravities
GM-CSF	Granulocyte Macrophage Stimulating Factor
GSU	Grey Scale Intensity Units
H&E	Haematoxylin and Eosin
HBSS	Hanks Balanced Saline Solution
HPF	High Power Field
h	Hours
H_2O_2	Hydrogen Peroxide
IAP	Inhibitors of Apoptosis
ICAD	Inhibitor of Caspase Activated Dnase
ICE	Interleukin-1β-Converting Enzyme
i.p	Intraperitoneal
IL-1β	Interleukin-1β
IL-4	Interleukin-4
IL-5	Interleukin-5
kDa	Dissociation Constant
LHS	Left Hand Side
LM	Lumen
LP	Lamina Propria
Min	Minutes
MT	Metallothionein
Mwt	Molecular Weight
μg	Micrograms
μM	Micromolar
μm	Microns

μl	Microlitre
mM	Millimolar
nM	nanomolar
nm	nano
OCT	Optimum Cooling Tissue Medium
OVA	Ovalbumin
PARP	Poly (ADP-ribose) Polymerase
PBS	Phosphate Buffered Saline
Prtn	Protein
PC3	Pro-Caspase-3
PC3-FITC	Pro-Caspase-3 FITC fluorescence
REC	Respiratory Epithelial Cells
RHS	Right Hand Side
RT	Room Temperature
ROS	Reactive Oxygen Species
RDI	Recommended Dietary Intake
SAL	Saline
sec	Seconds
NaPYR	Sodium Pyrithione
Th	T Helper Cells
TPEN	N,N,N',N'-tetrakis(2-pyridylmethyl)ethyl-enediamine
TSQ	N-(6-methoxy-8-quinolyl)-p-toluenesulfonamide
UV	Ultra Violet
XIAP	Human X-linked Inhibitor of Apoptosis Protein

Zinquin	2-methyl-8-p-toluenesulfonamido-6-quinolyloxy) acetate
Zn	Zinc
ZnT	Zinc Transporter
ZL	Zn Limited
ZN	Zinc Normal
ZR	Zinc Repleted
$ZnSO_4$	Zn Sulfate

LIST OF PUBLICATIONS ARISING FROM THIS THESIS

1. **Truong-Tran AQ, Ruffin RE, Foster PS, Koskinen AM, Coyle P, Philcox JC, Rofe AM and Zalewski PD.** Altered Zinc Homeostasis and Caspase-3 Activity in a Murine Model of Allergic Airway Inflammation. *American Journal of Respiratory Cell and Molecular Biology (in press).*

2. **Truong-Tran AQ, Ruffin RE and Zalewski PD.** 2001. New Insights into the Novel Role of Zinc in the Respiratory Airway Epithelium. *Immunology and Cell Biology.* 79:170-7 (2001).

3. **Truong-Tran AQ, Ruffin RE and Zalewski PD.** Visualisation and Function of Labile Zinc in Primary Ciliated Airway Epithelial Cells and Cell Lines. *American Journal Physiology: Lung Cellular Biology.* 279:L1172-L1183 (2000).

Other publications:

4. **Truong-Tran AQ, Ruffin RE and Zalewski PD.** The Role of Zinc in Caspase Activation And Apoptotic Cell Death. *Biometals.* 14: 315-330 (2001).

5. **Truong-Tran AQ, Chai F (equal first authors), Evdokiou A, Young GP and Zalewski PD.** Intracellular Zinc Depletion Induces Caspase Activation and p21$^{\text{Wafl/Cip1}}$ Cleavage in Human Epithelial Cell Lines. *Journal of Infectious Diseases.* 182: 85-92 (2000).

6. **Truong-Tran AQ, Ho LH, Chai F and Zalewski PD.** Cellular Zinc Fluxes and the Regulation of Apoptosis/Gene-Directed Cell Death. *Journal of Nutrition.* Vol 130 (5S Suppl):1459S-66S. (2000).

7. **Chai. F, Truong-Tran AQ, Ho LH and Zalewski PD.** Regulation of Caspase Activation and Apoptosis by Cellular Zinc Fluxes and Zinc Deprivation: A Review. *Immunology and Cell Biology.* 77:272-278 (1999).

SELECTED LIST OF PRESENTATIONS ARISING FROM

THIS THESIS

1. Truong-Tran A, Ruffin R and Zalewski P. Zinc and Apoptosis in Respiratory Epithelial Cells (April 2002. Oral Presentation at The Zinc Signals 2002 Congress, Grand Caymans).

2. Truong-Tran A, Ruffin R and Zalewski P. Dysregulation Of Zinc and Caspase-3 Homeostasis In A Murine Model Of Asthma (November 2001. Oral Presentation at The CRC *for* Asthma Conference 2001, Melbourne).

3. Truong-Tran A, Ruffin R and Zalewski P. Dysregulation Of Zinc Homeostasis In A Murine Model Of Asthma And Effects Of Zinc Deficiency On Airway Hyper-Reactivity. (October 2001. Oral Presentation at The Allen and Hanbury Young Investigator Award Session, Adelaide).

4. Truong-Tran A, Ruffin R and Zalewski P. Dysregulation Of Zinc Homeostasis In A Murine Model Of Asthma And Effects Of Zinc Deficiency On Airway Hyper-Reactivity. (October 2001. Oral Presentation at The Annual Queen Elizabeth Hospital Research Day Event, Adelaide). *Winner of the best oral presentation in the category of Higher Degree (Basic Science).*

5. Truong-Tran A, Ruffin R and Zalewski P. Role Of Cytoplasmic Zinc In Suppression Of Caspase-Activated Apoptosis In Respiratory Epithelial Cells (REC). (Poster Session, September 2001. European Respiratory Society Annual Meeting 2001, Berlin).

6. Truong-Tran A, Ruffin R and Zalewski P. Apical Cytoplasmic Zinc Inhibits Caspase-Activated Apoptosis In Respiratory Epithelial Cells. (March 2001. Oral Presentation, Young Investigator Award Session, The Thoracic Society of Australia and New Zealand Annual Meeting, Brisbane).

7. Truong-Tran A, Ruffin R and Zalewski P. New Insights into the Novel Role of Zinc in the Respiratory Airway Epithelium. Immunology and Cell Biology. (September 2000. Oral Presentation at QEHSM 2000 Symposium, Adelaide).

8. Truong-Tran A, Ruffin R and Zalewski P. The Involvement Of Zinc In The Regulation Of Apoptosis In Respiratory Epithelium. (January 1999. Oral Presentation at The Annual ANU JCSMR Apoptosis Conference, Canberra).

9. Truong-Tran A, Ruffin R and Zalewski P. Visualisation and Function of Labile Zinc in Primary Ciliated Airway Epithelial Cells and Cell Lines. (October 1999. Oral Presentation at The Annual Queen Elizabeth Hospital Research Day Event, Adelaide). *Winner of the best oral presentation in the category of Higher Degree (Basic Science).*

10. Truong-Tran A, Zalewski P and Ruffin R. The Involvement Of Zinc In The Regulation Of Apoptosis In Respiratory Epithelium. (October 1998. Oral Presentation at The Annual Queen Elizabeth Hospital Research Day Event, Adelaide). *Winner of the best oral presentation in the category of Honours degree (Basic Science).*

LIST OF FIGURES

LIST OF TABLES

CHAPTER 1
INTRODUCTION

CHAPTER 1 INTRODUCTION

The major aims of this thesis were to investigate the role of intracellular zinc (Zn) in regulating caspase activated apoptosis in respiratory epithelial cells (REC), to examine the localization of Zn in airway epithelium in the normal and inflamed states and to determine whether dietary Zn can influence the pathogenesis of allergic airway inflammation. To date there is limited information available on the physiological role of Zn in the normal and diseased respiratory system. However Zn has been demonstrated to be essential in all cell models previously studied and hence it is likely to also be critical for respiratory epithelial cell physiology. Knowledge of the interrelationship between Zn and AEC may lead to a greater understanding of the possible association between Zn deficiency and airway diseases.

This chapter provides an introduction to Zn, apoptosis and asthma and it amalgamates the information available to propose that Zn is essential in regulating apoptosis of REC in normal and diseased situations.

1.1 ZINC

The importance of Zn for the functional integrity of many organ tissue systems and its role as a structural component of hundreds of metalloenzymes and Zn finger transcription factors has emerged in the last four decades. Zn is a group IIb dietary metal, required for the healthy functioning of the body and is an essential nutrient necessary for a wide range of biochemical processes such as in the development of tissues, maintenance and priming of the immune system and in

epithelial tissue repair and regeneration (Vallee & Auld, 1993). This knowledge has been acquired in human (Baer & King, 1984) and animal (Beach et al., 1980) experimental models.

The Australian recommended dietary intake (RDI) of Zn is approximately 12 to 15mg/day and this is obtainable from protein rich foods such as red meat, seafood, dairy products and grains and nuts (Dreosti, 1993). Green vegetables and fruits contain adequate levels of Zn however the majority of this Zn is not in a bioavailable form.

There is currently limited information available on the consumption levels of Zn in the Australian diet, however the most recent data available is from an Australian random population survey conducted in 1991. This study reported that 67% of men and 85% of women consumed diets which contained Zn contents below 12 mg/day (reviewed in Dreosti, 1993). It was observed that the major individual food sources containing Zn were steak (11% of total Zn intake), bread (9%), milk (8%), cheese (6%), minced meat (4%) and breakfast cereals (3%).

1.1.1 Zn Homeostasis

Zn homeostasis is mostly regulated at the level of the gastrointestinal tract, by absorption and excretion and there are no constant stores of Zn in the body unlike iron (Fe), although bone and liver may act as Zn reservoirs (Vallee, 1988). Both stable isotopes and ^{65}Zn radioisotopes have been utilized in tracer studies to determine the efficiency of Zn uptake across the intestine in animals and to a lesser extent in humans (Hambidge, 2000). It has been reported that fractional absorption of Zn decreases when intestinal intraluminal concentrations of Zn are increased,

while Zn deficiency has the opposite effect. However, increased absorption of Zn can also occur in physiological states such as in pregnancy, lactation and infancy, where Zn demands are increased (Krebs, 2000).

Absorption of Zn from the diet occurs mainly through the brush border membrane of enterocytes lining the small intestine, especially within the distal duodenum or proximal jejunum (Lee et al., 1989). Kinetic studies investigating the rate of Zn absorption has been performed mainly in mice; with the majority of Zn found to be absorbed from the ileum and to a lesser extent from the jejunum, while the stomach and colon are insignificant sites for Zn absorption (Sorensen et al., 1998). Although mostly performed in rodents rather than humans, these studies have enhanced our understanding of the mechanisms of Zn absorption. Furthermore, these animal studies are comparable to the human kinetic studies previously published (Jackson et al., 1984; Wastney et al., 2000).

The Mechanisms Governing Zn Absorption

The mechanisms involved in the transport of Zn across the intestinal membranes are still being characterized (Reyes, 1996). Absorption across the intestinal mucosa may be both carrier-mediated or by simple diffusion of either ionic Zn or Zn complexed to various ligands including histidine, citric acid and picolinic acid (Vallee & Falchuk, 1993). Figure 1.1 is a schema showing the postulated mechanisms regulating Zn absorption and efflux within enterocytes. One candidate for Zn transport across the luminal surface of enterocytes is the divalent cation/metal ion transporter (DCT-1/DMT-1), a multi-specific metal ion transporter mediating Zn, Cu and Fe absorption (Gunshin et al., 1997).

Figure 1.1: Absorption Across the Enterocytes

(1) Dietary Zn is absorbed across the apical region of the brush border enterocytes by the cation transporter DCT-1 (blue). (2) Once inside, Zn is bound to CRIP which shuttles it from the apical cytoplasm to the basolateral surface of the cell. (3) Some of the Zn within the cytoplasm is sequestered into vesicles (light blue) by ZnT-2 (red) and ZnT-4 (purple). The sequestering of Zn into vesicles prevents unwanted activation or inhibition of cytoplasmic Zn regulated proteins and enzymes. These vesicles also act as storage compartments. (4) Zn export is likely to be mediated by the Zn efflux protein ZnT-1 (green) which transports Zn out into the plasma where most of this Zn will be bound to (5) albumin (yellow). Albumin acts as a plasma Zn transporter delivering Zn to cells and tissues within the body.

Lumen

Serosa

ZnT-4

Vesicles

Nucleus

(1) Zn^{2+}

(2) CRIP + Zn^{2+}

(3) Zn^{2+}

(2) CRIP + Zn^{2+}

(4)

(2) CRIP + Zn^{2+}

(4)

Nucleus

(5) Zn^{2+} + Albumin

ZnT-2

DCT1

C

N

ZnT-1

C

N

His-rich loop

C
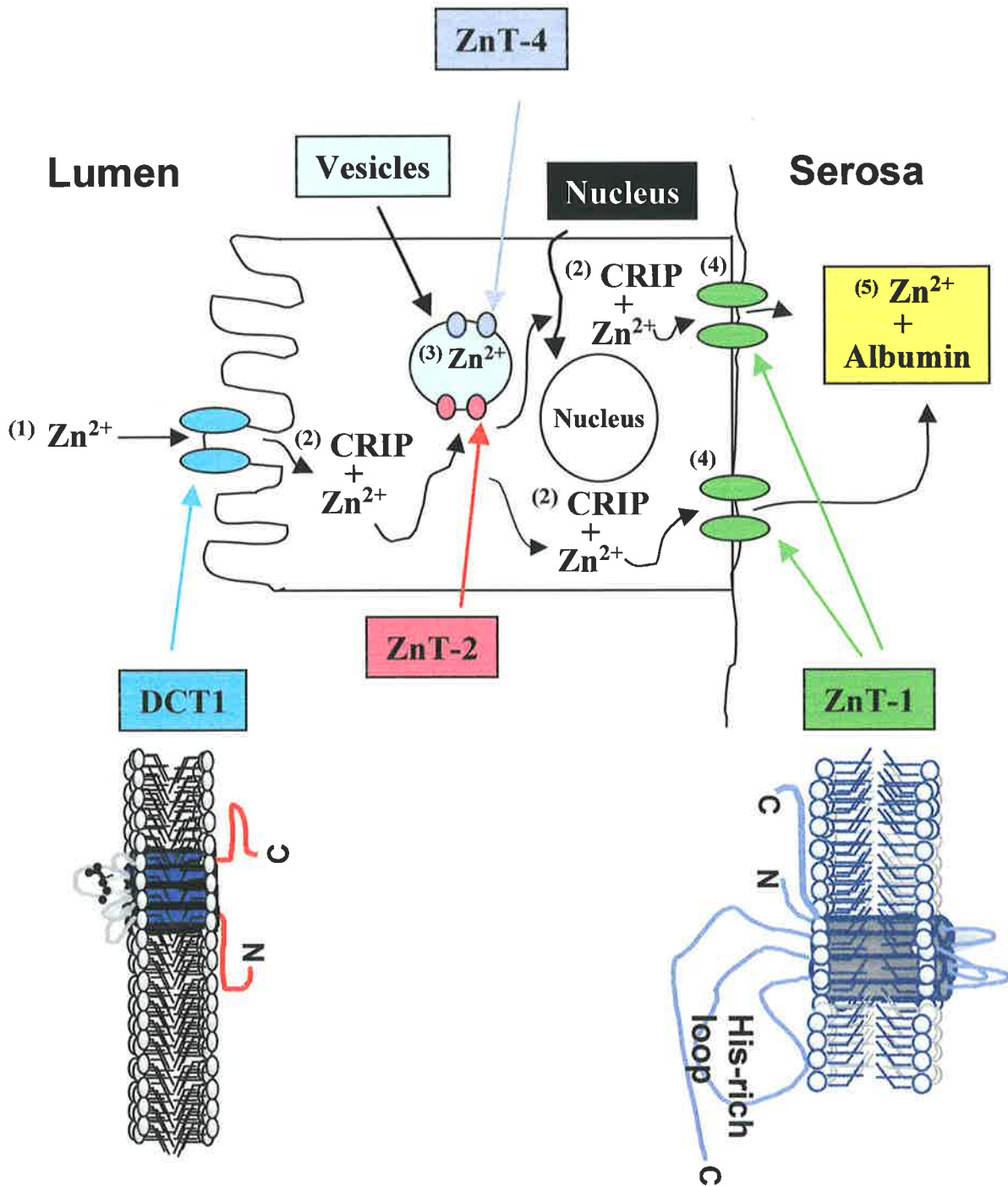
Once Zn is absorbed across the brush border, it is coupled to either cysteine-rich intestinal protein (CRIP) or to metallothionein (MT), another cysteine-rich protein (Cousins, 1989; Rolfs & Hediger, 1999). CRIP serves as a shuttle for Zn transport from apical to basolateral surfaces, analogous to mobilferrin for Fe. In rats fed a moderate amount of Zn, CRIP was found to be bound to a large proportion of Zn entering the intestinal cells whereas when Zn intake was excessive, the bulk of intestinal Zn was bound to MT (Cousins, 1989). This suggests that MT may retain Zn in enterocytes either for local usage or to prevent Zn overloading during periods of high dietary Zn intake (Davis et al., 1998).

At the basolateral surface, Zn export may be mediated by a Zn transporter protein, Zn Transporter-1 (ZnT-1) which is localised at the basal membrane of villous enterocytes lining the duodenum and jejunum (McMahon & Cousins, 1998; Palmiter & Findley, 1995).

Zn effluxed out of enterocytes by ZnT-1 enters the blood where it is carried by proteins, especially albumin, to the liver and other tissues. Approximately 70% of Zn in plasma is bound to albumin, while the remaining 30% is tightly incorporated into α_2-macrogolbulin (Vallee & Falchuk, 1993). The albumin-bound Zn represents 99% of the total exchangeable Zn in plasma which is then delivered to cells in the liver, pancreas, and blood or to the muscle and bone where it is retained for longer periods (Rowe & Bobilya, 2000; Wastney et al., 2000). The remaining 1% of the Zn not bound to albumin remains tightly associated with histidine and cysteine (Bloxam et al., 1984). Zn which is not required by the body is excreted, with a substantial proportion (70-80 %) of

it in faeces while only a small amount is normally lost in the urine (Vallee & Falchuk, 1993).

1.1.2 Regulation of Intracellular Zn Homeostasis by Zn Transporters

Zn is a highly charged ion unable to cross biological membranes by passive diffusion, hence the transport and intracellular homeostasis of this biometal must be regulated by the activity of specific proteins which are involved in Zn uptake, efflux and intracellular compartmentalization.

During the last decade there has been extensive research which has not only added new insights into the mechanism of Zn transport within a variety of cell types (Kruczynski et al., 1985; Takeda et al., 1997) but also resulted in the isolation of Zn transporter proteins in mammalian (Huang & Gitschier, 1997; Kambe et al., 2002; Murgia et al., 1999; Palmiter & Findley, 1995) and yeast cells (Guerinot & Eide, 1999; Zhao et al., 1998).

From these studies, a new family of specific Zn transporters (ZnT) have been identified. To date there are 5 known proteins which belong to the ZnT family, all of which have predicted multiple membrane spanning regions, a histidine-rich intracellular loop which is thought to act as the site of Zn binding and a C-terminal tail (Figure 1.2, panel A) (McMahon & Cousins, 1998). ZnT-1 was the first mammalian Zn transporter described and as such its discovery created the opportunity for researchers to use its gene sequence to identify other transporters from the same family (Palmiter & Findley, 1995). As previously mentioned, ZnT-1 is involved in Zn efflux from enterocytes and is therefore crucial for eliminating toxic levels of Zn from cells, while its absence accounts for

Figure 1.2: Predicted Topology Models of the Zn transporters (ZnT)

To date 5 known Zn transporter proteins have been identified.

Panel A: Figure depicts the predicted protein structure which contains 6 membrane spanning regions (blue), a histidine-rich intracellular loop (green) which act as the site of Zn binding and a C-terminal tail (red).

Panel B: depicts the amino acid sequence and putative functional domains of ZnT-4. ZnT-4 is a Zn transporter able to sequester Zn into cytoplasmic vesicles and is involved in the secretion of Zn from mammary glands into breast milk. Primary sequence of protein is depicted according to insertion topology within plasma membrane bilayer. Positions of consensus sequences for protein-protein interaction (Leu zipper) and metal binding (His region) are circled (pink and blue respectively). Dark red rimmed circle around the arginine residue at *position 297* marks point mutation that leads to synthesis of a truncated protein in the lethal milk mutant allele. Sequence of 14-amino-acid synthetic peptide used to raise polyclonal antibodies is indicated in italics. The abbreviation CYTO depicts the cytoplasmic side of the transporter.

A

ZnT-1, 2, 3, 4 & 5

OUT

IN

COOH

NH₂
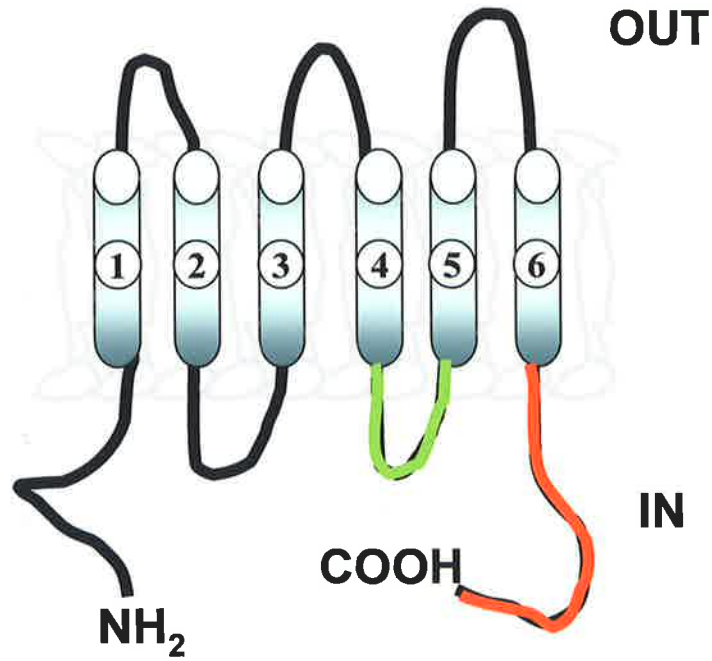
Figure taken from Rolfs and Hediger 1999

B
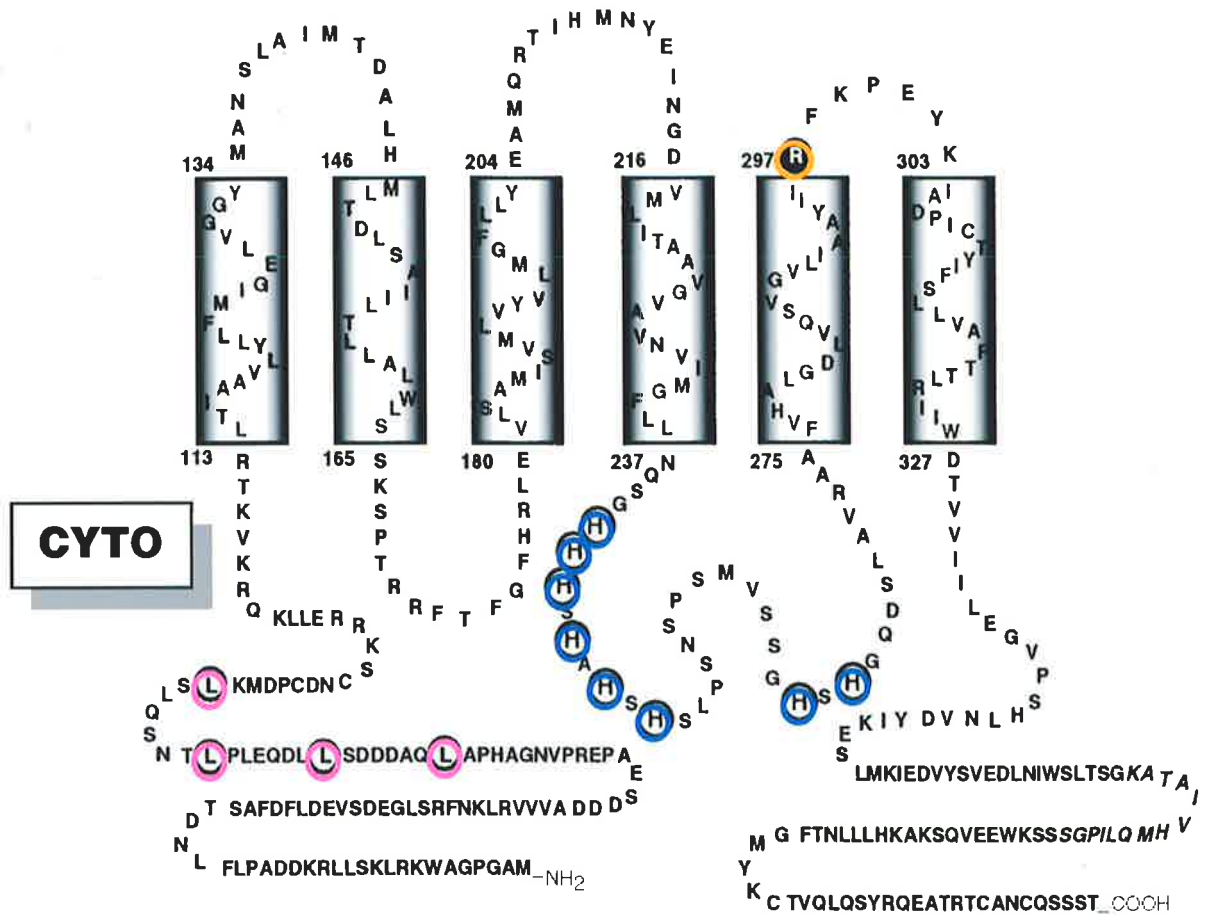
Figure taken from Murgia et al 1999

increased sensitivity of mutant cells to Zn toxicity (Palmiter & Findley, 1995). To date, the physiological significance and the precise mechanism of action of ZnT-1 and its other family members which are listed below, still require further investigation.

Other members of the ZnT proteins include:

- ZnT-2 and ZnT-3 are thought to protect cells from Zn toxicity by transporting intracellular Zn into endosomal/lysosomal compartments (Palmiter et al., 1996a) and in the case of ZnT-3, Zn is transported into synaptic vesicles of neurons (Palmiter et al., 1996b). The sequestering of labile Zn into vesicles may act as a mechanism for storing Zn and supplying it to metalloproteins or Zn requiring molecules and organelles within the cells (Suhy & O'Halloran, 1996).

- ZnT-4 is involved in efflux of Zn from mammary cells into breast milk (Huang & Gitschier, 1997; Michalczyk et al., 2002). Mutations in this protein result in the lethal milk mouse phenotype (Huang & Gitschier, 1997). Dams which carry this mutation produce Zn deficient milk, ultimately leading to the death of their pups prior to weaning (Ackland & Mercer, 1992). ZnT-4 has also been localised to the membrane of Zn containing vesicles of enterocytes and may have functions outside of the mammary gland. Figure 1.2 panel B illustrates the protein structure of ZnT-4.

- ZnT-5 has recently been identified as the Zn transporter responsible for delivering Zn into secretory granules of pancreatic beta cells (Kambe et al., 2002).

The Zn transporters described above, with the exception of DCT-1, are all involved with the export of Zn from cells or the sequestering of Zn into cytoplasmic vesicles. Recently, hZIP2 a human Zn transport protein was reported to be localised within the plasma membrane of K562 erythroleukemia cells (Gaither & Eide, 2000). This finding was recently supported by findings in the monocytic cell line THP-1 where there was an upregulation of hZIP2 mRNA expression in response to intracellular Zn depletion hence helping to protect these cells from cellular Zn deficiency (Cao et al., 2001). The studies reported by Gaither and colleagues are significant as they identify the first specific human Zn transporter involved in Zn influx.

To date, the mechanisms regulating Zn absorption and efflux, intracellular transport and control of Zn homeostasis in REC have not been studied and as such there is now a need to determine whether the Zn transporters discussed in this section may also influence the respiratory system. Currently these investigations have been initiated in the Department of Medicine forming the basis of a new Ph.D. project to be conducted by Dr. Dion Grosser (University of Adelaide).

1.1.3 Zn as a Biochemical Regulator

Zn is the most widely utilised biometal after Fe and is found in all organs, secretions, fluids and tissues of the body (Aggett & Comerford, 1995). The average 70 kg human adult is thought to contain 2-3 gm of Zn and, in the human body Zn is ubiquitously distributed within the nucleus, mitochondria, cytoplasmic vesicles and supernatant fractions (Bartholomew et al., 1959). Zn exists in two main states where, two thirds of this Zn is in a bound form held tightly by metalloproteins and Zn finger proteins, while the remaining one third exists in a more free or loosely

bound form which participates in intracellular Zn fluxes and is readily depleted in Zn deficiency (Jackson, 1989). For the purpose of this thesis, the loosely bound state of Zn is referred to as "labile intracellular Zn" and is thought to be the most exchangeable form of Zn. Although all organs contain labile intracellular Zn, the following tissues are particularly rich in labile Zn: hippocampus (Frederickson et al., 1992), testis (Singh & Nath, 1973) and secretory cells e.g. pancreatic β cells (Zalewski et al., 1994b) and mast cells (Danscher et al., 1980).

Zn is essential for the biochemical functioning of cells not only as a component of metalloenzymes and transcription factors but also as an anti-oxidant, microtubule stabiliser, anti-apoptotic agent, growth co-factor and anti-inflammatory agent in a variety of tissues. This is due to Zn possessing two main properties which make it an ideal participator in biological systems. Firstly, Zn is virtually non-toxic when ingested since the biochemical mechanisms which regulate Zn homeostasis are very effective. As such there are no chronic disorders associated with excessive Zn accumulation in contrast to the situation with other metals such as Fe, Cu and Ca (Bertholf, 1988). Secondly, the physical and chemical properties of Zn enables it to interact with a variety of enzymes and other proteins which participate in cellular metabolism as well as in the control of gene transcription (Vallee, 1988).

1.1.3.1 The Role of Zn in Metalloenzymes

Many enzymes and proteins utilise Zn to carry out their biological functions and in these cases, it is most often the tightly bound pools of Zn which are present in these molecules. Zn is a known regulator of at least 300 enzymes, which participate in gene expression and DNA synthesis (DNA polymerase),

detoxification of alcohol from the liver (alcohol dehydrogenase) and in tissue repair and wound healing (metalloproteinases) (Vallee & Falchuk, 1993). Zn's coordination flexibility and stable physical and chemical properties enable it to be either a catalytic, co-catalytic or structural component of these proteins (Vallee & Auld, 1990). For example, Zn ions within these molecules are able to contribute directly to the enzymatic reaction of Zn dependent enzymes by; 1) interacting with substrate molecules undergoing the reaction, 2) enhancing or diminishing the activity of the enzyme or by 3) stabilising the configuration and structure of numerous proteins and enzymes (Vallee & Auld, 1990).

1.1.3.2 The Role of Zn in DNA Binding Proteins

Zn was first discovered to be essential for gene transcription in 1983 when TFIIIA, a transcription factor protein from *Xenopus laevis* oocytes was identified as containing folded Zn finger domains with appropriately spaced cysteines and histidines that bind Zn (Hanas et al., 1983). Each of these Zn fingers facilitate the interaction between the transcription factor and the internal control region of the 5S RNA gene in the promoter/enhancer region of certain genes, thereby promoting gene transcription (Brown et al., 1985). Zn is a vital component for these processes since chelation of Zn atoms prevented TFIIIA from binding to the 5S RNA gene hence inhibiting transcription (Brown et al., 1985). Another example of a mammalian Zn finger protein is GATA-2, a transcription factor essential for the development of hematopoiesis (Vallee & Falchuk, 1993).

1.1.3.3 Metallothionein (MT), an Example of a Metalloprotein Essential for Zn Homeostasis

Zn is an important component of the anti-oxidant MT which functions to maintain metal homeostasis and regulate intracellular redox states (Maret, 2000). MT are small cysteine and Zn rich metal-binding proteins found in tissues such as the liver, kidney, pancreas, and intestines (reviewed in Davis & Cousins, 2000). The Zn which is present in MT is thought to be bound tightly however in the presence of reactive oxygen species (ROS), the sulfur donor atoms in the clusters are oxidised releasing Zn (Maret, 2000).

MT is essential for cell survival since it is induced during stress in response to heavy metal toxicity (especially cadmium), oxyradicals, inflammation, infection and in Zn deficiency (Mocchegiani et al., 2000). MT regulates intracellular metal metabolism and/or storage by detoxifying, transporting and donating Zn (and Cu) to target apometalloproteins and enzymes hence directly regulating Zn redistribution and homeostasis (Miles et al., 2000). In inflammation, once the acute phase response has passed, the MT gene is switched-off and much of the Zn stored in the liver is released back into the circulation for growth and repair mechanisms. This observation has been best demonstrated in the grastrointestinal (Coyle et al., 2002).

Whether MT proteins are altered in respiratory inflammation is not yet known. However, in one study it was reported that MT levels were transiently increased in response to cigarette smoke in rats suggesting that MT may also have important anti-oxidant properties in the lungs (Gilks et al., 1998). Future studies are now needed to determine whether MT proteins are involved in regulating the

redox states of specific cells within the lungs (e.g. inflammatory and REC) and whether they participate in the pathogenesis of respiratory diseases.

1.1.3.4 Zn as an Anti-Oxidant

Zn is a well-known cytoprotectant which protects and stabilizes cellular molecules (e.g. proteins and DNA), macromolecular complexes (e.g. microtubules) and subcellular organelles (e.g. membranes) from oxidation (Vallee & Falchuk, 1993). This observation has been demonstrated in animal studies where there is increased susceptibility of lung (Taylor & Bray, 1991), liver (Parsons & DiSilvestro, 1994) and testes (Oteiza et al., 1996) to oxidative damage in Zn deficient animals.

Zn is a very effective anti-oxidant whether in its tightly bound state or its labile state and this enables it to act as an anti-oxidant via a number of mechanisms. Firstly, labile pools of Zn ions can directly act as an anti-oxidant by stabilising and protecting sulfhydryl-containing proteins and Zn finger transcription factors from thiol oxidation and disulfide formation (Powell, 2000).

Secondly, Zn has only one oxidation state (II) and therefore cannot undergo redox reactions unlike metals such as Fe and Cu which have the ability to generate hydroxyl ions ($^{\cdot}OH$) and superoxide via the Fenton reaction during oxidative stress (Kappus, 1995). Zn can also displace these metals from macromolecular binding sites within the plasma membrane hence preventing lipid peroxidation (Chevion, 1991). Furthermore, Zn is able to accept a spare pair of electrons from oxidants and thereby neutralising their reactivity (Williams, 1987).

Thirdly, Zn can induce the synthesis of MT during high oxidative stress, which in turn releases Zn ions that can contribute to the anti-oxidant defense system (Jiang et al., 1998; McCormick et al., 1981).

Finally, Zn is an important component of the major anti-oxidant enzyme Cu-Zn superoxide dismutase (Cu-Zn SOD) found in abundance in the cytoplasm of airway and alveolar epithelial cells. Cu-Zn SOD is crucial for detoxifying superoxide anions released from the oxidative respiratory burst of eosinophils, neutrophils and macrophages in the respiratory tract (Greene, 1999). In a recent study, it was observed that the Zn dependent anti-oxidant Cu-Zn SOD had a protective effect against airway inflammation since transgenic mice with elevated levels of Cu-Zn SOD in the lungs were found to be more resistant to allergen-induced hyper-responsiveness than their wild-type counterparts (Larsen et al., 2000). Similarly, Cu-Zn SOD activity is decreased within the airway epithelium (De Raeve et al., 1997) and erythrocytes (Tekin et al., 2000) of patients with asthma, a disease in which there is increased oxidative stress and where a hypozincaemia is also thought to occur (Di Toro et al., 1987; el-Kholy et al., 1990; Goldey et al., 1984; Kadrabova et al., 1996; Vural et al., 2000; Wood et al., 2000).

1.1.3.5 Zn as a Membrane and Cytoskeletal Stabiliser

In addition to its role as an anti-oxidant, Zn is cytoprotective as it can protect plasma membrane proteins and nucleic acids from degradation, while stabilizing the microtubular cytoskeleton and other cellular membranes (reviewed in O'Dell, 2000). Supportive of this is the observation that Zn deficiency decreases cellular barrier functions in endothelial cells (Hennig et al., 1992) while also increasing membrane permeability of erythrocytes and platelets by altering the

lipid and protein composition of plasma membranes (O'Dell et al., 1987). Finally, Zn is also important for tubulin assembly since Zn deficiency causes disruption of microtubules (Hesketh, 1982). These studies confirm that the integrity and survival of a cell is highly dependent on its Zn status, but what remains unclear is the precise mechanism by which Zn deficiency influences the pools of Zn responsible for maintaining the plasma membrane integrity.

1.1.3.6 Zn is Essential for Growth and DNA Synthesis

One of the most obvious signs of Zn deficiency in both animals and humans is growth retardation. Zn is vital for pituitary growth hormone secretion and function (Henkin, 1976) and is needed for hepatic insulin like growth factor-1 (Matsui & Yamaguchi, 1995). Lack of these factors may be related to the anorexia, decreased food intake and decrease in growth rates observed in Zn deficient rats (Roth & Kirchgessner, 1997).

Cell proliferation is important in epithelial tissues (e.g. skin and gastrointestinal tract) where there is rapid cell turnover (Vallee & Falchuk, 1993). This may be related to Zn's presence in the cell nucleus, nucleolus and chromosomes and the abundance of Zn dependent metalloenzymes and Zn finger proteins within these structures. Furthermore, Zn is able to stabilise the structures of DNA and RNA, as well as being a vital cofactor for DNA polymerase, RNA polymerase and reverse transcriptase, all of which are vital enzymes necessary for DNA and RNA synthesis (MacDonald, 2000).

1.1.3.7 Wound Healing

Zn has been used for treatment of wounds for centuries (reviewed in Reed & Clark, 1985). The epithelium requires Zn and is sensitive to alterations in the levels of intracellular labile Zn within the plasma (Vallee & Falchuk, 1993). Many researchers have shown that topical Zn supplementation facilitates wound healing by enhancing the proliferation and regeneration of the epidermis (Hallbook & Lanner, 1972; Pories et al., 1967). In addition, Zn deficient patients suffering from poor healing of skin lesions and wounds are often treated by dietary Zn supplementation or by the use of Zn-impregnated bandages, both of which accelerate re-epithelialization of wounds (Agren, 1990; Vallee & Falchuk, 1993). One reason for the Zn dependence in wound healing is that there is an upregulation of the Zn dependent enzymes, metalloproteinases, (i.e. collagenases, stromelysins and gelatinases) which are essential for the degradation of the extracellular matrix (Lansdown et al., 1999; Ravanti & Kahari, 2000). Additionally, Zn promotes *in vitro* intestinal wound healing by enhancing epithelial cell restitution through a transforming growth factor-β-independent mechanism (Cario et al., 2000). Whether Zn supplementation enhances wound healing in the lung remains to be determined. However it is logical to suggest that exogenous Zn may be essential since metalloproteinases such as MMP-2 and gelatinase B are crucial for the *in vitro* wound healing of human respiratory epithelium (Buisson et al., 1996).

1.1.3.8 Anti-Inflammatory Effects of Zn

Labile intracellular Zn is important in the control of inflammation via a number of mechanisms with the most likely mechanism of actions described below.

Firstly, labile Zn ions can inhibit the activation of NF-κβ, a transcription factor implicated in the expression of many pro-inflammatory genes, by blocking the phosphorylation and degradation of the inhibitory proteins IκB and its multi-subunit IκB kinase (Jeon et al., 2000). Hence the inhibition of NF-κβ by Zn may prove important for a multitude of diseases where inflammation is the driving force.

Secondly, a switch from an initial cellular Th_1 predominance to a more humoral and pro-inflammatory Th_2 mediated immune response is a feature of inflammatory diseases such as asthma and food allergies (Sprietsma, 1999). This same switch favouring the Th_2 subset occurs in Zn deficiency and can be reversed by treating patients with oral Zn supplements (Shankar & Prasad, 1998). This will be discussed later in the context of a possible relationship between Zn deficiency and asthma in section 1.5.

Thirdly, many inflammatory diseases such as arthritis and asthma are associated with an increase in the inducible form of nitric oxide synthase resulting in enhanced NO formation. Labile Zn is able to inhibit lipopolysaccharide- and interleukin-1β-induced NO formation (Abou-Mohamed et al., 1998). To what extent Zn can modulate NO formation in other situations still remains to be determined.

Other mechanisms by which labile Zn can act as an anti-inflammatory agent include 1) blocking the binding of leukocytes to endothelial cells via inhibiting the interaction of leukocyte associated antigen 1 and intercellular

46

adhesion molecule-1 2) blocking the docking of human rhinovirus on intercellular adhesion molecule-1 of somatic cells, thereby preventing viral infections in the respiratory tract (Novick et al., 1997) and 3) inhibiting the release of pre-formed mediators from mast cells and basophils (eg. histamine) (Marone et al., 1986) and eosinophils (eg. eosinophil cationic protein) (Winqvist et al., 1985).

The studies mentioned above illustrate the diverse mechanisms by which Zn acts as an essential regulator of inflammation. Zn may be able to influence the pathogenesis of many diseases by exerting both its anti-inflammatory and anti-oxidant abilities.

1.1.3.9 Influence of Zn on Secretory Cells

In addition to the functions mentioned above, Zn is able to play a unique role in the secretory process of some specialized cells. For instance, neurons, pancreatic islet cells, prostate epithelial cells and mast cells have been reported to not only be rich in labile intracellular Zn but also to require Zn for the secretion of their specialised products. In these cells, labile intracellular Zn is concentrated within cytoplasmic vesicles and granules (Danscher et al., 1980; Frederickson, 2001; Huang & Arvan, 1995; Sorensen et al., 1997; Zalewski et al., 1994b).

It has been demonstrated that Zn in synaptic vesicles is co-secreted with the neurotransmitter glutamate upon excitation and this Zn is thought to modulate synaptic transmission (Huang, 1997). Likewise, in pancreatic islet cells, Zn is bound to proinsulin and is stored as Zn insulin microcrystals which are then secreted in response to glucose (Huang & Arvan, 1995). Similarly, the labile Zn within prostate epithelial cells is stored and secreted in a chelated form with

citrate (Sorensen et al., 1997). Finally, recent studies conducted in our laboratory suggests that labile Zn is secreted from mast cells during degranulation induced by compound 48/80 (personal communication Miss Lien Ho, Department Medicine, University of Adelaide). However, it is still controversial whether this Zn is complexed with histamine or other pre-formed mediators, since there is a lack of recent research conducted in this field (Marone et al., 1986; Uvnas et al., 1975).

Section 1.1.3 has described the multiple biochemical and physiological roles of Zn in the body, showing the importance of this biometal for cell survival and maintenance. Imbalances in Zn homeostasis leading to Zn deficiency therefore impacts on a number of biological systems.

1.1.4 Characteristics and Manifestations of Zn Deficiency

The classical symptoms of Zn deficiency in humans and animals include varying degrees of growth retardation, delayed sexual maturation, immunodeficiency, skin lesions, poor wound healing and gastrointestinal problems such as diarrhea (Prasad, 2001). Furthermore, rat pups born from Zn deficient mothers become severely Zn deficient while also developing numerous severe malformations which include an abnormal skeleton, fused or missing digits and a cleft palate. These pups are also low in birth weight, have skin lesions and are immunodeficient (Jackson, 1989; Record et al., 1985; Sandstead et al., 1975). These manifestations reflect the extreme sensitivity of those cells and tissues which have rapid cell turnover rates such as bone, thymus, epidermis and intestinal crypts, to available levels of dietary Zn (Solomons, 1988). Of particular interest, these tissues also become markedly atrophic with Zn deficiency as there is

impairment of DNA synthesis and increased cell death via apoptosis (Record et al., 1985).

One of the most interesting findings however is that even in severe Zn deficiency, the total cellular Zn (as measured by atomic absorption spectroscopy) is decreased only slightly or not at all. However, labile intracellular Zn levels become markedly decreased (Ploysangam et al., 1997). Other than plasma, tissue Zn levels of adult animals fed a Zn-deficient diet generally did not fall unless the deficiency extended for weeks (Vallee, 1988). From these observations, it can be speculated that it is the labile intracellular pools of Zn, rather than the tightly bound Zn in metalloproteins, which are crucial for the regulation of Zn homeostasis and the manifestations of the clinical symptoms observed in Zn deficiency.

Prevalence of Zn Deficiency

Recent information on Zn intake and prevalence of Zn deficiency in developed countries such as in Australia and USA is scanty. However, studies conducted during the early 1990s have suggested that a significant proportion of Western people are at risk of Zn deficiency since dietary intakes were either below or borderline to the RDI recommended (Sandstead, 1991). Furthermore, children and pregnant women and their fetuses were most at risk of Zn deficiency since their requirement for dietary Zn is significantly increased due to enhanced DNA synthesis and growth (Sandstead, 1991).

The prevalence of Zn deficiency in Australian infants is currently unknown. However, one unpublished study (Dr. Geoff Marks, University of Queensland, personal communication QEHSM 2000 conference) recently reported that

approximately 1 in 4 infants attending day care centers in Brisbane had low hair Zn and responded to Zn supplementation with increased growth and decreased diarrhea and respiratory infections. Similarly, an unpublished study in New Zealand (Dr. E. Ferguson, University of Otago, 2001) reported that 18% of infants had low plasma and hair Zn as well as increased diarrhea. If these findings are accurate and Zn deficiency is indeed a growing problem then there is now a need to monitor Zn status not only in children but also in the Australian adult population, both healthy and diseased to determine whether Zn deficiency is a common disorder in developed countries such as Australia.

Inadequate Intake of Bioavailable Zn Leads to Zn Deficiency

Bioavailability is the extent to which a substance is able to be absorbed and used by the body. The bioavailabity of Zn is dependent on many factors. One of the most important factors is the chemical form of the diet. For example, the presence of the following will greatly influence the absorption of dietary Zn; i) Zn antagonist ligands such as phosphates and oxalates which bind to Zn decreasing its absorptivity, ii) ligands such as carboxylic acids, glucose, amino acids such as histidine and methionine which increase uptake of Zn compared to diets rich in phytate and iii) competing metals such as iron and Cu (Aggett & Comerford, 1995). An example of how bioavailability influences the rate of Zn absorption is that of the vegetarian diet. This diet, despite containing an adequate level of Zn has low bioavailability since this Zn is largely chelated to fiber and phytic acid, hence decreasing absorption across the villi of the jejunum (Freeland-Graves et al., 1980).

Zn deficiency can occur due to the following reasons: 1) malnutrition, 2) defective uptake of the bioavailable Zn across the villi of the jejunum e.g. due to a genetic mutation in the Zn transporter as seen in Acrodermatitis Enteropathica, 3) excessive excretion of Zn in the urine as in diabetes mellitus and 4) increases in the demand of nutrients as in pregnancy and in childhood growth phases (Prasad, 2001).

Malnutrition

Malnutrition is the major cause of Zn deficiency in both developing countries (Bhan et al., 2001) and developed countries (Sandstead, 1995). Nutritional Zn deficiency was first observed in Egypt and Iran in the 1960s and it was found that this population consumed a staple diet adequate in Zn but rich in phytate; this resulted in a significant impairment in Zn absorption leading to the clinical symptoms of Zn deficiency (reviewed in Prasad, 1991). Similar observations have been reported for some indigenous populations including the Australian aborigines (Cheek et al., 1981). In developed countries, inadequate intakes of a balanced diet, presence of chronic diseases and loss of appetite are the major contributors of Zn deficiency in elderly people (Seiler, 2001). On the other hand, in developing countries, regardless of age, poverty is the major contributing factor to malnutrition-induced Zn deficiency (Sazawal et al., 1996).

Defective Zn Absorption

One of the major pathophysiological abnormalities contributing to secondary Zn deficiency is Zn malabsorption. Zn malabsorption can be mediated either by inborn errors of absorption as seen in Acrodermatitis Enteropathica where the CRIP gene is defective (Cousins, 1985), or by an acquired disease such as in

51

short bowel syndrome where half or more of the small intestine is removed (McClain et al., 1985). Treatment of patients with oral Zn sulfate therapy can result in complete clinical remission for both (Aggett et al., 1979; Beyer & Zawislak, 1978).

Excessive Zn Loss

In the healthy body, the 3 major routes of excretion of endogenous Zn are via the faeces, urine and sweat, therefore increases in the Zn content of these waste products due to a disease, can result in varying degrees of Zn deficiency (reviewed in King et al., 2000). For example, in diarrhea there is excessive Zn loss via the faeces (Semrad, 1999) and in diabetes mellitus (Kinlaw et al., 1983), Crohns disease (Salgueiro et al., 2000) and alcoholic cirrhosis (Milman et al., 1983) Zn is excessively excreted in the urine. In these diseases, Zn deficiency is a secondary complication and giving Zn supplements to these patients has proven to be beneficial (Licastro et al., 2001; Mocchegiani & Muzzioli, 2000; Naveh et al., 1997; Takagi et al., 2001; Zemel et al., 2002).

1.1.4.1 Therapeutic Effects of Zn supplementation

Imbalances in Zn homeostasis are easily managed and can be completely corrected by dietary and oral Zn supplementation. Zn supplements have been successfully used to treat Zn deficient children in developing countries where there are also increased risks of serious infectious diseases such as diarrhea, pneumonia and malaria (Black, 1998). Symptoms of Zn deficiency are normally reversed by increased dietary Zn intake or by oral Zn supplementation (Castillo-Duran & Uauy, 2001; Sazawal et al., 1995). For example, Zn supplementation using 10 mg Zn gluconate/day for 120 days in Indian infants aged between 6 and 41 months

was able to reduce the incidence of diarrhea by 17%, respiratory infections by 45% and malaria by 32% (Sazawal et al., 1997; Sazawal et al., 1998).

Zn supplementation is also beneficial in semi-developed countries. A recent study in Turkey found that supplementation by fortification of bread with Zn was an economical and readily accessible means of eliminating Zn deficiency in school children. Consumption of this Zn-fortified bread resulted in improvement of immune functions and significantly higher serum and leukocyte Zn concentrations (Kilic et al., 1998).

It is clear from these studies that diets containing adequate levels of Zn are essential for maintaining the well being of children and preventing the development of diseases which can be worsen by Zn deficiency.

1.1.5 Methods Associated with Zn Measurements

The measurement of total cellular Zn has routinely been performed since 1955 by using atomic absorption spectroscopy (AAS) with high sensitivity (Vallee, 1988). AAS measures the total Zn levels within a cell, which includes both the tightly bound non-exchangeable Zn and its corresponding labile intracellular Zn. However, this technique is unable to reveal the subcellular or tissue distribution of Zn without cellular disruption.

Until recently, understanding the role of intracellular labile Zn in cell biology has been limited partially by the inability to visualise and quantify this specialised pool of Zn since vital dyes for detection of intracellular labile Zn ions have not been as extensively developed as those for calcium. This limitation has led to the development of Zn specific fluorophores which can visualise labile

intracellular Zn without cellular disruption. In this thesis, these pools of "labile intracellular Zn" are defined as the pools of Zn which are freely available to interact with these fluorescent fluorophores. These pools are thought to 1) participate in Zn fluxes and ionic exchange, 2) be most readily altered in Zn deficiency, and 3) are not tightly bound to metalloproteins (Kd $\approx 10^{-11}$ to 10^{-13} M) (Zalewski et al., 1993).

The detection of labile intracellular Zn in a variety of different cell types has progressed extensively since the development of the first Zn specific fluorophore N-(6-methoxy-8-quinolyl)-p-toluenesulfonamide (toluene sulfonamide quinoline, TS-Q) (Frederickson et al., 1987a) and its esterified and methylated derivative 2-methyl-8-p-toluenesulfonamido-6-quinolyloxy) acetate (Zinquin) (Mahadevan, 1996; Zalewski et al., 1993).

TSQ was the first fluorescent Zn probe developed and it has been extensively used for the detection of histochemically active Zn in fixed cells and tissues, mainly from neurological samples (i.e. hippocampal mossy fibers terminals, synaptic vesicles & spinal cord) (Birinyi et al., 2001; Frederickson et al., 1987a; Varea, 2001). However one of the disadvantages of TSQ is that it readily precipitates forming rod like structures which interfere with the quality of the fluorescence observed (personal communications with Ms Sue Millard, Department of Surgery, TQEH, Adelaide).

Zinquin a UV-excitable Specific Fluorophore

In 1993, a non-toxic, membrane permeable UV-excitable intracellular Zn specific fluorophore, Zinquin was developed by this laboratory in collaboration

with other departments within the University of Adelaide (Zalewski et al., 1993). An advantage of this probe is its ability to monitor the more dynamic labile pools of Zn without disruption in living cells. Zinquin has excitation and emission wavelengths at 364 nm and 485 nm, and is able to form UV-excitable fluorescent complexes with labile pools of Zn ions in the nM to μM range in unfixed viable cells under physiological conditions. Zinquin has two separate binding constants of 2.7×10^6 and 11.7×10^6 l/mol which enables it to form 1:1 and 1:2 Zinquin-Zn complexes respectively (Zalewski et al., 1993).

As depicted by Figure 1.3, once inside the cell Zinquin binds to labile Zn through its two nitrogens, one contributed by the quinoline double ring group *(a)* and the other by the sulphonamido group *(b)*. Zinquin's ester group *(c)* is thought to be hydrolyzed by cellular esterases and the resulting acid is deprotonated at cellular pH, producing a negatively charged molecule which is retained within the cell. One of the major advantages of Zinquin is that it possesses a methyl group which prevents crystallisation with Zn ions while also increasing its specificity and affinity for Zn (Nasir et al., 1999). The free or loosely bound labile Zn labelled by Zinquin is then visualised as a blue fluorescence under UV light.

Zinquin has proven to be important for Zn research as it has been used to determine the spatial and temporal changes in labile Zn that accompany mitogenesis of lymphocytes, insulin secretion by pancreatic islet cells and the redistribution of Zn from plasma to liver cells in inflammation (Coyle et al., 1994; Zalewski et al., 1993; Zalewski et al., 1994a). Zinquin has also been used to detect labile intracellular Zn in a variety of cells and tissues by our group (Ho et al., 2000;

Figure 1.3: Chemical Structure and Specificity of Zinquin

Figure shows the structure of Zinquin. Zinquin is an esterified quinoline-based Zn specific fluorophore. The figure shows the binding of Zn to 2 nitrogens (N), one contributed by the quinoline double ring group *(a)* and the other contributed by the sulphonamido group *(b)*. Two Zinquin molecules bind one Zn ion with stepwise dissociation constants of 370nM and 85nM. Zinquin contains an ester group *(c)* which is thought to be cleaved by esterases within the cytoplasm of cells hence producing a negative charge which traps the Zinquin in the cell. It also contains a methyl group **(d)** which prevents crystallisation. The histogram shows the marked fluorescence (arbitrary spectrometric fluorescence units) of Zinquin (1.25 µM) for Zn ions (1 µM). Zinquin gives a small fluorescence signal with Cd, but not with any other metal ions (1 µM). Data represent means ± SD.

Zinquin

Kd$_1$ 370 nM
Kd$_2$ 85 nM
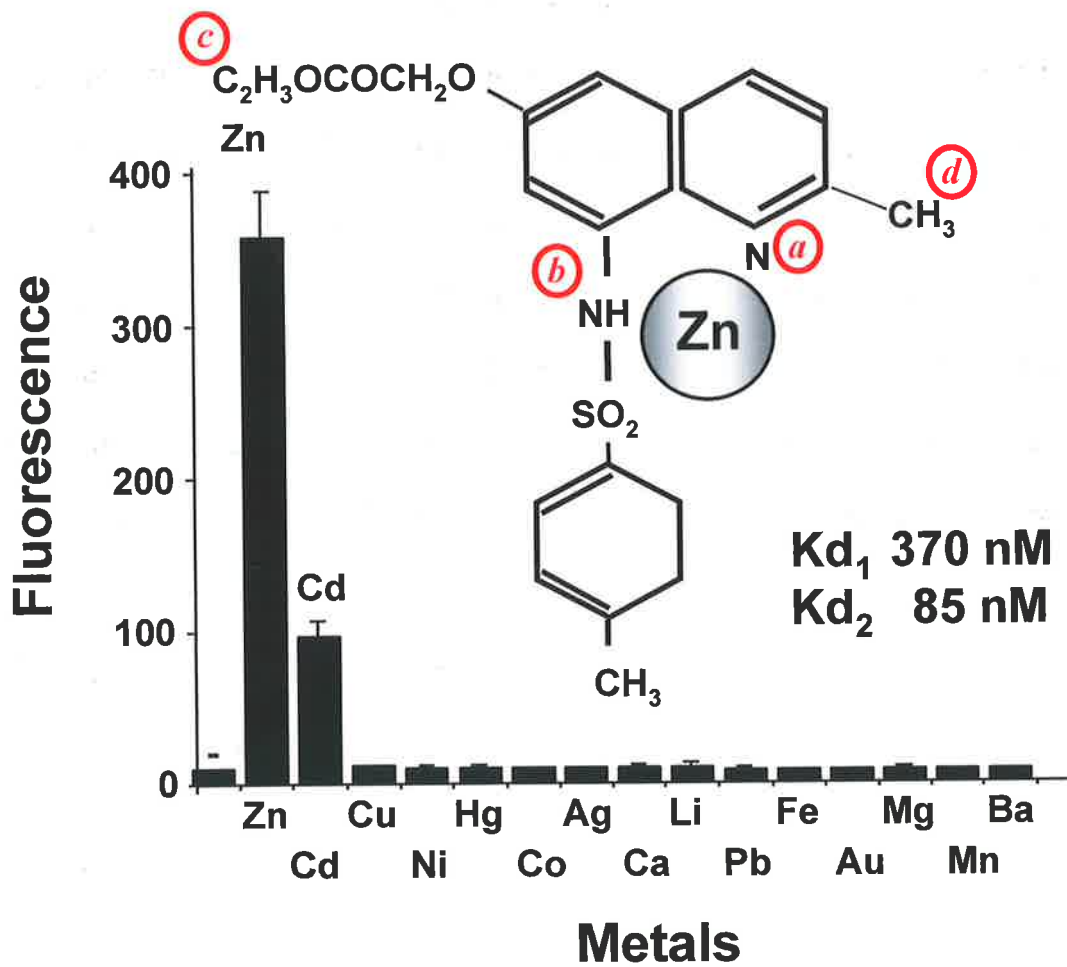
Figure taken from Zalewski et al 1994

Tran et al., 1999; Truong-Tran et al., 2000) and others (Nasir et al., 1999; Palmiter et al., 1996a; Qian et al., 2000; St Croix et al., 2002).

By using Zinquin, Zalewski and colleagues were the first group to report the importance of cellular Zn distribution in apoptosis demonstrating that levels of intracellular Zn inversely correlated with levels of apoptosis in a variety of different cell lines e.g. chronic lymphocytic leukaemia, HL60 cells and thymocytes (Zalewski et al., 1993). The observation that decreased Zn levels enhanced apoptosis was novel therefore acting as the catalysis for initiating studies which investigated the role of Zn as a regulator of apoptosis.

Since the synthesis of Zinquin, new Zn specific fluorohores modeled on Zinquin have been created. These include Newport green (Canzoniero et al., 1997; Lukowiak et al., 2001), ZnPYR4 and FuraZn (oral presentation of Dr Stephen Lippard, April 2002, Zinc Signals 2002 Conference, Grand Cayman).

1.2 APOPTOSIS

Apoptosis is a regulated biological mechanism required for the removal and deletion of superfluous, mutant or moderately damaged cells. In most healthy adult mammalian tissues, apoptosis occurs at a low rate, thereby complementing mitosis in a steady state of kinetics to determine tissue and organ size and shape (Wyllie, 1997). Apoptosis is prominent during embryonic and fetal development and in the immune response as well as being a target for growth factors, hormones and cytokines. In addition, it is a major mechanism of cell death in the body in response to toxic agents (eg X-irradiation) and its dysregulation (insufficient or excessive) is central to pathogenic mechanisms of many diseases (eg neurodegenerative disorders, AIDS,

autoimmune disease and malignancy) (Cohen & Duke, 1984; Kerr, 1997; Wyllie, 1997). As a result, a number of therapeutic strategies are aimed at correcting these imbalances by investigating the factors which regulate crucial molecular pathways which activate or inhibit the central mechanisms governing apoptosis.

1.2.1 Morphological Changes Associated with Apoptosis

Apoptosis is an active, energy-dependent process divided into two phases; the biochemical and the morphological phase. Cells entering death via apoptosis are recognised as undergoing a distinct set of structural changes which are consistent throughout all cell types (Wyllie, 1997). The morphological changes observed in apoptotic cells include: (i) the separation of the dying cell from its neighbours, (ii) loss of specialised membrane structures such as microvilli, (iii) contortion and blebbing of the membrane, (iv) irreversible condensation of cytoplasm, (v) increased cell density, and (vi) the compaction and segregation of the nuclear chromatin to form dense granular masses underlying the nuclear membrane (Kerr et al., 1972). This is followed by nuclear fragmentation and the budding of the cell as a whole, to produce membrane-bound apoptotic bodies. These apoptotic bodies are phagocytosed by nearby cells and degraded by lysosomes to produce lysosomal residual bodies. The formation of apoptotic bodies is an essential and distinct characteristic of apoptosis, preventing the initiation of an inflammatory reaction by keeping the apoptotic cell directly out of contact of the remaining healthy tissue (Wyllie, 1997). Hence these morphological and biochemical observations distinguish apoptosis from another type of cell death, necrosis.

1.2.2 Cell Necrosis

Necrosis, a pathological event caused by physical, chemical or osmotic damage results in the cessation of cellular synthetic functions, and therefore leads to consecutive disruptions of the internal and external membranes of the cell. During necrosis, the cytosol and nuclear structures swell and are dramatically altered; however, the cell maintains its nuclear pores and the general ratio of hetero- and euchromatin (Kroemer et al., 1995). This is in contrast to apoptosis where cells enter a regulated event which is dependent upon active metabolism and protein synthesis followed by the activation of endogenous caspase enzymes and the loss of membrane integrity (Kerr, 1997). Furthermore, cells dying from necrosis are affected as an entire population, whereas apoptotic cell death is limited to individual or randomly scattered cells in the tissue. Figure 1.4 demonstrates the morphological differences between cellular apoptosis and necrosis.

1.2.3 The Caspase Enzyme Family

In order to fully appreciate the distinctive biochemical pathways activated in apoptosis it is necessary to become acquainted with the major participators, the caspase protein family. As illustrated in Figure 1.5, there are currently fourteen caspases discovered and of these, seven are known regulators of apoptosis (Van de Craen et al., 1998). The name caspase is a general name proposed for all members of the family related to interleukin-1β-converting enzyme (ICE) a human cytoplasmic cysteine protease responsible for activation of pro-interleukin 1β (Cohen, 1997). The "C" in caspase denotes a cysteine protease while the "aspase" refers to the enzyme's ability to cleave after an aspartic acid residue. Some of these caspases may act in an auto-catalytic cascade (Cohen, 1997).

Figure 1.4: Comparison of Cells Undergoing Apoptosis and Necrosis

Figure shows the sequence of ultrastructural changes in apoptosis (RHS) and necrosis (LHS).

Apoptosis: A normal healthy cell (1). The earliest recognisable stage of apoptosis is characterised by compaction, margination of nuclear chromatin, condensation of cytoplasm and variable convolution of nuclear and cell membrane (2). These changes are followed by nuclear fragmentation, budding of the cell (blebbing) as a whole to produce membrane bound apoptotic bodies (3) which are phagocytosed by neighbouring cells (4) and degraded by lysosomes (5) to produce residual bodies.

Necrosis: The early signs of necrosis include irregular clumping of chromatin (7), swelling of all the cytoplasmic compartments, increased density of the mitochondrial matrix and focal disruption of membranes. The cell finally degenerates, ruptures, liberating cytosolic proteins and chemotactic factors eliciting an inflammatory response (8).

Necrosis

Apoptosis
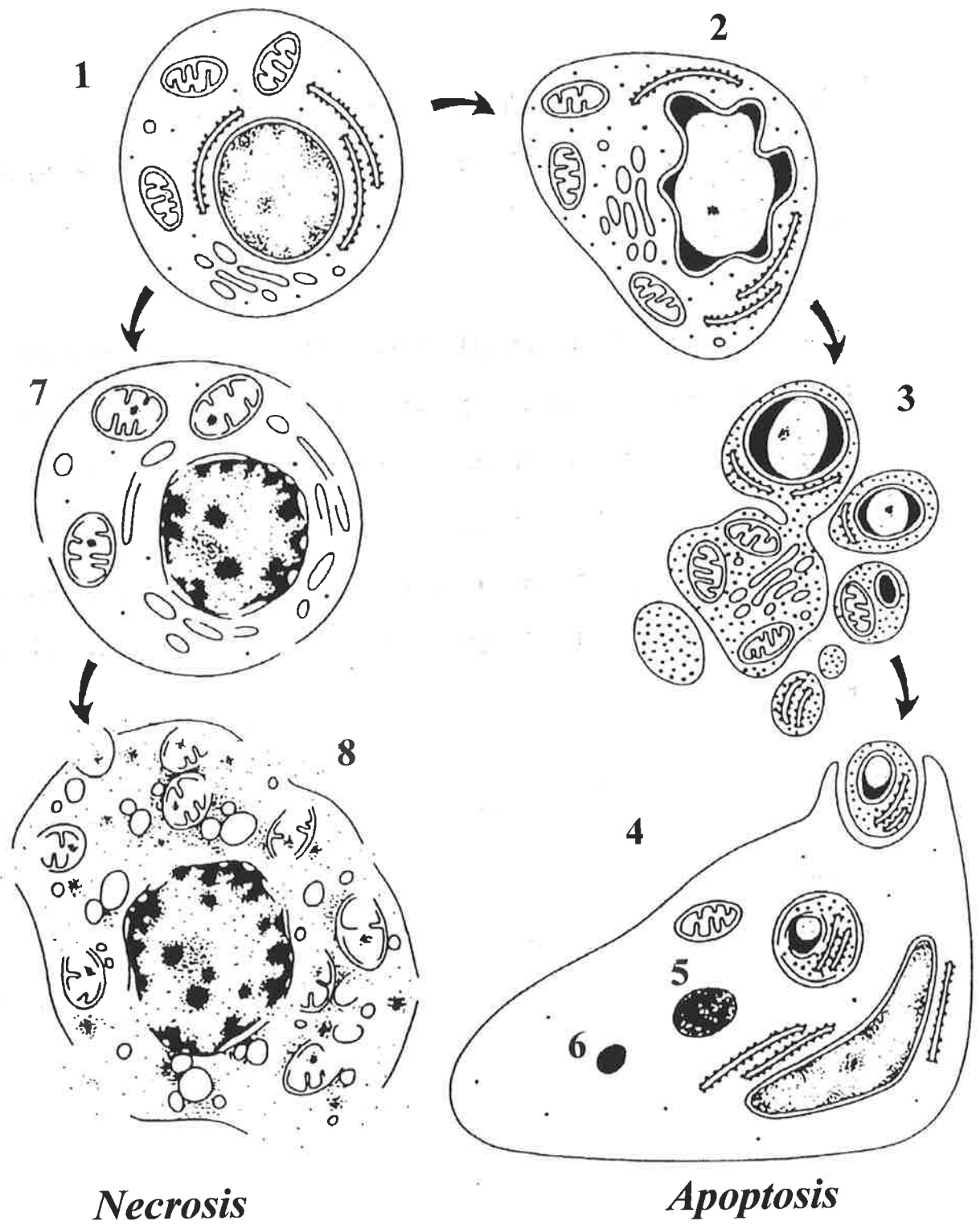
Figure taken from Wyllie 1987

Figure 1.5: Mammalian Caspase Family and C. elegans Caspase CED-3

All mammalian caspases are of human origin except for murine caspase-11 and -12, for which no human counterparts have been identified yet. Based on the substrate specificity, caspases are divided into three groups; the cytokine caspases (green), initiator caspases (blue) and effector caspases (red). Structural relationships are based on sequence similarity among the protease domains. Alternative names are listed in parentheses after each caspase. Dotted box, DED domains; wavy box, CARD domain; black box, large subunit; checked box, small subunit.

Key

▦	DED domain
◫	CARD Domain
▬	Large Subunit
▦	Small Subunit

Sequence Homology	Structure	Substrate Preference	Function

Prodomain Protease Domain

Caspase-4 (TX/ICH-2/ICE_ref-II) — (W/L)EHD ⎫

Caspase-5 (TY/ICE_ref-III) — (W/E)EHD

Caspase-13 (ERICE)

Caspase-11 (ICH-3)

Caspase-12 — Cytokine Activator

Caspase-1 (ICE) — WEHD ⎭

Caspase-14 (MICE)

Caspase-8 (MACH/FLICE/Mch5) — LETD ⎫

Caspase-10 (Mch4)

Caspase-2 (ICH-1/mNEdd2) — DEHD — Apoptosis Initiators

Caspase-9 (ICE-LAP6/Mch6) — LEHD ⎭

Caspase-3 (CPP32/apopain/Yama) — DEVD ⎫

Caspase-7 (Mch3/ICE-LAP3/CMH-1) — DEVD — Apoptosis Effector

Caspase-6 (Mch2) — VEHD ⎭

CED-3 — DETD

Large Subunit   Small Subunit

500   400   300   200   100   0

Amino Acids

Figure modified from Chang and Yang 2000

The first study investigating apoptosis related genes was performed in the nematode *Caenorhabditis.elegans* in 1986 and identified the genes *ced-3* and *ced-4* (abbreviated for cell death abnormal) as being essential for initiating apoptosis (Ellis & Horvitz, 1986). Subsequent studies conducted by the same group found that not only did these genes code for a cysteine protease but they also possessed similar structural and functional properties to ICE (Hengartner & Horvitz, 1994; Yuan et al., 1993). These cysteine proteases were later termed the "caspase proteins"

Family of Caspases

There are three families of caspases; 1) the cytokine activators, 2) the initiator caspases and 3) the executioner caspases. The cytokine activators (caspase-1,4, 5, 13, and 14) are involved in regulating inflammation and at present there is limited data available on the precise mechanism of action of these caspases (Gallaher et al., 2001). The second family of caspases are the initiator caspases (such as caspases-2, 8, 9 and 10) which act upstream and transduce signals from specific input pathways. For example, membrane apoptotic signals activate caspase-8 while the release of cytochrome *c* from the mitochondria triggers caspase-9 activation. These caspases cleave and activate the third family of caspases, the executioner caspases (such as caspases-3 and-6 and 7) which lead to the cleavage of critical substrates, resulting in downstream events and ultimately apoptosis (Chang & Yang, 2000; Gallaher et al., 2001; Thornberry & Lazebnik, 1998).

Caspase Processing

Caspases are synthesized as inactive zymogens (pro-caspases) (Cohen, 1997). All pro-caspases contain a highly homologous protease domain which is further divided into two subunits, a large subunit of approximately 20kDa (p20) and a smaller subunit of approximately 10kDa (p10). Each pro-caspase also contains a pro-domain which is an N-terminal peptide of variable length. Initiator and cytokine caspases have pro-domains of over 100 amino acids while the effector caspases have shorter domains of less than 30 amino acids. The long domain of the pro-caspase protein contains the death effector domain (DED) and the caspase recruitment domain (CARD) (Chang & Yang, 2000; Thornberry & Lazebnik, 1998). During apoptosis, initiator pro-caspases are activated by undergoing oligomerisation which converts the pro-caspase proteins into the tetrameric active form containing an active site at the QR163 D residues (Chang & Yang, 2000).

Proteolytic cleavage of substrates at the aspartic residues removes the N-terminal pro-domain, liberating the large and small subunits to form a tetrameric structure which is the active enzyme (reviewed in Thornberry & Lazebnik, 1998). This mechanism also enables the caspases to regulate the activation and cleavage of other caspases and substrates which are downstream of themselves in an autocatalytical manner, otherwise known as the transactivation phenomenon, resulting in the processing of a multitude of other caspases (Wyllie, 1997).

Caspase Substrates

To date approximately 60 proteins have been identified as substrates for the caspase proteins (Table 1.1). These can be divided into two groups; the first are a group of proteins essential for the regulation and execution of apoptosis and the second, a smaller group which act as pro-inflammatory cytokine precursors (Chang & Yang, 2000). Caspases result in cell death by disassembling and re-organising the cells structures via processes dependent on the cleavage of their substrate proteins at distinct tetra-peptide aspartic acid residues. For example in the case of caspase-3, the motifs are Asp-Xaa-Xaa-Asp (DXXD) which can be found within the cytoskeleton (i.e. gelsolin and actin) and the nucleus (i.e. inhibitor of caspase activated DNase; ICAD) (Thornberry & Lazebnik, 1998). These substrates are either activated or inactivated by proteolysis. One example is the cleavage of ICAD by caspase-3 which results in the release of activated CAD and ultimately cell DNA fragmentation (Thornberry & Lazebnik, 1998). DNA fragmentation is now recognised as one of the hallmarks of cell death but it was not linked with apoptosis until the 1980s (Wyllie, 1987).

Based on the known cleavage site of caspase substrates, invaluable synthetic fluorogenic coumarin derivatives, such as Ac-DEVD-AMC for caspase-3, have been developed as a method for measuring caspase activity in cytosolic extracts (Gillardon et al., 1997).

1.2.4 Caspases Measured in This Thesis

Apoptosis was assessed in REC by measuring the activity levels of caspases-1, 2, 3, 4, 5, 6 and 9. This was performed using their related synthetic coumarin substrates as discussed in Chapter 4 of this thesis.

61

Table 1.1: Caspase Substrates

Substrates

Cell Death Proteins
 Bcl-2
 Bcl-x$_L$
 IAP
 P35
 Pro-caspases

Cell Cycle Regulation
 Cyclin A
 p21$^{cip1/Waf1}$
 Retinoblastoma protein

Cytoskeleton
 Actin
 Fodrin
 Gelsolin
 Keratin -18 and –19
 Lamins protein

Cytokine precursors
 Pro-interleukin-1β
 Pro-interleukin-16
 Pro-interleukin-18 (IGIF)

DNA Metabolism
 DNA-dependent protein kinase (DNA-PK)
 ICAD
 PARP
 Ca^{2+}/Mg^{2+} Endonucleases

RNA Metabolism
 Eukaryotic Initation Factor 2α
 Heteronuclear Ribonuclear Proteins C1 and C2

Signal Transduction
 Calmodulin-Dependant Kinase IV
 Focal Adhesion Kinase
 Protein Kinase C (Delta and theta)

Transcription factors
 Heat Shock Factor
 GATA-1
 IκB-α
 NF-κB (p50, p65)
 Sterol-regulatory element-binding proteins

Others
 Phospholipase A2
 Transglutaminase

Caspase-3 is the major focus of this thesis and was chosen as it is one of the major executioners of apoptosis. Caspase-3 can be found at intermediate to high levels in a variety of cells such as; epidermal keratinocytes, cartilage chondrocytes, bone osteocytes, heart myocardiocytes, epithelial cells of the stomach, intestine, and colon, vascular smooth muscle cells and bronchial epithelium. In contrast, little or no caspase-3 immunoreactivity is observed in endothelial cells, alveolar pneumocytes, kidney glomeruli, mammary myoepithelial cells, Schwann cells, and most types of brain and spinal cord neurons (Krajewska et al., 1997). As previously mentioned, caspase-3 proteolytically cleaves many essential protein substrates e.g. ICAD, poly (ADP-ribose) polymerase (PARP) and p21$^{Wafl/Cipl}$ (Chai et al., 2000; Enari et al., 1998; Tewari et al., 1995).

Caspases-1, 4 and 5 are involved in mediating inflammation (Black et al., 1989) and are thought to be insignificant for apoptosis (reviewed in Cohen, 1997). On the other hand, caspase-6, 9 and until recently 2, are recognised as essential participators in the pathways regulating apoptosis. For instance, capase-6 is an executioner caspase able to cleave the nuclear lamin scaffold proteins at a unique conserved VEID sequence resulting in the fragmentation of the nucleus (Takahashi et al., 1996). It also contributes to the transactivation phenomenon by cleaving caspase-3 (Srinivasula et al., 1996). Caspase-9 is an essential component of the apoptosome (as discussed in the following section) and once activated, cleaves other caspases which results in the ultimate destruction of cells (Jiang & Wang, 2000). On the other hand, caspase-2 was recently reported as an initiator caspase able to release cytochrome c from the mitochondria hence triggering early events in apoptosis (Guo et al., 2002).

At the time when this Ph.D. was commenced there were only a limited number of studies documenting apoptosis in REC with many of these lacking a description on the biochemical pathways involved (Ohno et al., 1999; Shapiro et al., 1999; Zhang et al., 1999). The majority of these studies were also conducted in malignant lung cell lines with the aim of successfully identifying novel methods for lung cancer treatment rather than determining the mechanisms by which apoptosis was regulated (Ohno et al., 1999). Nevertheless, since 2000, there has been a surge in the number of publications focusing on apoptosis in different cells within the respiratory system. The data reported in this thesis provides new understanding of caspase mediated apoptosis of REC.

1.2.5 Distinctive Biochemical Characteristics Associated with Apoptosis

Research conducted over the years has provided invaluable insight into the mechanisms which regulate apoptosis. It can now be stated that the mitochondria is an essential component in the early stages leading up to apoptosis and the late stages facilitating caspase activation. The mitochondria directly coordinates the various pro-apoptotic input signalling pathways and channels them onto a central path governed by the mitochondrial-associated anti-apoptotic (Bcl-2) and pro-apoptotic (Bax) families of regulators (Strasser et al., 2000). Whether the cell proceeds into apoptosis is determined by the ratio of Bcl-2/Bax proteins; this has also been referred to as the Bcl-2/Bax rheostat and serves as a major check-point for commitment of the cell to death (Korsmeyer et al., 1993). Once the cell is committed to apoposis it undergoes distinctive biochemical pathways mediated by two converging caspase cascades; the extrinsic and the intrinsic pathways.

The extrinsic pathway is initiated by a pro-apoptotic membrane receptor such as Fas, which when bound by its cognate ligand activates the Fas cell surface receptor. This results in the recruitment of the death inducing signalling complex to the Fas cytoplasmic domain which ultimately recruits pro-caspase-8 (Kischkel et al., 1995). Once caspase-8 binds to the adaptor proteins within the death inducing signalling complex, it undergoes auto-activation releasing activated caspase-8 which then promotes the cleavage of pro-caspase-3 (PC3) protein to its activated form (Kischkel et al., 1995). Activated caspase-3 (AC3) protein ultimately cleaves its specific substrates and other down stream caspases such as caspase-6 and 10 leading to the destruction of the cell.

On the other hand, the intrinsic pathway is thought to be regulated by the mitochondrion. This organelle acts via the formation of an essential complex named the apoptosome (Zou et al., 1999). The intrinsic pathway is initiated by cellular insults such as oxidative stress, DNA damage and heat shock which induce the release of cytochrome c from the mitochondria into the cytosol. Released cytochrome c plays an essential role by binding to the c-terminus of the apoptosis protease activating factor-1 protein (Apaf-1) within regions which contain multiple WD-40 motifs, thereby resulting in the hydrolysis and oligomerization of Apaf-1 (Benedict et al., 2000). This process triggers the recruitment of pro-caspase-9 to the CARD motif, with binding occurring at a 1:1 stoichiometric ratio at the Apaf-1 N-terminus (Zou et al., 1999). The complexing of Apaf-1 with multiple molecules of pro-caspase-9 forms the apoptosome complex which is approximately 700kDa in size (Cain et al., 2000) and this eventually triggers a cascade of caspase activation. Once activated, caspase-9 dissociates from the complex and becomes available to cleave and activate caspase-3 and 7 (Adrain & Martin, 2001; Zou et

al., 1999). Figure 1.6 illustrates the intrinsic and extrinsic apoptotic pathways described.

1.2.6 Inducers of Apoptosis

Apoptosis is inducible in cells by a variety of stimuli which include various chemical agents e.g. butyrate (Medina et al., 1997), the withdrawal of growth factors, irradiation of cells by UV or x-rays or by the specific activation of cell death receptors such as Fas (Wyllie, 1997).

Another major inducer of apoptosis is the reactive oxygen species (ROS). ROS are highly unstable compounds (e.g. superoxide anion, singlet oxygen, hydrogen peroxide (H_2O_2) and nitric oxide) capable of oxidizing lipids, proteins and nucleic acids within plasma membrane and other cellular components (Halliwell, 1991). It has been proposed that apoptosis evolved primarily to rid the body of oxidatively-damaged cells (Frade & Michaelidis, 1997). Thus, many agents which induce apoptosis are either oxidants or are stimulators of cellular oxidative metabolism while typical anti-oxidants such as Zn, vitamin E, and N-acetylcysteine (precursor for the antioxidant glutathione) have anti-apoptotic properties (Evans & Halliwell, 2001). In fact, the anti-apoptotic protein Bcl-2 is thought to also possess anti-oxidant properties (Dimmeler et al., 1997; Hennig et al., 1993).

Effect of Hydrogen Peroxide (H_2O_2) on Apoptosis

Numerous *in vitro* studies have confirmed that H_2O_2 is an effective apoptotic agent which acts via three major pathways. These include 1) the

Figure 1.6: Two Distinct Pathways Governing Apoptosis

Apoptosis is regulated by two distinctive pathways which result in the activation of the caspases. Caspase activation can be triggered by either (A) the extrinsic pathway (blue, LHS of Figure) or (B) the intrinstic pathway (green, RHS of Figure). Activation of caspase-3 is a common step for both pathways therefore supporting the observation that it is a major executioner of apoptosis.

The extrinsic pathway (LHS) is activated via the binding of specific ligands (such as FasL; blue ovals) to their death receptors (such as Fas; red cylinders). This oligomerization results in the recruitment of the adaptor molecules (such as FADD; green cylinders) and the activation of the initiator caspase-8 (purple cylinders). Activated caspase-8 then triggers the processing of the effector pro-caspase-3 to activated caspase-3, which culminates in the cleavage of caspase-3 specific cellular substrates, destruction of the cell and ultimately apoptosis.

Alternatively the intrinsic pathway (RHS) is activated by the cytosolic release of cytochrome c from the mitochondria. Cytochrome c then binds to Apaf-1 and triggers the recruitment of pro-caspase-9 to the cytochrome c Apaf-1 complex which results in the formation of the apoptosome. Hence, the apoptosome consists of cytochrome c, Apaf-1, and the initiator procaspase-9 (green/yellow oval complex). Pro-caspase-9 within the apoptosome is then activated leading to the recruitment and activation of the effectors pro-caspase-3 (pink cylinders) and 7 (purple cylinders) to activated caspase-3 and 7 which proceed to cleave their specific substrates ultimately resulting in cell death. For example, caspase-6 (yellow cylinders) can be activated by caspase-3. This results in, amongst other things, the cleavage of the nuclear lamin proteins and nuclear collapse.
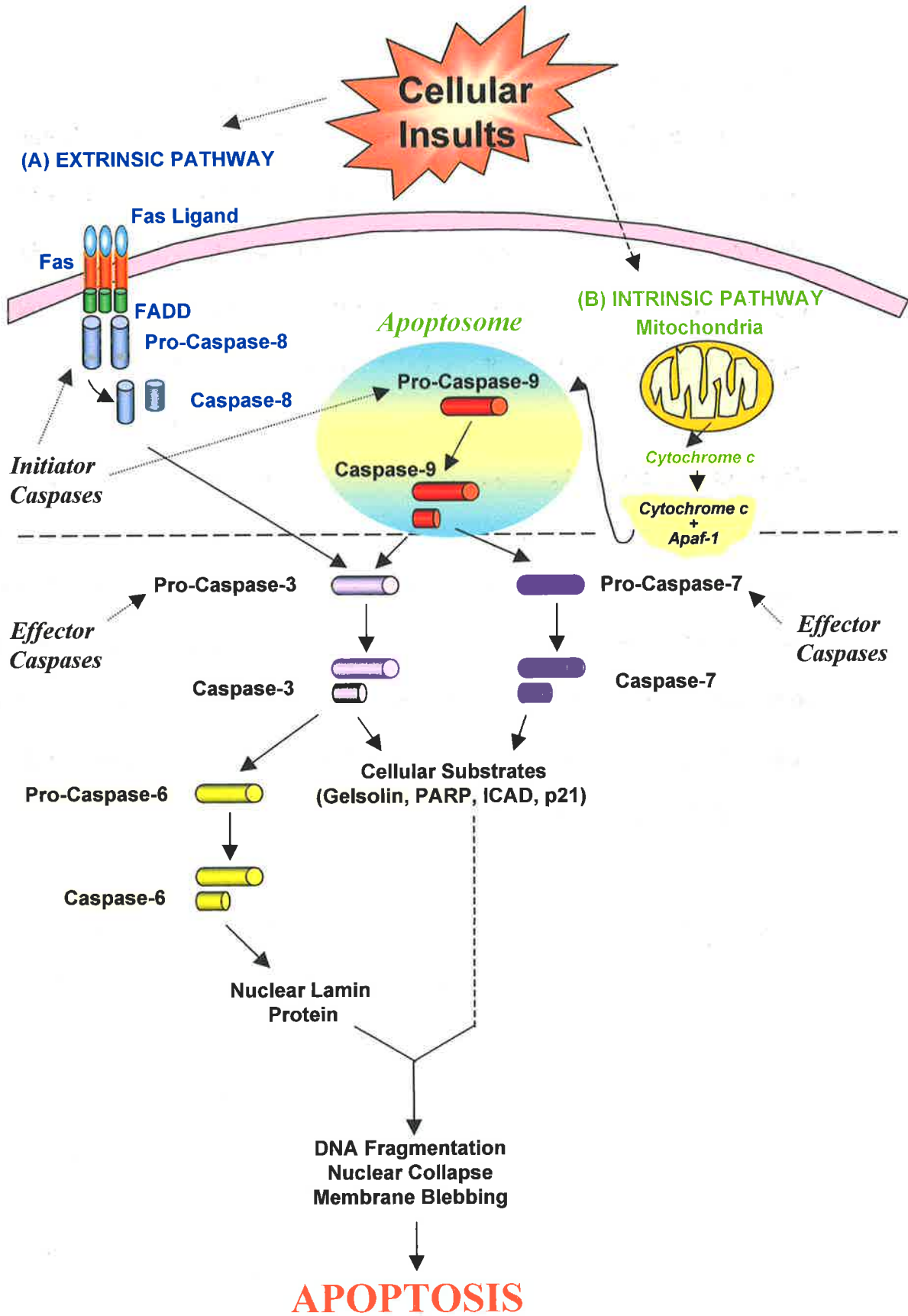
Figure modified from Holcik and Korneluk 2001

activation of the c-Jun-N-terminal kinase pathway, 2) the release of cytochrome c and 3) the generation of the sphingolipid ceramide (Goldkorn et al., 1998; Ramachandran et al., 2002; Stridh et al., 1998). To date, it is unclear which mechanism H_2O_2 preferentially acts by and this may be due to cell specificity, concentration of H_2O_2 used and the individual pathways investigated by the researchers. As such it is possible to also speculate that these three pathways may influence one another or they are at least participators of the one mechanism induced by H_2O_2. Currently, there are no studies which investigate all three mechanisms in one cell type. However, it is interesting to note that in one recent publication, exogenous N-Acetyl-sphingosine a C2-ceramide molecule, was able to induce cytochrome *c* release from the mitochrondria, caspase-3 activation and apoptosis in human neuroblastoma cells (SK-N-MC) (Ito et al., 1999). This observation is interesting as it suggests that interrelationships between two of the three proposed pathways may exist

What is well known though is that H_2O_2 damages cell DNA leading to two forms of cell deaths; at low concentrations it initiated the activation of caspases resulting in apoptosis, while at high concentrations ($H_2O_2 \geq 200$ μM) caspase activation was suppressed hence forcing cells into necrosis (Hampton & Orrenius, 1997). This observation has been confirmed in endothelial cells (Burlacu et al., 2001) human lung fibroblasts (Teramoto et al., 1999) and in Burkitt's lymphoma cell line JLP 119 (Lee & Shacter, 2000).

In the lungs, it has been proposed that H_2O_2 causes acute epithelial cell damage resulting some pulmonary diseases however the mechanism by which it

acts remains controversial (Halliwell et al., 1992). It was first thought that H_2O_2 increased c-fos and c-jun mRNA levels and nuclear proteins, leading to increased membrane permeability and apoptosis in rat lung epithelial cells (Janssen et al., 1997). However, studies conducted in primary human tracheobronchial epithelial cells during the last three years point to an alternative mechanism mediated by ceramide (Goldkorn et al., 1998; Lavrentiadou et al., 2001). Ceramide is thought to be produced within 5 to 10 mins of H_2O_2 treatment and is linked to the DNA fragmentation which appears 6 to 12 hr thereafter (Goldkorn et al., 1998). Of particular interest, ceramide levels were increased at the same time points as when glutathione, a major antioxidant within REC, were depleted (Lavrentiadou et al., 2001).

Hence taken together one could therefore speculate that H_2O_2 may induce apoptosis via the following steps:

1. H_2O_2 activates the hydrolysis of phospholipid sphingomyelin by sphingomyelinase in the plasma membrane to generate ceramide.

2. In the presence of H_2O_2, glutathione levels are depleted decreasing the anti-oxidant properties of cells. These cells have increased oxidative stress which may generate ROS from the mitochondria hence facilitating apoptosis.

3. Ceramide targets the mitochondria activating the pro-apoptotic protein BAX and triggering the release of cytochrome c.

4. Cytochrome c triggers the formation of the apoptosome by recruiting Apaf-1 binding to caspase-9 molecules.

5. Caspase-9 within the apoptosome becomes activated triggering activation of caspase-3, which targets the endonucleases by cleaving ICAD.

6. Cleavage of substrates leads to membrane blebbing, condensation and fragmentation of the cell, DNA fragmentation and formation of apoptotic bodies which are removed.

1.2.7 Regulators of Apoptosis

Apoptosis is a tightly regulated mechanism carefully controlled by a variety of anti-apoptotic agents. This section will discuss three major regulators of apoptosis; Bcl-2, XIAP and Zn. For the purpose of this thesis, Zn was investigated as a regulator of caspase activated apoptosis in REC and this is reported in Chapter 4.

1.2.7.1 The Bcl-2 Family

Bcl-2 and Bcl-X_L belong to a family of proteins which regulate apoptosis during development and homeostasis. There are at least 15 Bcl-2 anti-apoptotic protein family members identified in mammalian cells and these are able to inhibit apoptosis in cells treated with various cytotoxic agents and stimuli such as in γ-ultraviolet-irradiation, cytokine withdrawal, dexamethasone and cytotoxic drug induced apoptosis (Adams & Cory, 1998).

Bcl-2 proteins are anchored on the cytoplasmic face of the outer mitochondrial membrane, the endoplasmic reticulum and the nuclear envelope therefore exposing the active site of Bcl-2 to the cytosol (Nguyen et al., 1993) Once triggered, Bcl-2 can inhibit the release of cytochrome *c* and adenosine

triphosphate (ATP) from the mitochondria hence suppressing apoptosome

formation, caspase activation and apoptosis (Cai et al., 1998).

1.2.7.2 Inhibitors of Apoptosis Proteins (IAP)

In 1996 a new family of human-X-linked inhibitors of apoptosis (XIAP)

were identified (Rajcan-Separovic et al., 1996). These proteins contain several Zn

fingers within the N-terminal baculovirus IAP repeat (BIR) motifs and a C-

terminal RING finger and are homologous to the inhibitor of apoptosis protein

(IAP) family originally identified in baculoviruses (Crook et al., 1993). XIAPs

inhibit apoptosis by binding caspases to the CARD domain of the protein. As

depicted by Figure 1.7, once bound, the Zn fingers within the BIR units contain a

linker peptide which interacts directly with the active site of the caspase protein

thereby inhibiting their activation (Shi, 2002). For example, XIAP are though to

inhibit caspase-3 activation via the BIR2 domain and caspase-9 via the BIR3

domain (Holcik & Korneluk, 2001). Despite the current information available,

appreciation of the full potential of XIAPs as inhibitors of apoptosis still needs to

be determined. As such it remains unclear how and when these proteins are

regulated, recruited or are activated during apoptosis. Furthermore, studies are now

required to determine whether XIAP binding temporarily or permanently interferes

with the functionality of caspases and whether intracellular Zn homeostasis of cell

influence XIAP function.

1.2.7.3 Zn as a Regulator of Apoptosis

Numerous *in vivo* studies have demonstrated the importance of Zn on

apoptosis, noting the increased populations of apoptotic cells in a variety of tissues

Figure 1.7: Model for Inactivation of Caspases by XIAP

In the presence of an apoptotic trigger, mitochondria cytochrome c (black spheres) is released into the cytosol. Cytochrome c binds to Apaf-1, resulting in the recruitment of pro-caspase-9 to form the apoptosome.

The apoptotic inhibitor XIAP becomes associated with the apoptosome and is able to efficiently inhibit caspase-3 activation at the BIR2 domain and caspase-9 at the BIR3 domain. Hence, XIAP are able to intercept and regulate both the extrinsic and the intrinsic pathways of apoptosis by suppressing caspase activation.

Apoptotic Trigger

APAF-1

Cytochrome *c*

Pro-Caspase-9

Mitochondria

Pro-
Caspase-3

Caspase - 3

Caspase-9

BIR 1   BIR 2   BIR 3   RING

XIAP

Apoptosome
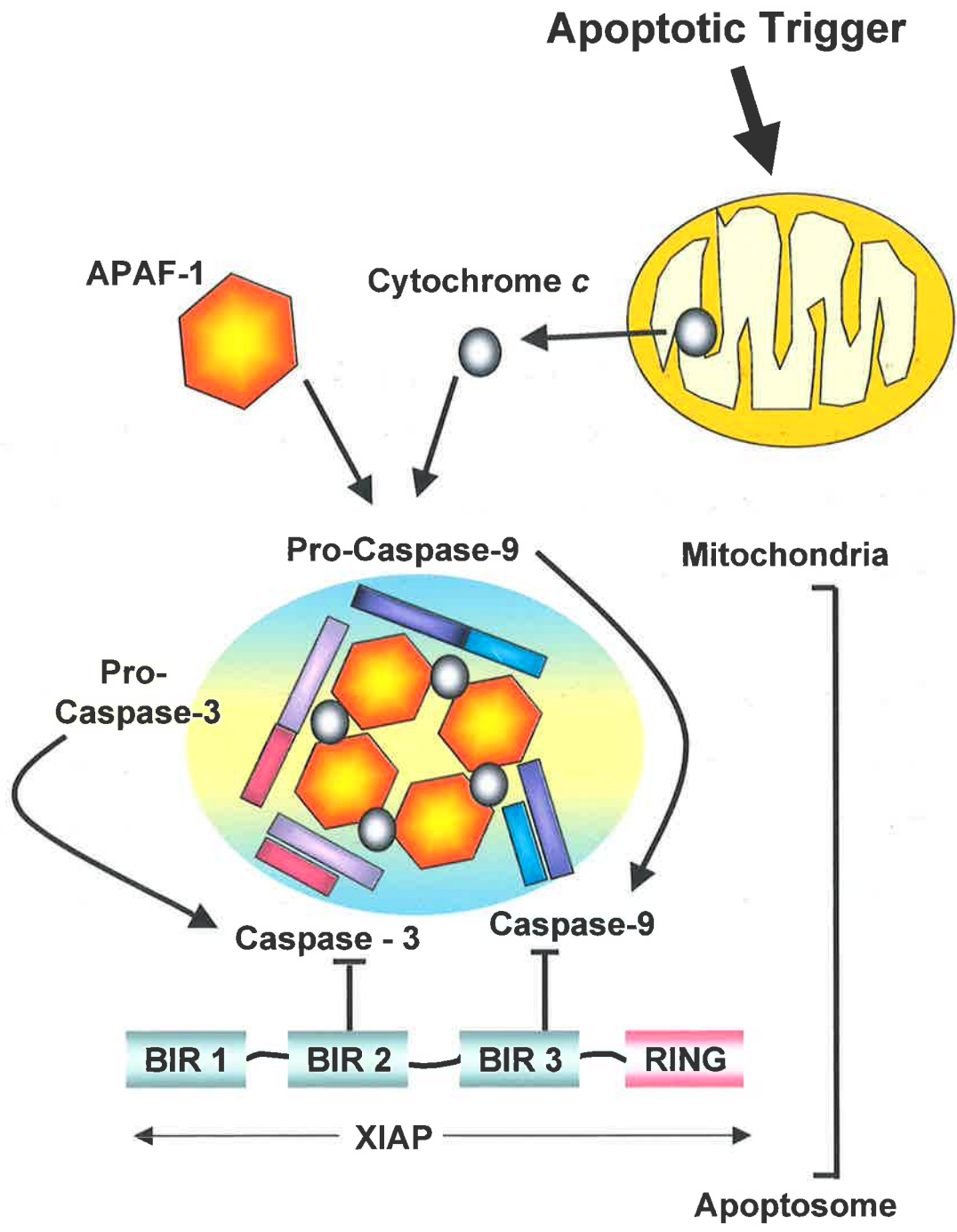
Figure modified from Holcik and Korneluk 2001

including the intestinal epithelium, skin, thymus, testis and pancreas of Zn deficient animals (Elmes, 1977; Nodera et al., 2001; Sunderman, 1995) For example, recent studies have reported that dietary Zn deficiency significantly inhibits chondrocyte proliferation and induced cell apoptosis in the growth plate of juvenile chickens (Wang et al., 2002). Similarly, rats given a completely Zn deficient diet (0% Zn) had increased rates of apoptosis within the thymus and testis within 1 and 3 weeks after the administration of the diet, respectively (Nodera et al., 2001). Interestingly, in the same study, apoptotic cells within the kidney and liver appeared after 13 and 34 weeks, respectively, suggesting that tissues rich in Zn are better protected against apoptosis (Nodera et al., 2001). Whether these abnormalities apply in humans is not known; however, it has been reported that there is increased apoptosis of keratinocytes around vesicular lesions of patients with moderate to severe levels of Zn deficiency (Mori et al., 1996). Similarly, patients with Down's syndrome, a disease associated with Zn deficiency, also had elevated frequencies of pre-apoptotic DNA nicks in peripheral leukocytes which were substantially decreased after 6 months of oral Zn supplementation (Antonucci et al., 1997). The knowledge gained from these *in vivo* studies had provided the foundation for numerous *in vitro* experiments to be conducted in an attempt to better understand how Zn may regulate mammalian cell apoptosis (Chai et al., 2000; Fraker & Telford, 1997; Zalewski et al., 1994a). Despite the extensive knowledge available, there have been no studies to date reporting on the susceptibility of the respiratory system to Zn deficiency induced apoptosis *in vivo* or *in vitro*.

In vitro Studies of Zn and Apoptosis

In vitro studies have advanced our understanding of the biochemical mechanisms by which Zn deficiency triggers apoptosis. Numerous studies have

shown a direct stimulatory effect of apoptosis in Zn depleted cells cultured either overnight in Zn-free medium (Martin et al., 1991) or depleted by membrane-permeant Zn chelators such as N,N,N',N'-tetrakis(2-pyridylmethyl)ethyl-enediamine, TPEN (Treves et al., 1994; Zalewski et al., 1993). These cells exhibit all of the characteristic features of apoptosis and in some cells, Zn deprivation also resulted in necrosis (Martin et al., 1991). Studies performed in lymphocytes have reported an inverse correlation between the level of intracellular labile Zn, varied with pre-treatment of cells with a Zn ionophore sodium pyrithione (NaPYR) or a Zn chelator TPEN, and apoptosis (Zalewski et al., 1991). For example, Zn depletion with TPEN significantly elevated caspase-3 activation in cells. The observations reported by these authors were the first to demonstrate that intracellular labile Zn levels could directly regulate apoptosis by influencing caspase activation and have since been confirmed by others (Chimienti et al., 2001).

Zn is a Potent Inhibitor of Apoptosis

There are now several studies reporting on the beneficial effects of Zn supplementation both *in vivo* and *in vitro* on suppression of apoptosis. Some interesting *in vivo* experiments include the protective effects of Zn salts against whole body irradiation in mice (Floersheim et al., 1992) and sporidesmin-induced immunosuppression in sheep (Waring et al., 1990). Similarly, i.p injections of 1-5 mg/kg of Zn chloride reduced cardiac allograft rejections in an *in vivo* rat transplantation model by suppressing caspase-3 mediated apoptosis (Kown et al., 2000). These findings are consistent with the cytoprotective and anti-apoptotic effects of exogenous Zn *in vivo* in diverse animal models.

Similarly, numerous studies have shown that addition of exogenous Zn sulfate ($ZnSO_4$) suppresses apoptosis in both cell free and cellular *in vitro* models (Sunderman, 1995; Zalewski et al., 1993). One of the earliest *in vitro* biochemical studies supportive of Zn as an anti-apoptotic agent was performed in 1983. It was found that Zn could inhibit the activity of Ca/Mg-dependent endonucleases responsible for nuclear DNA fragmentation in thymocytes (Duke et al., 1983). Studies later performed in the 1990s observed micromolar concentrations of Zn suppressing the activation of caspase-3 (Perry et al., 1997) and 6 (Stennicke & Salvesen, 1997; Takahashi et al., 1996).

Finally, Zn is also able to regulate apoptosis via a pathway independent of caspase activation. It was recently reported that Zn supplementation raised the Bcl-2/Bax ratio hence increasing the resistance of the monocytic cell line U937 cells to H_2O_2-induced apoptosis (Fukamachi et al., 1998). Whether Zn is able to suppress apoptosis in REC remains to be determined and will therefore be tested in the studies described in this thesis.

Of the three mechanisms described above it can be speculated that the most likely pathway inhibited by Zn may be via the inhibition of caspase-3 activation. This is because *in vitro* studies by our group and others have demonstrated that caspase-3 activation occurs rapidly after Zn chelation while Zn supplementation suppresses this process and down stream events of apoptosis (Aiuchi et al., 1998; Chai et al., 2000; Chimienti et al., 2001). Furthermore, rat embryos taken from Zn deficient dams had increased caspase-3 activity and cell death. Hence by suppressing caspase activation then one would also be able to suppress DNase mediated DNA fragmentation since these enzymes are substrates of caspase 3.

Figure 1.8: Structure of the Trachea and the Major Bronchi

The upper conducting airways consist mainly of the trachea, which passes from the larynx to the trachea where it then divides into the two main bronchi. The bronchi then enter the right and left lobes of the lungs further dividing to form smaller airways termed the bronchioles. The trachea and bronchi are mainly supported by rings of cartilage, groups of elastic fibres arranged in longitudinal bundles, numerous mucous glands and nerve bundles, all of which contribute to the ridged effect in the inner lining of the trachea.

Cricothyroid ligament Thyroid cartilage
Cricoid cartilage

Connective tissue sheath
Cartilage
Elastic fibres
Gland
Small artery
Lymph vessels
Nerve
Epithelium

Connective tissue
sheath (cut away)

Intercartilaginous
ligaments

Tracheal
cartilages

Anterior wall

Cross section
through trachea

Posterior wall

Mucosa showing
longitudual folds
formed
by dense collections
of elastic fibres

Nerve
Small arteries
Gland
Elastic fibres

Trachealis muscle
Oesophageal muscle
Epithelium
Lymph vessels

© Novartis

Eparterial
bronchus

To
upper
lobe

To
upper
lobe

To
lingula

To
middle
lobe

R. main
bronchus

L. main
bronchus

To
lower
lobe

To
lower
lobe

Intrapulmonary

Extrapulmonary

Intrapulmonary

Figure modified from Netter 1995

Figure 1.9: Ultrastructure of Bronchus and Bronchioles

Panel A depicts the histology of a section of medium-sized bronchus (large image) and a section of bronchiole (smaller image). These airways are predominantly lined by a pseudostratified, ciliated, columnar epithelium in which all cells are attached to the basement membrane. Beneath the basement membrane exists the lamina propria which consists of a vast amount of blood vessels, elastic fibers, smooth muscle, submucosal glands, nerve fibers, lymph vessels and cartilage plates.

Panel B is a high power image of a bronchiole. Note the pseudostratified ciliated epithelial cells (C), goblet cells (G) and the basal cells (B) which are attached to the basement membrane (BM). The epithelium is supported by a lamina propria abundant in blood vessels (V), lymphoid tissue (LT) and connective tissue (CT).

A

Section of medium-sized bronchus

Ciliated columnar epithelium
with many goblet cells

Basement membrane

Blood vessels

Lamina propria with
elastic fibers

Smooth muscle

Submucosal glands

Nerve fiber

Lymph vessels

Cartilage

Alveoli
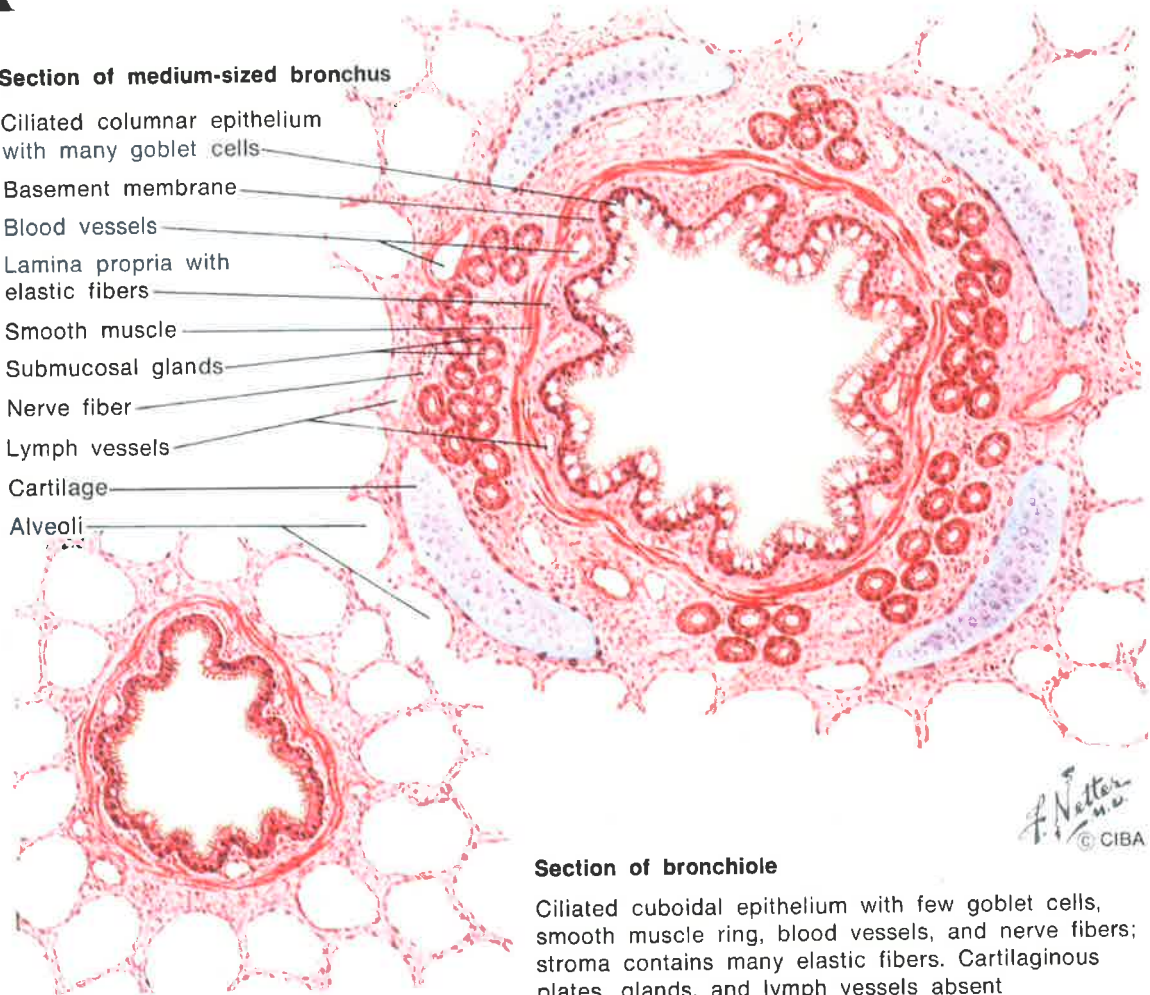
Section of bronchiole

Ciliated cuboidal epithelium with few goblet cells,
smooth muscle ring, blood vessels, and nerve fibers;
stroma contains many elastic fibers. Cartilaginous
plates, glands, and lymph vessels absent

Figure from Netter 1995

B
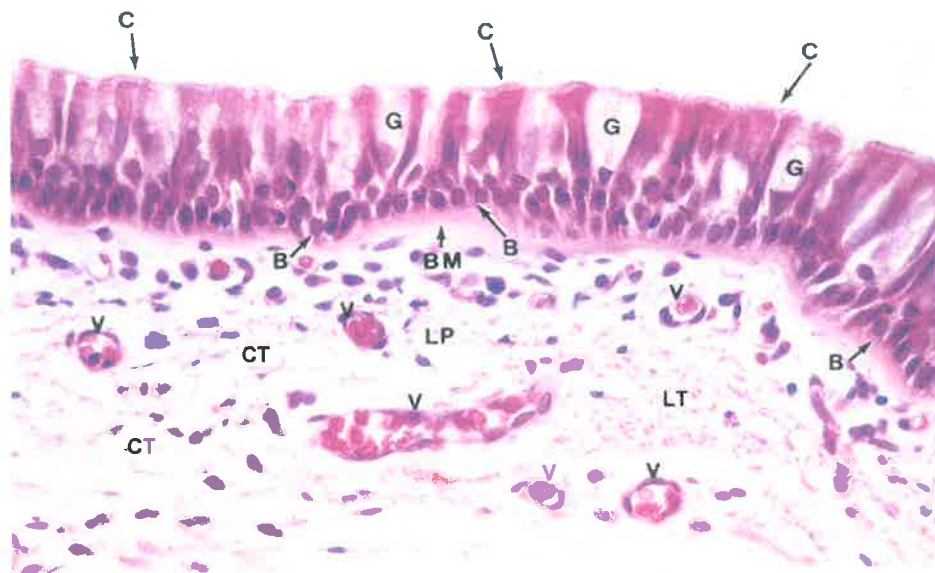
Figure from Burkitt et al 1993

Figure 1.10: Subdivisions and Structure of Intrapulmonary Airways

Figure illustrates the subdivisions of the airways and highlights the structure of the terminal bronchioles, respiratory bronchioles and the alveolar airsacs and alveoli. Between the trachea and the alveolar sacs, the airways divide 23 times. The first 16 generations of passages form the conducting zone of the airways and are made up of bronchi, bronchioles and terminal bronchioles. The remaining seven generations form the transitional and respiratory zones where gas exchange occurs, and are made up of respiratory bronchioles, alveolar ducts and alveolar sacs. These multiple divisions greatly increase the total cross-sectional area of the airways. Pulmonary capillaries surround the alveoli and in most areas the structures between the air and the capillary blood, across which O_2 and CO_2 diffuse, are very thin. There are 300 million alveoli in humans and the total area of the alveolar walls in contact with capillaries in both lungs is about 70 m^2.

Segmental bronchus

Large subsegmental bronchi (about 5 generations)

Small bronchi (about 15 generations)

Cartilage

Terminal bronchioles

Lobule

Respiratory bronchioles (3 orders)

Alveolar ducts and alveolar sacs

Acinus

Acinus

Terminal bronchiole
Smooth muscle
Elastic fibres
Alveolus

1st order
2nd order
3rd order

Respiratory bronchioles

Alveolar ducts

Alveolar sacs and alveoli

Pores of Kohn

© Novartis

Figure modified from Netter 1995

Whether Zn is able to influence Bcl-2/Bax ratios remains controversial and requires further investigations.

Although rates of apoptosis in different regions of the respiratory tract have yet to be studied, it was recently shown that PC3 protein measured by immunocytochemistry is much higher in the bronchial epithelium compared to alveolar pneumocytes (Krajewska et al., 1997).

1.3 RESPIRATORY SYSTEM

The respiratory system consists of the conducting airways which begin at the nasal cavities, leading into the larynx and the trachea which then branches into the main right and left bronchi (Figure 1.8). The trachea is relatively rigid as it contains a number of horseshoe cartilage rings, and is lined by pseudostratified ciliated epithelial cells composed mainly of tall ciliated columnar, secretory goblet and basal cells (Netter, 1995). The bronchi resembles the trachea in structure and are also lined by the same type of epithelial cells (Burkitt et al., 1993). After entering the lungs, the two main bronchi divide to form smaller lobular bronchi. As the branching progresses, the individual airways become narrower, are less rigid, have increasing amounts of smooth muscle and elastic fibers and contain less cartilage. Figure 1.9 depicts the histology of the bronchus, a bronchiole and high magnification image of the airway epithelium. The smaller bronchi then subdivide creating airways termed bronchioles which further branch into the respiratory bronchioles and finally terminating to form several alveolar ducts and air sacs (Figure 1.10). The principal epithelial cell type of an alveolus is the type I simple squamous cell which lines the alveolar air sacs. The alveolus also contains a type II cuboidal cell which produces surfactant hence decreasing lung surface tension. Type I cells rest on a basement membrane fused with endothelial cells from the

73

surrounding capillaries to form the blood-air barrier and it is across this membrane that gases diffuse between the inhaled air and the blood. Also associated with the alveolar wall are the alveolar macrophages which phagocytose dust particles removing debris from the alveolar air sacs (Le Souef, 2001).

As a result, the function of the conducting airways is carrying air into and out of the lungs, and, filtering and removing foreign antigens and particles from inspired air, while the respiratory portion consisting of alveolar air sacs, participates in gaseous exchange (Le Souef, 2001).

The physiological structure of the upper conducting airways plays an important role in normal lung defense mechanisms (reviewed in Cantin, 2001) Goblet cells produce a rich layer of viscoelastic mucus which moistens the air, absorbs water soluble gases and is responsible for trapping inhaled dust and foreign particles. The ciliated columnar epithelial cells remove these mucus enclosed packages by the mucociliary escalator, propelling the tracheobronchial secretions towards the pharynx where these secretions are eliminated from the respiratory system by swallowing or expectoration (Crapo et al., 2000).

Cellular pathways governing the differentiation and cell turn-over of the pseudostratified tracheobronchial epithelium have only recently been studied. Over the past decade several investigators have supported the role of the basal cell as a progenitor cell type (Boers et al., 1998; Inayama et al., 1988). Basal cells may also act as precursors to other epithelial cells within the airways such as the mucus cells (Boers et al., 1998). In contrast to this, secretory cells have also been reported as an alternative progenitor cell type able to regenerate a complete pseudostratified

74

epithelium (Kelsen et al., 1993). Studies into the differentiation of the respiratory epithelium are now feasible due to the development of well established air-liquid interface cell culturing techniques and also the commercial availability of primary normal human tracheobronchial epithelial cell cultures. For example, it was recently reported that mucus cells appeared as rapidly as 10 to 14 days after seeding, while ciliated epithelial cells appeared later at days 21-28 (Gray et al., 2001). Hence use of these cell cultures will undoubtedly provide an advance knowledge in the near future.

As previously discussed, the respiratory system consists of two major epithelial cells, the first type are columnar or cuboidal in shape and line the entire airways, extending from the nasal cavities down to the terminal bronchioles and are therefore termed the airway epithelial cells (AEC). The second, are the squamous alveolar epithelial cells (type I and II) which line the alveolar ducts and airsacs. In this thesis the term respiratory epithelial cells (REC) will be used to describe the mixed population of cells which line both the airways and the alveolar region, while the term AEC will refer only to the epithelial cells which are derived from the airways.

1.3.1 *The Respiratory Epithelium as a Protective and Pharmacologically Active Physical Barrier*

The airway epithelium is a complex and highly-regulated barrier separating the human airway from the external environment and is therefore constantly exposed to a variety of exogenous agents (e.g. allergens, inhaled pollutants and viruses) capable of initiating an inflammatory reaction. Traditionally, this tissue is regarded as a protective barrier however, the epithelium is also able to act as a

metabolically active regulatory system by producing chemokines, cytokines, growth factors and many pro-and anti- inflammatory mediators (Thompson, 1998). Some of the products secreted by the epithelium include: lymphocytic chemoattractant factor, granulocyte macrophage- colony stimulating factor (GM-CSF, promotes differentiation, survival and recruitment of inflammatory cells), Interleukin-1β (IL-1β, activator of B lymphocytes & monocytes, regulator of acute phase protein synthesis and eosinophil and neutrophil inflammation), IL-8 (activator and chemoattractant for neutrophils and eosinophils) and nitric oxide (vasodilator, bronchodilator and increases Th_2 T lymphocytes) (Holgate, 2000; Thompson, 1998).

1.3.2 Inflammation and Diseases of the Respiratory System

Airborne irritants, such as tobacco smoke, industrial chemicals, fumes and domestic and environmental pollutants are critical factors in the etiology of respiratory diseases. These irritants damage the respiratory epithelium and repeated damage ultimately changes the morphology by increasing its thickness, goblet cell hyperplasia and the number of alveolar macrophages in the proximal airways (Lewis & Jakins, 1981; Rahman & MacNee, 1999).

Chronic respiratory diseases such as pneumonia and chronic obstructive pulmonary disease are inflammatory diseases which result in the damage to both the bronchial and alveolar epithelium if left untreated. This damage is due to the recruitment and activation of inflammatory cells such as the eosinophils, mast cells and neutrophils which release tissue damaging proteases, chemotactic cytokines and toxic reactive oxygen species thereby exacerbating the inflammatory response (Shaw et al., 2002).

1.4 ASTHMA IS A CHRONIC INFLAMMATORY DISEASE OF THE AIRWAYS

Asthma is a common disease currently affecting approximately 12% of the Australian adult population, 25% of children and 14% of teenagers nationally (SA Asthma Foundation 1997). Similarly, a survey conducted by the South Australian Spring Health omnibus survey in the period of 1992-1995, stated that the prevalence in self reported adult cases had increased from 15.7% to 20.3% ($p <$ 0.0005) (Adams et al., 1997). This rise was thought to be due, in part to, increased public awareness through education and better patient-clinician contact and is consistent with those reported internationally (Anonymous, 1995; Rutten van-Molken & Feenstra, 2001; Woolcock et al., 2001).

Asthma is a chronic inflammatory disorder of the airways in which many cells play a role, resulting in inflammation. This inflammation causes symptoms associated with widespread but variable airflow obstruction that is often reversible either spontaneously or with treatment (Busse & Lemanske, 2001). Patients with asthma suffer episodes which may be triggered by the inhalation of foreign extrinsic allergens such as grass pollen, pollutants and irritants in the environment. Of indoor allergens, dust mites, domestic animal dander and cockroach allergens are thought to be strong risk factors for asthma (Rosenstreich et al., 1997; Sporik et al., 1995; Squillace et al., 1997).

Asthma can also be precipitated by exercise, cold air, viral infections and exposure to fumes in the work place, producing one or more of the following symptoms of coughing, wheezing, shortness of breath and chest tightness (Busse & Lemanske, 2001). These symptoms are due to pathological changes in the bronchi including increases in: 1) the fragility of the epithelium resulting in sloughing and

desquamation of cells, 2) the chemotaxis of leukocytes which release inflammatory factors targeting mucus and smooth muscle cells and affecting sensory nerves and 3) collagen deposition in the basement membrane leading to fibrosis and irreversible obstructions of the airways (Holgate, 2000).

1.4.1 Prevalence of Asthma

Over the last 100 years there has been a significant decline in the prevalence of previously common childhood infections. This is so because serious viral and bacterial diseases are now preventable by vaccination or antibiotics. On the other hand, many studies have documented the increasing prevalence of childhood and adult asthma throughout the world over the last two decades. In the United States, asthma in 6-11 year old children has increased from 4.8% in 1974 and 1976 to 7.6% in 1980-1984 (Gergen et al., 1988). As previously mentioned, prevalence of asthma in adults has also significantly increased globally (Janson et al., 2001; Pearce et al., 2000).

In Australia, the prevalence of asthma has continued to rise during the 1980's and the late 1990s and this is most evident in the child population. This was confirmed by Peat and colleagues who conducted two major studies monitoring the prevalence of asthma and wheezing in Australian children during 1982 and 1992 and recently, between 1992 and 1997 (Peat, 1998; Peat et al., 1994). These serial cross sectional studies were of populations of children aged between 8 and 10 years and living in two different climatic town in New South Wales: Belmont and Wagga Wagga (Peat et al., 1994). Peat and colleagues reported that the prevalence of wheeze had significantly increased from 10.4% in 1982 to 27.6% in 1992 (p < 0.001) in Belmont and from 15.5% in 1982 to 23.1% in 1992 in Wagga Wagga (Peat et al., 1994). Airway hyper-responsiveness, as determined by the histamine

78

inhalation challenge, had also increased two fold in Belmont to 19.8% (p < 0.001) and 1.4 fold in Wagga Wagga to 18.1% (p < 0.05). The investigators suggested that exposure to higher allergen levels (e.g. dust mites and ryegrass) may have contributed to these findings. Similar results were recently obtained by the same group showing increasing prevalence of wheeze (up by 5.1%), asthma diagnosis (up by 8.1%) and atopy (up by 6.7%) in Wagga Wagga for the period between 1992 and 1997 (Downs et al., 2001). In this study, Peat and colleagues also concluded that increases in the prevalence of diagnosed asthma, wheezing and use of asthma drugs were due to increased awareness and recognition of the symptoms of this disease. The findings reported by these two studies were similar to those found by the Australian leg of the "International Study of Allergies and Asthma in Childhood" which was conducted in Melbourne, Sydney, Adelaide and Perth (Robertson et al., 1998) and also internationally in 16 other countries (Pearce et al., 2000).

However, it still remains to be determined whether this increase in the prevalence of childhood and adult asthma is due to increased rates of diagnosis or to a real increase in the disease. The current general consensus is that increased prevalence of asthma is due to a variety of factors, some of which are environmental. However, the suggestion that asthma prevalence has increased due to better diagnosis is also highly plausible since there is now increased awareness of symptoms and better education of both the public and the general practitioners.

To provide a definitive answer, there is a need to establish a prospective long-term study which measures the prevalence rate of a population using controlled diagnostic techniques.

1.4.1.1 Why is the Prevalence of Asthma Increasing?

Asthma is a unique disease which is multi-factorial and therefore many theories have been generated to better understand the increase in the prevalence of asthma.

Westernisation

Many authors have reported that "Westernisation" may play a role in this increase. This theory is based on the assumption that as a country progresses and becomes more affluent there are many changes made to the lifestyle of its occupants. Westernisation has therefore been associated with; 1) a decline in the family size, 2) improvements in house hold amenities, 3) prevention of viral infections, 4) increases in exposure to indoor house hold allergens (dust mites and cockroach faeces) and 5) lack of ventilation because of tight buildings leading to a higher exposure to volatile organic compounds.

One interesting country for epidemiological investigations is Germany. The unification of Germany in 1990 has provided an excellent opportunity to study the impact of environmental factors on the development of asthma in ethnically similar populations (von Mutius et al., 1994). Studies performed shortly after the unification of Germany found that children (aged 9-11 years) living in the former East Germany (Leipzig) had lower incidence of asthma and atopy than those in the former West Germany (Munich) (von Mutius et al., 1994). Five years after unification, it was observed that although the prevalence of diagnosed asthma had increased for both regions, East Germany was now catching up with West Germany suggesting that Westernisation was a major contributing factor in the increase of asthma and allergy (Weiland et al., 1999)

Hygiene

If Westernisation is indeed an important predisposing factor in asthma then hygiene becomes a critical player in this theory. One interesting study conducted in 1989 found that hygiene, household size and position within a family were the most influential variables in determining the susceptibility of a child to allergic diseases (Strachan, 1989). This study suggested that improvements in hygiene and reduced opportunities for cross infections between siblings had increased the vulnerability of the second child (and thereafter) to allergic diseases such as hay fever and eczema. It has been suggested that exposures to early postnatal infections, especially that of a viral origin could alter the Th_1/Th_2 balance therefore decreasing the risk of developing allergic diseases such as asthma (Strachan, 2000).

Diet

The changing diet and its relationship with asthma has attracted a large amount of attention during the past 10 to 15 years. Numerous epidemiological studies have attempted to investigate the role of various dietary minerals (magnesium, potassium, sodium and selenium), vitamins (Vitamin C and E) and fatty acids (*n-6* and *n-3* polyunsturated fatty acids) and their influence on asthma (reviewed in Fogarty & Britton, 2000b; Greene, 1999; Hodge et al., 1998; Nagakura et al., 2000; Schwartz & Weiss, 1990; Schwartz & Weiss, 1994; Soutar et al., 1997; Sprietsma, 1999). Recent studies have reported that diets from developed countries are now higher in fat and meat and lower in carbohydrates and fibre than in previous years (Popkin, 2001). This trend is also coupled with decreased intakes of fresh fruits, green vegetables and fish, all of which are rich in

anti-oxidants (Fogarty & Britton, 2000a). While acknowledging that these epidemiological studies are important, it still is controversial whether dietary intake levels of specific nutrients in certain populations are correlated with the incidence of asthma, and especially whether dietary supplements which have been used as therapeutic intervention have been completely beneficial. However, diet is unlikely to be the one major cause of asthma since not all patients with asthma are also nutrient deficient and vice versa. Like many of the putative explanations, it is more likely to be a contributing factor.

1.4.2 Histopathological Changes Noted in the Pathogenesis of Asthma

In all asthmatics, the bronchial epithelium is fragile, with a tendency to desquamation and shedding. Bronchial biopsies taken from asthmatic patients demonstrate profound epithelial destruction which include sloughing of mucosal epithelium, and the swelling of ciliated columnar cells giving the epithelium a "fragile appearance" (Laitinen et al., 1985). The airway inflammation present in asthma is characterised by increases in neutrophils, lymphocytes, monocytes, mast cells, and basophils . However, infiltration of eosinophils is a particular feature of asthma when compared with other respiratory diseases (Busse & Lemanske, 2001; Burkitt et al., 1996). In asthmatic responses, mast cells and eosinophils, through their release of toxic granule proteins, cause damage and desquamation of bronchial epithelial cells (Cai et al., 1998; Chanez et al., 1999; Gompertz & Stockley, 2000; Laitinen et al., 1985). Figure 1.11 panel A illustrates the changes observed in asthmatic airways, while Figure 1.11 panel B depicts the histopathological changes observed in a patient with chronic asthma.

Figure 1.11: Histopathological Changes Observed in Chronic Asthma

Panel A is a cartoon depicting the morphological changes of airways in asthma patients (RHS) compared with the airways of normal patients (LHS). Variable airflow obstruction and bronchial hyperreactivity (specific and non-specific) are central features in asthma and are due to the presence of increased smooth muscle tissue, mucus plug formation, thickened epithelium and enhanced collagen deposition which thickens the basement membrane.

Panel B depicts the airway histology of a patient who had chronic asthma. Note the thickened bronchial walls due to hypertrophy of smooth muscle (M), hyperplasia of submucosal mucus glands (G), increased edema and marked infiltration of eosinophils. The bronchial lumen also becomes obstructed by mucus (Mu).

A

Normal airway

Constricted airway
in asthma

Epithelium

Basement
membrane

Smooth
muscle

Mucus plug

Mucus
glands
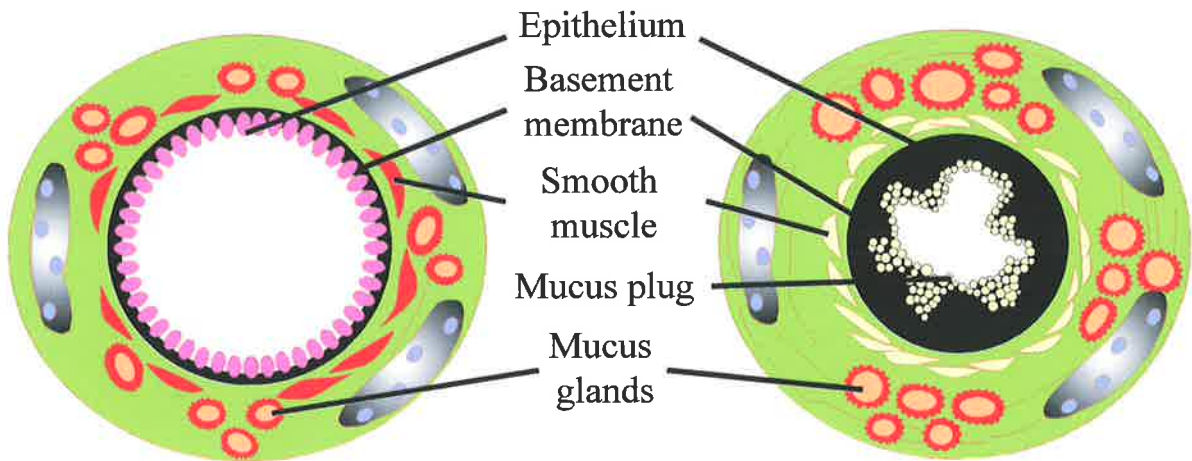
Figure taken from Cotran 1999

B
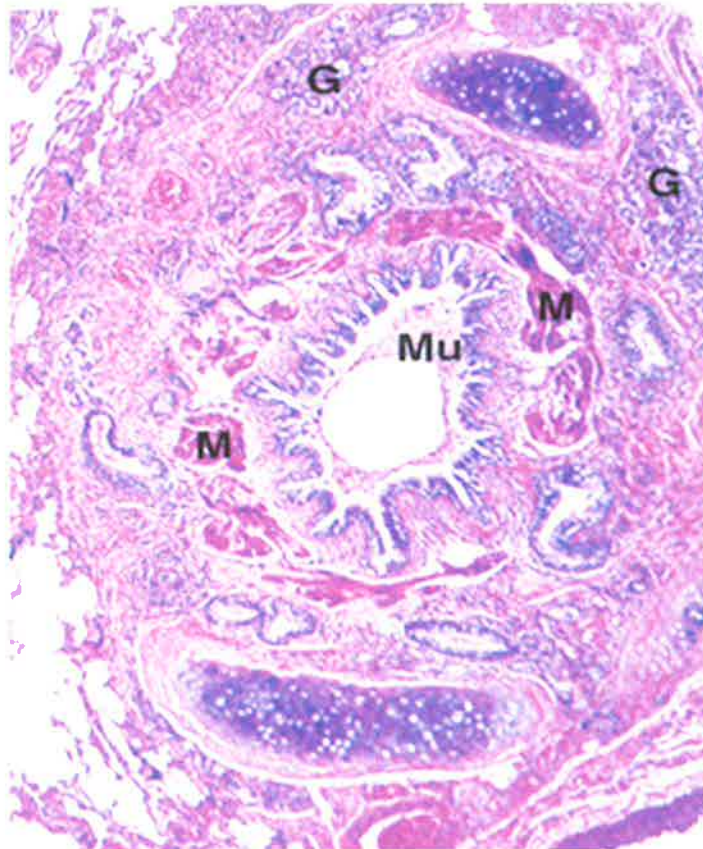
Figure taken from Burkitt et al 1996

1.4.3 The Immunobiology of Asthma

Asthma is associated with hypersensitivity towards specific allergens and elevated serum IgE levels and the immunobiology of this disease is complex as it involves a variety of cell types and mediators (Hamelmann et al., 1999). The first cells which encounter the allergen in the airways are the antigen presenting dendritic cells. These dendritic cells play an important role in the uptake and processing of the antigen. Once the antigen has been processed, dendritic cells present the processed peptide fragments to T lymphocytes which modulate the immune response and release of cytokines (Lambrecht et al., 2001). T lymphocytes belong to two main subsets, one which has the $CD8^+$ marker, is involved in suppressing the immune response and is cytotoxic to target cells, while the other T lymphocytes carry the $CD4^+$ marker which can influence immunoglobulin production in B lymphocytes. In genetically pre-disposed individuals, cytokines secreted from the $CD4^+$ T lymphocytes are predominantly Th_2 cytokines and include IL-4 and Il-13. The production of IL-4 and IL-13 promotes synthesis of IgE from the B lymphocytes which is central to the pathogenesis of asthma and atopy (Greenfeder et al., 2001). In the presence of allergens, pro-inflammatory cytokines released from the Th_2 lymphocytes are increased while the anti-inflammatory Th_1 derived cyokines such IL-2 and IFN-α are decreased (reviewed in Greenfeder et al., 2001). Factors which influence the Th_1 and Th_2 phenotypes are illustrated in Figure 1.12.

Cytokines Govern the Inflammatory Response

The major players in the pathogenesis of asthma are the Th_2 derived cytokines which are generated upon antigen presentation to the $CD4^+$ T lymphocytes. Cytokines are extracellular signalling proteins capable of inducing

Figure 1.12: The Importance of Establishing a Balance between Th_1-Type and Th_2-Type Cytokine Responses

Numerous factors, including alterations in the number or type of infections early in life, the widespread use of antibiotics, adoption of the Western lifestyle, and repeated exposure to allergens, may affect the balance between Th_1-type and Th_2-type cytokine responses and increase the likelihood that the immune response will be dominated by Th_2 cells and thus will ultimately lead to the expression of allergic diseases such as asthma.

Factors favoring the Th1 phenotype

Presence of older siblings

Early exposure to day care

Tuberculosis, measles, or hepatitis A infection

Rural environment

Factors favoring the Th2 phenotype

Widespread use of antibiotics

Western lifestyle

Urban environment

Diet

Sensitization to house-dust mites and cockroaches

Th1

Th2

Protective immunity

Cytokine balance

Allergic diseases including asthma

Figure taken from Busse and Lemanske 2001

the production of many pro-inflammatory mediators in a variety of diseases. These mediators are responsible for the recruitment, maintenance and activation of eosinophils, mast cells and lymphocytes. Numerous studies have reported the increase in cytokine levels of the following type: IL-4, IL-5, IL-13 and IL-2 (Busse & Lemanske, 2001). Figure 1.13 illustrates the interactions between the CD4$^+$ T lymphocytes and the B lymphocytes in the synthesis of IgE.

Of the cytokines mentioned, IL-4, IL-5 and 13 are those most increased in the bronchoalveolar lavage fluid, serum, and induced sputum samples of human asthmatics (Bodey et al., 1999; Huang et al., 1995; Kroegel et al., 1996). As such there has been intense interest in how these molecules modulate the pathogenesis of asthma. It is now apparent that these cytokines account for the majority of the pathophysiological manifestations of allergic asthma such as increasing IgE production, eosinophil recruitment and mucus metaplasia, hypersecretion and enhanced airway hyperresponsiveness (AHR) (Romagnani, 2002). For instance, IL-4 regulates the recruitment and adhesion of inflammatory cells to endothelial cells which are then transported to the airways via the circulation (Hickey et al., 1999; Kopf et al., 1993). IL-4 is also responsible for Th$_2$ lymphocyte commitment and isotype switching of B lymphocytes to the IgE phenotype, two crucial factors which regulate the inflammatory response in the presence of an antigen. In support of these observations, *in vivo* studies conducted in mice, have found that inactivation of the IL-4 receptor either with anti-IL-4 antibodies or specific blockers, inhibits airway eosinophilia, airway hyperreactivity and globlet cell metaplasia during aerosolisation with ovalbumin (Corry et al., 1996; Gavett et al., 1997). IL-5 on the other hand, can also greatly influence the inflammatory process in asthma as it directly regulates the production, survival, and activation of

Figure 1.13: Interactions between CD4$^+$ T Cells and B Cells That Are Important in IgE Synthesis

Interleukin-4 and interleukin-13 provide the first signal to B cells to switch to the production of the IgE isotype. The second signal is provided by accessory pairs of molecules, such as L 2 integrin and intercellular adhesion molecule 1 and CD40$^+$ and its ligand. The engagement of allergen by the complex of the T-cell receptor and CD3 on major-histocompatibility-complex (MHC) class II B cells results in the rapid expression of the CD40$^+$ ligand and increased production of IgE. Once formed, IgE antibody circulates in the blood, eventually binding to both high-affinity IgE receptors (FcRI) and low-affinity IgE receptors (FcRII, or CD23). After subsequent encounters with antigens, binding to the high-affinity IgE receptors results in the release of preformed and newly generated mediators. Once released, mediators may produce various physiological effects, depending on the target organ.
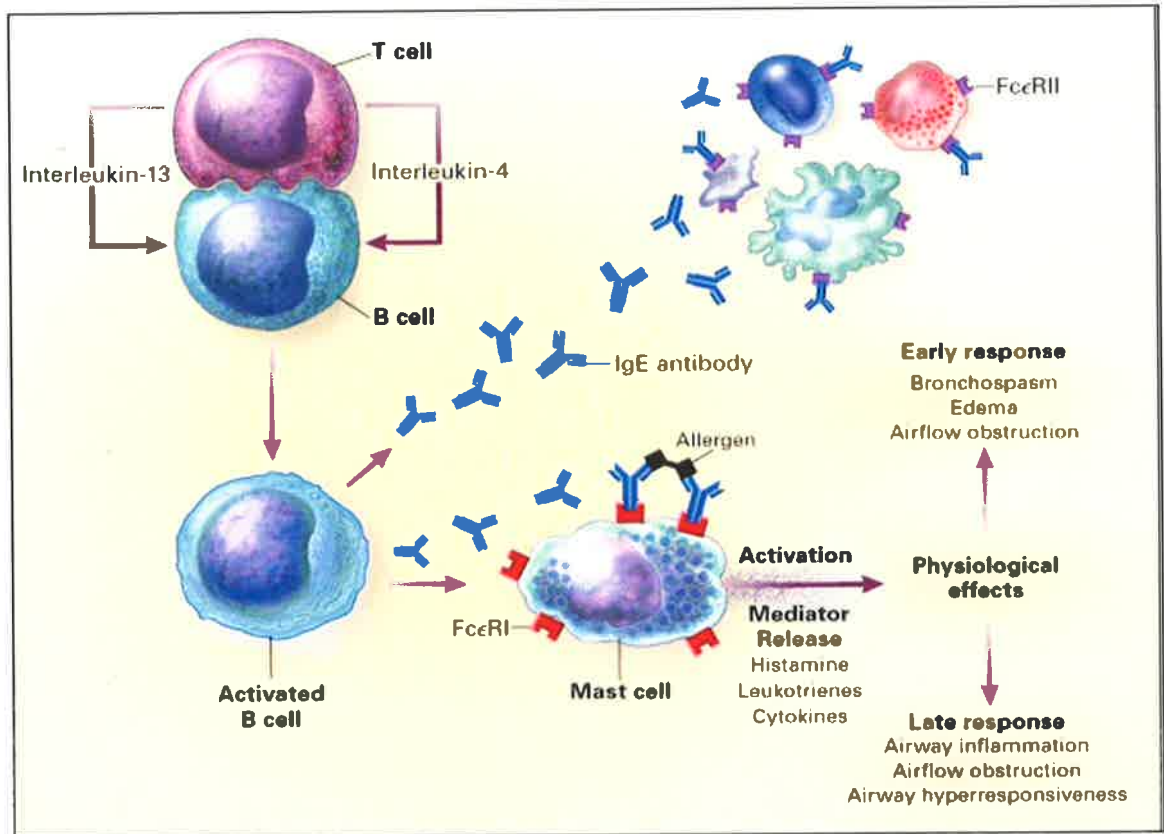
Figure taken from Busse and Lemanske 2001

eosinophils in allergic airway inflammation. This has best been demonstrated in numerous studies using murine models of inflammation (Hamelmann & Gelfand, 2001; Lopez et al., 1988) where allergic animals administered with monoclonal antibodies directed towards IL-5 have significantly decreased bronchial pulmonary eosinophilia and hyperresponsiveness (Nakajima et al., 1992). Similarly, IL-5 knockout mice lack the characteristic eosinophilia, airways hyperreactivity, and lung damage normally observed in the wild type mice made allergic by treatment with ovalbumin (Foster et al., 1996). Finally, studies conducted by various groups have implicated IL-13 as a major participator in regulating eosinophilia, mucus secretion and AHR in both allergic humans and animals. IL-13 is also known to bind to the α chain of the IL-4 receptor and hence can also signal similar pathways influenced by IL-4 (Lefort et al., 1995).

Eosinophils

Eosinophils are major effector cells in the pathogenesis of asthma (Figure 1.14). In asthma, eosinophilopoiesis is up regulated by the cytokines IL-5, IL-13, and GM-CSF hence resulting in peripheral blood, tissue and lung eosinophilia (MacKenzie et al., 2001). Eosinophils migrate from the circulation via the endothelium to the airways via "cell roll" a phenomenon mediated by the L-selectin receptors located on the surfaces of the eosinophils (Sriramarao et al., 1994). Once activated, eosinophils release oxyradicals which damage epithelial cells and generate pre-formed mediators such as GM-CSF which not only promote their survival but also exacerbate the inflammatory response by further enhancing the recruitment of other inflammatory cells (Fujisawa et al., 2000).

Figure 1.14: The Role of Eosinophils in Allergic Inflammation

Inhaled antigens activate mast cells and Th_2 lymphocytes in the airway. This in turn induces the production of pro-inflammatory mediators (such as histamine and leukotrienes) and cytokines which include interleukin-4 (IL-4) and interleukin-5 (IL-5). IL-5 travels to the bone marrow and causes terminal differentiation of eosinophils. Circulating eosinophils enter the area of allergic inflammation and begin migrating to the lung by rolling, through interactions with selectins, and eventually adhering to endothelium through the binding of integrins to members of the immunoglobulin superfamily of adhesion proteins: vascular-cell adhesion molecule 1 (VCAM-1) and intercellular adhesion molecule 1 (ICAM-1). As the eosinophils enter the matrix of the airway through the influence of various chemokines and cytokines, their survival is prolonged by interleukin-5 and granulocyte–macrophage colony-stimulating factor (GM-CSF). On activation, the eosinophil releases inflammatory mediators such as leukotrienes and granule proteins which injure airway tissues. In addition, eosinophils can generate granulocyte–macrophage colony-stimulating factor to prolong and potentiate their survival and contribution to persistent airway inflammation. MCP-1 denotes monocyte chemotactic protein, and MIP-1 macrophage inflammatory protein.
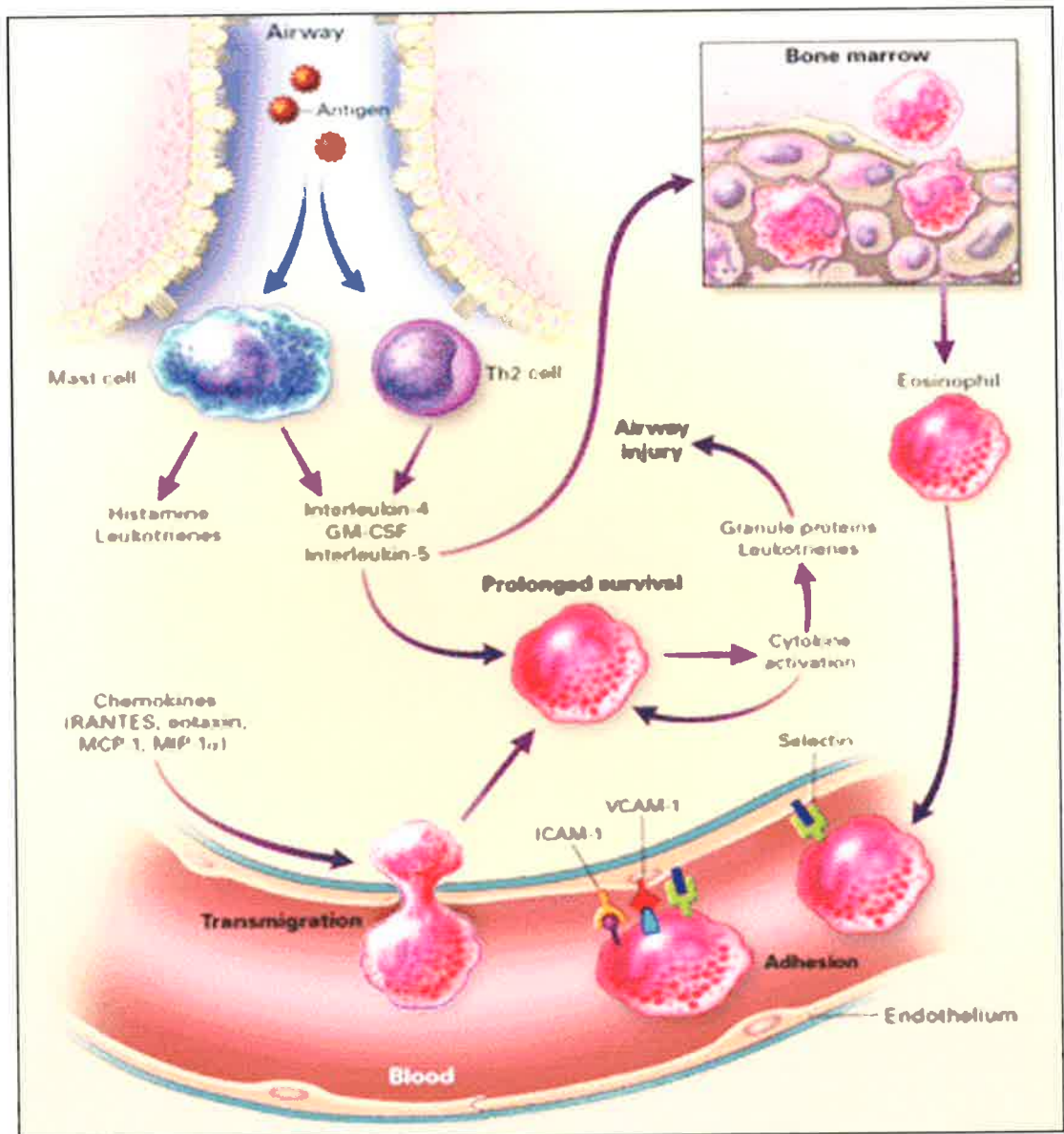
Figure taken from Busse and Lemanske 2001

Mast cells

A very important inflammatory cell involved in asthmatic responses is the mast cell. During inflammation, mast cells release a heterogeneous group of multi-functional pre-formed mediators such as: histamine, neutral proteases, proteoglycans (heparin/chondroitin sulfates), cytokines (IL-2, IL-3, IL-4, IL-5, IL-6, TNF-α and IFN-γ), and acid hydrolases (Kitamura & Fujita, 1989; Pawankar, 2001). Other mediators released by mast cells include: platelet activating factor and products of lipid-derived arachidonate metabolism (PGD2, LTB4, LTC4). Mast cells also release chemokines and eosinophil chemotactic factors which increase the migration of eosinophils in asthma and allergic reactions (Dvorak, 2002; Galli et al., 1984).

1.4.4 Animal Models of Asthma

To investigate the mechanisms controlling the pathogenesis of asthma, one important tool used in asthma research is the animal model of allergic asthma. A variety of allergic models have been established over the past two decades to mimic bronchial asthma in animals such as guinea pigs (Graziano et al., 1981; Pretolani & Vargaftig, 1993), rabbits (El-Hashim et al., 1999; Shampain et al., 1982) sheep (Ahmed et al., 2000; Patterson & Kelly, 1974), rats (Haczku et al., 1996; Holme & Piechuta, 1981), cats (Padrid et al., 1995), dogs (Theodorou et al., 1997) and mice (Foster et al., 1996; Hamelmann et al., 1997; Temelkovski et al., 1998). This section will discuss three major animal models commonly used.

The use of animal models has been an effective tool enabling not only the study of the immune and inflammatory mechanisms involved in asthma but it has also been beneficial in evaluating the efficacy of new asthma drugs (Leong & Huston, 2001).

86

Guinea pigs

Guinea pigs have been routinely used to investigate airway responses to antigen, mediators of asthma such as histamine and new drugs for many decades now (reviewed in Bice et al., 2000). They are easily sensitised to antigens such as ovalbumin (OVA), can produce an anaphylatic response characterised by cytokine and chemokine pathways similar to those observed in humans and they have a sustained lung eosinophilia (Underwood et al., 1995). Furthermore, antigen challenges also result in histamine mediated broncho-constriction (Santing et al., 1994), and agonist-dependent AHR (Underwood et al., 1995). However despite these advantages, the major limitation in this model is that the immune responses are produced by a subclass of IgG rather than IgE immunoglobulin and this does not correlate to the atopic asthma seen in humans (Andersson, 1980).

Rabbits

Rabbits are also valuable for evaluating asthma drug efficacy and if immunised 24 h after birth and sensitised later in life, they produce IgE and IgG antibodies, pulmonary inflammation and airway edema (Shampain et al., 1982). However major disadvantages of this model are; 1) the level of airway AHR reported does not correlate to the level of inflammation present within the airways and 2) the major inflammatory cell present is the heterophil which functionally resembles the human neutrophil rather than the eosinophil (Minshall et al., 1996).

Rodents

Rats (Wistar, Lewis and Sprague-Dawley) are commonly used to investigate airway inflammation by OVA sensitisation with alhydrogel (Szelenyi, 2000). House dust mite antigen and Bordetella pertussis have also been used as

allergens to produce adequate AHR, increased numbers of goblet cells, activation of β_2- agonist receptors and increased infiltration of eosinophils and neutrophils. One major disadvantage of the rat model however is the weak level of bronchoconstriction observed and therefore higher levels of agonists such as histamine and β-methacholine are required when compared to the responses observed in the guinea pigs (Leong & Huston, 2001).

The murine model of allergic asthma has been chosen as the ideal animal model for this Ph.D project for 3 main reasons, 1) it is relatively easy and cheap to establish in the laboratory, 2) the immune responses and genetics of mice are better characterised than any of the other species mentioned and 3) there is now a wider range of molecular and immunological tools available which can be used to study the immunological responses in these animals (reviewed in Leong & Huston, 2001). The murine model of asthma has been successfully used to determine the influence of T cells, dendritic cells and other co-stimulatory molecules which are important in the development of airway eosinophilia and AHR. However one of the major limitations of any animal model is the inability to produce all of the distinct characteristics reported for human asthma in one animal model (Szelenyi, 2000; Vargaftig, 1999). An in depth discussion on the murine model of asthma is provided in Chapter 5. This chapter will also discuss why it is perhaps more appropriate to refer to these models as murine models of allergic airway inflammation rather than as models of asthma.

1.5 ZINC AND ASTHMA

1.5.1 Is Zn Important for the Respiratory Tract?

As presented in section 1.12, Zn is crucial for many biological processes and therefore imbalances in Zn levels will ultimately affect a number of different systems. To date, there are limited studies which have focused on the physiology of Zn in the respiratory epithelium. However, it can be speculated that the AEC of the respiratory system are likely to respond to alterations in Zn homeostasis similar to other epithelial cells of the gastrointestinal tract, endothelium and the skin. If this is true, then some of the beneficial effects of Zn for example, as an anti-oxidant, enhancer of proliferation and wound healing, anti-inflammatory agent and anti-apoptotic agent may also be important for the respiratory system.

Studies are now needed to be performed in the conducting airways to determine whether Zn is indeed essential for the respiratory system since oxidative stress is greatly increased in AEC as a consequence of inflammation, exogenous exposure and also leakage from actively respiring mitochondria (Thompson, 1998). Zn may be important for maintaining the integrity and function of cilia and plasma membranes in AEC and by regulating cell proliferation and tissue repair in the respiratory epithelium in a similar way to that reported for the endothelium (Hennig et al., 1992).

1.5.2 Is Zn Beneficial or Detrimental for Respiratory Diseases?

Excessive inhalation of Zn salts such as Zn oxide, has previously been implicated in causing metal fume fever, an influenza-like illness which results from an acute or subacute respiratory tract inflammation (mild interstitial

89

pneumonia) and is characterised by bronchial hyper-responsiveness, myalgias and fever. If left untreated or undetected, fume fever can also lead to occupational asthma (Fuortes & Schenck, 2000).

On the other hand brief exposures to Zn sulfate aerosols have been shown to protect against allergic bronchoconstriction in guinea pigs, possibly by blocking histamine release from mast cells (Cho et al., 1977). Oral Zn supplementation has also be shown to directly decrease the incidence of respiratory infections in Zn deficient children of developing countries (Sazawal et al., 1998).

Similarly, Zn may be beneficial in reducing the severity of the common cold symptoms. However, there has been conflicting data arguing the pros and cons of Zn lozenges in the treatment of colds (Prasad et al., 2000; Turner & Cetnarowski, 2000). For example, studies by Turner and colleagues found only a slight improvement in the duration of colds (2.5 days vs 3.5 days) but no effect on symptom severity in patients given Zn lozegenes when compared to those on the placebo (Turner & Cetnarowski, 2000). However, a randomised, double blinded, placebo-controlled study published in the same year was supportive of Zn. This study reported a shorter overall duration of cold symptoms (4.5 vs. 8.1 days), cough (3.1 vs. 6.3 days), and nasal discharge (4.1 vs. 5.8 days) when compared to the placebo group (Prasad et al., 2000). Furthermore, a recent study found that routine oral Zn supplementation for a period of four months substantially reduced the incidence of pneumonia in Indian children who had also received vitamin A (Bhandari et al., 2002). The inconsistencies in the data available are due to the high degree of bias present. For example, in the study conducted by Turner and Colleagues, the participants were not adequately blinded since 44% of the

treatment group reported that they could taste the metallic study medication and were likely to be aware that they had received medication (Turner & Cetnarowski, 2000). Hence, better controlled studies are now required to confirm whether Zn lozegenes are effective treatments for the common cold. Nevertheless, it has previously been proposed that Zn is beneficial in the treatment of colds as it may prevent viral docking, capsid formation and replication in the respiratory epithelium (Novick et al., 1997). Several factors such as the dosage, route of administration and the form of the Zn salts given may influence the outcome of whether Zn is good or bad for the respiratory system. Another issue which needs to be taken into account is whether certain diseases have an underlying hypozincaemia for example in chronic inflammatory diseases such as rheumatoid arthritis (Jeon et al., 2000). This may influence the recovery rate when supplemented with exogenous Zn.

1.5.3 Is There a Connection Between Asthma and Zn Deficiency?

The connection between low Zn levels (hair and serum) in chronic bronchial asthmatics treated with corticosteroids was first observed in 1976 by Ellul-Micallef and colleagues. This study reported that patients receiving corticosteroid therapy had significantly ($p < 0.001$) lower serum Zn levels than non-treated asthmatics (Ellul-Micallef et al., 1976).

The increase in prevalence of asthma is strongly dependent on environmental factors including the diet. Numerous studies have suggested that significant decreases in the intake of dietary anti-oxidants may be an important contributing factor in the increasing incidence of asthma over the last three decades (Soutar et al., 1997). One of the first studies investigating the Zn status of

bronchial asthmatics was conducted in 1984 by Goldey and Colleagues. This American study reported a reduction in hair Zn content in asthmatics but due to a limited sample size these results were not considered statistically significant (Goldey et al., 1984). However in 1987, a larger study conducted in Italy reported a significant decrease in Zn hair status in allergic and asthmatic children suggesting that asthmatic children were at risk of Zn deficiency (Di Toro et al., 1987). Two other clinical studies, conducted in Egypt and the Slovak Republic, reported similar results but extended these observations by reporting lower serum Zn levels (el-Kholy et al., 1990; Kadrabova et al., 1996). It was therefore proposed that adequate dietary intake and Zn supplementation may decrease the severity of asthmatic attacks by correcting this underlying hypozincaemia (Kadrabova et al., 1996). Further to this, a recent Australian study reported a significantly lowered level of plasma Zn in asthmatics at 11.5 ± 0.4 μmol/L compared to the healthy population which had 12.8 ± 0.4 μmol/L ($p = 0.027$) therefore suggesting that Zn status may be perturbed in asthma (Wood et al., 2000). However, this Australian study is not totally convincing as the sample size was relatively small (n = 15/group) and Zn levels of both the asthmatic and the healthy group reported were still within the normal reference ranges (~9-18 μmol/L). It is perhaps inaccurate to state that asthmatics are Zn deficient since the accepted level of Zn deficiency in Australia is below 9 μmol/L, rather it may be more appropriate to suggest that asthmatics are more susceptible to Zn deficiency. What is important though is that in almost all the studies quoted, asthmatic patients were found to have significantly lower levels of serum and/or hair Zn levels when compared to the control group. Nevertheless, a recent study by Picado and colleagues reported no association between micronutrient/antioxidant intake or plasma/serum levels of micronutrients/antioxidants and asthma (Picado et al., 2001).

On the other hand low serum Zn levels and dietary Zn intake may play an important role in regulating respiratory functions. Of particular relevance, Schwartz and Weiss in 1990 obtained data conducted in the American Second National Health and Nutrition Examination Survey (n = 9,074). This study found a negative relationship between wheezing and serum Zn:Cu ratio (Schwartz & Weiss, 1990). Furthermore, in a separate earlier Scottish study, Soutar and colleagues investigated the relationship between allergic diseases and dietary anti-oxidants and noted that there was an increase in the presence of atopy, bronchial reactivity and the risk of allergic type-symptoms in adults with the lowest intake of dietary Zn (Soutar et al., 1997).

Despite these studies, the significance of these correlations between the severity of asthmatic symptoms and low Zn levels is not yet fully understood. Hence, future studies are required to fully appreciate the importance of varying Zn status and its effect on clinical symptoms and pathological changes noted in asthma.

1.5.6 Possible Mechanisms of Altered Zn homeostasis in Asthma

While acknowledging that dietary changes over the past several decades have resulted in a decreased intake of fresh foods containing anti-oxidants, it is proposed that several intrinsic factors may contribute to a low Zn status in asthmatics. Firstly, like other inflammatory diseases, a redistribution in plasma Zn to the liver can occur during excessive stress, especially during the acute phase response. This has been attributed to the release of leukocyte endogenous mediator from activated phagocytes, which then stimulates movement of Zn from plasma to hepatocytes in allergic reactions (el-Kholy et al., 1990). Secondly, the immune

system is extremely dependent on the availability of Zn for maintaining its homeostasis. Inflammatory diseases can cause an increase in the demand for Zn as: (i) Zn is essential for producing the thymic hormone thymulin necessary for regulating T-cell development and activation; and (ii) Zn is crucial for the activation of natural killer cells, phagocytic cells and for granulocytes, such as mast cells and eosinophils (Wellinghausen & Rink, 1998). As a result, greater demand for Zn by the immune system could be a contributing factor to the reported Zn deficiency noted in inflammatory diseases. Zn deficiency itself is detrimental for inflammation as it results in large increases in the number, size and activation state of mast cells (Wellinghausen & Rink, 1998). This further exacerbates damage via increasing chemotaxis of eosinophils and neutrophils, which creates a continuous cycle of oxidative damage. Zn deficiency can also cause a premature switch from the Th_1 dependent cellular immune response to a Th_2 dependent pro-inflammatory humoral response (Shankar & Prasad, 1998). This shift in the Th_1/Th_2 balance promotes enhanced levels of IL-4, IL-5, leukotriene B$_4$ (LTB$_4$) and prostaglandins E$_2$ (PGE$_2$) release, all of which have been implicated in promoting the pathogenesis of allergic diseases such as asthma (Wellinghausen & Rink, 1998). Thirdly, although reactive oxygen species are formed as a normal component of cellular respiration, in asthma there is a reported imbalance between the flux of oxidants generated and the presence and/or activation of cellular anti-oxidant defence mechanisms such as Cu-Zn SOD. One possible explanation is that In order for the body to compensate for increased oxidative stress, it must upregulate its anti-oxidant production, hence increasing its need for biochemically active Zn. Therefore, if a hypozincaemia exists and tissue Zn levels becomes limited during inflammation, then the activity of Cu-Zn SOD may be compromised (De Raeve et al., 1997; Tekin et al., 2000). Finally, the inflammatory cells such as

94

eosinophils and mast cells are rich in Zn and their continual activation and removal from the body through coughing during asthmatic episodes, may further deplete Zn reserves.

1.6 AIMS AND HYPOTHESIS

The importance of labile intracellular Zn for many biological systems has been widely reported, however to date, the function of this biometal within the respiratory system is virtually unknown. Hence In order to investigate the functionality of Zn within the respiratory system, the following hypotheses and aims were established.

Hypotheses:
1. REC contain an abundance of labile intracellular Zn within the cytoplasm
2. Zn plays an important role by protecting REC from oxidative damage and apoptosis.
3. Decreased Zn levels may contribute to increased oxidative stress, chronic inflammation and decreased protection of the airway epithelium.
4. Low AEC Zn levels may facilitate the development of airway disease or the clinical expression of airway diseases by increasing apoptosis of AEC.

Aims:
- To determine the levels and localisation of intracellular Zn within the normal and allergic airway epithelium.
- To elucidate the physiological role of Zn in the regulation of caspase-mediated apoptosis in a variety of REC, both primary and transformed.
- To determine whether alterations in Zn homeostasis are an influencing factor in the pathogenesis of asthma, by using a murine model of allergic airway inflammation.
- To examine the influence of allergic inflammation *per se* on levels of intracellular Zn, PC3 and apoptosis in AEC.

CHAPTER 2

MATERIALS AND METHODS

CHAPTER 2 MATERIALS AND METHODS

The experiments described in this thesis conform to the National Health and Medical Research Council of Australia Animal ethics guidelines and have been approved by the Animal Ethics Committee at the University of Adelaide and the Queen Elizabeth Hospital. For suppliers of materials, formulation of buffers and a list of the equipment used please refer to Appendix 1, 2 and 3, respectively.

2.1. RESPIRATORY TISSUES USED

Animal lungs were removed from freshly sacrificed pigs and sheep with permission from the T&R Pastoral Abattoirs at Gepps Cross and Murray Bridge and the Lobethal Abattoirs in Lobethal, South Australia.

2.1.1 Processing of Animal Tissues

Lungs obtained from the abattoirs were immediately trimmed to remove excess adipose tissues, dissected into segments of trachea, bronchi and alveolar tissue which also contained the bronchioles and briefly rinsed in phosphate buffered saline solution (PBS, pH 7.4) to remove excess blood. Tissues of 1cm x 2cm dimensions were then either placed immediately into yellow capped specimen containers containing neutral buffered formalin for fixation or frozen directly with Optimum Cooling Tissue Medium (OCT).

Fresh Tissues

For frozen tissues, 1 cm x 0.5 cm blocks were excised and quickly placed into plastic cryoembedding trays containing OCT and snapped frozen in a glass beaker containing 50 ml of isopentane by immersion into liquid nitrogen.

Paraffin Embedded tissues

After 48 hrs, tissues fixed in 10% neutral buffered formalin were placed into plastic tissue cassettes and processed using the following protocol outlined in Table 2.1.

Table 2.1 Tissue Processing for Paraffin Embedding

Step Number	Reagent	Duration
1	70% Ethanol	1 h
2	90% Ethanol	1 h
3	100% Ethanol	1 h
4	100% Ethanol	2 h
5	100% Ethanol	2 h
6	100% Ethanol	1 h
7	100% Chloroform	2 h
8	100% Chloroform	2 h
9	100% Chloroform	3 h
10	100% Paraffin Wax	2 h
11	100% Paraffin Wax	2 h
12	100% Paraffin Wax	3 h
Total		**22 h**

Tissue blocks were then sectioned at 5 μm thickness and sections were stained for routine morphological assessment as described in section 2.3.

2.1.2 Isolation and Percoll Separation of Primary Tracheal Ciliated AEC

Animal tracheas were carefully dissected, rinsed in 1 X PBS (pH 7.4) then transferred using plastic forceps into sterile 50ml centrifuge tubes containing RPMI 1640 media. These tubes were then transported on ice to the Department of Medicine's Research laboratory. Approximately 8-12 tracheas were obtained per visit with a total of 10 visits conducted.

To prepare isolated AEC, excised segments were incubated at 4°C overnight in RPMI 1640 medium containing 0.05% Streptomyces griseus pronase E. Dissociated cells were removed by vigorous agitation for 5 min, and enzymatic digestion was terminated with fetal bovine serum (10% final concentration). Cells were centrifuged at 150 g for 5 min to produce a cellular pellet containing isolated mucus cells, ciliated cells, and non-ciliated basal cells that were used for Zinquin fluorescence studies.

To obtain a highly enriched population of AEC for apoptosis assays, the percoll separation technique was used (Takizawa et al., 1990). Fresh percoll (density of 2.141) was diluted using 10x Hanks Buffered Saline Solution (HBSS) without Ca^{2+}/Mg^{2+} (pH 7.4) to reach the desired density of 1.045. 3 mls of this percoll solution was mixed gently with 4 mls of cell suspension to ensure an even distribution of AEC and percoll and centrifuged at 800 g for 20mins. Cells were then collected by aspirating the upper band using a sterile glass pipette and viability determined by trypan blue exclusion; only preparations with >90%

viability were used. The upper band collected contains a highly enriched population of ciliated cells that were used for apoptosis studies. AEC were cultured in a modified serum-free LHC-9 medium supplemented with 2 mM L-glutamine, 25 μM amphotericin B, 1 μg/ml of insulin, 1 μg/ml of transferrin, 10 ng/ml of EGF, and 10 ng/ml of retinoic acid. Where extensive clumping had occurred, AEC suspensions were passed two times through a 20-gauge needle before being seeded into wells.

2.2 HUMAN BRONCHIAL BRUSHINGS AND BRONCHOALVEOLAR LAVAGE

Human bronchial brushings and lavage fluid were collected from consenting patients undergoing bronchial biopsies at The Queen Elizabeth Hospital. Human nasal brushings were obtained using a cytology brush from consenting volunteers. Samples were taken from the healthy looking tissues lining the bronchi through a vigorous brushing action and AEC placed in a sterile saline solution for immediate use. All procedures were approved by The Human Ethics Committee of The Queen Elizabeth Hospital.

2.3 ROUTINE STAINING PROCEDURE

The dyes used to stain tissue sections in this thesis were Haematoxylin and Eosin (H&E) for general morphological assessment, Weigert's Haematoxylin and van Gieson's stain for detection of collagen, Alcian Blue/Periodic Shifts Reagent for detection of mucus containing cells and Lendrum's Carbolchromotrope for identification of eosinophils.

The routine steps in staining and mounting of sections involve the complete removal of wax from the tissues by a 45 min incubation with histoclear. Sections were hydrated by treating sequentially with graded alcohol (100% then 90%) for 2 min each and a water wash for 30 secs, then stained with the appropriate dyes. Once the staining was completed, sections were dehydrated in graded alcohol (70%, 90% and 100%) for 1 min, cleared of all water in histoclear for 2 min then mounted with histomount medium.

2.3.1 Haematoxylin and Eosin Staining Procedure for Routine Morphological Assessment of Tissues.

Tissue sections were dewaxed and hydrated as described above. Slides were then stained with Erhlich's haematoxylin for 8 minutes, washed in running water for 2 min and excess staining removed from the tissue sections by quickly dipping sections into a 1% acid alcohol solution. Sections were then washed in tap water for 2 min and counterstained with Eosin for 5 min. Once the staining was completed, sections were dehydrated, cleared and mounted as previously described. Cell nuclei are stained blue, red blood cells are stained red and muscle and collective tissue are stained with varying shades of pink.

2.3.2 Weigerts Haematoxylin and Van Geison's Stain for Identification of Collagen

Weigert's haematoxylin and Van Gieson's dyes were a kind gift from the histopathology department at the University of South Australia. Tissue sections were removed of wax and hydrated as described in section 2.3. Weigert's haematoxylin consisted of two solutions: solution 1 is a 1% iron haematoxylin dye

while solution 2 contains a 30% aqueous ferric chloride solution with a 1% hydrochloric acid base. Solutions 1 and 2 were mixed in equal volumes just prior to use. Sections were stained with Weigert's haematoxylin for 25 min, washed in tap water for 2 min and excess stain removed by quickly dipping sections with 1% acid alcohol and straight into tap water afterwards. Sections were then counterstained by flooding the tissue with Van Gieson's stain for 1 min and the excess stain removed by flicking solutions off the slide. Sections were then dried by blotting with paper, cleared in histoclear and mounted with histomount. Cell nuclei are stained blue black, collagen a bright red colour and the remaining cytoplasm, muscle fibers and red blood cells are stained yellow.

2.3.3 Alcian Blue/Periodic Acid Schiff's Reagent for Identification of Mucus Containing Cells

Alcian Blue, Periodic Acid and Schiff's Reagent were a kind gift from the histopathology department at the Queen Elizabeth Hospital. Tissue sections were removed of wax and hydrated as described in section 2.3. Sections were stained with alcian blue for 5 min, rinsed in tap water for 2 min, and oxidised in 1% periodic acid for 10 min. The sections was then washed in running water for 2 min, rinsed in distilled for a further 2 min and treated with Schiff's reagent for 8 min. Sections were then washed in running water for 2 min, dehydrated in graded alcohol for 2 min, cleared in histoclear and mounted with histomount. Acidic mucins are stained blue, neutral mucins are magenta and mixtures of acid and neutral mucins are purple in colour.

2.3.4 Carbolchromotrope for Identification of Eosinophils

Tissue sections were stained with Lendrum's Carbochromotrope by technicians at the John Curtin School of Medical Research in Canberra. Sections were treated with Mayer's Haematoxylin for 1 min, rinsed in tap water and stained with Carbolchromotrophe for 30 min. Sections were then washed in water dehydrated in graded alcohol, cleared and mounted in histomount. Eosinophils are easily identified by their intense red granules and blue nuclei. Cell nuclei of surrounding tissues are stained blue, red blood cells are stained red and muscle and collective tissue are stained with varying shades of pink.

2.3.5 May Grunwald and Giemsa Stain

Leukocytes from peripheral blood and BALF samples were stained with May Grunwald Giemsa by technicians at the John Curtin School of Medical Research in Canberra and the staff at the Haematology Department at the Queen Elizabeth Hospital. Slides were stained in May-Grunwald for 3 mins, washed with MilliQ water to remove excess stain for 1 minute, then stained with 10% Giemsa stain (stock solution diluted 1:10 in Sorenson's Buffer) for 7-10 minutes. Slides were then washed twice in MilliQ water for 3 mins each, air dried and mounted in histomount. Stained nuclei/micronuclei of leukoctyes appear deep reddish/purple while the cytoplasm appears a pale blue-purple.

2.4 VISUALISATION OF INTRACELLULAR LABILE POOLS OF ZINC WITH ZINQUIN

The localisation of labile intracellular Zn was determined by labelling cryostat lung tissue and primary AEC with Zinquin, ethyl-(2-methyl-8-p-

toluenesulfonamido-6-quin-olyloxy) acetate, (Zinquin) a novel Zn specific fluorophore. Under UV light, intracellular Zn labelled with Zinquin is visualised as a bright blue fluorescence, allowing quantification and localisation.

2.4.1 Labelling of Intracellular Zn with Zinquin in Cryostat Sections of Lung Tissue

Cryostat sections of 8 μm thickness from animal airways and alveolar tissue were fixed in 100% chilled acetone for 5 min at room temperature (RT) then rinsed in PBS (pH 7.4) for 30 secs. Cryostat sections were labeled with 25 μM Zinquin and incubated for 30 min at RT in dark and humidified conditions. Sections were then washed 3x with milliQ water and mounted with an anti-fade fluorescence mounting medium. An autofluorescence control (PBS alone) was set up for each section as a negative control to ensure the specificity of Zinquin for Zn.

2.4.2 Labelling of Intracellular Zn with Zinquin in Primary AEC

Primary AEC were incubated with 25 μM Zinquin as cell suspensions immediately after isolation for 30 min at RT in the dark. In some experiments, intracellular Zn was either depleted or supplemented before addition of Zinquin.

2.5 DEPLETION AND AUGMENTATION OF INTRACELLULAR LABILE ZN IN REC

To deplete intracellular Zn, REC were incubated with varying concentrations (up to 50 μM) of TPEN (N,N,N',N'-tetrakis-{2-pyridylmethyl}-ethylenediamine) for 1 h at 37ºC in complete culture medium. TPEN was stored as

a 5 mM stock solution in DMSO at -20°C and added to cultures at a dilution of at least 1/200. To increase intracellular Zn, cells were incubated with 25 μM Zn which is a typical plasma concentration, in the presence of 1 μM of NaPYR. $ZnSO_4$ was added just prior to addition of NaPYR. TPEN functions by depleting the labile pools of Zn within the cells, while NaPYR facilitates exogenous Zn ion transport across the plasma membrane.

2.6 DETERMINATION OF SERUM AND LIVER ZINC CONCENTRATIONS BY ATOMIC ABSORPTION SPECTROSCOPY

Serum and liver Zn levels were determined as previously described (Coyle et al., 1994). Serum Zn levels were assayed using Graphite Atomic Absorption Spectroscopy. Liver samples were diluted with 5 volumes of cold Tris HCl buffer (0.01M, pH 8.2) and homogenised using a Potter-Elvehjem homogeniser (Wheaton, NJ). Aliquots of liver homogenate were then dried at 70°C for 48h before nitric acid digestion as appropriate for Zn analysis by flame atomic absorption spectroscopy (Perkin-Elmer 303 Atomic Absorption Spectrophotometer, Uberlinger, Germany). Serum samples were diluted 1:100 to a final volume of 1 ml while liver samples were diluted 1:15 to a final volume of 3 ml with Zn free buffer solution (see Appendix 2).

2.7 IMAGE ANALYSIS

2.7.1 Epifluorescence Microscopy

Slides were examined using an Olympus (BH-2) fluorescent microscope, equipped with a UV B dichroic mirror for low wavelength excitation, and connected to a CCTV

video colour camera and computer work station. Both fluorescence images and corresponding phase contrast images were captured and stored.

2.7.2 Confocal Microscopy

A Bio-Rad MRC-1000 UV Laser Scanning Confocal Microscope System, equipped with a UV-Argon laser, was used in combination with a Nikon Diaphot 300 inverted microscope in fluorescence mode. For Zinquin, fluorescence excitation was at 351/8 nm and emission at 460LP while for FITC, fluorescence was at excitation 488/10 nm and emission at 522/35. Images were collected using a 40x water immersion objective lens with NA 1.15. Each image was averaged over 6 scans by Kalman filtering. Prior to the capturing of images, the laser settings of the confocal microscope were adjusted to a level which excluded background fluorescence. The laser strength for Zinquin fluorescence was 3% and for FITC fluorescence, the laser was 10%. Where dual staining was performed, fluorescence images were merged to demonstrate co-localisation of Zinquin and pro-caspase-3 staining using Confocal Assistant (Version 4.02) software package.

2.7.3 Quantification of Zinquin Fluorescence by Video Pro Image Analysis System

AEC Suspensions

For quantification of mean cellular Zinquin fluorescence, lines were drawn around the borders of AEC and fluorescence intensity, as measured by grey scale intensity units (GSU) within the borders, was measured using the Video Pro Image Analysis System (Leading Edge Pty Ltd, South Australia). Background illumination in an area not occupied

by cells was subtracted from the readings. At least 200 cells in each group (from duplicate wells) were analyzed.

Cryostat Sections

For the quantification of Zinquin fluorescence in the sheep and pig cryostat lung sections for Chapter 3, both fluorescence images and corresponding phase contrast microscope images were captured and stored using a 20x objective lens. The outline of the airway epithelium was traced, stored and copied onto the corresponding fluorescence image. A profile line was then drawn at 90° to the epithelial surface so that it spanned the entire epithelium. Zinquin fluorescence intensities were quantified at 1 pixel intervals along the profile line. For each image, 7 randomly positioned profiles were obtained and the mean fluorescence intensity was calculated for each 2.5% distance across the epithelium. As a result, 40 intervals were measured, the first beginning at the lumenal surface and the last terminating at the basement membrane. For the alveolar cryostat tissue sections, 20 squares were drawn as overlays within the boundaries of the epithelium on the light images. These overlays were transferred to the corresponding fluorescence image and intensities measured. The mean fluorescence intensity was collated from 7 images.

2.7.4 Quantification of Zinquin Fluorescence in Confocal Images by the CoMOS Software Package

For the quantification of Zinquin and PC3-FITC fluorescence in the mouse cryostat lung sections for Chapter 7, both fluorescence images and corresponding bright field images were captured and stored using a 40x water objective lens with 3x zoom. For each image, 5 randomly positioned profiles lines were drawn at 90° to the epithelial surface so that they spanned the entire epithelium. The mean fluorescence intensity was

calculated for each of 15 evenly spaced intervals across the epithelium, the first beginning at the lumenal surface and the last terminating at the basement membrane. Apical region is defined as intervals from 1 to 5 and the basal region as intervals from 6 and 15. Fluorescence was quantified using the CoMOS software package results expressed as GSU between 0 and 255 units. The mean fluorescence intensity was collated from at least 2 mice per group, each having 5 to 6 airways assessed.

2.8 TRANSMISSION ELECTRON MICROSCOPY OF SHEEP TRACHEAL CILIATED AEC

Cells (10^6cells/ml) obtained by protease treatment and percoll separation were centrifuged at 800 g and the pellet resuspended in 1ml of EM fixative mixture (1.5% glutaraldehyde and 4% formaldehyde in 0.1M sodium cacodylate buffer) overnight at 4°C. The cell suspension was centrifuged between each of the following processing steps for 1min at 800 g. The cell pellet was post-fixed in 2% osmium tetroxide and stained *en bloc* in 2% uranyl acetate. Cells were then dehydrated through graded series of alcohols (70%, 90%, 100%) and further processed through 100% epoxypropane, a 50/50 mixture of epoxypropane and Procure 812 resin (Electron Microscopy Sciences Fort Washington PA) and 2x 100% Procure 812 resin. The pellet was embedded in polythene capsules and cured overnight at 90°C. Survey sections were cut at approximately 2 μm and stained with toluidine blue. Thin sections were cut at silver-gold colour (approx 100 nm) and mounted on Cu grids. Sections were stained with Reynold's lead citrate and examined with a Hitachi H-600 transmission electron microscope at a potential difference of 75kV.

2.9 CULTIVATION OF CELL LINES

All cell cultures were at 37°C in an atmosphere of 95% medical grade air and 5% CO_2. All cell culture work was performed using aseptic techniques in a biological safety cabinet, Class 2.

A549 cells

A549 cells obtained from Dr. P. Thompson (University of Western Australia) were cultured in Ham's F12 medium (HEPES-buffered pH 7.4, and supplemented with 2 mM glutamine, 100 µg/ml penicillin, 100 µg/ml streptomycin, 160 µg/ml gentamicin) and 10% foetal bovine serum (FBS). Confluence of cells was reached within 48 to 72 h of incubation. These cells grow as adherent monolayers.

A frozen vial of A549 cells were thawed out from the -70°C liquid nitrogen freezer. These cells were transferred aseptically via a pasteur pipette into a sterile 10 ml yellow capped tube. Eight mls of Hams F12 medium supplemented with 10% FBS was added drop wise to the cells until the top of the tube was reached. The tube was then capped and gently shaken to allowing even mixing of cells and centrifuged at 400g at 4°C for 15 min. Following centrifugation, the supernatant was decanted, and fresh medium added to the cells. Tubes were inverted to resuspend the cells before centrifuging again at 400 g at 4°C for 15 min. After the second centrifugation, supernatant was removed and 4 mls of fresh medium added, before re-suspension of the cell pellet. The resuspended A549 cells were transferred into a 25cm^2 flask. Fresh Hams F12 medium with 10% FBS was added to the culture flask to make up a total volume of 10 mls of cell suspension.

NCI-H292

NCI-H292 provided by Dr. D. Knight (University of Western Australia) were cultured in RPMI 1640 (HEPES-buffered pH 7.4, and supplemented with 2 mM glutamine, 100 μg/ml penicillin, 100 μg/ml streptomycin, 160 μg/ml gentamicin) and 10% FBS in a humidified atmosphere (37°C), containing 5% CO_2. Confluence of these adherent cells was reached within 24-48 h of incubation.

The NCI-H292 cells arrived in this laboratory confluent in a $25cm^2$ flask. Upon arrival, the old medium was removed enabling the cells to be washed three times with phosphate buffered saline solution (PBS), pH 7.4. The cells were split by treatment with 0.3% Trypsin/EDTA to cause detachment from the culture flask surface. 10 mls of fresh RPMI-1640 supplemented with 10% FBS was added to the trypsinised cells to stop the reaction. A 2 ml volume of this cell suspension was placed into each of the 3 new vented $25cm^2$ flasks and topped up with 8 mls of fresh RPMI-1640 medium with 10% FBS.

2.9.1 Splitting of Cell Lines

Malignant cells were allowed to grow to confluence prior to splitting. Cells were split 1:10 using the standard procedures outlines above where the old media was removed from the flasks, adherent cells were washed three times with PBS, pH7.4 and then trypsinised with 0.3% Trypsin/EDTA. Proteolysis was terminated by adding 10 mls of fresh RPMI medium containing 10% FCS.

2.10 INDUCTION OF APOPTOSIS IN PRIMARY AND TRANSFORMED CELL CULTURES

Percoll-separated primary ciliated cells (4×10^4 cells/ml) were cultured as cell suspensions with hydrogen peroxide (H_2O_2) in 24 well plates in serum free modified LHC-9 medium. H_2O_2 (30%w/v) was prepared immediately prior to use as a 200 mM stock solution and serially diluted into the plates to give the final concentrations of 0.125 mM, 1.0 mM and 2.0 mM. Cells treated with H_2O_2 where incubated for 18 h. A549 and NCI-H292 cells were seeded into 6-well plates and allowed to grow to near confluence for 48 h prior to the addition of apoptotic stimuli (TPEN & H_2O_2) while primary sheep AEC were used as cell suspensions. For experiments involving TPEN alone, cells were incubated with varying concentrations of TPEN (0-50 μM) for 4 h at 37°C. In experiments involving interaction between TPEN and H_2O_2, cells were initially treated with H_2O_2 (0-0.125 mM) for 18 h at 37°C before the addition of TPEN for a further 4 h. For experiments involving the effects of Zn supplementation on apoptosis, NaPYR (1 μM) and $ZnSO_4$ (25 μM) were added 1 h prior to the addition of apoptotic inducer.

2.10.1 Harvesting of Cell Cultures

Adherent cells were harvested into separate aliquots. The medium containing any detached cells was collected into non-sterile labelled disposable test tubes and centrifuged at 400g at 4°C for 5 min. The supernatant was discarded carefully so as to retain the cell pellet. Remaining adherent cells were lysed directly in the wells by 750 μl of NP-40 lysis buffer, for 10 min at room temperature. Primary AEC were collected directly into disposable tubes, centrifuged at 400g and lysed with 750 μl of NP-40 lysis buffer, for 10 min at

111

room temperature. The cell lysate was transferred via pasteur pipettes into a labelled eppendorf tube and spun in a microcentrifuge at 4°C for 5 min to pellet the organelles. The supernatant was immediately aliquoted into various volumes depending on the different biochemical assays (20 µl for protein assays and 50 µl for caspase activity assays), the rest was stored as 400 µl aliquots at -20°C.

2.10.2 Determination of Protein Concentration

Protein concentration was determined using the DC protein Assay kit. A 20 µl aliquot of cytosol was incubated with 2 µl of Reagent S (a detergent solution), 100 µl of Reagent A (alkaline Cu tartrate solution), and 800 µl of Reagent B (a dilute Folin Reagent), for 15 min at room temperature. A standard curve was constructed using varying concentrations of purified bovine serum albumin dissolved in NP-40 lysis buffer to produce final concentrations within the ranges of 0 mg/ml to 1.6 mg/ml and the reaction quantified using a Varian Techron DMS 200 spectrophotometer at maximum absorbance of 750nm.

2.11 ASSAY FOR APOPTOSIS

Apoptosis was assessed in cells and tissues by measuring caspase activity, morphological features associated with apoptosis, as determined by chromatin condensation and increases in active caspase-3 (AC3) protein and cleavage of cytokeratin 18 (CK18), a substrate of caspase-3. PC3 protein levels were also determined by immunohistochemistry. The methods used for measuring these parameters are described below.

2.11.1 Assay for Caspase Activity

Based on the knowledge that caspases are able to cleave substrates which all contain a common aspartatic acid residue motif such as Asp-Xaa-Xaa-Asp (DXXD), specific synthetic substrates have been developed for the purpose of measuring caspase activation in vitro. These model synthetic fluorogenic substrates such as DEVD-AFC (for caspase-3) and VEID-AFC (for caspase-6) all enable specific types of caspase activity to be measured in cell lysates, hence providing a convenient, quantifiable, biochemical indicator of apoptosis (Nicholson et al., 1995).

Caspase activity was quantified by its enzymatic cleavage of substrate, hence releasing the free coumarin derivative, AFC. The free AFC compound produces a yellow-green fluorescence when exposed to UV light at 505nm. For caspase-3 activity the fluorogenic substrate used was DEVD-AFC. Other substrates used were YVAD-AFC (caspase-1), VDVAD-AFC (caspase-2), LEVD-AFC (caspase-4), WEHD-AFC (caspase-5), VEID-AFC (caspase-6) and LEHD-AFC (caspase-9). A 50 µl aliquot of cytosol was incubated with 1ml of caspase protease substrate buffer, containing 2.5 µM of synthetic fluorogenic substrate, for 18 h at room temperature. Caspase activity was quantified in a Perkin Elmer LS50 spectrofluorometer (excitation 400nm and emission 505nm) and is reported in units of caspase-3 activity/mg Ptn/hr. Corresponding caspase activity for samples were divided firstly by the obtained protein concentration (section 2.9.2) and then by 18 h, which was the incubation time of cell lysate with the fluorogenic substrate.

2.11.2 Detection of Chromatin Condensation by Hoechst dye #33342 Dye In AEC

AEC required for examination of apoptotic morphology labeled with 1 mg/ml stock solution of Hoechst #33342 dye which was diluted 100x with MilliQ water, producing a working dye concentration of 10 µg/ml and incubated at 37°C for 10 min. Fluorescence was visualised using a fluorescent microscope. Images displaying nuclear chromatin fragmentation were recorded to confirm that apoptosis had occurred.

2.11.3 Detection of the PC3 Protein and AC3 Protein Levels by Immunohistochemistry.

Caspase-3 protein expression was determined using the primary rabbit anti-human precursor 32kDa caspase-3 antibody and a primary rabbit anti-human active 17kDa caspase-3 antibody both of which were cross-reactive with mouse PC3 protein. Acetone-fixed cryostat lung sections of 8µm thickness were washed 3 times for 5 min each with a 2%BSA/PBS solution and incubated with a 1:250 dilution of the primary antibody overnight at 4°C. Visualisation was performed using a 1:100 dilution of a goat anti-rabbit fluorescein isothiocyanate (FITC)-conjugated secondary antibody for 1h at room temperature in humidified atmosphere. Negative controls lacked the primary antibody.

2.11.4 Co-localisation of PC3 Protein and Zn

In some experiments, dual staining was performed. After the PC3 protein immunostaining procedure was completed, sections were washed 3 times in PBS to remove excess secondary antibody and incubated sequentially with 25µM Zinquin

114

for 30 min at RT in dark and humidified conditions (as described in section 2.2). Sections were then re-washed in milliQ water and permanently mounted with fluorescent mounting medium.

2.11.5 Detection of a Caspase Cleavage Product of Cytokeratin 18 (CK18) by Immunohistochemistry.

To confirm apoptosis, the M30 Cytodeath Kit was used to detect cells which had undergone apoptosis in acetone-fixed cryostat sections of mice lung tissue. This kit uses a mouse IgG_{2b} monoclonal antibody which detects an epitope formed during the cleavage of CK18 by caspases in the early stages of apoptosis. The primary CK18 antibody was used at a final dilution of 1:50 and pipetted onto the tissue section which was then incubated for 18h at 4°C; an anti-mouse FITC-conjugated secondary antibody (gift of Dr C. Murgia, Institute for Food and Nutrition, Rome) was used at a dilution of 1:150 for 1h at 4°C in a humidified atmosphere. Negative controls lacked the primary antibody.

2.12 MURINE MODEL OF ALLERGIC AIRWAY INFLAMMATION

2.12.1 Animals Used

Specific pathogen free 6 week old female BALB/c mice were purchased from the University of Adelaide Animal Center, Adelaide, South Australia and fed New Joint Stock Ration Normal mouse food (Ridley Agri Products, South Australia, Australia). Animals were housed at 21°C with a 14-h light/10-h dark cycle.

2.12.2 Sensitisation and Aerochallenge of Female BALB/C Mice with Ovalbumin

Allergic inflammation was induced using the method of Xiong and colleagues, a protocol that produces an inflammatory process which is localised within the bronchi and the lungs. Mice were injected intraperitoneally (i.p) on days 1 and 12 with 50 µg of ovalbumin (OVA) per 1 ml of adjuvant alhydrogel in 0.9% sterile saline (Xiong et al., 1999). Saline treated mice (SAL) received alhydrogel in 0.9% sterile saline alone. Sensitised mice (OVA-treated) were then aerochallenged with 10 mg/ml of OVA in 0.9% saline from day 19 to day 29, 3 times a day for 30 min every second day using a RapidFlo nebuliser bowl which produced particles of 3-5 µm. SAL-treated mice were nebulised with 0.9% saline only. On day 30, mice (n = 10 per group) were bled by cardiac puncture and sacrificed by cervical dislocation for collection of tissues.

2.12.3 Collection of Blood

Mice were anesthetized and blood collected by performing a cardiac puncture using a 23 gauge needle connected to a 1 ml sterile syringe which was inserted into the apex region of the right ventricular wall. A drop of blood was immediately transferred to a clean glass slide and a blood smear created. Leukocyte differential counts were performed by staining the slide with May Grunwald and Giemsa solutions (section 2.3.5). Cells were identified by morphological criteria and a total of 800 leukocytes were quantified per mouse. To obtain serum, blood was collected and allowed to coagulate overnight at 4°C. Samples were centrifuged at 12,000g for 5 min at 4°C and the serum transferred into Eppendorf microtubes and stored at −20°C until tested.

2.12.4 Collection and Assessment of Bronchoalveolar Lavage Fluid (BALF) Inflammatory Cell Infiltration.

BALF samples were obtained from 5 mice per group. After anesthesia, the trachea was cannulated with a blunted $18^{1/2}$ gauge needle, lavage performed by perfusing the lungs twice with 1 ml of 1x HBSS (pH 7.4), fluid withdrawn into tubes and stored on ice. The total recovery volume of lavage collected was 1.7 ml which was then centrifuged at 600g for 5 min at 4°C. The supernatant was decanted and the cell pellet re-suspended with 500 µl of 1X HBSS and cytospin preparations were performed. Cells were stained with May Grunwald and Giemsa (stained by the department of haematology, IMVS, The Queen Elizabeth Hospital, Adealide) and using a 40x objective lens, a differential leukocyte count of a total of 800 cells per mouse was performed in duplicates using standard morphological criteria. A count of the number of cells at 40x magnification within 4 different field of view was performed and counts are expressed as total cells/ 40x field of view.

2.12.5 Processing of Mice Lung Samples

Tissues for histopathological assessment were collected 24h after the final aerosolisation. Animals were sacrificed as described above and blood from the pulmonary capillary bed eliminated by injecting 2 x 1 ml of 0.9% saline directly into the right ventricle. Lungs were then inflated using a blunted $18^{1/2}$ gauge needle into the trachea with 1 ml of 10% phosphate buffered formalin for paraffin sections or with OCT for cryostat sections, tied off with cotton thread and processed accordingly. After an overnight fixation with formalin, lung tissues representing the central (bronchi) and the peripheral (bronchioles) airways were horizontally sliced from the mid-zone of a single lobed lung and embedded in paraffin.

For frozen tissues, the entire lung was tied off, excised and sections of the trachea and lobes were quickly placed into plastic embedding trays containing OCT and snapped frozen in a glass beaker containing 50 mls of isopentane by liquid nitrogen. Frozen tissue blocks were stored at $-70°C$ until used for immunohistochemistry. When required, sections were cut at 8 μm thickness and allowed to adhere onto poly-L-lysine coated glass slides at room temperature for 20 min. Sections were fixed in 100%-chilled acetone for 10 min at $-20°C$ prior to tissue staining.

2.12.6 Assessment of Tissue Histology

Ribbons of 5 μm thickness from paraffin embedded lung tissues were cut from paraffin embedded blocks and stained with Charbol's chromotrophe haematoxylin (section 2.3.4) for identification of eosinophils, Weigert's Haematoxylin and van Gieson's (section 2.3.2) for collagen deposition, and alcian blue/ periodic acid-Schiff (section 2.3.3) for enumeration of mucin-secreting cells. Eosinophils and mucus-containing cells were identified by morphological criteria as described by Foster and colleagues (Foster et al., 1996).

Tissue eosinophils and mucus containing cells were examined and quantified using a 100x oil immersion and a 40x normal objective lens, respectively. Firstly, eosinophils were counted in the epithelium and subepithelial tissue ($2mm^2$ area directly beneath the epithelial basement membrane) in 6 airways of 3 different mice from both the SAL-treated and OVA-treated and are expressed as mean $\pm$ SEM eosinophils/High powered field (100xHPF). Secondly, mucus-containing cells were counted within 6 peripheral airway epithelium of 3 different

mice from both the SAL-treated and OVA-treated groups were quantified and are expressed as mean ± SEM mucus cells/HPF.

2.12.7 Assessment of IL-5 and IgE Levels

Levels of IL-5 in Serum and BALF

The Endogen Mouse Interleukin-5 (IL-5) ELISA kit was used to quantify IL-5 levels in BALF (neat) and serum (1:200 dilution) samples following the methods provided by the manufacturer. Reactions were performed in duplicate on 96-well anti-mouse IL-5 pre-coated ELISA plates. Optical density was read on a microplate reader at 450 nm and a standard curve generated by plotting the average absorbance intensity obtained for each of the standards on the vertical y-axis against the corresponding IL-5 concentrations on the horizontal x-axis. The resultant concentration was expressed as pg/ml.

IgE Serum and BALF levels

The murine OptIEA™ IgE ELISA kit was used to quantify IgE levels in BALF (neat) and serum (1:20 dilution) samples following the methods provided by the manufacturer. Reactions were performed on 96-well Nunc Maxisorp ELISA plates containing the samples and the murine IgE standards, performed in duplicates and absorbances were read on a microplate reader at 450 nm. The standard curve was generated by plotting the average absorbance intensity obtained for each of the standards on the vertical y-axis against the corresponding IgE concentrations on the horizontal x-axis. The resultant concentration was expressed as ng/ml.

2.12 STATISTICAL ANALYSIS

Data reported in this thesis are expressed as means ± standard error of the mean (SEM) unless otherwise stated. Where appropriate, the student t test was performed. Differences were considered statistically significant at $*p < 0.05$, $** p < 0.005$. For the animal experiments conducted in Chapter 6, results were analysed by the student t test and in some cases also interpreted using analysis of variance (ANOVA) with Tukey's post-hoc test using the General Linear Model on Minitab.

CHAPTER 3

VISUALISATION OF LABILE INTRACELLULAR ZINC IN RESPIRATORY EPITHELIUM

CHAPTER 3 VISUALISATION OF LABILE

INTRACELLULAR ZINC IN RESPIRATORY EPITHELIUM

3.1 INTRODUCTION

The airway epithelium participates in a range of functions which vary from acting as a physical barrier to the external environment to regulating the host defense mechanisms of the respiratory system by synthesizing and releasing mediators which participate in airway inflammation (Holgate, 2000). Continual exposure of this tissue to inhaled gaseous and particulate matter increases the epithelium's vulnerability to damage, which not only compromises its protective barrier function, but also leads to decreased production of smooth muscle relaxant factor and increased release of pro-inflammatory cytokines e.g. IL-6 and GM-CSF (Marini et al., 1992).

As previously discussed in Chapter 1, Zn is an essential cytoprotectant and biochemical regulator of many biological systems. Zn is especially important as an anti-oxidant, anti-inflammatory and anti-apoptotic agent able to influence the integrity and the growth and repair of epithelial tissues, especially in the skin and gastrointestinal tract (Agren, 1991; Elmes, 1977). It has been previously reported that epithelial and endothelial cells are highly sensitive to Zn since inadequate availability of Zn results in increased oxidative stress and enhanced rates of apoptosis in a range of organs (Nodera et al., 2001). However, to date the role of Zn in the respiratory epithelium has not yet been studied. As such, Zn may also act as an essential cytoprotectant against toxins and inflammatory mediators within the

respiratory tract tissues, in a similar way to that reported for the endothelium (Hennig et al., 1999; Hennig et al., 1992).

In order to understand the biochemical functions of Zn within the respiratory system it was necessary to first determine the localisation and distribution of labile intracellular Zn in a variety of respiratory cells and tissues. Taking into account that these cells are constantly exposed to inhaled particulate matter and therefore require adequate cytoprotection, it was hypothesised that REC contain an abundance of labile intracellular Zn within the cytoplasm

Hence the aim of the experiments described in this chapter was to determine the localization of labile intracellular Zn in the respiratory epithelium of pigs, sheep and humans using Zinquin, a novel Zn specific fluorophore developed by this department (Zalewski et al., 1993). As previously mentioned in section 1.13, Zinquin is a Zn specific fluorophore capable of entering cells to form UV-excitable fluorescent complexes with Zn in the nM to μM range thereby allowing for the visualisation and quantification of intracellular Zn without cellular disruption.

3.2 METHODS

3.2.1 Respiratory Cells and Tissues Used

For this study, respiratory tissues and primary ciliated AEC were obtained from pigs, sheep and human subjects and the methods to prepare these are

described in sections 2.1.1 and 2.1.2 for the animal AEC and section 2.2 for the human AEC.

3.2.2 Assessment of Histology

Tissues were stained with Haematoxylin and Eosin (H&E) for routine morphological assessment using the method described in section 2.3.1 and with Weigert's and Van Gieson for detection of collagen as described in section 2.3.2. Cells were prepared for electron microscopy (EM) as described in section 2.8.

3.2.3 Zinquin Studies

Cells and tissues were labeled with Zinquin as described in section 2.4. Intracellular Zn levels were manipulated in primary ciliated AEC using the Zn chelator TPEN and the Zn ionophore NaPYR as described in section 2.5. In order to better localise Zinquin fluorescence in AEC, UV laser confocal images were obtained as described in section 2.7.2. The gain settings on the camera were kept constant for all the Zinquin images taken for quantification purposes, unless otherwise mentioned in the text. Quantification of Zinquin fluorescence in tissues was determined by using the image analysis program Video Pro™ (section 2.7.3).

There were insufficient sections of sheep trachea to do multiple analyses hence tissues from pig were also used. Autofluorescence determinations were made on a separate set of images derived from sections incubated without Zinquin. Zinquin fluorescence was expressed as GSU (0-255) $\pm$ S.E.M. The level of statistical significance was determined by the Student's unpaired t-test.

3.3 RESULTS

3.3.1 Zinquin Fluorescence is Higher in the Airway Epithelium than in the Alveolar Epithelium

Zinquin fluorescence was examined in frozen sections of pig and sheep tracheobronchial and alveolar tissue. A total of 6-8 images from sections of pig and sheep trachea and bronchiole were quantified and background fluorescence was subtracted to give the specific Zinquin fluorescence.

Figure 3.1 is a montage of images of pig and sheep respiratory epithelium. Panels A and B are corresponding bright field and UV fluorescence images of pig trachea treated with PBS only (no Zinquin) and therefore act as autofluorescence controls. Autofluorescence was largely confined to the walls of blood vessels (not shown) and to the lamina propria where it was co-localized with collagen (*, panel B). This was confirmed by using a microscope with polarised lenses and by staining with Weigert's Haematoxylin and van Gieson's stain. The presence of collagen is shown by the bright red staining under the basement membrane where the autofluorescence was most prominent (panel C). The autofluorescence within the lamina propria was more prominent in areas where collagen was more densely packed and organised, particularly in the bronchi and bronchiolar regions of pig, when compared with trachea or sheep tissues. Importantly, there was no autofluorescence in the epithelia of any of the sections examined.

Panel D & E, which are not serial sections, show typical H&E stained and Zinquin fluorescence images, respectively, of frozen sections of pig trachea. The pseudostratified, ciliated epithelium was lined, continuously, at the luminal surface

Figure 3.1: Zinquin Fluorescence in Cryostat Sections of Pig and Sheep

Figure shows the intense lumenal Zinquin fluorescence in cryostat sections of pig and sheep bronchi and trachea.

Panel A: Bright field image (panel A) of unlabelled pig trachea (negative control). White arrow in panel A depicts the lumenal surface of the epithelium. Black double headed arrow shows the area in which collagen is deposited in the lamina propria of pig trachea. 500x initial magnification.

Panel B: Corresponding UV image of unlabelled pig trachea. The fluorescence seen in the lamina propria (*) is UV autofluorescence due to abundance of collagen below the basement membrane (BM). Note the lack of autofluorescence in the epithelium of pig trachea (arrowed). 500x initial magnification.

Panel C: Weigert's Haematoxylin and van Gieson's staining of pig bronchi. Collagen was stained brightly red, while smooth muscle and other cytoplasmic proteins were stained a brown/yellow colour. Note the abundance of collagen below the BM (*). 500x initial magnification.

Panel D: Pseudostratified columnar ciliated epithelium (EP), basement membrane (BM) and lamina propria (LP) of pig trachea stained with H&E. 500x initial magnification.

Panel E: Zinquin fluorescence image of pig trachea (similar orientation to panel D but this is not a serial section of D). Image depicts a continuous concentration of labile Zn along the luminal surface (arrowed) of the epithelium. 500x initial magnification.

Panel F & G: Corresponding bright field image (panel F) of Zinquin-labelled pig bronchi (panel G). Note the similar luminal distribution of Zinquin fluorescence. The fluorescence in the lamina propria (*) is UV autofluorescence due to abundance of collagen below the BM. Autofluorescence was never seen in epithelium of any species. 500x initial magnification.

Panel H: High magnification image of Zinquin fluorescence in the apical region of the pig bronchi. 2500x initial magnification.

Panel I & J: Zinquin fluorescence in sheep trachea (H) and sheep bronchi (I). A similar pattern of Zinquin fluorescence was noted in sheep epithelium. Note the autofluorescence (*) in the lamina propria. 500x initial magnification.

A

B Autofluorescence (500x)

C Pig Trachea (500x)

D EP BM LP Pig Trachea (500x)

E Pig Trachea (500x)

F Pig Bronchi (500x)

G Pig Bronchi (500x)

H Pig Bronchi (2500x)

I Sheep Trachea (500x)

J Sheep Bronchi (500x)
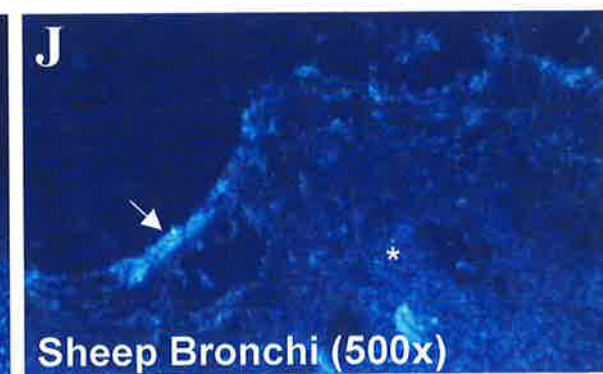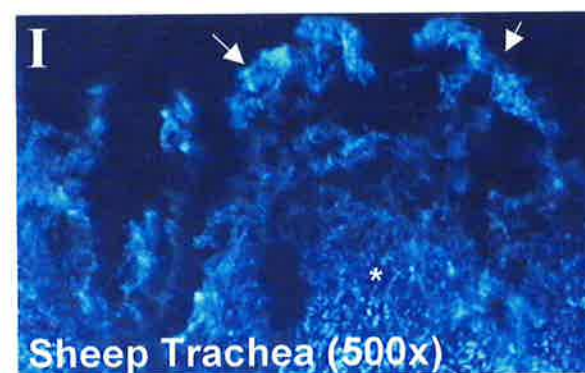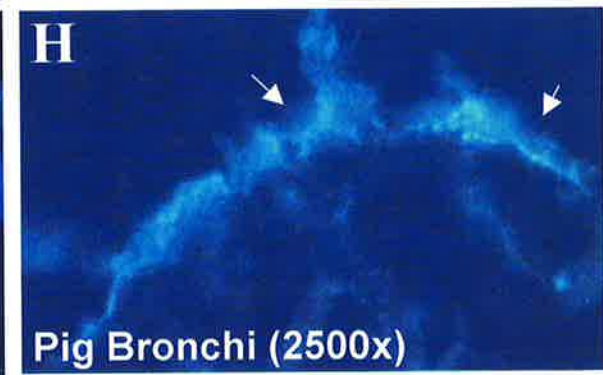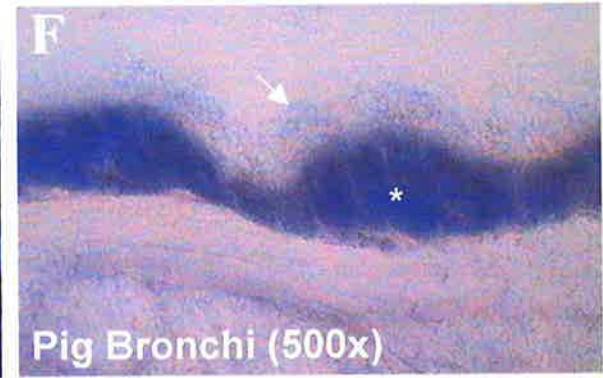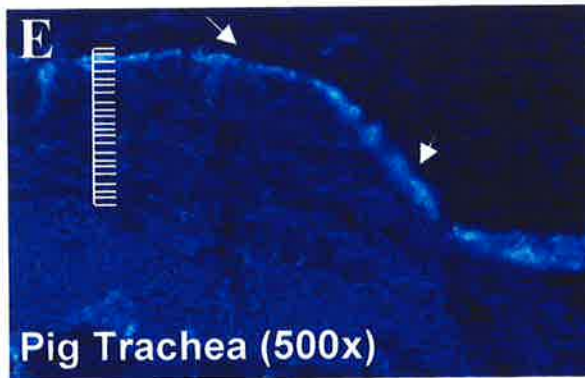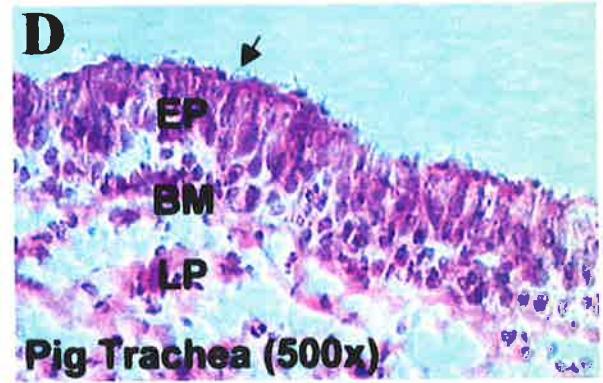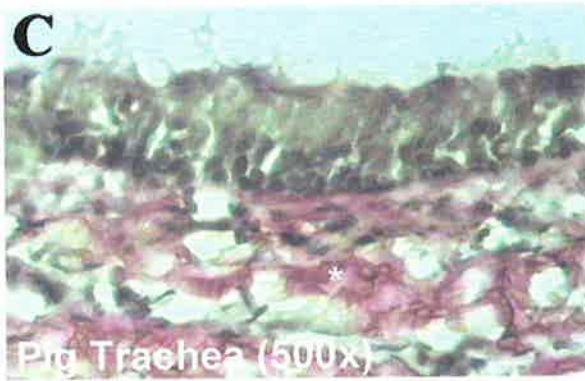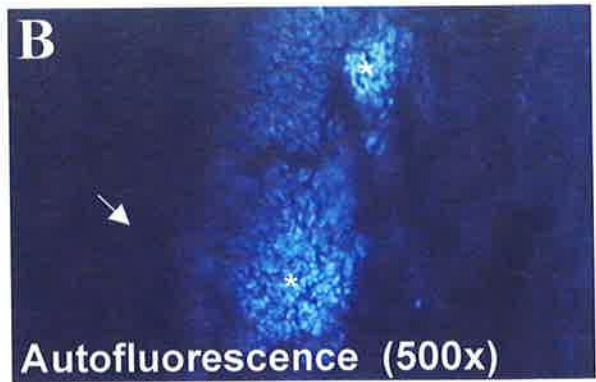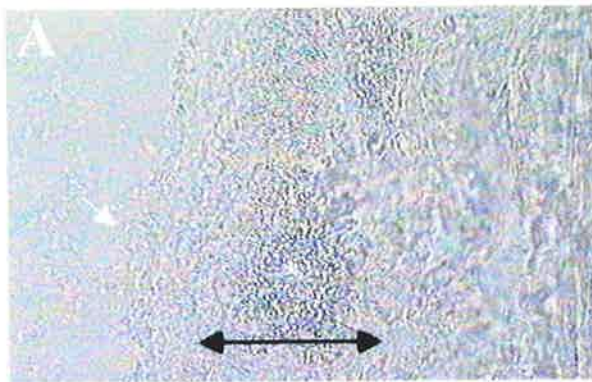
(arrow) by a region of intense Zinquin fluorescence (panel E). This luminal distribution of Zinquin fluorescence was also noted in pig bronchi (panel G). Note again the autofluorescence in the lamina propria (*). Panel H shows a representative section from pig bronchi at a higher magnification, and reveals the striking demarcation between the labile Zn-rich outer area and the relatively Zn-poor middle to inner layers of the epithelium. Similar patterns were observed with sheep trachea (panel I) and bronchi (panel J) where there was intense Zinquin fluorescence at the luminal surface. As noted in the pig respiratory tissues, there was significant autofluorescence within the region of collagen deposition (*, Figure 3.1I).

The alveolar epithelium in both pig (Figure 3.2, panel B) and sheep (Figure 3.2, panel D) had a typically dull Zinquin fluorescence when compared to the bright fluorescence noted in pig trachea (panel F). No distinction in fluorescence was evident between the type I and II epithelial cells.

3.3.2 Quantification of Zinquin Fluorescence Across Respiratory Epithelial Tissue

Figure 3.3 shows a compilation of data from all of the cryostat sections analysed.

Panel A shows the pooled mean data for the two pig trachea (n = 56 profile measurements). This graph shows the specific Zinquin fluorescence, after subtraction of the background readings which were negligible (lower panel). The highest Zinquin fluorescence intensities were recorded in the apical region which is between the 1st and the 5th intervals (from 0% to 12.5% of the epithelial width

125

Figure 3.2: Zinquin Fluorescence in Alveolar and Tracheal Tissue

Panel A, C, E are bright field light images of pig (A) and sheep (C) alveolar tissue and pig trachea. Panels B, D & F are the corresponding Zinquin fluorescence images. Note the weak Zinquin fluorescence noted in the alveolar epithelial tissue when compared with the high fluorescence seen in pig trachea (F). No differences in fluorescence distribution was evident between the type I and II epithelial cells. 500x initial magnification.

Bright Field

Zinquin Fluorescence
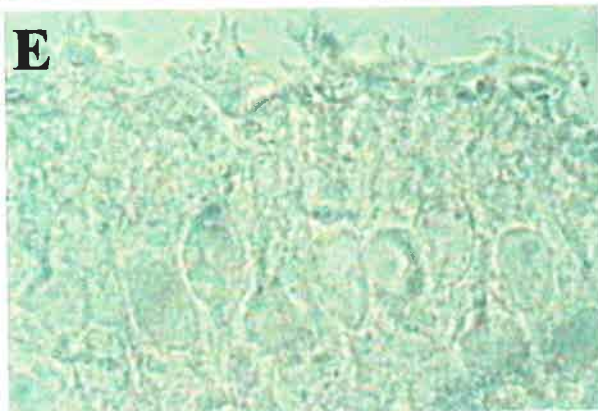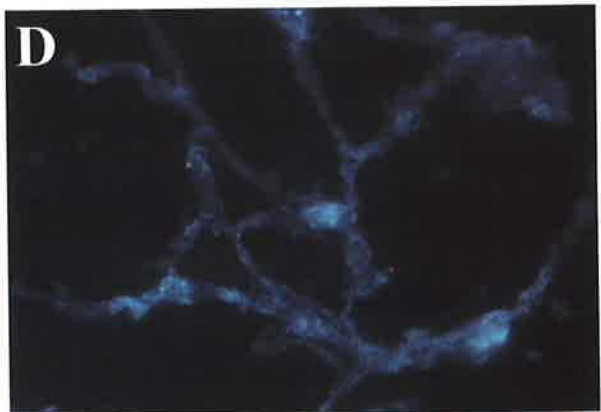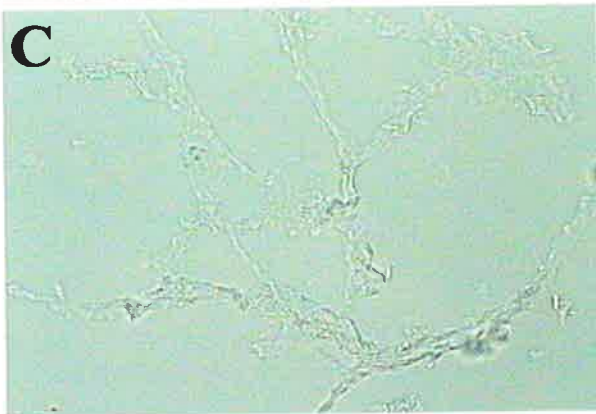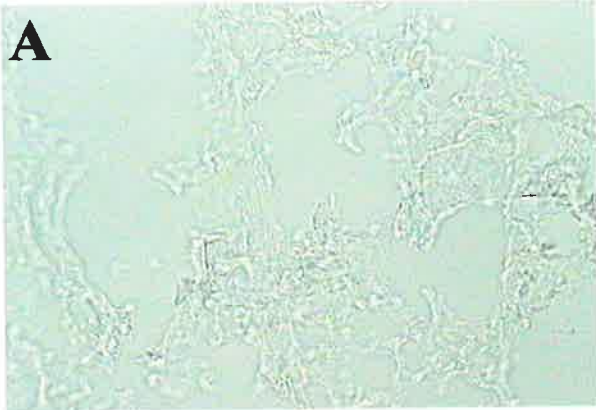
Figure 3.3: Quantification of Zinquin Fluorescence Across Respiratory Epithelium

Figure shows pooled data expressed as mean fluorescence intensity for each of 40 evenly-spaced intervals spanning the epithelia from the luminal surface (relative position 0) to the basement membrane (relative position 1). Bars indicate standard error of mean. Data were collated for several images from different sections and from at least two different animals. Upper segment of each panel shows specific Zinquin fluorescence while lower segment shows autofluorescence (no Zinquin added).

Panel A: Pig trachea (n = 56 profile measurements).

Panel B: Pig bronchiole (n = 35).

Panel C: Sheep bronchiole (n = 28).

Far right upper column in B and C show corresponding mean specific Zinquin fluorescence intensities for alveolar epithelium from pig (n = 72 measurements) and sheep (n = 45), respectively, while lower columns show corresponding mean autofluorescence intensities.

A

Pig Trachea
Specific Zinquin Fluorescence

37.7 ± 5.4

17.6 ± 0.8

Autofluorescence

B

Pig Bronchiole
Specific Zinquin fluorescence

37.6 ± 1.9

16.1 ± 2.9

Autofluorescence

Pig Alveolar Epithelium

12.6 ± 1.6

C

Sheep Bronchiole
Specific Zinquin Fluorescence

21.7 ± 4.3

7.9 ± 0.7

Autofluorescence

Sheep Alveolar Epithelium

7.0 ± 0.4

Zinquin Fluorescence Intensity (GSU)

Relative position within the epithelium

0.25   0.5   0.75   1.0

inward from the surface). For quantitative purposes, it was noted that most of the Zinquin fluorescence was contained within the first 7 intervals (corresponding to the outer 17.5% of the epithelium) and hence fluorescence data from these intervals were collated to give an average mean ± SEM apical fluorescence intensity of 36.7 ± 5.4 GSU. The remaining portion was found to contain an average of 17.6 ± 0.8 GSU (n = 77 profile measurements). The autofluorescence of pig trachea (lower panel of A) was 2.9 ± 0.6 (n = 43). Panel B shows similar data for the pig bronchiole having an apical fluorescence of 37.6 ± 1.9 GSU, while the basal region had 16.1 ± 2.9 GSU (n = 35). The autofluorescence was 0.7 ± 0.6 (n = 43). A similar pattern was observed in panel C for sheep bronchiole (n = 77) where the Zinquin fluorescence quantified in the apical and basal regions were 21.7 ± 4.3 GSU and 7.9 ± 0.7 GSU, respectively. The autofluorescence for this tissue was 0.5 ± 0.3 GSU (n = 43).

For comparison, the corresponding intensities for alveolar epithelium of pig and sheep are shown in the far right panels of B (12.6 ± 1.6 GSU) and C (7.0 ± 0.4 GSU), respectively (pig; n = 72, sheep; n = 45). Autofluorescence intensities for these alveoli tissue were also insignificant, while the Zinquin fluorescence intensities were similar to those in the labile Zn-poor regions of the bronchiolar epithelium (Figure 3.3 lower panel B & C).

3.3.3 Zinquin Fluorescence is Localised in an Apical Manner in Primary Ciliated AEC

Figure 3.4 shows a transmission electron micrograph of a typical sheep tracheal ciliated AEC (processed as described in section 2.8) showing the presence of cilia, basal bodies and mitochondria in the apical region of the cell.

Primary cells were incubated with 25 μM Zinquin as wet suspensions and fluorescence analyzed by fluorescence image analysis. No autofluorescence was seen in cells incubated with PBS alone. Figure 3.5 shows a montage of typical images of bright field (panel A & B) and Zinquin fluorescence (C to J) in Zn manipulated pig (LHS) and sheep (RHS) epithelial cells. Panel C & D show the Zinquin fluorescence of cells which were not Zn manipulated and are the corresponding light images of panel A & B, respectively. An apical fluorescence was seen in the cytoplasm below the cilia (white arrowheads) and in some cells, Zinquin fluorescence was also concentrated within the basal bodies of the cilia (yellow arrowheads). This apical pattern is consistent with the Zinquin fluorescence observed in the cryostat tracheobronchial tissue sections.

To confirm that the Zinquin fluorescence of these cells was Zn-dependent, the effect of the Zn chelator TPEN on Zinquin fluorescence was determined. Cells were incubated with 25 μM Zinquin in the presence or absence of 6.25 μM TPEN to create a mild Zn deficiency. Zinquin fluorescence was strongly reduced by TPEN as seen in panel E & F. Next, a dramatic increase in Zinquin fluorescence was noted when cells were Zn supplemented with 1 μM of the Zn ionophore NaPYR and 25 μM $ZnSO_4$ (panel G & H). In order to determine which compartments of the cells have been most affected by this supplementation, it was

127

Figure 3.4: Electron Micrograph of Isolated Sheep Tracheal Ciliated Epithelial Cells

Figure shows a ciliated epithelial cell, still joined to its neighbours by desmosomes (D), with the typical abundance of mitochondria (M) and basal bodies (B) in the apical cytoplasm. Axonemes of cross-section of cilia are also evident (Ax). Scale bar indicates 1 µm.
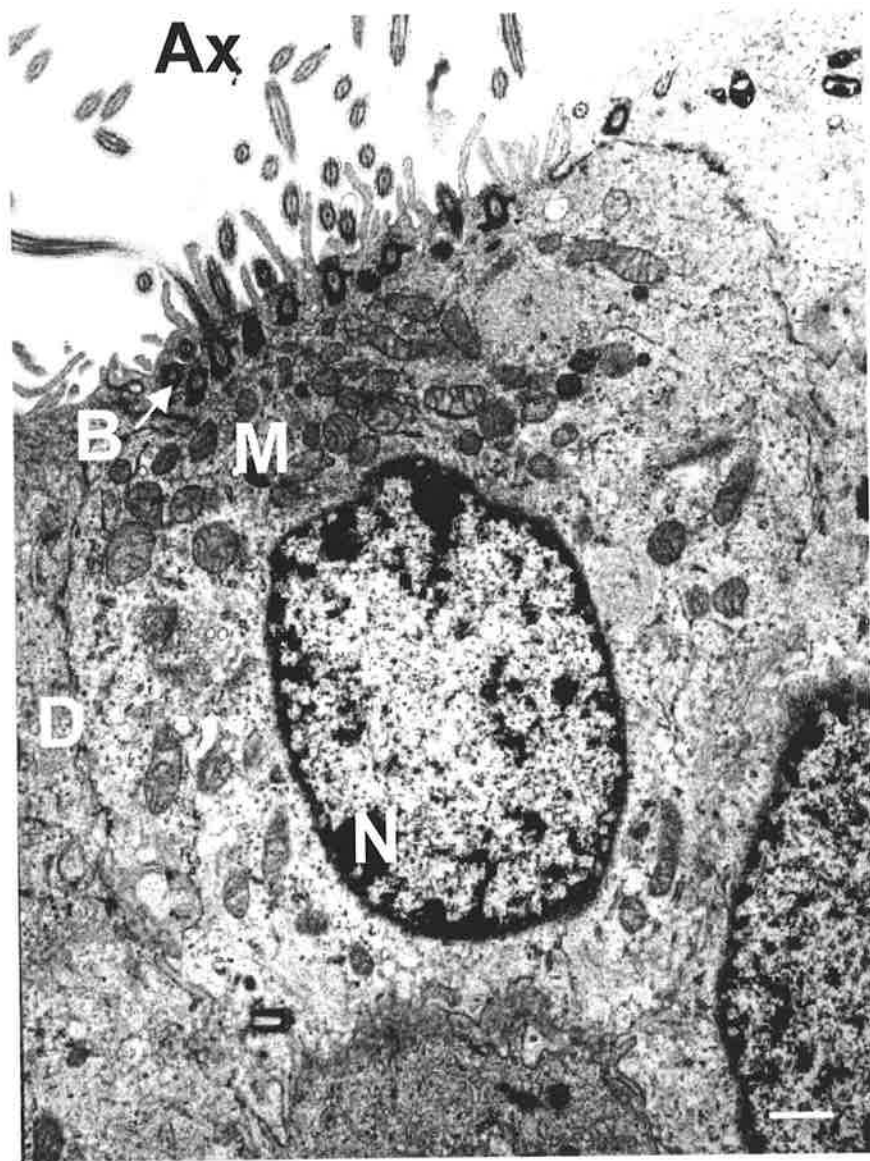
Figure 3.5: Localisation of Zinquin Fluorescence in Primary Pig and Sheep Tracheobronchial Cells

Epifluorecence images of isolated primary pig (left panels) and sheep (right panels) tracheobronchial epithelial cells showing labile Zn distribution as detected by the intense apical distribution of Zinquin fluorescence. Typical images are shown. White arrows depict cilia of cells.

Panel A & B: Bright field images corresponding to Zinquin fluorescence in panels C & D, respectively. 1000x initial magnification.

Panel C & D: Zinquin fluorescence of untreated tracheobronchial ciliated AEC showing apical fluorescence in the cytoplasm, cilia (white arrows) and in some cells, distinct fluorescence within basal bodies of cilia (yellow arrows). 1000x initial magnification.

Panel E & F: Zinquin fluorescence was quenched when AEC were pre-incubated with 6.25 μM of TPEN. 1000x initial magnification.

Panel G & H: Marked increases in Zinquin fluorescence was noted in Zn supplemented AEC incubated with exogenous Zn using 25 μM $ZnSO_4$ and 1 μM of NaPYR. 1000x initial magnification. Scale bar in panel H represents 10 μm.

Panel I & J: Higher magnification images of Zn supplemented cells. A lower gain setting was used in order to increase the resolution of Zinquin fluorescence. Zn supplementation resulted in enhanced Zinquin fluorescence in the same apical region. 2500x initial magnification. Scale bar in panel J represents 7 μm.

	Pig	Sheep
Light		
Normal ZQ^n		
TPEN Treated		
Zn + NaPYR Treated		
Zn + NaPYR Treated		
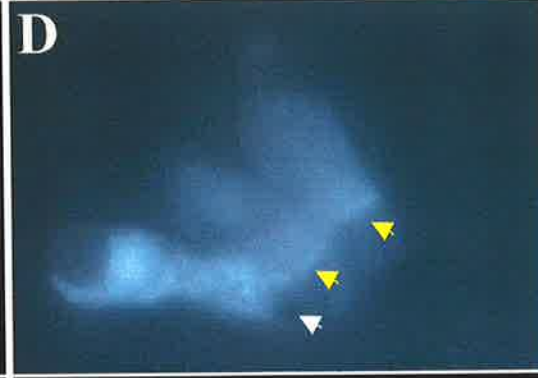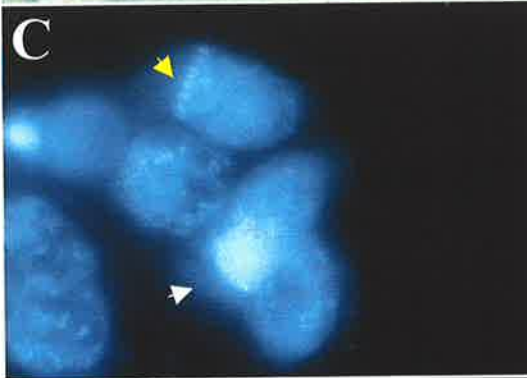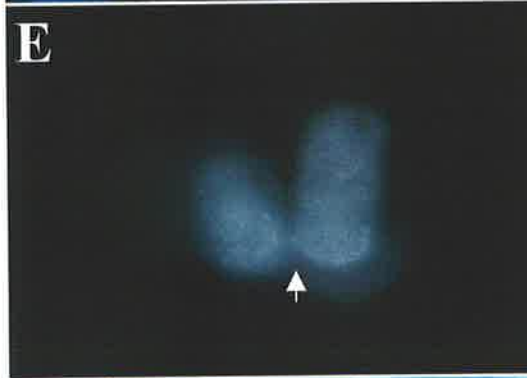
10 μm

7 μm
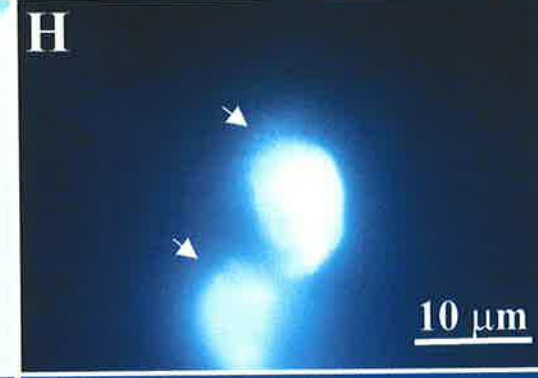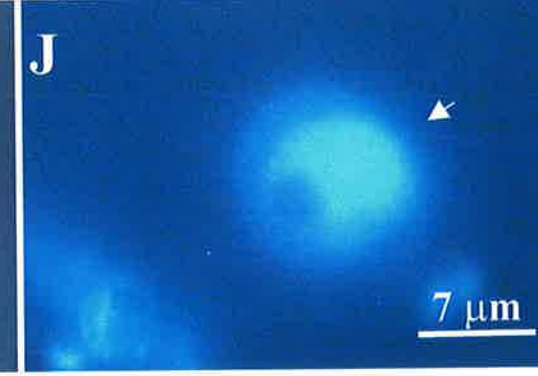
necessary to decrease the gain setting of the camera control unit. This is shown in panels I & J at a higher final magnification where intense fluorescence was still compartmentalised within the apical region. The increases in fluorescence were seen both in the region containing basal bodies (I) and in a more diffuse and perinuclear pattern (J). However, there were no differences in the Zinquin patterns between the two species used. Thus a decrease in labile intracellular Zn decreases Zinquin fluorescence, while an increase in intracellular Zn results in an increase in Zinquin fluorescence.

3.3.4 Quantification of Zinquin Fluorescence in Primary AEC

In order to quantify levels of intracellular labile Zn, 40 to 70 tracheal epithelial cells from each group were examined at high magnification using a 100x oil immersion lens, images captured and fluorescence intensity quantified by image analysis (see section 2.7.3) as reported in Figure 3.6. Firstly, in the absence of TPEN, mean basal fluorescence ($\pm$ SEM) intensity was 46.9 $\pm$ 4.9 GSU in pig and 46.5 $\pm$ 9.5 GSU in sheep cells. 6.25 μM TPEN decreased Zinquin fluorescence to 26.0 $\pm$ 10.0 GSU in pig and 27.7 $\pm$ 3.7 GSU in sheep, respectively (p < 0.005). A higher concentration of TPEN (25 μM) further lowered fluorescence to 11.7 $\pm$ 8.6 GSU in pig and 16.1 $\pm$ 1.6 GSU in sheep, respectively. Further increasing the concentration of TPEN in sheep epithelial cells did not completely remove all the labile Zn present in these cells. Sheep AEC treated with 50 μM TPEN had a fluorescence of 9.4 $\pm$ 0.6 GSU while cells exposed to 100 μM TPEN had a fluorescence of 11.0 $\pm$ 0.9 GSU. Therefore, maximal reduction of Zinquin fluorescence by TPEN can be achieved when using concentrations within the range of 6.25 μM to 25 μM. Zinquin fluorescence was substantially increased by

Figure 3.6: Changes in Zinquin Fluorescence in Zn Manipulated Primary Pig and Sheep Tracheobronchial Epithelial Cells

Zinquin fluorescence was measured by image analysis in primary pig (filled columns) and sheep (unfilled columns) ciliated AEC. Data represents means ± SEM in 40-100 cells per group and is expressed as grey scale units (GSU). Two TPEN concentrations were used since the aim was to create both a mild (6.25 μM TPEN) and a more severe (25 μM TPEN) level of Zn deficiency in these cells. Zinquin fluorescence was increased in AEC treated with 25 μM $ZnSO_4$ and 1 μM NaPYR. Statistical analysis was performed by unpaired student t test. Comparisons were made between cells from the same species and between basal and different treatments.
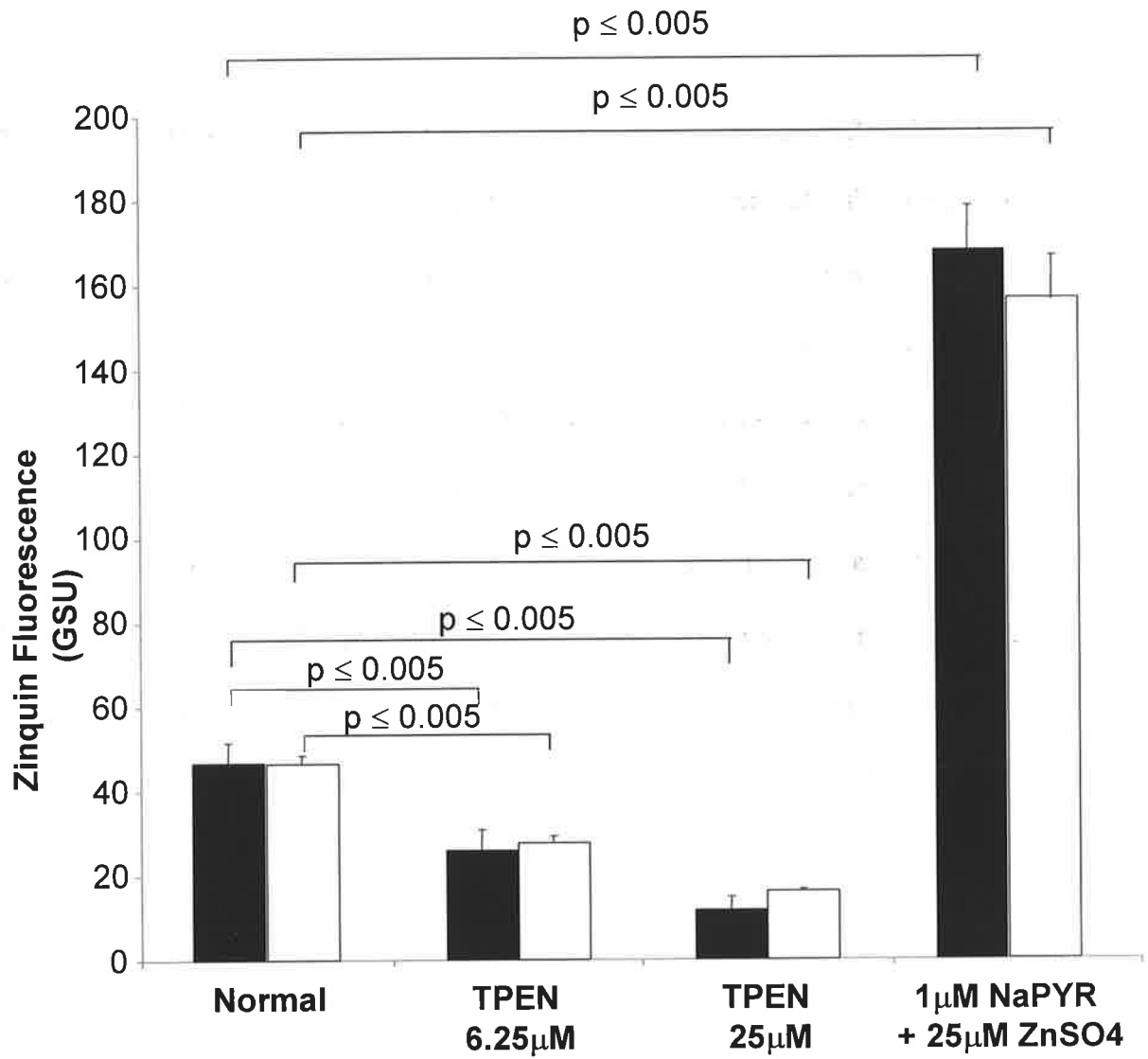
preloading of the cells with exogenous Zn, using 25 µM $ZnSO_4$ and 1 µM of NaPYR (Figure 3.6). Zinquin fluorescence increased to 167.8 ± 45.0 GSU in pig and 156.4 ± 14.5 GSU sheep.

3.3.5 Standard Curve for Zinquin Fluorescence in Mouse Splenocytes

In order to convert Zinquin fluorescence to intracellular Zn concentrations [Zn^{2+}], it was essential to have a standard curve which could be applied to a range of different cells and tissues. For this section, intracellular Zn will be referred to as [Zn^{2+}] since the aim was to deduce a Zn concentration for the Zinquin fluorescence recorded by constructing a standard curve. Mouse splenocytes were chosen for this task for the following three reasons. Firstly, it is known that these cells contain a very low basal level of Zinquin fluorescence. This was useful as there was a very low background noise prior to loading cells with $ZnSO_4$, allowing for accurate quantification of increasing increments in Zinquin fluorescence. Secondly, these cells have a relatively homogeneous pattern of Zinquin fluorescence and, thirdly, splenocytes are readily available in large numbers and are easily harvested.

Freshly isolated mouse splenocytes were incubated with 1 µM of NaPYR and with increasing extracellular concentrations of $ZnSO_4$ within the range of 0-50 µM. This range is typical of Zn^{2+} concentrations found within extracellular fluids such as plasma. NaPYR was used to rapidly equilibrate [Zn^{2+}] concentrations between the extracellular and intracellular environment across the plasma membrane. The standard curve was constructed by plotting the Zinquin fluorescence (GSU) against the standard [Zn^{2+}] concentrations loaded within the splenocytes. Figure 3.7 illustrates the proportional increase in intensity of Zinquin

Figure 3.7: Construction of a Zinquin Fluorescence Standard Curve

Splenocytes were used in this study since they have low basal levels of Zinquin fluorescence and they are readily available in large numbers. Mouse splenocytes were loaded with increasing concentrations of $ZnSO_4$ (0-50 µM, as indicated in the figure) using 25 µM $ZnSO_4$ and 1 µM NaPYR. Images were captured using a 100x oil immersion objective lens and typical images are shown. A and L represent corresponding bright field images. Note the increase in fluorescence intensity and its vesicular nature. Scale bar represents 7 µm.

A. 0 μM B. 0 μM C. 0.625μM D. 1.25μM E. 2.5 μM F. 5 μM G. 10 μM H. 15 μM I. 20 μM J. 25 μM K. 50 μM L. 50 μM
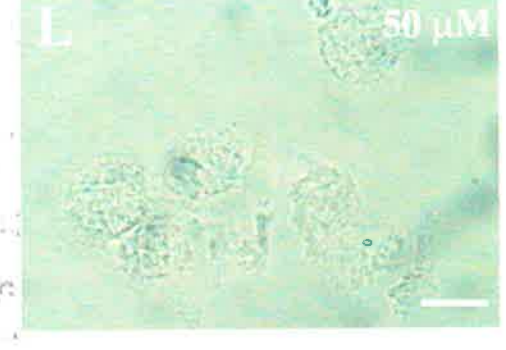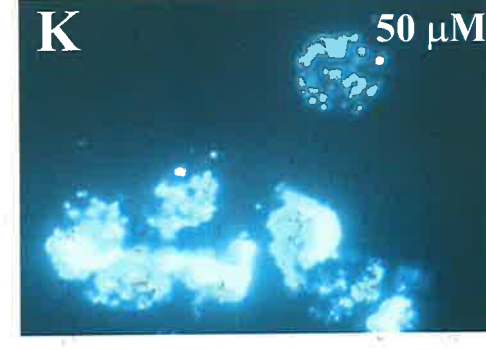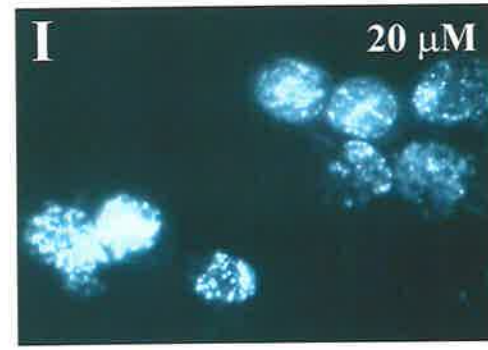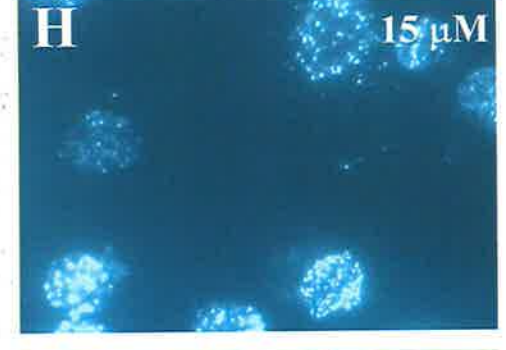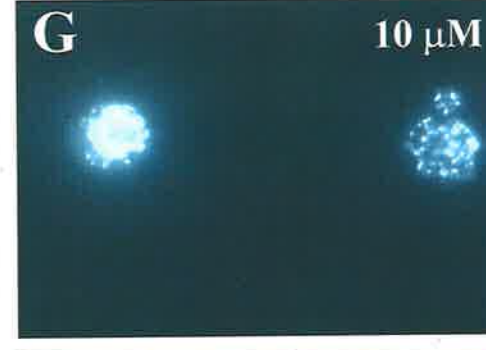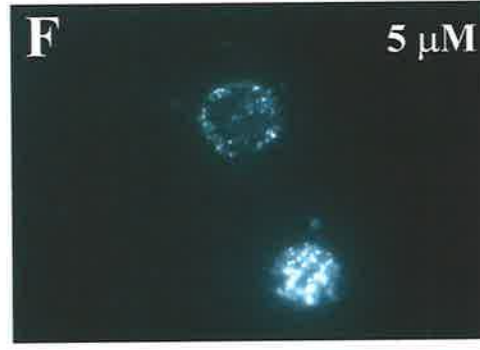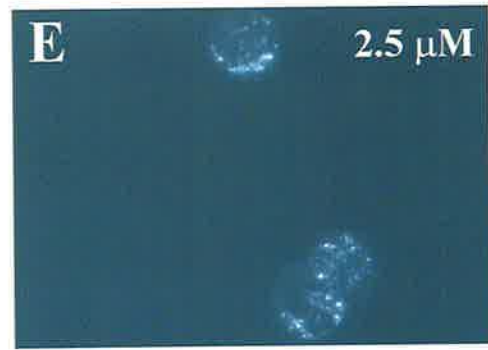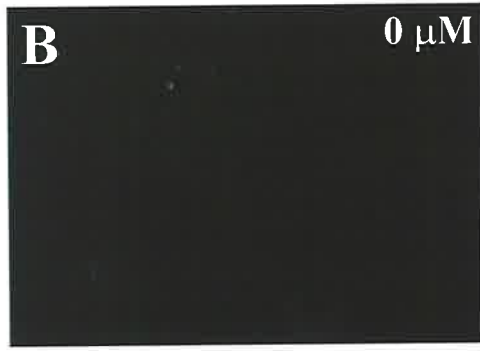
fluorescence with the concentration of exogenously added [Zn^{2+}]. Of particular interest, this Zn was compartmentalized within vesicles, the numbers and size of which were increased with greater Zn loading.

Figure 3.8 shows the standard curve generated from this experiment where the calculated regression equation was $y = 5.63x$ ($r^2 = 0.92$). "y" is the Zinquin fluorescence intensity expressed as GSU and "x" is the [Zn^{2+}] μM. This equation was then used to determine the approximate concentration of [Zn^{2+}] within cells and tissues labeled with Zinquin.

[Zn^{2+}] concentrations in the cryostat tissue sections ranged from 1.2 ± 0.1 μM in sheep alveolar epithelium to 6.7 ± 0.4 μM in the apical region of the pig bronchi epithelium. For the isolated primary ciliated AEC, [Zn^{2+}] concentrations were 8.3 ± 0.9 μM for the pig and 8.3 ± 0.4 μM for the sheep. These decreased by 75% to 2.1 ± 0.6 μM for the pig and by 65% to 2.9 ± 0.1 μM for the sheep when AEC were treated with 25 μM TPEN. Zinquin fluorescence increased by 360% to 29.8 ± 2.0 μM in the pig and by 335% to 27.8 ± 2.0 μM in the sheep when AEC were treated with 25 μM $ZnSO_4$ and 1 μM NaPYR. A summary of Zinquin fluorescence and the corresponding Zn concentrations are presented for pig and sheep respiratory tissues and cells in Table 3.1.

3.3.6 Localisation of Zinquin Fluorescence in Primary Ciliated AEC by UV Laser Confocal Microscopy

For qualitative purposes, UV laser confocal microscopy was also performed on these cells to determine whether an increase in resolution of the

Figure 3.8: Standard Curve of Zinquin Fluorescence in Mouse Splenocytes

Zinquin fluorescence (GSU) was quantified from 200 cells per concentration of $ZnSO_4$ from images taken with a 20x objective lens (typical images at 100x objective lens magnification are shown in Figure 3.2). The curve was approximately linear up to 25 μM $ZnSO_4$. This curve was used to convert fluorescence to intracellular Zn concentrations (μM). The data represents means ± SD.
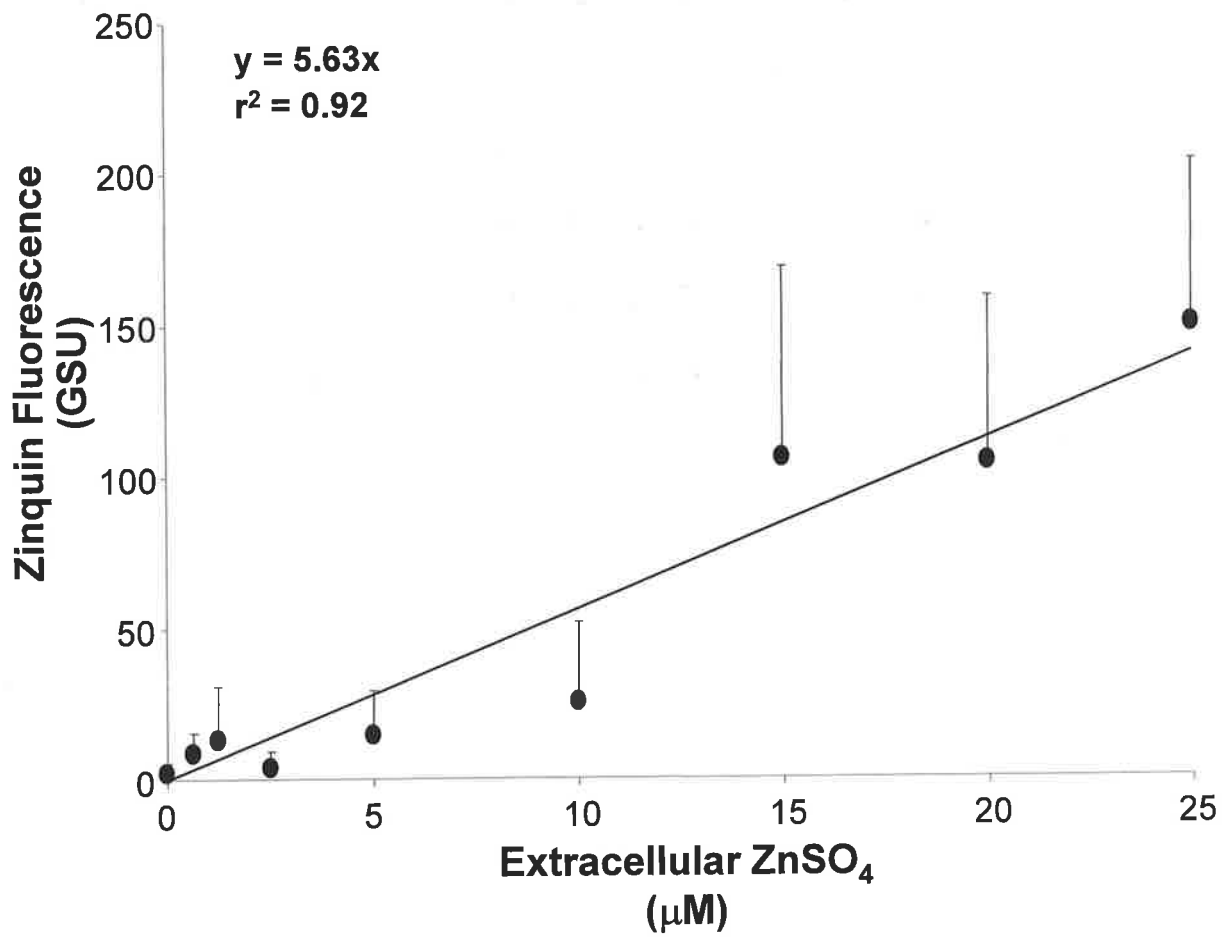
Table 3.1: Summarised Results of Zinquin Fluorescence and Corresponding Zn Concentrations in Airway Epithelial Tissues and Cells

Species	Tissue Type	Zinquin Fluorescence (GSU)	Zn Concentration (μM)
Pig	**Trachea** *Apical Region*	36.7 ± 5.4	6.5 ± 1.0
	Trachea *Basement Membrane Region*	17.6 ± 0.8	3.1 ± 0.1
	Bronchi *Apical Region*	37.6 ± 1.9	6.7 ± 0.4
	Bronchi *Basal Region*	16.1 ± 2.9	3.0 ± 0.5
	Alveolar Tissue *Epithelial cells*	12.6 ± 1.6	2.2 ± 0.3
	Isolated Epithelial Cells	46.9 ± 4.9	8.3 ± 0.9
	Isolated Epithelial Cells *+ TPEN 6.25 μM*	26.0 ± 10.0	4.6 ± 0.9
	Isolated Epithelial Cells *+ TPEN 25 μM*	11.7 ± 8.6	2.1 ± 0.6
	Isolated Epithelial Cells *+ NaPYR 1μM + 25 μM ZnSO$_4$*	167.8 ± 45.0	29.8 ± 2.0
Sheep	**Bronchi** *Apical Region*	21.7 ± 4.3	3.9 ± 0.8
	Bronchi *Basal Region*	7.9 ± 0.7	1.4 ± 0.1
	Alveolar Tissue *Epithelial cells*	7.0 ± 0.4	1.2 ± 0.1
	Isolated Epithelial Cells	46.5 ± 9.5	8.3 ± 0.4
	Isolated Epithelial Cells *+ TPEN 6.25μM*	27.7 ± 3.7	4.9 ± 0.3
	Isolated Epithelial Cells *+ TPEN 25μM*	16.1 ± 1.6	2.9 ± 0.1
	Isolated Epithelial Cells *+ NaPYR 1μM + 25 μM ZnSO$_4$*	156.4 ± 14.5	27.8 ± 2.0

subcellular distribution of Zinquin fluorescence could be achieved. For this experiment, bright-field images and their corresponding fluorescence images were captured. Autofluorescence was negligible at the fluorescence gains used to capture the images.

Figure 3.9 is a collection of UV laser confocal images of Zinquin fluorescence in pig (panel A to F) and sheep (panel G to J) tracheobronchial AEC. Fluorescence images have been pseudo-coloured, where white indicates highest Zn content, followed by magenta and then by black (no fluorescence). These images were captured approximately half way through the thickness of the cells and cilia are depicted by arrows. Typical images were obtained from different pigs and sheep and representative cells are displayed. The images confirm the findings which were obtained with epi-fluorescence; Zn was concentrated within the apical cytoplasm immediately beneath the cilia (panel D, F, H & J) and in some cases in a perinuclear manner (panel F, H & J). This apical distribution of Zinquin fluorescence was a consistent feature in greater than 95% of all ciliated cells examined in both pig and sheep. In addition to Zinquin fluorescence in the apical cytoplasm, some fluorescence was also evident within the cilia themselves (e.g. arrowed in panels D, F, H & J).

3.3.7 Zinquin Fluorescence in Primary Human Ciliated AEC

Zinquin distribution was determined in human AEC obtained from patients undergoing bronchoscopy. Cells were collected either as brushings, which were taken from regions which appeared morphologically healthy, or as bronchoalveolar lavage washes with sterile saline. Bronchial AEC collected from bronchial brushings are shown in Figure 3.10 panels A, B, C, D, E & F, while AEC collected

Figure 3.9: UV Laser Confocal Imaging of Zinquin Fluorescence in Isolated Primary Pig Ciliated Tracheobronchial Epithelial Cells

UV laser confocal images of isolated primary pig (panel A to F) and sheep (panel G to J) tracheobronchial epithelial cells showing labile Zn. Panel B is the negative control showing lack of autofluorescence in primary pig epithelial cells. Left hand side panels depict bright field transmission images. Right hand side panels depict Zinquin fluorescence as pseudocoloured images where white indicates highest Zinquin fluorescence followed by magenta then black. Zinquin fluorescence was most intense in the apical region beneath the cilia of epithelial cells (panel D, H & J) and in some cases existed in a perinuclear manner (panel F, H & I). Typical images are shown. Arrows depict cilia of cells. Scale bar indicates 10 μm.

Bright Field

Zinquin Fluorescence
(Pseudocoloured)

Pig
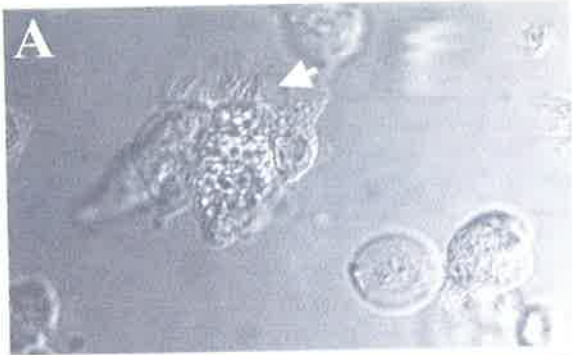
Pig

Pig

Sheep

Sheep

10 µm
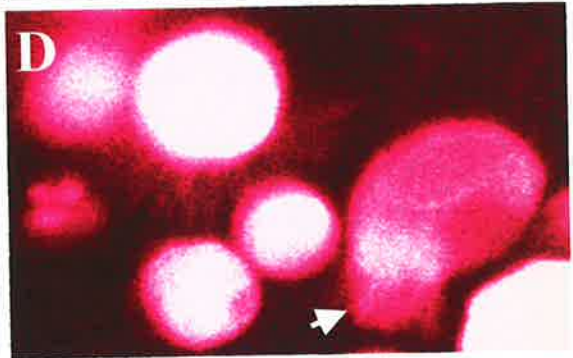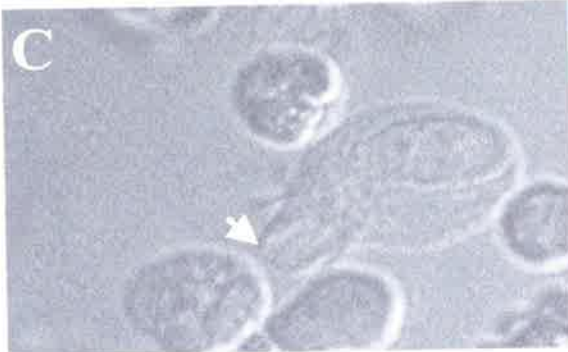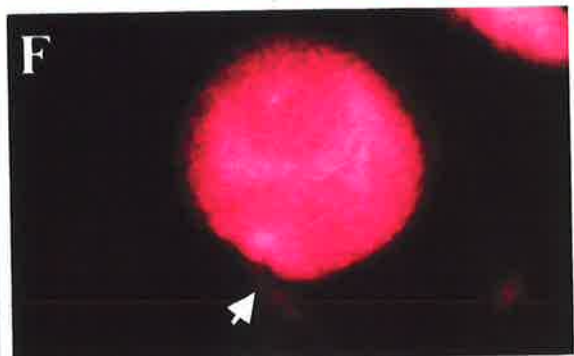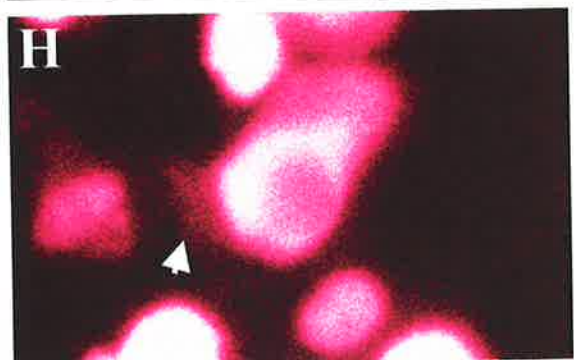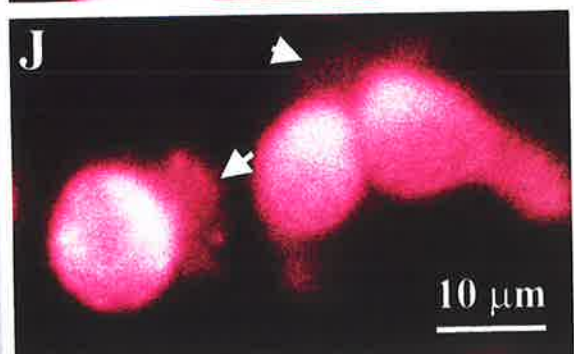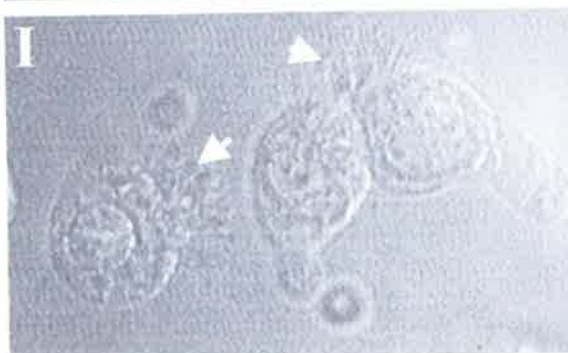
Figure 3.10: Localisation of Zinquin Fluorescence in Primary Human Ciliated AEC

Bright field images are illustrated on the left hand side (LHS panels A, C, E & G). These correspond to the Zinquin epifluorescence images shown on the right hand side (RHS panels B, D, F & H). Panel B is the negative control showing lack of Zinquin autofluorescence in human ciliated AEC. Epifluorecence images of untreated isolated human epithelial cells obtained by bronchial brushings (panel D & F) and bronchoalveolar lavage washes (panel H, I & J) and demonstrate intense apical distribution of Zinquin fluorescence mainly within the apical cytoplasm (panels D, H & I). Intense Zinquin fluorescence was also observed within cilia (panel D & I) and basal bodies of cilia (panel F, H & J). Typical images are shown. 2500x initial magnification.

10 μm
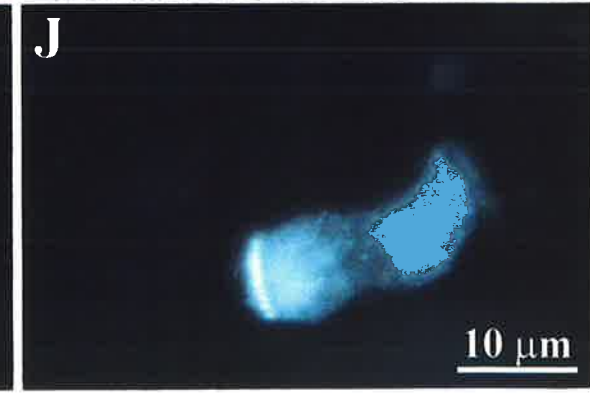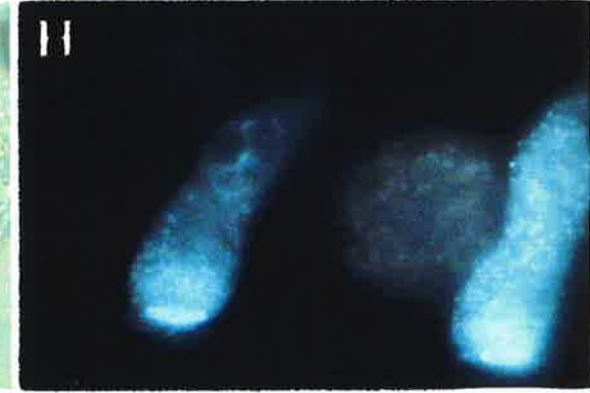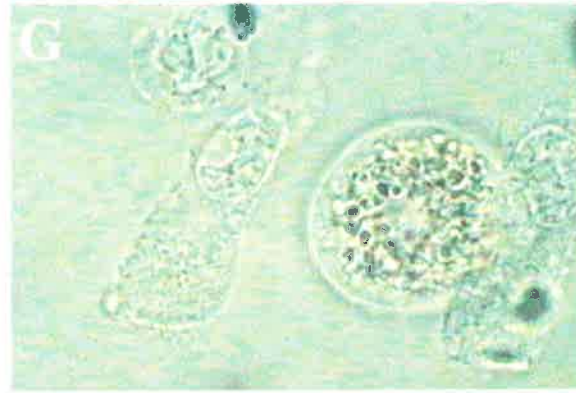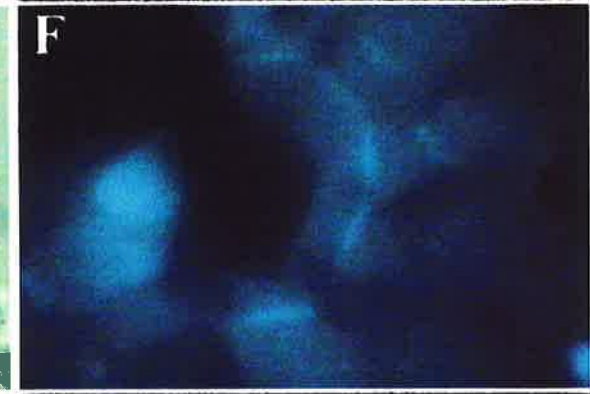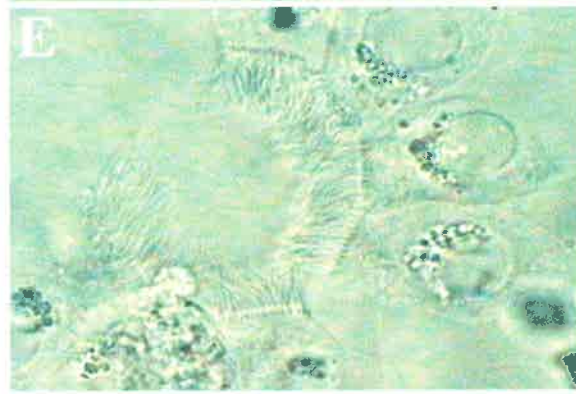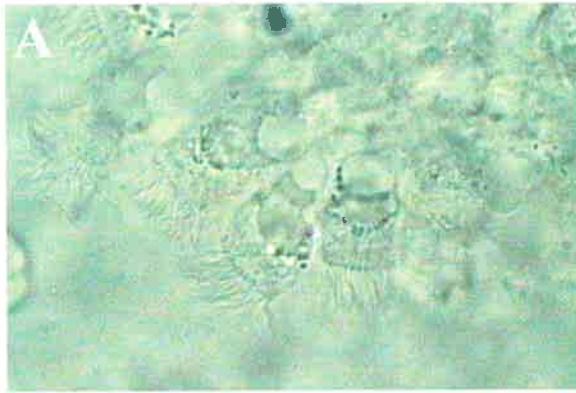
from bronchoalveolar lavage washes are shown in panels G, H, I & J. Autofluorescence was negligible as seen in panel B where cells were treated with PBS only and therefore acted as a negative control. Panel A is the corresponding light image. Zinquin fluorescence was found to be most intense within three compartments of these cells; 1) in the apical cytoplasm (panels D, H, I & J), 2) within cilia of some cells (panel D & I) and 3) in structures which appear to be basal bodies of cilia (panel F, H & J).

3.4 DISCUSSION

These studies are the first to report the visualisation and quantification of labile intracellular Zn in different populations of airway epithelium. There have been no previously reported studies of Zn distribution in the respiratory system due to lack of sensitive techniques to visualize and quantify tissue Zn.

The major findings reported in this chapter are: 1) Zn lines the luminal regions of the trachea, bronchi and bronchioles, 2) primary ciliated AEC are rich in labile Zn, compared with alveolar epithelial cells and other cell types, 3) this Zn is especially concentrated in the apical cytoplasmic region immediately below the cilia (within vesicles and basal bodies) and within cilia themselves.

The first finding of labile Zn lining the apical and luminal side of the conducting airways, may have an analogy with the concept of Zn in galvanisation, where Zn acts to protect the underlying steel from oxidation and corrosion. The distribution of intense Zinquin fluorescence in an apical manner directly beneath the cilia of primary AEC confirms the previous finding of high Zn levels within the luminal side of the epithelium which was observed with the cryostat epithelial

132

tissues. Since these cells are the first site of contact between the inhaled air and the respiratory tissue, they may require higher concentrations of Zn for survival compared to the alveolar cells. It has been proposed that Zn became particularly important in eukaryotic cell evolution at about the time the atmosphere was becoming oxygen-rich and cells were developing mitochondria (Da Silva, 1991). Therefore, Zn, as one of the major anti-oxidants in the body, may play an important role in the protection of the respiratory epithelium. Zinquin reacts with labile Zn rather than the tightly bound pools of Zn found in metalloenzymes and so it is unlikely that the apical Zn is representing Zn in metalloenzymes.

The finding of low labile Zn in alveolar epithelium when compared with the tracheal and bronchial tissue, suggests that these cells types (squamous versus columnar) may have either different capacities for Zn uptake (e.g altered levels of Zn transporters in the cell membrane) or different metabolic requirements for Zn (e.g for cell proliferation). It would therefore be interesting to quantify the mRNA and protein levels of the family of Zn transporters in these cells, and to determine their localisation within the respiratory epithelium. It is hypothesized that the higher Zn content in the upper conducting airway epithelium, reflects the greater need to protect these cells from foreign inhaled particles and other noxious agents, rather than the alveolar cells which are further down the respiratory tract.

The distribution of total Zn is not known but is likely to be similar to the distribution of metalloenzymes in these cells and therefore uniformly distributed throughout the cellular organelles (Vallee & Falchuk, 1993). It has proven difficult to determine the real concentrations of intracellular labile $[Zn^{2+}]$ from Zn binding dyes and fluorophores. One attempt to quantify this pool of Zn in terms of actual

intracellular concentration is that by Savage and colleagues. This paper describes the embedding of solutions containing known concentrations of Zn standards in a plastic medium. These plastic-embedded standards were then sectioned, mounted onto a slide and reacted with a Zn fluorophore (Savage et al., 1989). However, there are limitations with this technique. Firstly, there is no real comparison between standard solutions embedded within plastic and that of the Zn within cells. For example, Zn within cells is bound to various proteins and lipid ligands, or concentrated within vesicles or other organelles, whereas, the Zn within the plastic medium remains in a free state. This would suggest that for a given concentration of Zn there would be a higher fluorescence intensity for plastic embedded Zn standards than with the cells. Secondly, the authors do not take into account whether the uptake and concentration of Zn fluorophore within the cells differs from that in the plastic.

This chapter describes a potentially relatively simple method using a standard curve derived from cells pre-loaded with increasing concentrations of Zn. This method is probably more realistic than the method described above since it takes into account the intracellular environment of the fluorophore and the exogenous Zn loaded. However, this method is still unable to give an accurate concentration of Zn within these cells for the following reasons and was therefore not used for the remaining experiments in this thesis. Firstly, a major assumption is that the NaPYR equilibrates the Zn concentration across the plasma membrane. This is often assumed but has not been proven and raises the question of how much Zn NaPYR transports into cells in a given period of time. A second limitation is that when a concentration has been determined from the standard the value is an average throughout the total cell and does not take into account differences in

subcellular distribution of the Zn bound to Zinquin, for example within vesicles versus the nucleus. An alternative method which could be used is by incubating red cell ghosts with known concentrations of $ZnSO_4$ then resealing them before labelling with Zinquin. A standard curve could then be derived from these cells.

As discussed earlier in Chapter 1, Zn may have a special anti-oxidant role in the vicinity of mitochondria which release potentially damaging oxyradicals during the generation of energy (Halliwell et al., 1992). This is a particular hazard for the ciliated cells lining the airways, since these cells rely heavily on this energy for the rapid beating of the cilia. Supportive evidence would be finding other anti-oxidants similarly concentrated in this apical region. Of particular relevance, the antioxidant enzyme peroxiredoxin capable of neutralizing oxidizing chemical agents was recently reported to be localised within the apical region of olfactory, trachea and bronchi AEC (Novoselov et al., 1999). Similarly, unpublished observations from this laboratory have since shown an abundance of Cu-Zn SOD within the same apical region as the intracellular Zn. However it is unlikely that the labile Zn visualied by Zinquin includes that in Cu-Zn SOD since this Zn is tightly bound and probably unavailable to Zinquin.

Apical Zn may be derived from Zn reservoirs existing in a possible vesicular and perinuclear pattern. In the primary ciliated AEC, the perinuclear concentration of Zn was most pronounced on the apical side of the nucleus and is reminiscent of the distribution of Zn in secretory cells such as the Zn-rich pancreatic islets (Zalewski et al., 1996). Whether any of the apical Zn is contained within secretory granules and is destined for secretion into the pericellular fluid is not yet clear. Measurements of the Zn content of this fluid should be informative.

These studies have also indicated a significant content of labile Zn within the cilia themselves. Zn is a well-known stabilizer of microtubules (Oteiza et al., 1990) and may have a similar role in the axonemes of the cilia.

One limitation of these studies is the lack of comparison between Zinquin and other Zn detecting technique. Future studies would include confirming the localisation of Zn observed in these cells using a technique with greater resolution. One suggestion is the autometallography (AMG) method developed by Danscher and colleagues in 1997 which relies on the precipitation of zinc sulfide by reaction of the labile Zn with sodium sulfide within tissues. This reaction is visualized by silver enhancement and can reveal Zn localisation at the ultrastructural level using EM (Danscher & Andreasen, 1997). While this technique has been useful in visualising Zn in brain sections, it involves numerous washes and incubations which may pose a technical problem for the more fragile respiratory tissues. Furthermore, AMG requires intravenous injection of sodium sulfide followed by transcardial fixation to produce a constant staining which would have been difficult since fresh lungs and tracheas were obtained from the local abattoir.

In summary, the findings presented in this chapter show for the first time that AEC are rich in Zn. This pool of intracellular labile Zn was confined within the apical region of AEC and extends from the trachea down to the bronchioles and may act to further enhance the protective abilities of the respiratory epithelium. Zn is known to be protective as it promotes cell proliferation while suppressing apoptosis. In order to determine part of the functionality of this intracellular labile pool of Zn in AEC, caspase-3 activation was investigated in experiments described in Chapter 4.

Some of the results reported in this chapter are in the following published manuscripts:

1. Visualization of labile zinc and its role in apoptosis of primary airway epithelial cells and cell lines (Truong-Tran et al., 2000).

CHAPTER 4

INVESTIGATION OF ZINC AS AN ANTI-APOPTOTIC AGENT IN RESPIRATORY EPITHELIAL CELLS

CHAPTER 4 INVESTIGATION OF ZINC AS AN ANTI-APOPTOTIC AGENT IN RESPIRATORY EPITHELIAL CELLS

4.1 INTRODUCTION

The studies described in Chapter 3 show the localisation of Zn in the apical cytoplasm of AEC. This chapter reports experiments which were designed to investigate the possible functional role of labile intracellular Zn in caspase activated apoptosis in REC.

As discussed in Chapter 1 section 1.2, of this thesis, apoptosis is characterised by two distinct phases. The first is the biochemical phase which involves activation of caspases and the cleavage of specific cellular substrates, while the second is the morphological phase which results in the ultimate destruction of the cells characterised by membrane blebbing, formation of apoptotic bodies and nuclear fragmentation (Wyllie, 1997).

One potential role of labile Zn in REC is as a survival factor able to regulate apoptosis. This is based on the knowledge that Zn deficiency enhances rates of apoptosis in a variety of cells and animals, while, Zn supplementation inhibits apoptosis via a number of mechanisms which have been described in detail in section 1.2.7.3 (Nodera et al., 2001; Truong-Tran et al., 2001). However, despite these studies little is known about the physiology of Zn within the respiratory system and its influence on apoptosis. Hence, it was hypothesised that labile intracellular Zn plays an important role by protecting REC from oxidative damage and apoptosis.

The aim of this study was therefore to elucidate the role of Zn in regulating caspase activation in REC by biochemically measuring the activity levels of caspases-1, 2, 3, 4, 5, 6 and 9 using their related synthetic coumarin-tagged substrates as described in the methods section of this chapter. Apoptosis was also morphologically confirmed in selected samples by staining cells with Hoechst dye #33342 to detect chromatin fragmentation.

The experiments reported in this chapter describe the effects of 1) Zn depletion induced by the Zn chelator TPEN, 2) H_2O_2 alone, 3) a combination of TPEN and H_2O_2 and 4) Zn supplementation (by the Zn ionophore sodium NaPYR with exogenous $ZnSO_4$) in combination with H_2O_2 and TPEN. For this study a variety of REC were used: NCI-H292 and A549 (malignant cell lines often taken to be representative of bronchial and alveolar epithelium respectively) and primary sheep and human ciliated AEC.

4.2 METHODS

4.2.1 REC Used

Primary sheep ciliated AEC were isolated using the method described in section 2.1.2 and primary human cilaited AEC were obtained as described in section 2.2. Transformed A549 and NCI-H292 cell lines were obtained and cultured as in sections 2.9.

4.2.2 Alterations in Intracellular Zn Levels of REC

Intracellular Zn levels were manipulated in cells using the Zn chelator TPEN and the Zn ionophore NaPYR as discussed in section 2.5.

4.2.3 Apoptosis Studies

To investigate whether H_2O_2 increases apoptosis in REC, cells were treated with increasing concentrations of H_2O_2 (as described in section 2.10) and caspase-3 activity levels measured (as in section 2.11.1).

For this series of experiments, a synthetic fluorogenic peptide substrate DEVD-AFC was used to measure caspase-3 activity (Medina et al., 1997). The enzymatic cleavage of this substrate, releases the free coumarin derivative compound, AFC, producing a yellow-green fluorescence measured at 505 nM (as described in section 2.11.1). Other substrates used for the detection of various caspase activities in these experiments were YVAD-AFC (caspase-1), VDVAD-AFC (caspase-2), LEVD-AFC (caspase-4), WEHD-AFC (caspase-5), VEID-AFC (caspase-6) and LEHD-AFC (caspase-9). For simplicity, the different caspase activities will be hereon be referred to by their caspase number. However, it should be mentioned that although these substrates are preferentially cleaved by the indicated caspases, there may be some overlap. The caspase activities were expressed as fluorescence units/μg prtn/h ± S.E.M. In some experiments apoptosis was confirmed by staining cells with Hoechst dye # 33342 as outlined in section 2.11.2. Protein concentrations of cell lysates were determined by the Lowry assay as in section 2.10.2. The data reported in this chapter were derived from the

average of 2 to 4 separate experiments, each performed in triplicates. The level of statistical significance was determined by the Students *t* test.

4.3 RESULTS

4.3.1 Caspase Activation and Apoptosis is Increased In Zn-Manipulated REC

A) Induction of Caspase-3 Activation and Apoptosis by the Zn chelator TPEN in Primary Sheep Ciliated AEC and Malignant Cell Lines

Figure 4.1 shows the large increase in caspase-3 activity in TPEN-treated primary (A) and NCI-H292 (B) cells (C3, red diamond symbol). Primary ciliated cells had a control level of caspase-3 activity of 1.02 ± 0.05 caspase units/µg prtn/h. This was increased to 1.89 ± 0.09 caspase units/µg prtn/h when treated with 6.25 µM TPEN ($p < 0.05$). Increases in caspase-3 levels were dependent on TPEN concentration and plateaued at 12.5 µM TPEN (2.87 ± 0.13 caspase units/µg prtn/h). For the NCI-H292 cells caspase activity was increased in a linear manner rising from 0.03 ± 0.01 caspase units/µg prtn/h in untreated cells to 0.13 ± 0.09 caspase units/µg prtn/h with 12.5 µM TPEN. Caspase-3 activity continued to rise without plateauing at 25 µM TPEN (0.35 ± 0.161 caspase units/µg prtn/h, $p < 0.05$). These data show that the primary cells treated with TPEN had approximately a 10 to 20-fold higher level of caspase-3 activity when compared to the TPEN treated transformed NCI-H292 cell line.

A range of other caspase activities were assayed to determine whether Zn chelation also affects these caspases. Caspase-6 (VEID-caspase, blue rectangle

Figure 4.1: Induction of Caspase Activity and Apoptosis in Zn-Depleted AEC

Panel A & B: Primary ciliated AEC (A) and NCI-H292 cells (B) were treated with increasing concentrations of TPEN for 4 h. Lysates were assayed for various caspases. Large increases in caspase-3 (C3; red diamond symbols) and caspase-6 (C6; blue square symbols) and small increases in caspase-2 (C2; purple circles) were seen with increasing concentrations of TPEN in both cell populations. There were no significant differences noted in any of the other caspases: caspase-1 (C1; green square symbol), caspase-4 (C4; orange circle symbol), caspase-5 (C5; black triangle) or caspase-9 (C9; blue triangle). Data were collated from 3 separate experiments each in triplicates. Significant differences refer to comparisons with untreated control cells: * $p < 0.05$; ** $p < 0.005$.

Panel C & D: Corresponding bright field (C) and Hoechst dye 33342 epifluorescence (D) images of a typical sheep ciliated AEC undergoing apoptosis after overnight intracellular Zn depletion with 6.25 μM of the Zn chelator TPEN. Note the formation of apoptotic bodies in panel C and the presence of fragments of the nucleus (revealed by chromatin staining) in two of these bodies in panel D. Scale bar indicates 10 μm.

Symbols used are:
Caspase-1 (C1; green square symbol),
Caspase-2 (C2; purple circles)
Caspase-3 (C3; red diamond symbols),
Caspase-4 (C4; orange circle symbol)
Caspase-5 (C5; black triangle),
Caspase-6 (C6; blue square symbols)
Caspase-9 (C9; blue triangle).

A — Primary ciliated cells

Caspase Activity/μg prtn/hr vs TPEN (μM)

** C3
** C6
** C2
C1,C4
C5,C9

B — NCI-H292

Caspase Activity/μg prtn/hr vs TPEN (μM)

* C3
* C6
** C2,C4
C1,C5,C9

C

D
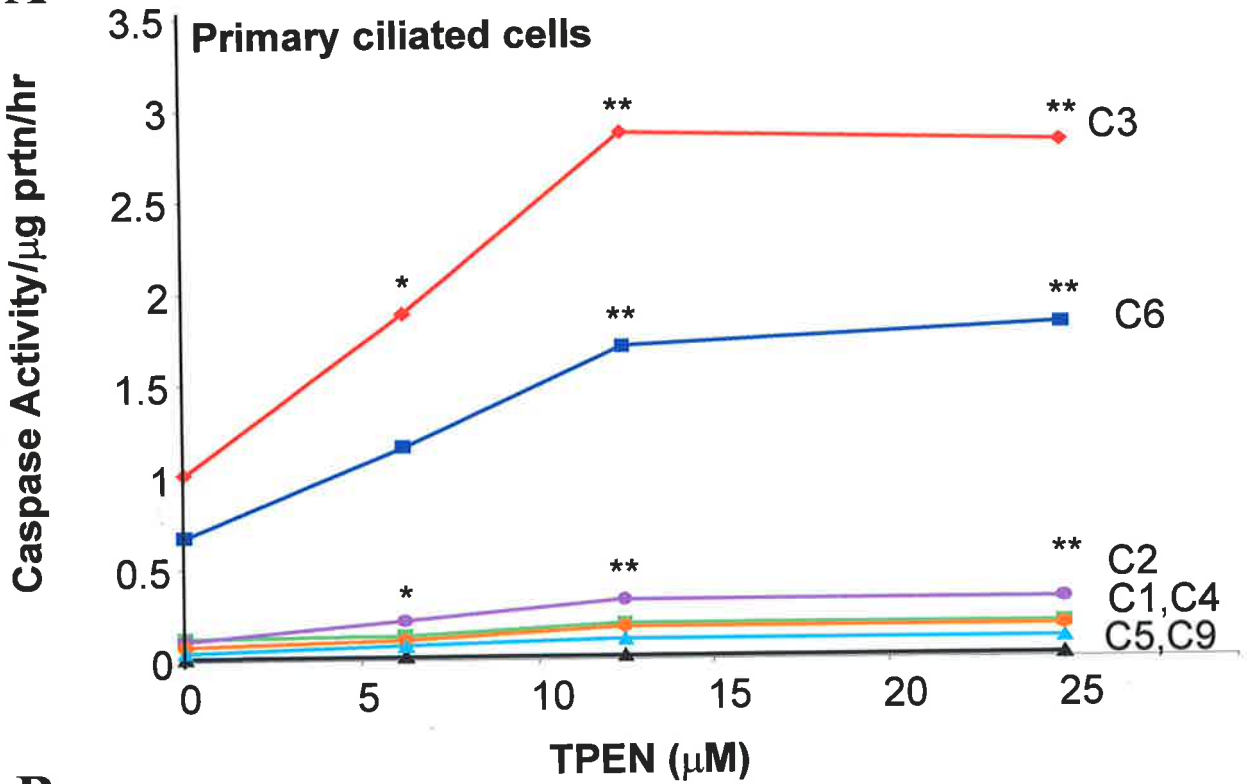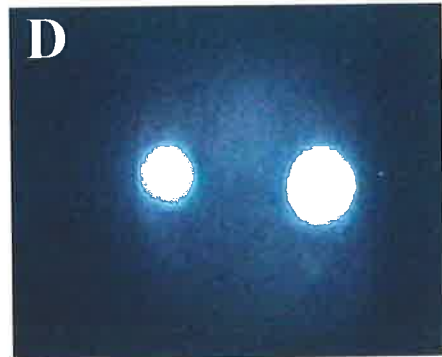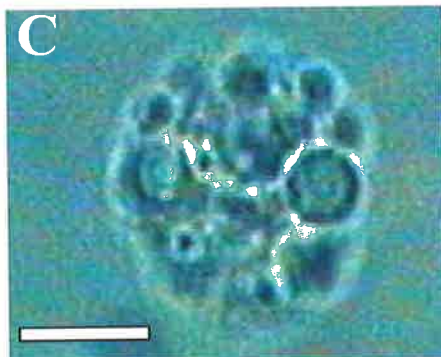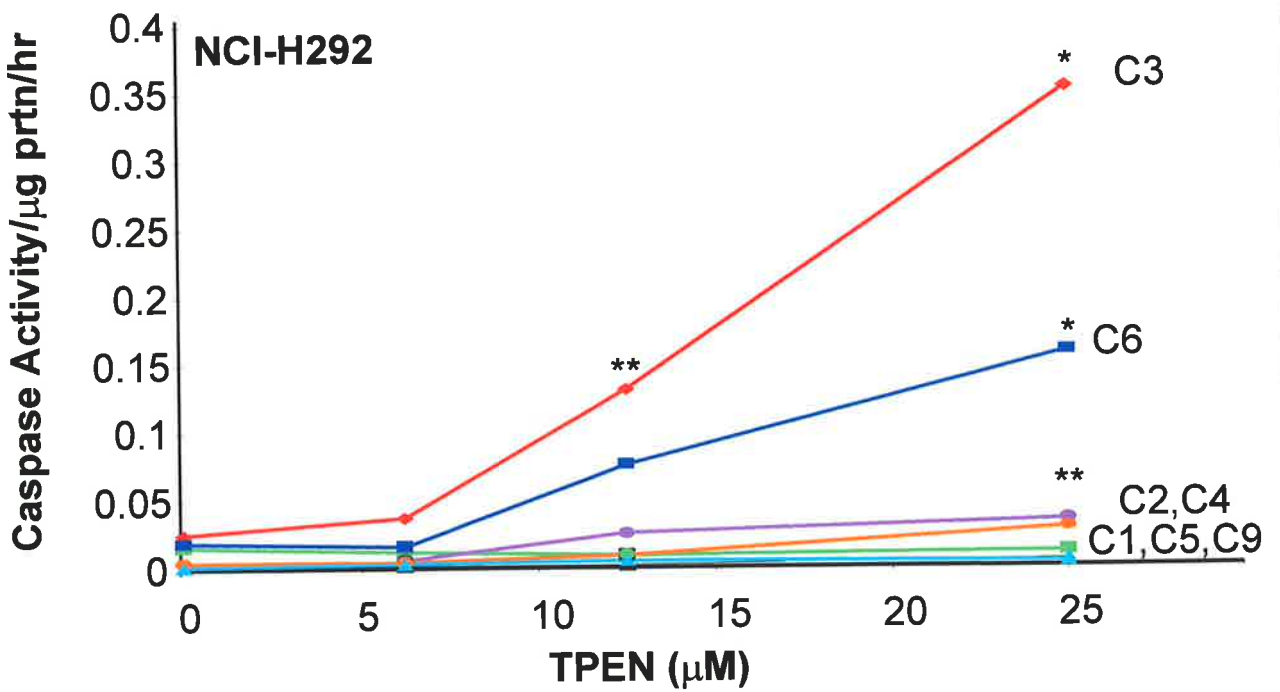
symbol) was increased in both cell types; at 25 μM TPEN, the caspase-6 activities were 1.81 ± 0.18 caspase units/μg prtn/h for primary ciliated AEC ($p < 0.05$) and 0.16 ± 0.00 caspase units/μg prtn/h for the NCI-H292 cells ($p < 0.05$). This was increased over the control levels of 0.67 ± 0.01 caspase units/μg prtn/h in primary ciliated AEC and 0.02 ± 0.00 caspase units/μg prtn/h in NCI-H292 cells. Caspase-2 (VDVAD-caspase, purple circle symbol) was weakly induced; at 25 μM TPEN the caspase-2 activities were 0.33 ± 0.04 caspase units/μg prtn/h for primary cells and 0.03 ± 0.01 caspase units/μg prtn/h for the NCI-H292 cells although the increases after TPEN addition were still significant ($p < 0.05$ and $p < 0.005$, respectively). No significant increases were seen for caspase-1, (YVAD-caspase, green square symbol) caspase-4 (LEVD-caspase, orange circle), caspase-5 (WEHD-caspase, black triangle symbol) and caspase-9 (LEHD-caspase, blue triangle).

Apoptosis is normally accompanied by distinct morphological changes which can be detected by staining cells with the chromatin dye Hoechst dye #33342 using UV microscopy. Figure 4.1 panel C (bright field) and D (fluorescence) show a typical primary sheep AEC undergoing fragmentation into apoptotic bodies (C) and chromatin fragmentation (D) induced by 6.25 μM TPEN.

Figure 4.2 demonstrates similar morphological changes induced in primary human bronchial ciliated AEC treated with 12.5 μM TPEN for 18h. Untreated cells were found to have intact nuclei and low Hoechst fluorescence (Hoechst staining, LHS panels A, B & C) with ≥ 95% of these cells being viable as determined by the trypan blue exclusion assay. Live cells with cilia had a weak fluorescence. Some

142

Figure 4.2: Morphological Changes Observed in Apoptotic Primary Human Ciliated AEC Detected by the Nuclear Stain Hoechst Dye # 33342

Figure 4.2 are typical images depicting the morphology of untreated (LHS) and Zn depleted (RHS) primary human ciliated AEC which have been labelled with the chromatin stain Hoechst dye #33342. Hoechst dye #33342 strongly fluoresces with condensed chromatin under UV light highlighting apoptotic cells. Experiments were performed twice in duplicate and approximately 100 cells per slide were examined using a 100x oil immersion lens.

LHS panels: Panels A to C show cells which have not undergone apoptosis and therefore have intact nuclei (**) with a weak level of nuclear fluorescence. Panel A & C are dual light and fluorescence images showing the healthy morphology of primary human ciliated AEC. Panel B is the corresponding fluorescence image of A and depicts weak nuclear fluorescence and the absence of chromatin fragmentation. Live beating AEC (*) within the same image were not stained with the Hoechst dye. 2500x initial magnification

RHS panel: Panel D to F show the strong nuclear fluorescence and distinct chromatin fragmentation of cells which have been treated with 12.5 µM TPEN overnight. Panel D & F are dual light and fluorescence images showing a combination of live (*) and apoptotic cells (arrowed). Panel E is the corresponding fluorescence image of D and shows the distinct nuclear chromatin fragmentation observed within apoptotic cells. Note the distinct fragmentation of chromatin highlighted by the bright blue fluorescence within the arrowed primary ciliated AEC in panel F. 2500x initial magnification.
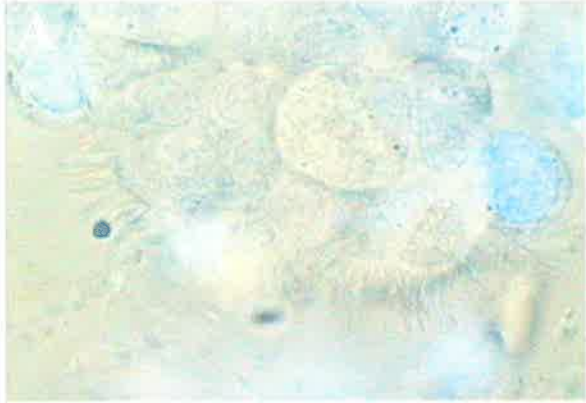
Untreated   **12.5μM TPEN**
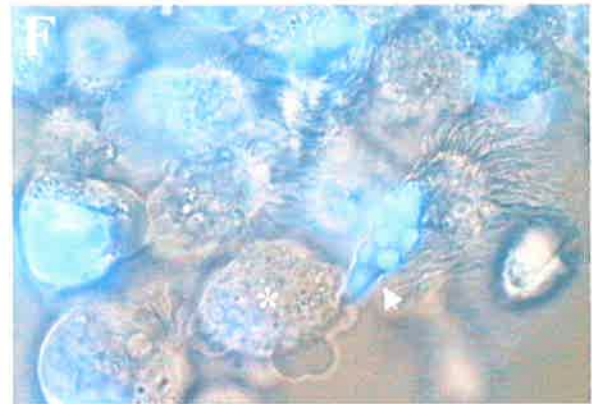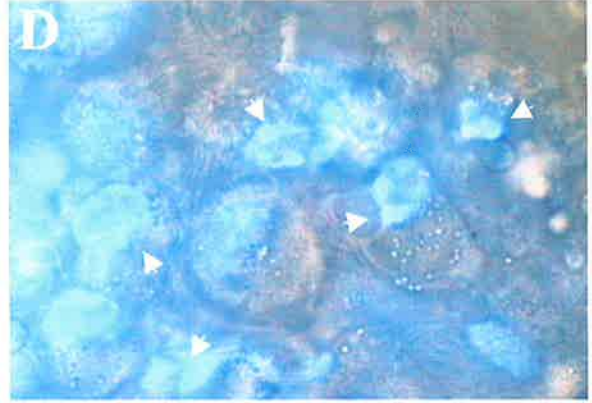
cells without beating cilia had a stronger fluorescence and may represent early stage apoptosis. Cells treated with 12.5 µM TPEN overnight (panel D, E & F) had distinct patterns of chromatin fragmentation (arrowed) and strong nuclear fluorescence confirming that apoptosis is being induced. Due to the limited number of human cells available, caspase-3 activity levels were not measured.

B) Time-Course of Caspase Activation by TPEN

The aim of the following experiment was to determine how rapidly caspases were activated following the decline in intracellular labile Zn induced by 25 µM TPEN. Due to limitations in the number of highly purified primary cells, this time course was performed only in NCI-H292 cells. Experiments were performed in triplicates. To monitor Zinquin fluorescence in the cells, NCI-H292 cells were cultured on sterile glass coverslips, while the caspase-3 activity was determined in the same cells which had grown on the bottom of the six well culture plates. TPEN was added at time zero to both populations and, at varying intervals up to and including 4 h, cells were harvested and assayed for caspase-3 activity.

Zinquin fluorescence was determined in 17-18 image fields (total of 140-260 cells) for each time-point and is expressed in GSU. Figure 4.3 panel A (blue line) shows mean fluorescence intensity decreased by $38 \pm 6\%$ in the first 30 min after adding 25 µM TPEN (from the control value of 23.64 ± 1.31 GSU, $p < 0.005$) and by a further $11 \pm 4\%$ (not significant) in the next 30 min to 13.03 ± 1.05 GSU. Caspase-3 activity (red lines) did not increase in the first 60 min, but there was a $76 \pm 42\%$ increase over the next 75 min and a further $80 \pm 42\%$ increase over the following 60 min ($p < 0.005$).

Figure 4.3: Time Course for Induction of Caspases in Zn-Depleted NCI-H292 Cells

NCI-H292 cells were treated with 25 μM TPEN and assayed at time 0 and at 30-60 min intervals. 25 μM TPEN was used to give a maximal response. Symbols are depicted below.

Panel A: Decrease in labile Zn content after 0.5 h of TPEN treatment (quantified by Zinquin fluorescence, blue rectangle symbol, left hand Y-axis) is followed by a rapid increase in caspase-3 activity (red diamond, right hand Y-axis) at 1.5h. Data were collated from 2 separate experiments each in triplicates. Bars indicate SEM. Significant differences refer to comparisons with untreated control cells: * $p < 0.05$; ** $p < 0.005$.

Panel B shows marked increase in caspase-6 activity, weak increase in caspase-2 activity and no significant increases in other caspases. Data were collated from 3 separate experiments each in triplicates. Significant differences refer to comparisons with untreated control cells: * $p < 0.05$; ** $p < 0.005$.

Symbols used are:

Caspase-1 (C1; green square symbol)

Caspase-2 (C2; purple circles)

Caspase-3 (C3; red diamond symbols)

Caspase-4 (C4; orange circle symbol)

Caspase-5 (C5; black triangle)

Caspase-6 (C6; blue square symbols)

Caspase-9 (C9; blue triangle).

A

NCI-H292 cells

Labile Zn

Caspase-3

B

NCI-H292 cells
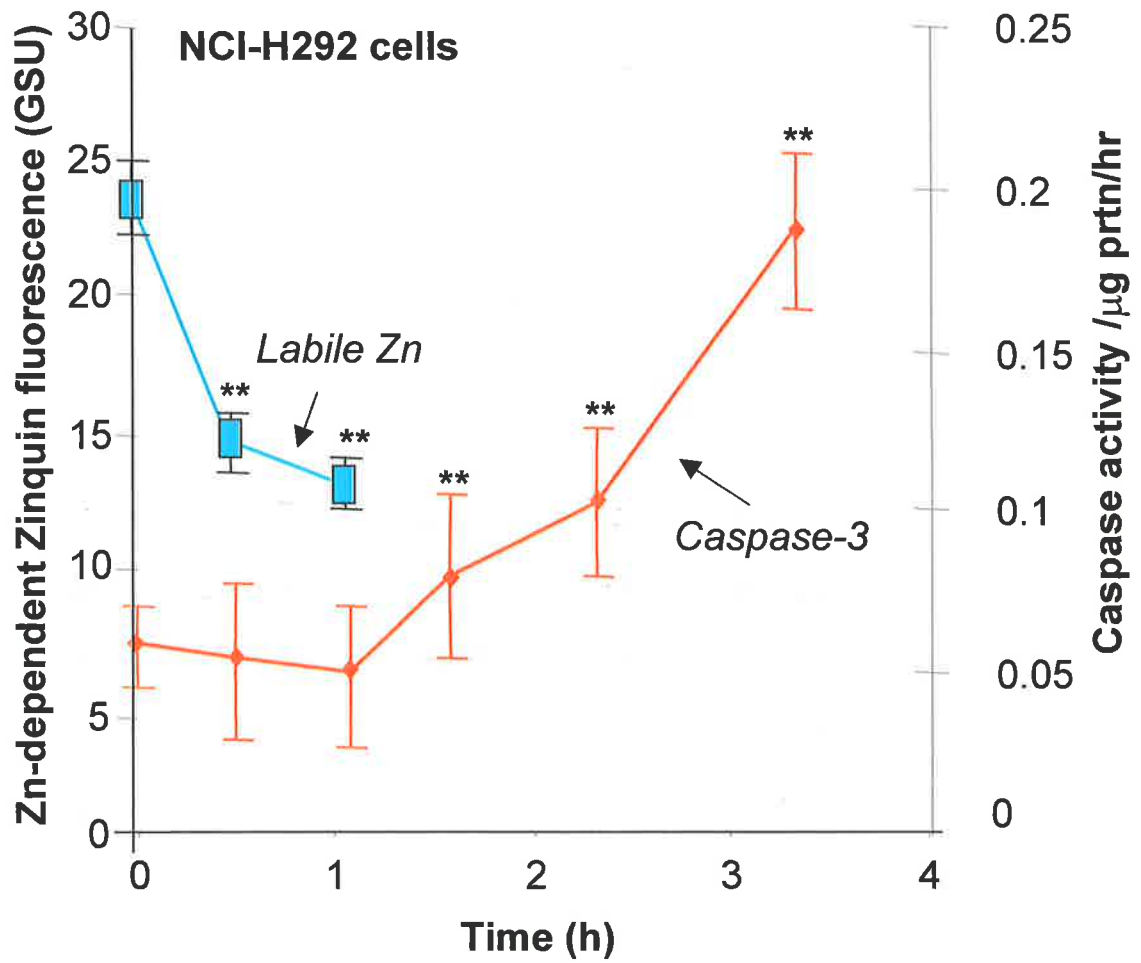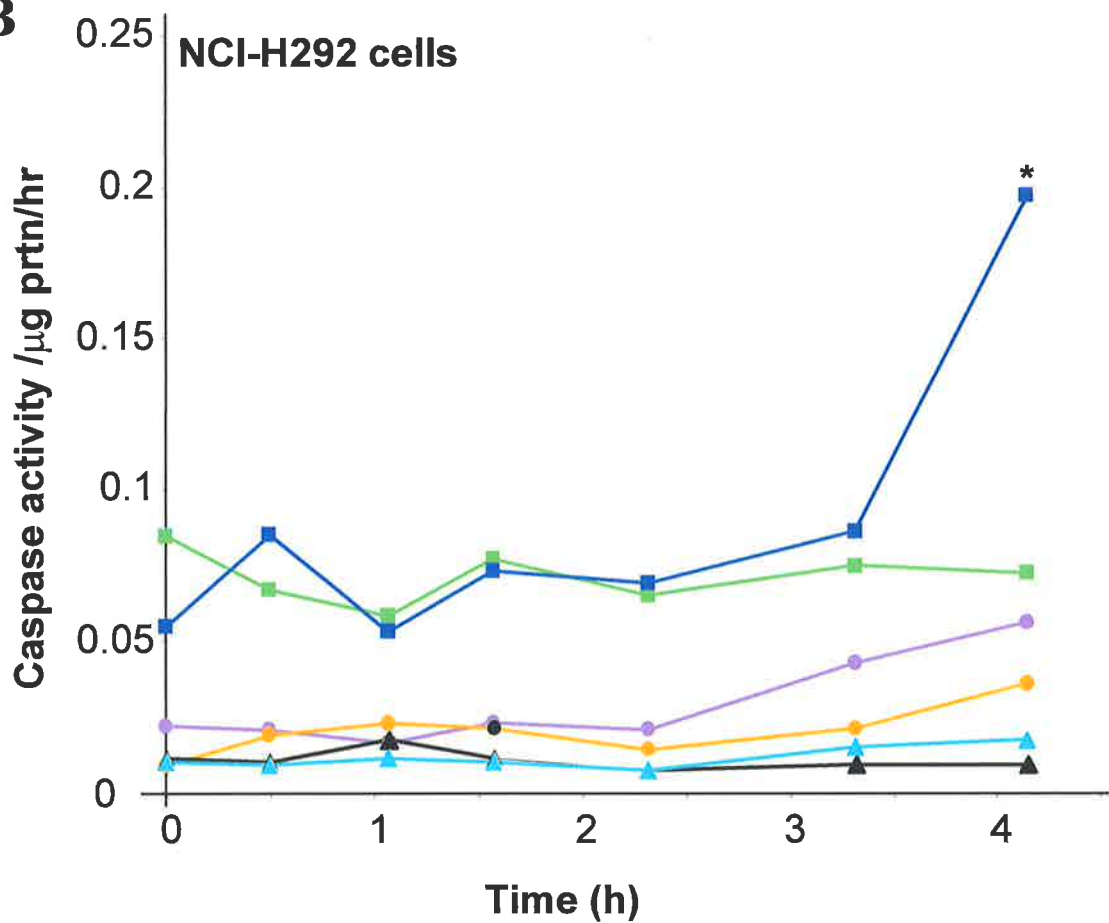
Since caspase-3 is activated from the zymogen form by other caspases (including caspase-6 and -9), it was of great interest to determine whether any of these caspases were activated prior to caspase-3 in TPEN-treated cells. Fig 4.3 panel B shows a large increase in VEID-caspase/caspase-6 activity (blue line) from the control value of 0.06 ± 0.01 to 0.2 ± 0.00 caspase units/μg prtn/h ($p < 0.05$). However, this occurred between 3 and 4 h after the addition of TPEN. There were no early increases in caspase activity of any of the other caspases (1, 2, 4, 5 or 9) tested.

4.3.2 Caspase-3 Activation and Apoptosis is Enhanced in REC Treated with H₂O₂

Inflammatory diseases within the respiratory tract are often characterised by increased H_2O_2 release from the activation of neutrophils and eosinophils, resulting in lung injury (Henricks, 2001).

Primary Ciliated AEC

Figure 4.4 panel A describes the results obtained for primary ciliated AEC treated with varying concentrations of H_2O_2. Primary ciliated AEC had control caspase activity levels of 0.89 ± 0.12 caspase units/μg prtn/h. The addition of 0.125 mM H_2O_2 increased caspase-3 activity to 1.89 ± 0.08 caspase units/μg prtn/h ($p < 0.005$). Caspase-3 activation did not further increase when AEC were treated with 0.25 mM H_2O_2 (2.15 ± 0.39 caspase units/μg prtn/h), however a decrease in caspase activity to 1.17 ± 0.32 caspase units/μg prtn/h was noted in cells receiving 0.5 mM H_2O_2. Cells within wells receiving 0.5 mM H_2O_2 appeared swollen, were

Figure 4.4: Caspase-3 Activation in Response to the Oxyradical Hydrogen Peroxide (H_2O_2) in REC

Figure demonstrates that H_2O_2 induces modest caspase-3 activation in primary ciliated AEC (A) and A549 cells (C) but not in the NCI-H292 cells (B). Cells were treated with increasing concentrations of H_2O_2 for 18 h. Optimum concentrations for inducing caspase-3 activity were 0.125 mM H_2O_2 for primary ciliated AEC, and 0.5 mM for A549 cells. Data were collated from 4 separate experiments each in triplicates. Bars indicate SEM. Significant differences refer to comparisons with untreated control cells: * $p < 0.05$; ** $p < 0.005$.

A Primary ciliated cells

B NCI-H292 cells

C A549 cells

H$_2$O$_2$ (mM)
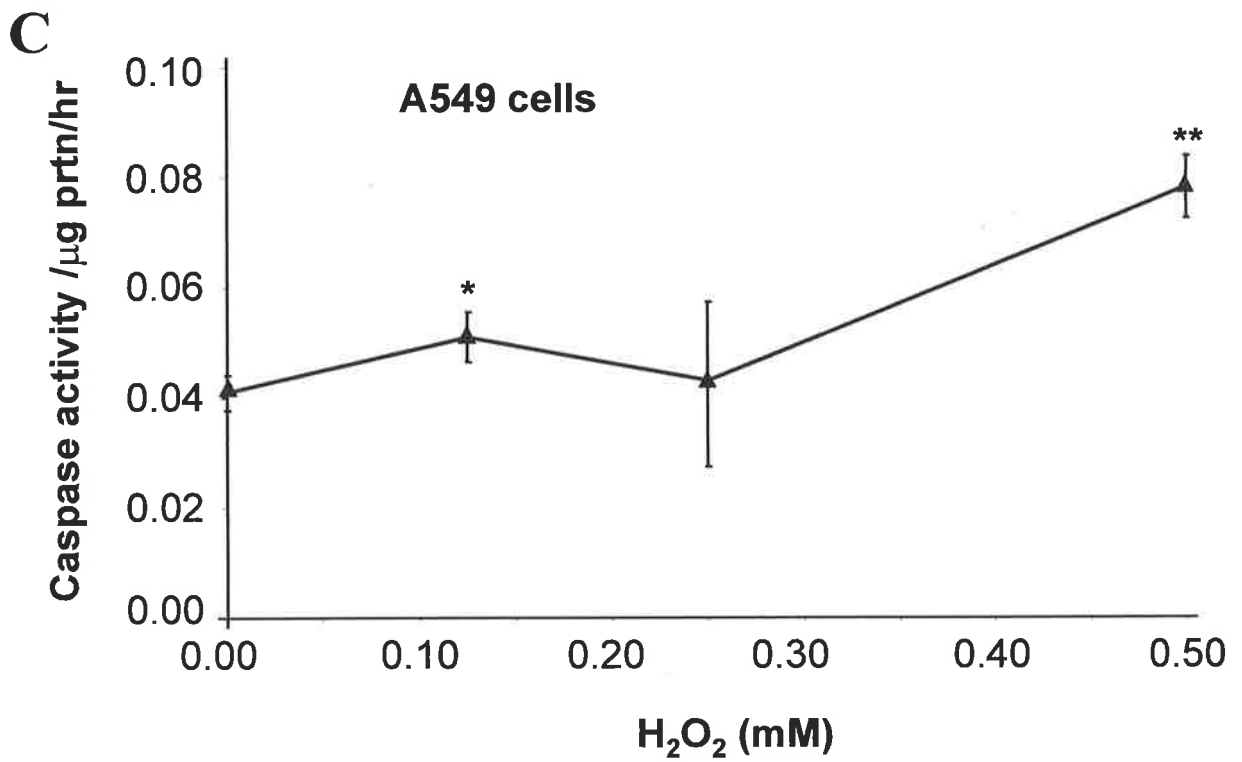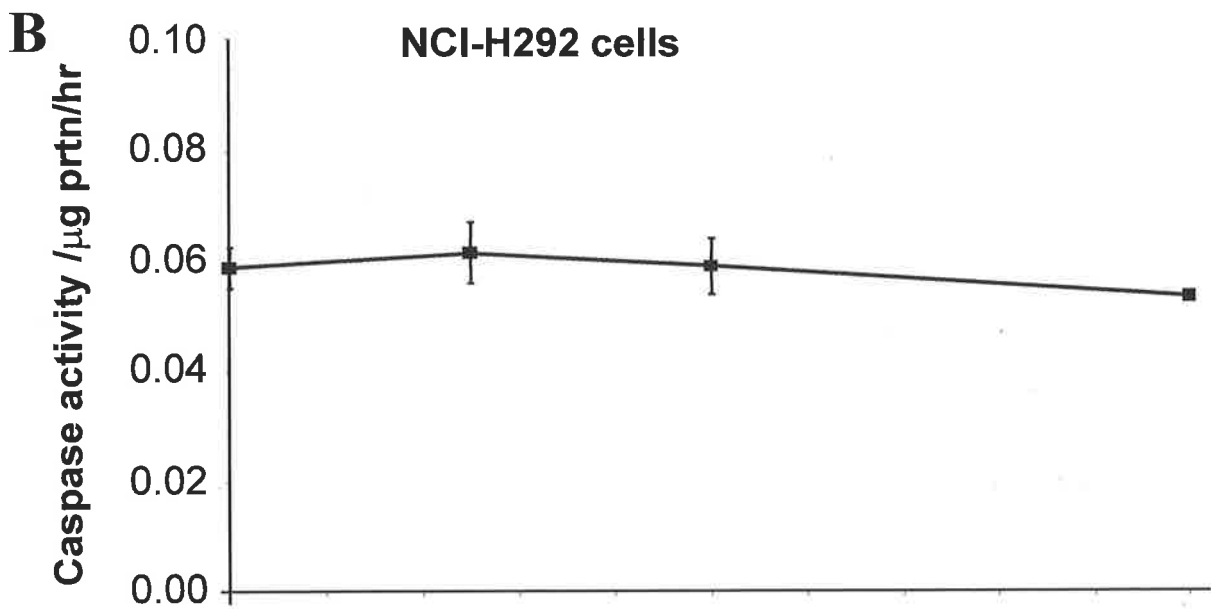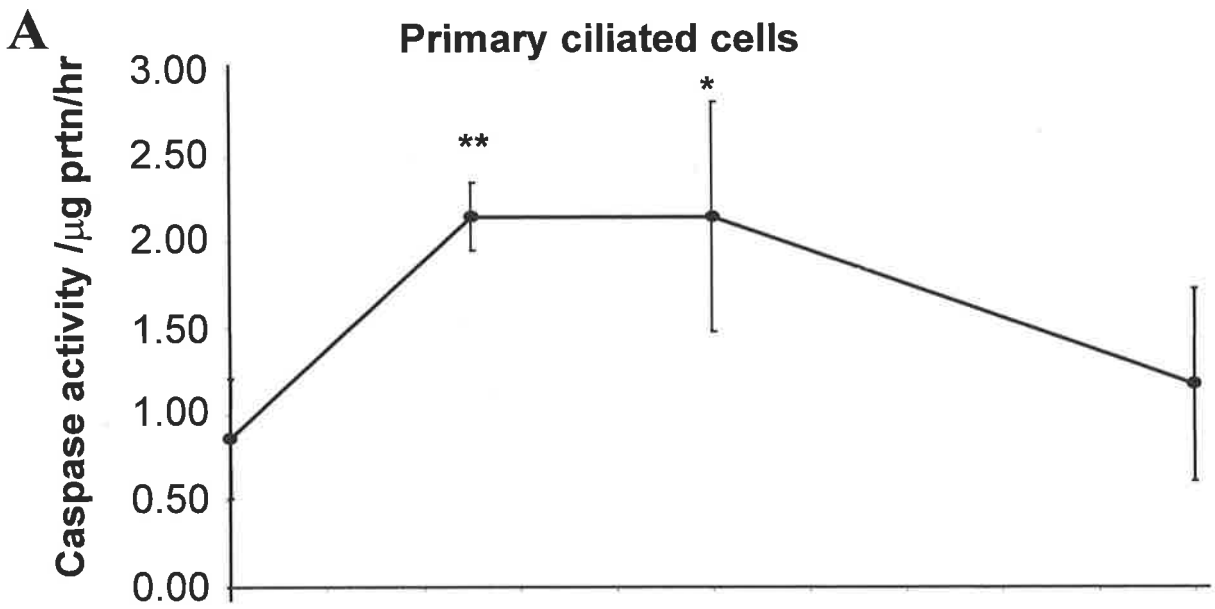
trypan blue positive and had decreased caspase-3 activity, all of which are characteristic of necrosis rather than apoptosis.

Malignant NCI-H292 Bronchial Epithelial Cells

Figure 4.4 panel B shows the results obtained for NCI-H292 cells treated with H_2O_2. NCI-H292 cells had control caspase activity levels of 0.06 ± 0.00 units/μg prtn/h which did not significantly increase when cells were treated with H_2O_2 within the range of 0.125 mM to 0.5 mM.

Malignant A549 Alveolar Epithelial Cells

Figure 4.4 Panel C shows the pattern of caspase-3 activation for A549 cells. A549 cells had a control caspase activity level of 0.05 ± 0.00 units/μg prtn/h. The addition of 0.125 mM H_2O_2 was found to increase caspase-3 activity to 0.06 ± 0.00 caspase units/μg prtn/h ($p < 0.005$) while 0.5 mM H_2O_2 increased levels to 0.08 ± 0.01 caspase units/μg prtn/h ($p < 0.05$). Hence caspase-3 activity was increased by 1.2 fold and 1.6 fold at H_2O_2 concentrations of 0.125 mM and 0.5 mM, respectively.

4.3.3 Caspase-3 Activation is Synergistically Increased in REC Treated with Both TPEN and Hydrogen Peroxide

In order to determine if Zn depletion influences H_2O_2-mediated caspase-3 activation the following experiments were performed. Results were collated from 4 separate experiments performed in triplicates.

145

Figure 4.5 demonstrates caspase-3 activity REC treated with increasing concentrations of H_2O_2 and TPEN.

Firstly, Zn depletion using TPEN (within the ranges of 6.25-25 μM) alone was able to increase caspase-3 activity levels in all cell types tested (depicted by red diamond symbols in panel A-C). In the primary ciliated AEC (panel A) treated with 6.25 μM TPEN alone there was a 0.68 ± 0.06 increase in caspase-3 activity/μg prtn/hr above the untreated cells ($p < 0.05$). Similarly, caspase-3 activity in NCI-H292 cells (panel B) increased over the control value by 0.01 ± 0.01 caspase-3 units/μg prtn/hr ($p < 0.05$). This same trend was also noted in A549 cells (panel C) where there was an increase over the control by 0.02 ± 0.01 caspase-3 units/μg prtn/hr ($p < 0.05$).

Primary Ciliated AEC

Cells treated with H_2O_2 plus 6.25 μM TPEN had significant increases in caspase-3 activity over cells treated with H_2O_2 alone. For example, in primary ciliated AEC 0.125 mM H_2O_2 induced 1.28 ± 0.19 caspase-3 units/μg prtn/hr while 6.25 μM TPEN induced 0.679 ± 0.06 caspase-3 units/μg prtn/hr. In combination they induced 2.80 ± 0.98 caspase-3 units/μg prtn/hr ($p < 0.005$). Although this increase was found to be more than additive (1.96 ± 0.15 caspase-3 units/μg prtn/hr, Figure 4.6, dashed line Panel A), it was not considered to be synergistic since the p value for synergy was 0.109. The same trend was noted in cells treated with 0.125 mM H_2O_2 and 6.25 μM TPEN ($p = 0.15$). Higher concentrations of H_2O_2 resulted in a decrease in caspase-3 levels (Figure 4.5 panel A).

Figure 4.5: Increased Caspase-3 Activation in Zn Depleted REC Treated with H₂O₂

Figure shows the levels of caspase-3 activity in REC (primary AEC, panel A, NCI-H292, panel B and A549, panel C) treated with combinations of TPEN and H_2O_2. These combinations were TPEN (6.25 μM; red diamond, 12.5 μM; blue circle and 25 μM; light blue triangle) and varying concentrations of H_2O_2. Cells were treated with H_2O_2 for 18 h followed by treatment with TPEN at the stated concentrations for a further 4 h. Caspase-3 activities were measured and are expressed as increase over the control (no H_2O_2 or TPEN). Data were collated from 4 separate experiments each in triplicates. Bars indicate SEM.
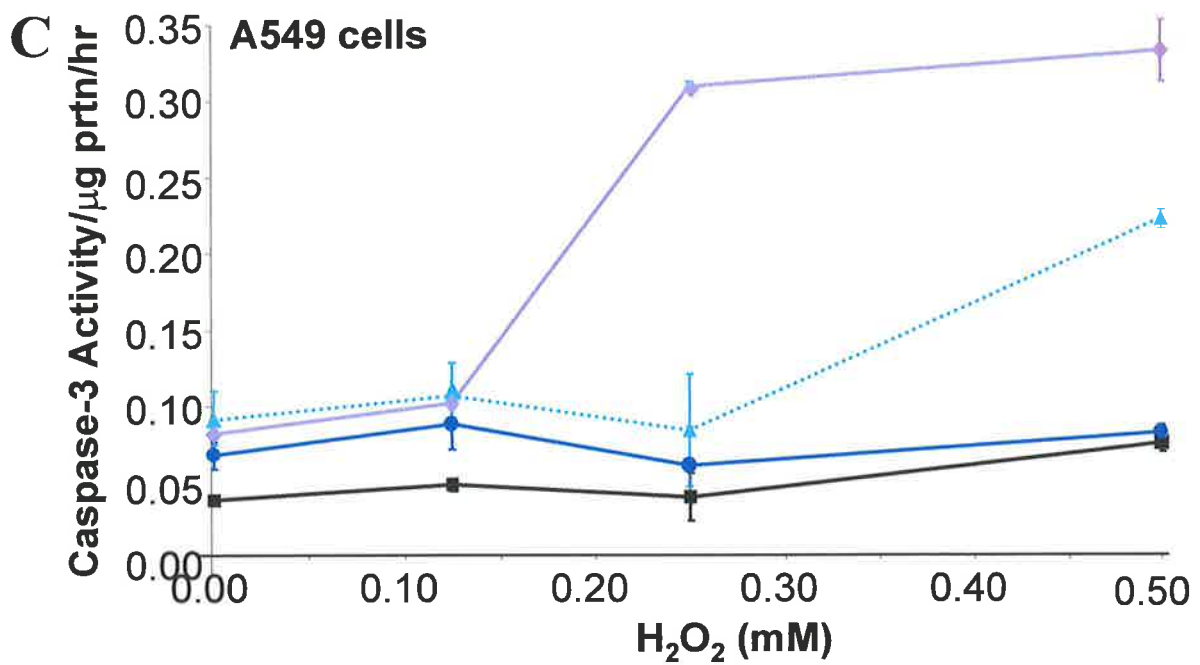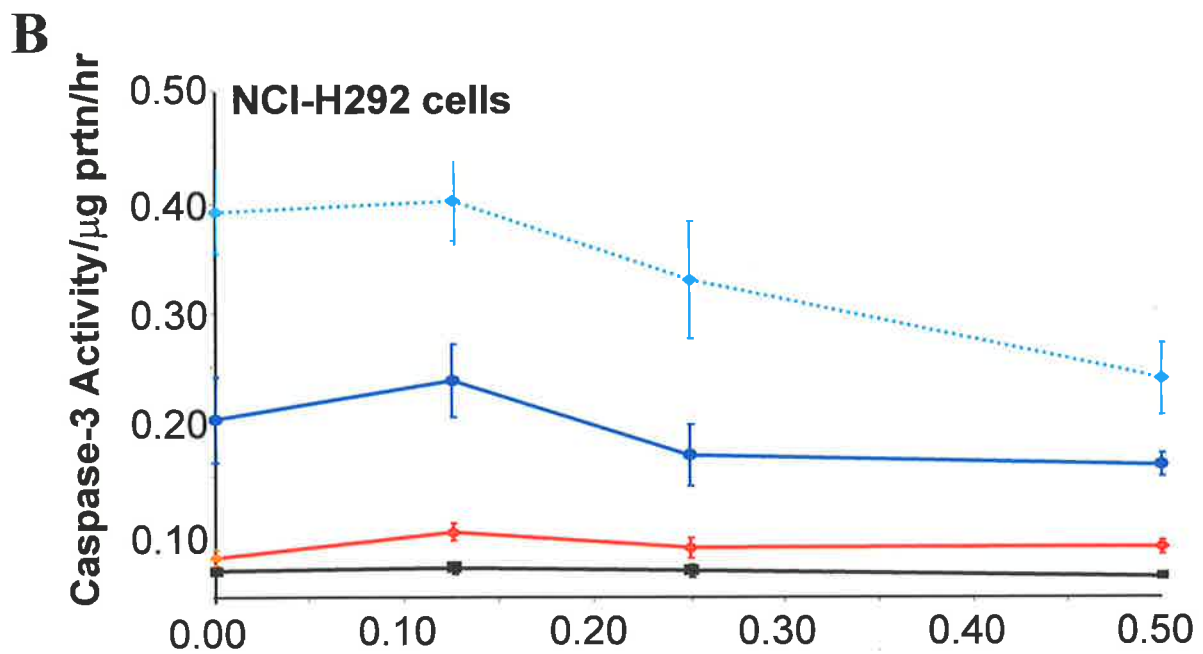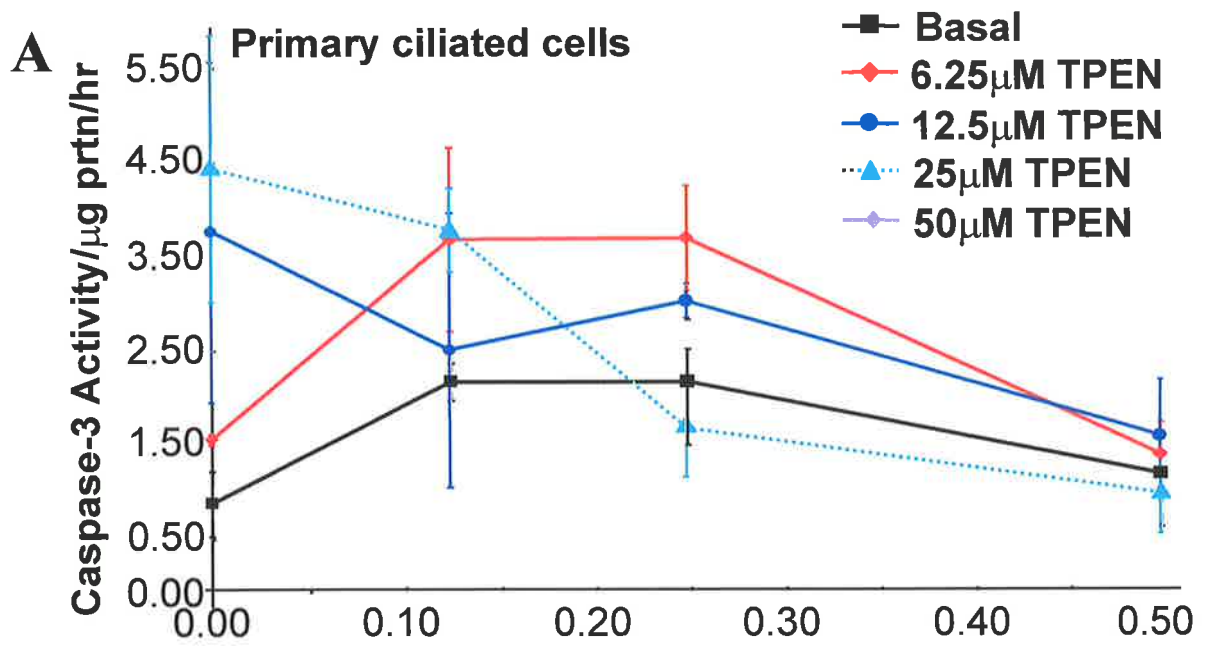
NCI-H292 Bronchial Epithelial Cells

For the NCI-H292 cells, 0.125 mM H_2O_2 alone did not have a significant effect on caspase-3 activity; however, in combination with 6.25 µM TPEN, caspase-3 levels were significantly increased (Figure 4.5 Panel B). For instance, 0.125 mM H_2O_2 alone increased caspase-3 activity over the control by 0.01 ± 0.01 caspase-3 units/µg prtn/hr, 6.25 µM TPEN induced 0.07 ± 0.00 caspase-3 units/µg prtn/hr, but in combination, 0.189 ± 0.01 caspase-3 units/µg prtn/hr were induced. As depicted in Figure 4.6 Panel B, this increase was over the level which would have been expected if it were an additive effect (0.02 ± 0.01, caspase-3 units/µg prtn/hr, $p < 0.050$). Greater concentrations of H_2O_2 and TPEN (at 12.5µM and 25µM) did not have this synergistic effect.

Increasing TPEN concentrations to 12.5 µM (dark blue circle symbols) and 25 µM (dotted light blue diamond symbols) alone continued to raise caspase-3 activity levels and this was best seen in the primary ciliated (panel A) and malignant NCI-H292 (panel B) cells. However when primary ciliated and NCI-H292 cells were treated with increasing concentrations of H_2O_2 in combination with these TPEN concentrations, caspase-3 levels were significantly decreased (panel A and B).

A549 Alveolar Epithelial Cells

For the A549 cells, since 6.25 µM TPEN in combination with H_2O_2 did not increase caspase-3 activity greatly, higher concentrations of TPEN between the ranges of 12.5 µM and 50 µM were then used to treat these cells at the given increasing concentrations of H_2O_2. There were small increases in caspase activity

147

Figure 4.6: Interactions Between H_2O_2 and TPEN in Caspase-3 Activation of REC

Figure summarises the interactions between H_2O_2 and TPEN, in the induction of caspase-3 activity.

Panel A & B: Primary sheep ciliated AEC (panel A) and NCI-H292 cells (panel B) were treated with either 6.25 µM TPEN (white column) and 0.125 mM H_2O_2 (red column) alone or in combination (black column). In combination, cells were treated with H_2O_2 for 18 h followed by treatment with TPEN at the stated concentrations for a further 4 h. Caspase-3 activities were measured and are expressed as increase over the control (no H_2O_2 or TPEN).

Panel C: A549 cells were treated either with 50 µM TPEN (white column) and 0.25 mM H_2O_2 (pink column) alone or in combination (dark blue column) as described for the primary ciliated AEC and NCI-H292 cells. Modest amounts of caspase activity were induced by either reagent alone but a much larger increase was seen when cells received both reagents.

Dashed lines indicate the expected values for a combination of H_2O_2 and TPEN, assuming the interaction was additive. In all cases the interaction was more than additive but significant only for NCI-H292 and A549 cells (double asterixes denote synergism: * $p < 0.05$; ** $p < 0.005$). Data are means of triplicates pooled from 4 separate experiments. Bars indicate SEM.

A Primary Ciliated Cells

Y-axis: Increase in Caspase-3 Activity/μg prtn/hr (0.00 to 4.00)

X-axis: Basal, 6.25μM TPEN, 0.125mM H2O2, TPEN+ H2O2

B NCI-H292 cells

Y-axis: Increase in Caspase-3 Activity/μg prtn/hr (0.00 to 0.05)

X-axis: Basal, 6.25μM TPEN, 0.125mM H2O2, TPEN+ H2O2 **

C A549 cells

Y-axis: Increase in Caspase-3 Activity/μg prtn/hr (0 to 0.30)

X-axis: Basal, 50μM TPEN, 0.25mM H2O2, TPEN+ H2O2 **
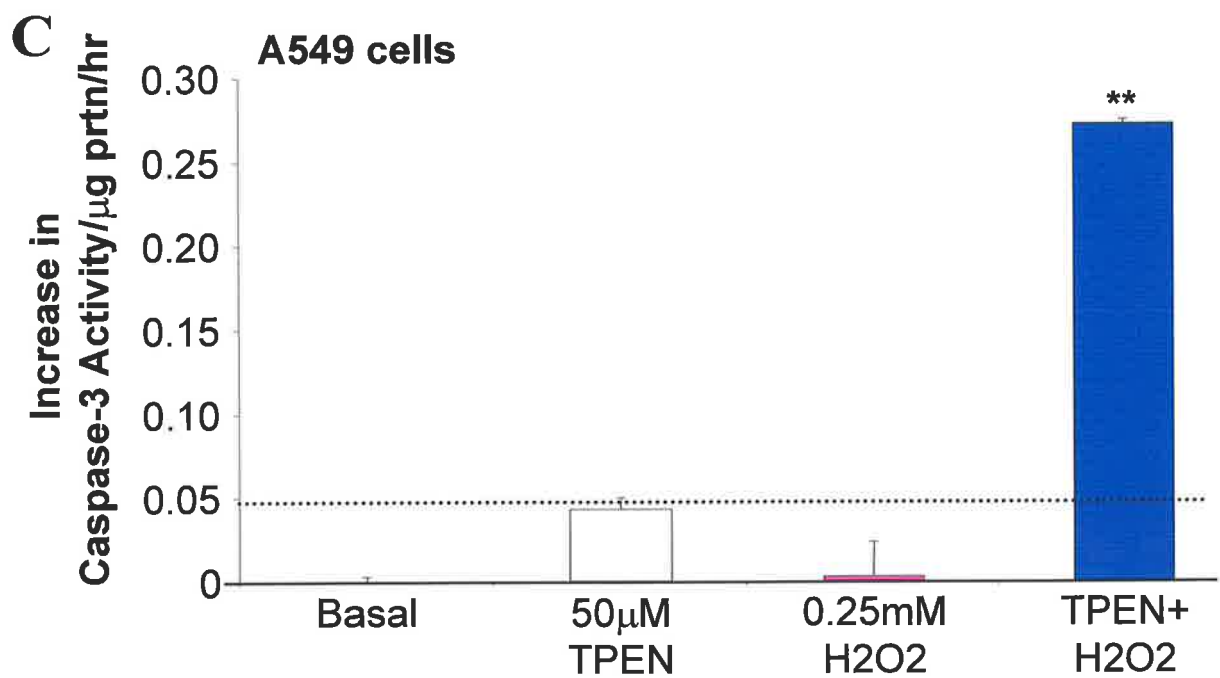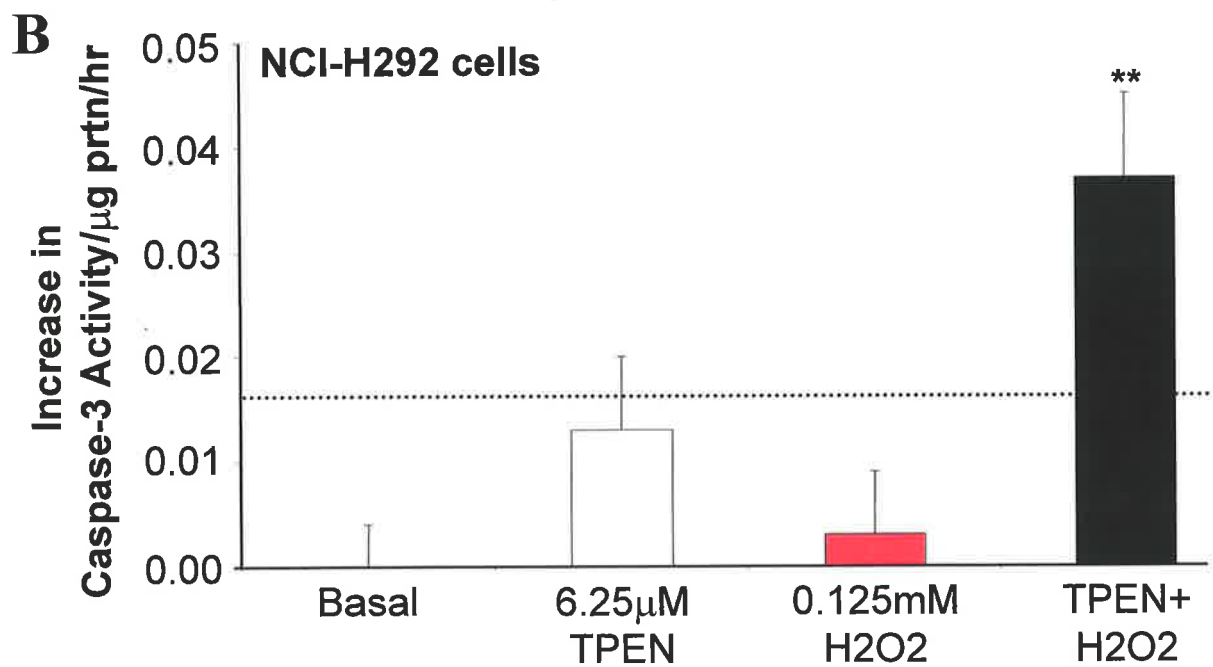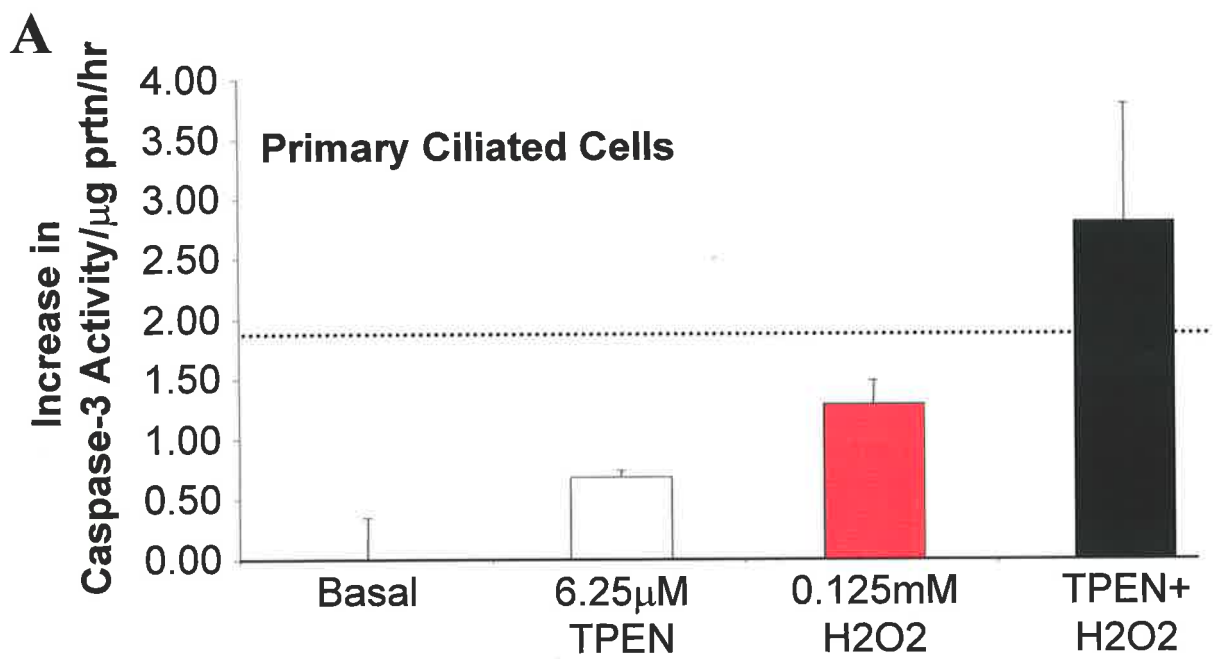
in A549 cells treated with 0.125 mM H_2O_2 and 12.5 µM TPEN. 0.125 mM H_2O_2 induced 0.01 ± 0.01 caspase-3 units/µg prtn/hr, 12.5µM TPEN induced 0.02 ± 0.01 caspase-3 units/µg prtn/hr, but in combination these reagents induced 0.06 ± 0.00 caspase-3 units/µg prtn/hr. However, this level was found to be no more than additive (0.05 ± 0.01, caspase-3 units/µg prtn/hr, $p = 0.28$). A synergistic effect was noted when A549 cells were treated with a higher concentration (50 µM) of TPEN in combination with 0.25 mM H_2O_2. 50 µM TPEN induced 0.03 ± 0.01 caspase-3 units/µg prtn/hr, 0.25 mM H_2O_2 induced 0.02 ± 0.01 caspase-3 units/µg prtn/hr, while in combination 0.27 ± 0.00 caspase-3 units/µg prtn/hr was induced ($p < 0.05$). Caspase-3 activity levels in A549 cells continued to rise when treated with 50 µM TPEN and 0.5 mM H_2O_2 (panel C).

Figure 4.6 is a summary of the above data illustrating the synergism between H_2O_2 and TPEN in the induction of caspase-3 activity.

Despite the marked level of synergism seen in NCI-H292 and A549 cells, the results reported in this chapter have shown that primary cells had approximately a 10-fold higher level of caspase-3 activity when compared to the two transformed cell lines.

4.3.5 Suppression of Caspase-3 Activation in Zn-Supplemented Primary REC

The effect of increasing intracellular labile Zn content of REC on caspase-3 activity was next determined. To investigate the optimal concentration of NaPYR needed, A549 cells were treated with 0.125 mM H_2O_2 to induce caspase activation

after intracellular labile Zn levels were increased in cells for 1 h by using increasing concentrations of NaPYR (0 μM-1 μM) plus 25 μM ZnSO$_4$. The data presented in this section was pooled from 3 separate experiments, each performed in triplicate.

Figure 4.7 depicts the suppression of caspase-3 activation in Zn supplemented A549 cells. A549 cells treated with 0.25 mM H$_2$O$_2$ alone had a caspase-3 activity level of 0.07 $\pm$ 0.02 caspase-3 units/μg prtn/hr (panel A). Caspase-3 activity was significantly decreased by 21% with 0.125 μM PYR (0.06 $\pm$ 0.01 caspase-3 units/μg prtn/hr), 40% with 0.25 μM PYR (0.04 $\pm$ 0.00 caspase-3 units/μg prtn/hr) and by 50% with 1 μM PYR (panel A). Panel B (green triangle) demonstrates the potent effect of Zn supplementation in suppressing 68% and 81% of caspase-3 activity in A549 cells treated with 0.125 mM and 0.25 mM H$_2$O$_2$, respectively, when compared to cells which had not been supplemented (black circles). The inhibition of caspase-3 activity was also noted in primary ciliated AEC and NCI-H292 cells supplemented with the optimal concentration of 1 μM NaPYR and 25 μM ZnSO$_4$. Zn supplementation significantly decreased caspase-3 activity levels by 95% in primary ciliated cells treated with 0.125 mM H$_2$O$_2$ from 2.15 $\pm$ 0.20 down to 0.11 $\pm$ 0.07 caspase-3 units/μg prtn/hr (p < 0.005). The same high level of inhibition (96%) was also noted in primary cells which had been pre-loaded with Zn then treated with both 6.25 μM TPEN and 0.125 mM H$_2$O$_2$. A similar trend was also noted for the NCI-H292 cells where Zn supplementation suppressed 89% and 96% of caspase-3 activity in cells treated with 0.125 mM H$_2$O$_2$ alone or in combination with 6.25 μM TPEN, respectively (p < 0.005).

Figure 4.7: Suppression of Caspase-3 Activation By Zn Supplementation Using the Zn Ionophore NaPYR and Exogenous ZnSO$_4$

Figure 4.5 demonstrates the strong inhibitory effect of intracellular labile Zn on caspase-3 activation in A549 cells. Cells were treated with 0.25 mM H$_2$O$_2$ after pre-loading with increasing concentrations of NaPYR and 25 μM ZnSO$_4$ for 1 h. Panel A shows that NaPYR at 1 μM suppressed caspase-3 activity by 50% in cells treated with 0.25 mM H$_2$O$_2$ while, panel B demonstrates that 1 μM NaPYR suppressed caspase-3 activation at all concentrations of H$_2$O$_2$ tested. Data were collated from 3 separate experiments each in triplicates. Bars indicate SEM. For panel A, significant difference is from cells treated with 0.25 mM H$_2$O$_2$ only. Significant differences refer to comparisons with untreated control cells: * $p < 0.05$; ** $p < 0.005$.

A — A549 Cells Treated with 0.25 mM H2O2

Y-axis: Caspase-3 Activity/μg prtn/hr
X-axis: NaPYR (μM)

* ** ** **

B

Y-axis: Caspase-3 Activity/μg prtn/hr
X-axis: H_2O_2 (mM)

- No NaPYR
- 1μM NaPYR

** ** **
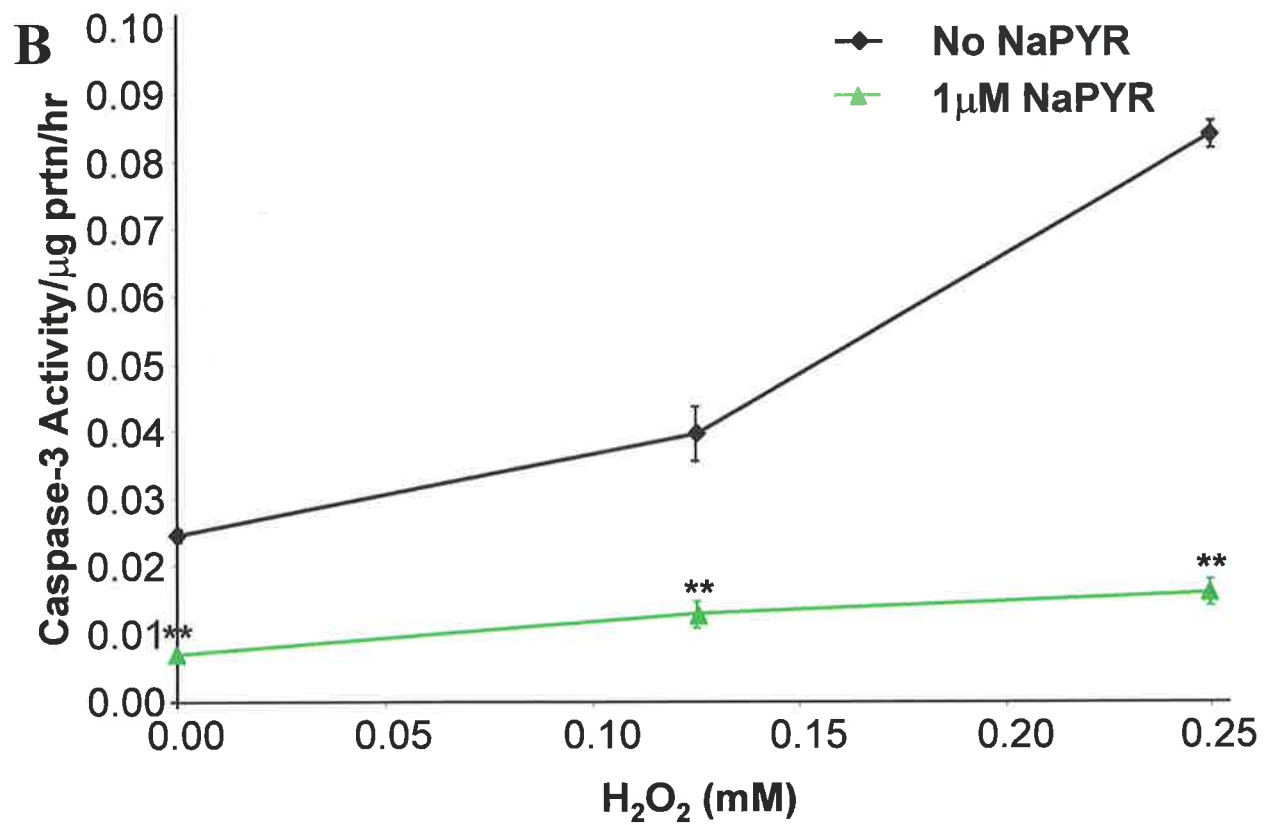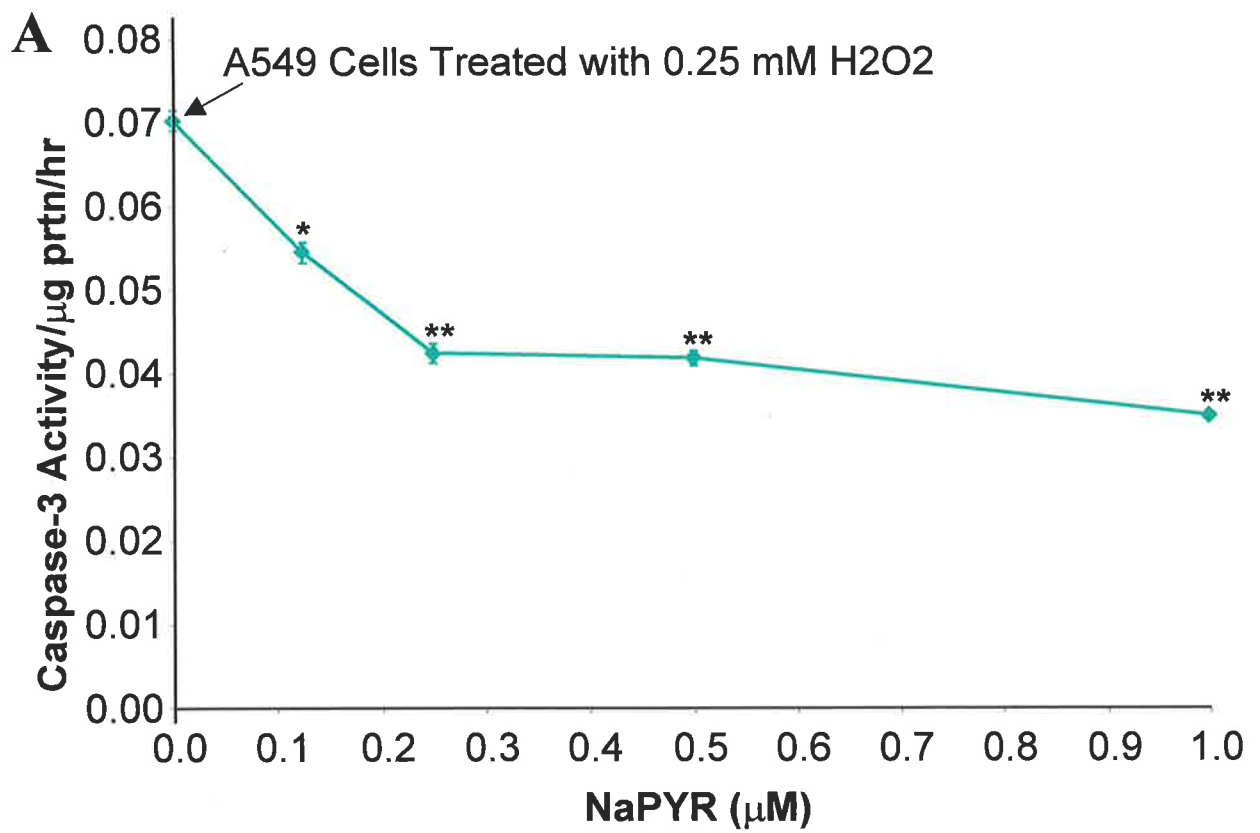
4.4 DISCUSSION

The studies reported in this chapter are the first to show that intracellular Zn can be modulated in REC *in vitro* to strongly influence caspase activation and morphological changes of apoptosis.

The major findings of these experiments chapter are: 1) treatment with the Zn chelator TPEN rapidly increases activation of caspase-3 and 6, 2) primary AEC had higher levels in caspase-3 activity both in the control state and after induction of apoptosis than the malignant NCI-H292 and A549 cell lines, 3) Zn depletion enhanced the susceptibilty of respiratory epithelial cell to the oxyradical H_2O_2 resulting in a synergistic increase in caspase-3 activation and 4) treatment with the Zn ionophore NaPYR and exogenous $ZnSO_4$ suppressed caspase-3 activation by greater than 50% in all cell types.

In Chapter 3, it was proposed that one of the major functions of apical labile Zn in the ciliated AEC was as a cytoprotective agent which may have a direct effect on the regulation of cell death by apoptosis and perhaps also necrosis. It is therefore interesting to mention that a recent publication from this laboratory has reported that PC3 protein, the zymogen form of the major executioner enzyme in apoptosis caspase-3 (as detected by immunocytochemistry) was found within the same apical region as labile intracellular Zn in human tracheobronchial AEC (reviewed in Truong-Tran et al., 2000). The experiments reporting this observation were part of an honours thesis by Miss. Joanne Carter in our laboratory. This observation is also similar to that of Krajewska and colleagues who were the first to report a higher level of procaspase-3 within bronchial epithelium and limited levels within alveolar epithelium of human fixed tissues (Krajewska et al., 1997).

One of the interesting findings reported in this chapter is the rapid activation of caspase-3 occurring 1.5 h after the addition of the TPEN. Furthermore, this increase in caspase-3 activity was found to be concentration dependent. These findings, together with the observation that Zn is co-localised with PC3 protein, suggests that labile intracellular Zn plays an important role in stabilising and regulating the activation of this protein. TPEN may directly remove Zn ions which would normally be suppressing the activation or the catalytic activity of these cytoplasmic caspases. Zn depletion by TPEN was also able to induce morphological changes consistent with apoptosis, such as chromatin condensation and the formation of apoptotic bodies in primary ciliated cells (as detected by Hoechst dye #33342). Future studies looking at the levels of Zn in PC3 protein before and after Zn depletion are now needed to confirm that Zn depletion directly induces caspase-3 activation. In order to investigate this, a technique which will enable measurement of Zn in these enzymes now needs to be developed. However, immunoprecipitating PC3 protein and AC3 protein in Zn depleted cells should be informative. Another caspase strongly activated in the Zn depleted REC used was caspase-6. Caspase-6 has been reported to be both an initiator and an effector caspase (Earnshaw et al., 1999; Takahashi et al., 1996), however in the experiments described in this chapter, caspase-6 was activated relatively late (3 h after TPEN treatment) after caspase-3 and may have been required during the effector phase where it cleaves lamin proteins within the nuclear membrane leading to nuclear collapse (Takahashi et al., 1996). The induction of both caspase-3 and 6 in the Zn depleted respiratory cells is consistent with other models of apoptosis (Takahashi et al., 1996). The model used in this chapter was unable to detect increases in the initiator caspases 1, 2, 4, 5 and 9 in the Zn depleted cells tested. One possible explanation is that these particular

151

enzymes could be absent (with the exception of caspase-1 which is involved in inflammation), or are in concentrations which were undetectable in primary sheep ciliated and NCI-H292 epithelial cells.

In the experiments described in this chapter, the oxyradical H_2O_2 was used at physiological concentrations (range 0.125 - 0.5 mM) similar to those applied by Goldkorn et al (Chan & Goldkorn, 2000; Goldkorn et al., 1998). At the time when this project was started the evidence for induction of apoptosis in REC by H_2O_2 was unclear and caspase activation in REC treated with H_2O_2 had not yet been investigated. The results described in this chapter have shown that H_2O_2 at the concentrations tested did not significantly induce caspase-3 activation in NCI-H292 while A549 cells treated with H_2O_2 had significantly increased caspase-3 levels. These levels were however not as great as in the primary ciliated AEC. In my Honours thesis, I reported that NCI-H292 had double the intensity of Zinquin fluorescence as did A549 cells suggesting twice as much labile intracellular Zn. The high content of labile Zn within NCI-H292 cells may therefore protect these cells from damage by oxidative stress. The results presented in Chapter 3 of this thesis show a significantly high level of labile Zn within primary tracheobronchial AEC and tissues and it was speculated that this labile Zn had an enhanced protective effect. However, the results reported in this chapter have shown that the same primary sheep ciliated cells also had the highest basal caspase-3 activity levels (greater than 10 times the control caspase-3 levels than the malignant cell lines per weight of protein). One possible explanation for the increased levels of caspases observed is that the primary sheep ciliated AEC used were more exposed to oxyradicals in the environment and are more vulnerable to toxin induced injury.

In the *in vivo* enivironment, these cells may have been primed to respond to cell damage rapidly by inducing caspase-3 activation. Furthermore, these cells are primary and not transformed, hence they are less likely to be resilient to apoptosis than the malignant A549 and NCI-H292 cells since it is well known that cancerous cells have lower levels of apoptosis (Allan et al., 1992). To test this hypothesis, one should compare primary AEC with primary alveolar epithelial cells.

A major finding was the synergistic increase in caspase-3 activation in REC treated in combination with TPEN and H_2O_2. Both A549 and NCI-H292 cells had a synergistic increase in caspase-3 activity when treated with both H_2O_2 and TPEN while the primary cell had an increase in caspase-3 which trended towards synergism. These results suggest that the two pathways triggered facilitate each other. The first speculation is that H_2O_2 may have signaled a cellular pathway which is responsible for inducing enzymes which trigger ceramide synthesis (i.e sphingomyelin/ceramide pathway), warning the cells that they are damaged. However, this signal may have been insufficient to completely activate the biochemical pathways of apoptosis. Recent studies have reported that induction of apoptosis with H_2O_2 also results in a depletion of the anti-oxidant glutathione (Lavrentiadou et al., 2001) which also leads to ceramide production and apoptosis. Whether H_2O_2 influences labile intracellular Zn levels in the same way, as gluathione remains to be determined. H_2O_2-induced intracellular Zn depletion may also faciliate the activation of caspases in these damaged cells forcing them into apoptosis. However this now needs to be prove. The measurement of other major apoptosis markers such as Bcl-2, Bax, Apaf-1 and other substrates of the caspases

153

ie p21 may provide important insights into the mechanisms governing this synergism.

The close proximity of labile Zn, with PC3 protein and the rapid activation of this enzyme following Zn depletion, raises the question of whether apical cytoplasmic Zn can suppress the induction of this caspase. To further understand how Zn was involved in regulating apoptosis in these cells, the cells were supplemented with exogenous $ZnSO_4$. Firstly, In order to determine the optimal concentration of NaPYR needed, these experiments were conducted in A549 cells. This is due to the limited numbers of primary ciliated cells available and also because NCI-H292 cells did not produce an adequate increase in caspase-3 activation when treated with H_2O_2 alone. Pre-loading cells with Zn was found to significantly decrease (by greater than 50%) caspase-3 levels in all cells treated with H_2O_2 alone or in combination with TPEN. This observation is important as it confirms caspase-3 activation in these experiments is at least partly Zn regulated since Zn depletion by TPEN enhanced caspase-3 catalytic activity while supplementation of Zn by NaPYR with $ZnSO_4$ significantly decreased it almost to those of the control cells. Whether Zn blocks the activation of pro-caspase 3 or the catalytic activity of the already activated caspase 3 in REC now needs to be determined perhaps by using cell free models and recombinant caspase-3 proteins. What is known though is that in non-REC, Zn suppresses the activation of PC3 protein in cell free models (Medina et al., 1997), catalytic activity of recombinant caspase-3 and 6 (Maret et al., 1999; Perry et al., 1997; Stennicke & Salvesen, 1997), and pro-caspase-9, which is essential for the activation of the apoptosome (Wolf & Eastman, 1999). From these studies it appears that Zn can inhibit apoptosis by suppressing caspase activation and down stream events of apoptosis,

however the precise step in the caspase cascade that is inhibited by Zn remains unclear and now needs to be determined. One could speculate that inhibition by Zn is mediated by the IAP proteins. As previously mentioned, XIAPs are potent caspase inhibitors containing Zn finger BIR domains which directly control caspase activation (Shi, 2002). Hence alterations in the intracellular Zn levels of cells may trigger the activation or suppression of the XIAPs. For example, adequate (normal cell) or increased levels of Zn (supplemented cells) may trigger XIAPs to bind to the caspases hence inhibiting apoptosis and therefore promoting cell survival. Decreased levels of Zn (ie. in Zn deficiency) may remove the Zn atoms within the BIR domains and inactivate the XIAPs therefore allowing the caspases to be activated and apoptosis to occur. Hence future studies are required to determine whether Zn depletion and supplementation influences XIAP activity in the *in vitro* Zn studies described above.

The *in vitro* experiments described in this chapter with primary and malignant REC support the hypothesis that Zn deficiency renders the airway epithelium more susceptible to damage by apoptosis-inducing agents such as H_2O_2. However, once caspase-3 has been activated and XIAP are suppressed in a damaged cell, then that cell is more likely to be committed to apoptosis, regardless of the presence of Zn. Zn will suppress the death of those cells which have not yet had their caspase-3 enzymes activated. On the other hand, supplementing cells with exogenous Zn *in vitro*, and possibly also *in vivo*, may decrease the susceptibility of cells and tissues to spontaneous or toxin-induced apoptosis, even when the cells apparently have a normal Zn status. Finally, Zn is clearly an important factor in the regulation of apoptosis as demonstrated by these results, but it is not the only factor involved. Future studies are now required to investigate the

interplay between Zn and other known regulatory factors involved i.e. Bcl-2, growth factors and cell death genes.

The aim of this chapter was to elucidate the role of Zn in regulating caspase activation in AEC. While this study does show how Zn may influence caspase activation and apoptosis it requires further investigations into the direct mechanisms involved. Some limitations of this study are the inability to determine what are the relevant pools of Zn directly responsible for caspase processing, how much Zn is being altered by a given concentration of TPEN or NaPYR, and whether these alterations are physiological. Furthermore, the relevance of the *in vitro* experiments now need to be better understood by conducting similar experiments in an *in vivo* rodent model of hyperoxia and perhaps examining the apoptotic rates of epithelial cells from the lungs. These animals could then be Zn supplemented and apoptotic rates compared with their Zn deficient counterparts since the greatest oxidative damage in lungs has been reported to occur in animals made Zn deficient (Taylor & Bray, 1991).

In conclusion, the results reported in this chapter have provided some insights into: which caspases are regulated in response to Zn depletion and H_2O_2 in AEC; the suppression of caspase-3 by Zn supplementation, and the more than additive increase in caspase-3 activity due to the combination of TPEN and H_2O_2. These results provide a foundation for further understanding the physiology of Zn in airway epithelium and may point to a hitherto unrecognised role for Zn in the survival of REC. To take these studies one step further, there was a need to determine whether changes in respiratory epithelial cell Zn status can influence inflammatory respiratory diseases where oxidative damage is central to their

pathogenesis. To investigate this, a murine model of allergic airway inflammation was established and is described in Chapter 5.

Some of the results reported in this chapter are in the following published manuscripts:

2. Intracellular zinc depletion induces caspase activation and p21 Waf1/Cip1 cleavage in human epithelial cell lines (Chai et al., 2000).

3. Visualization of labile zinc and its role in apoptosis of primary airway epithelial cells and cell lines (Truong-Tran et al., 2000).

CHAPTER 5
ESTABLISHMENT OF A MURINE MODEL OF ASTHMA

CHAPTER 5 ESTABLISHMENT OF A MURINE MODEL OF ALLERGIC AIRWAY INFLAMMATION

5.1 INTRODUCTION

To investigate the mechanisms controlling the pathogenesis of asthma, *in vitro* and *in vivo* experimental models have been developed which can be used to identify factors that influence or modulate the inflammatory process. These models are also vital for studying the distinct physiological and morphological abnormalities noted in the airway epithelium of asthmatics. Knowledge gained from these studies can be used to better understand the pathogenesis of human asthma.

Originally, animal models of "asthma" were developed to measure only airway responses to antigen and/or mediators (e.g histamine) and the effects of new drugs on AHR, mainly in guinea pigs and rabbits (Cheng & Townley, 1982; Shampain et al., 1982). However, during the past decade many researchers have chosen to use murine models of allergic asthma to also investigate the pathways governing eosinophilia (MacKenzie et al., 2001; Pope et al., 2001), cytokine regulation and production (Tang et al., 2001), recruitment of inflammatory cells (Burr et al., 2001), goblet cell hyperplasia (Zuhdi Alimam et al., 2000) and the histopathological changes which occur in the airway epithelium (Gajewska et al., 2001). One major advantage of using this animal is that the immune responses and genetics of mice are better characterised than any of the other species mentioned. Furthermore, a wider range of molecular and immunological probes such as monoclonal antibodies directed towards most mouse cytokines, immunoglobulins,

and T cell markers have been developed for this species (reviewed in Leong & Huston, 2001).

Nevertheless, it is recognised that no animal model accurately represents the human disease as human asthma is complex and not all of the features of human asthma are reproduced in the one animal system. In view of the alveolitis and lack of true airway remodeling in some murine models of asthma, these should be referred to more accurately as models of acute allergic bronchopulmonary inflammation rather than true models of human asthma (Kumar, 2001). The limitations of these allergic murine models are discussed further in section 5.4.

The aim of the experiments in this chapter was to set up a previously reported murine model of allergic airway inflammation, which could be used in subsequent experiments to investigate the physiology of Zn in normal and allergic airway tissue. The mice used in these experiments are referred to throughout the rest of this thesis as group 1 since tissues used from these mice were also used in experiments described in Chapter 7.

5.2 METHOD

5.2.1 Animals Used

Specific pathogen free 6 week old female BALB/c mice were purchased from the University of Adelaide Animal Center, Adelaide, South Australia, fed New Joint Stock Ration Normal mouse food and housed as described in section 2.12.1.

5.2.2 Sensitisation and Aerochallenge of BALB/c Mice with Ovalbumin (OVA)

In experiments described in this chapter, allergic airway inflammation was induced in BALB/c mice using a 30 day protocol outlined in section 2.12.2, which involves sensitising and aerochallenging BALB/c mice with ovalbumin (an antigen to which they give a high IgE response). Control mice were treated with 0.9% saline only. Figure 5.1 shows the equipment used for nebulisation of the mice. Plastic two tiered inserts (panel A) were placed within a 300 mm diameter glass desiccator (panel B) to create a nebulisation chamber (panel C). These inserts were 255 mm in diameter with 5 mm holes drilled into the plastic to allow even airflow within the chamber. Four plastic blocks were placed on the rim of the desiccator to prevent a tight seal when the lid was placed on top of the chamber, thereby enabling adequate ventilation for the mice. Figure 5.2 panel A illustrates the protocol used while panel B shows the nebulisation of mice in the chamber.

A range of tissues such as blood, BALF and lung tissue were collected as outlined in section 2.12.3, 2.12.4, and 2.12.5, respectively and the methods by which they were obtained are illustrated in Figure 5.3.

5.2.3 Assessment of Blood Samples and Bronchoalveolar Lavage Fluid

Blood and BALF samples were stained with May Grunwald and Giemsa stain and leukocyte diferential counts determined as described in section 2.12.3 and 2.12.4, respectively. Cells were identified by standard morphological criteria with a total of 800 leukocytes quantified per mouse using a 40x magnification lens and are expressed as percentages. In some cases, BALF cell counts are expressed as total cells/ 40x field of view.

Figure 5.1: Construction of a Nebulisation Chamber

Figure shows the equipment used for nebulisation of mice which consisted of 1) a set of two tiered perspex plastic inserts (255 mm diameter) with evenly spaced holes of 5 mm drilled into the plates (panel A) which allow for even airflow within the chamber and 2) a glass desiccator of 300 mm diameter. Panel C shows the completed nebulisation chamber.

A

B

C
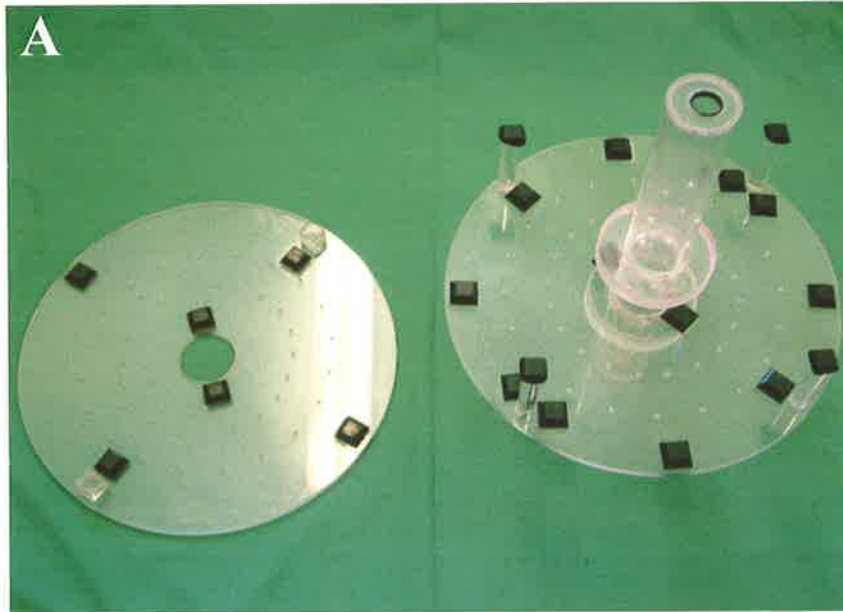
Figure 5.2: Protocol for Ovalbumin Sensitisation and Subsequent Ovalbumin Aerochallenge by Nebulisation

Mice were induced to have allergic airway inflammation by using the following protocol.

Panel A: Six week old BALB/c mice were i.p sensitised with 50 μg OVA/1ml alhydrogel in 0.1% saline on day 0 and a second booster i.p given on day 12. Mice were subsequently aerochallenged by nebulisation at 30 min intervals, 3 times a day with 1% OVA in 0.9% saline on days 19, 21, 23, 25, 27 and 29, sacrificed on day 30 and tissues collected.

Panel B: Nebulisation of BALB/c mice was performed in a glass desiccator using a sidestream nebuliser (*).

A

50μgOVA/ ml alhydrogel
in 0.9% SAL

1% OVA in 0.9% Saline

i.p sensitisation
of 6 wk female
BALB/c mice

i.p booster

Sacrifice

Nebulisation
(3 x 30min)

0 2 4 6 8 10 12 14 16 18 20 22 24 26 28 30

DAYS OF PROTOCOL
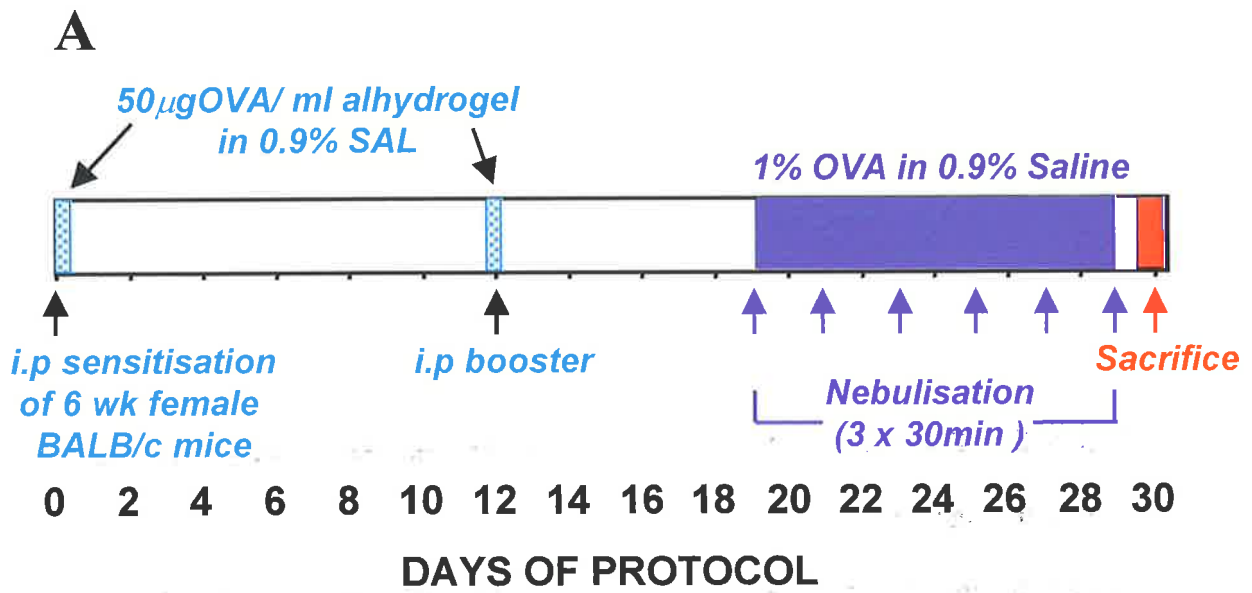
B

Figure 5.3: Collection of Samples

A range of specimens were collected from SAL and OVA-treated mice.

Panel A: Blood was collected from an anesthetised mouse by cardiac puncture using a 23 gauge needle which was inserted into the ventricular wall of the heart and blood withdrawn via a 1 ml syringe.

Panel B: Collection of bronchoalveolar lavage fluid (BALF) was performed on mice using a blunted $18^{1/2}$ gauge needle inserted into the trachea and connected to a 1 ml syringe for recovery of fluid. A total of 2 ml of 1x HBBS solution was injected down the trachea and approximately 1.7 ml recovered.

Panel C: To obtain good quality frozen tissue sections, lungs were inflated with approximately 1 ml of optimum cooling temperature medium (OCT). The lungs were then tied off with a piece of cotton and the lobes excised and processed for frozen tissue (*not shown*).
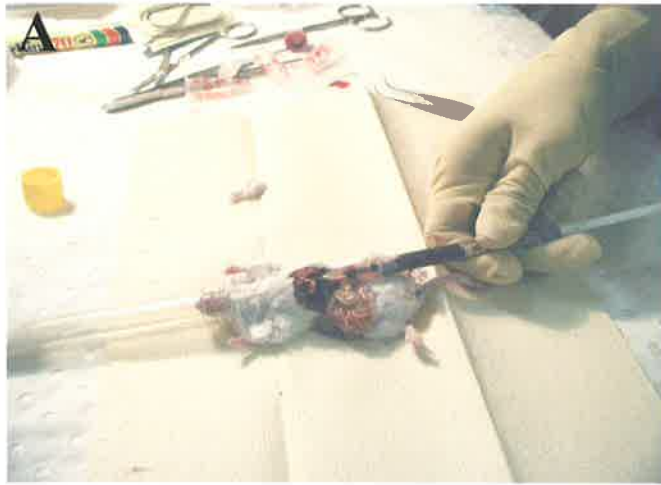
5.2.4 Assessment of Lung Tissue Histology

The lung tissues were mophologically assessed as outlined in section 2.12.6 by staining with Alcian Blue/Periodic Acid-schiff for assessment of mucus cells, Charbol's chromotrophe haematoxylin for detection of eosinophils and Weigert's and van Gieson's for collagen deposition. Tissue eosinophils and mucus containing cells were examined and quantified using a 100x oil immersion and a 40x normal objective lens, respectively. Eosinophils were counted in the epithelium and subepithelial tissue (2 mm^2 area directly beneath the epithelial basement membrane) in 6 airways of 3 different mice from both the SAL-treated and OVA-treated groups and are expressed as mean ± SEM eosinophils/High powered field (100xHPF). On the other hand, mucus-containing cells were counted within 6 fields of peripheral airway epithelium of 3 different mice from both the SAL-treated and OVA-treated groups and are expressed as mean ± SEM mucus cells/HPF.

5.2.5 Assessment of IL-5 and IgE Levels

IL-5 and IgE levels were determined in serum and BALF samples using the methods discussed in section 2.12.7. Determination of IL-5 levels was performed using the Endogen Mouse Interleukin-5 (IL-5) ELISA kit (Endogen, Maryland, USA) to quantify IL-5 levels in BALF (neat) and serum (1:200 dilution) samples and the resultant concentrations expressed as pg/ml. IgE levels were determined using the murine OptIEA™ IgE ELISA kit (PharMingen, California, USA) in BALF (neat) and serum (1:20 dilution) samples and the resultant IgE concentrations expressed as ng/ml.

The data reported in this chapter were derived from the collation of 2 to 4 separate experiments, which contained 10 mice per group. Data are expressed as means ± standard error of the mean (SEM) and the level of statistical significance was determined by the students *t-test*. Differences were considered statistically significant at p < 0.05, unless otherwise stated.

5.3 RESULTS

A number of differences were observed between SAL and OVA-treated mice and these are summarised in Table 5.1 and discussed in detail below.

5.3.1 Histopathological Changes in OVA Sensitised and Challenged BALB/c Mice

As depicted by Figure 5.4, panels D, E & F, sensitisation and challenge of BALB/c mice with OVA induced marked histopathological changes consistent with allergic airway inflammation in comparison to mice treated with saline which had normal airway epithelial morphology (Figure 5.4, panel A, B & C). Lung tissue in the OVA-treated mice was characterised by thickening of the epithelium (panel D, *), a marked infiltration of inflammatory cells into the lamina propria and the epithelium (panel D, **), thickening of the epithelial basement membrane due to enhanced collagen deposition (panel E), and increased numbers of mucus containing cells (panel F).

Table 5.1 Summary of Indices of Inflammation

[1]Indices of Inflammation, (n = # mice used)	SAL-Treated	OVA-Treated	[4]p-value
Eosinophils			
Blood Eosinophils *(n = 10)*	[3]3.0 ± 0.4 %	13.8 ± 1.2 %	< 0.005
BALF Eosinophils *(n = 5)*	ND[2]	77.1 ± 3.3 %,	
Tissue Eosinophils *(n = 3)*			
Epithelial	0.2 ± 0.2 eosinophils/HPF	6.1 ± 1.5 eosinophils/HPF	< 0.005
Subepithelial	0.3 ± 0.3 eosinophils/HPF	46.1 ± 5.5 eosinophils/HPF	< 0.005
Mucus Containing Cells			
Epithelial *(n = 3)*	0.3 ± 0.3 mucus cells/HPF	137.6 ± 11.6 mucus cells/HPF	< 0.005
IL-5 Levels			
BALF (n = 5)	1.6 ± 0.005pg/ml	32.3 ± 0.1 pg/ml	< 0.005
Serum (n = 10)	441.8 ± 3.1pg/ml	439.7 ± 3.9pg/ml	< 0.5
IgE Levels			
BALF (n = 5)	3.3 ± 0.4ng/ml	10.1 ± 3.3 ng/ml	< 0.05
Serum (n = 10)	45.0 ± 2.8pg/ml	374.2 ± 51.8ng/ml	<0.005

[1] The numbers of eosinophils, mucus cells and levels of IL-5 and IgE in SAL and OVA-treated mice are shown.

[2] ND; there were insufficient cells to determine the differential count in the SAL-treated mice.

[3] Data represents mean ± SEM.

[4] Significant differences between SAL and OVA-treated mice.

Figure 5.4: Histopathological Changes in SAL and OVA-Treated Mice

Figure depicts the histopathological changes present 24 h after the final nebulisation at day 30. Tissues from SAL (LHS panel) and OVA (RHS) treated mice stained with H&E for routine analysis (top panel), Weigert's hematoxylin and van Gieson's stain (middle panel) and Alcian Blue/Periodic Acid Schiff's base (PAS) solution (bottom panel).

Note the epithelial thickening (black arrows, panel D, E & F) and infiltration of inflammatory cells in the subepithelial tissue of OVA-treated mice (*, panel D, 250x initial magnification). These mice also had enhanced collagen deposition beneath the epithelial basement membrane (yellow arrows, panel E, 500x initial magnification) and mucus cell hyperplasia within the epithelium (PAS positive cells, panel F, 500x initial magnification). Alveolitis was also observed in the OVA-treated mice (**, panel B). SAL-treated mice lacked these histopathological changes (panel A, B & C, 500x initial magnification).

SAL-Treated | OVA-Treated

H & E

A | D

Weigerts/
Van Geison

B | E

Alcian Blue/
PAS

C | F
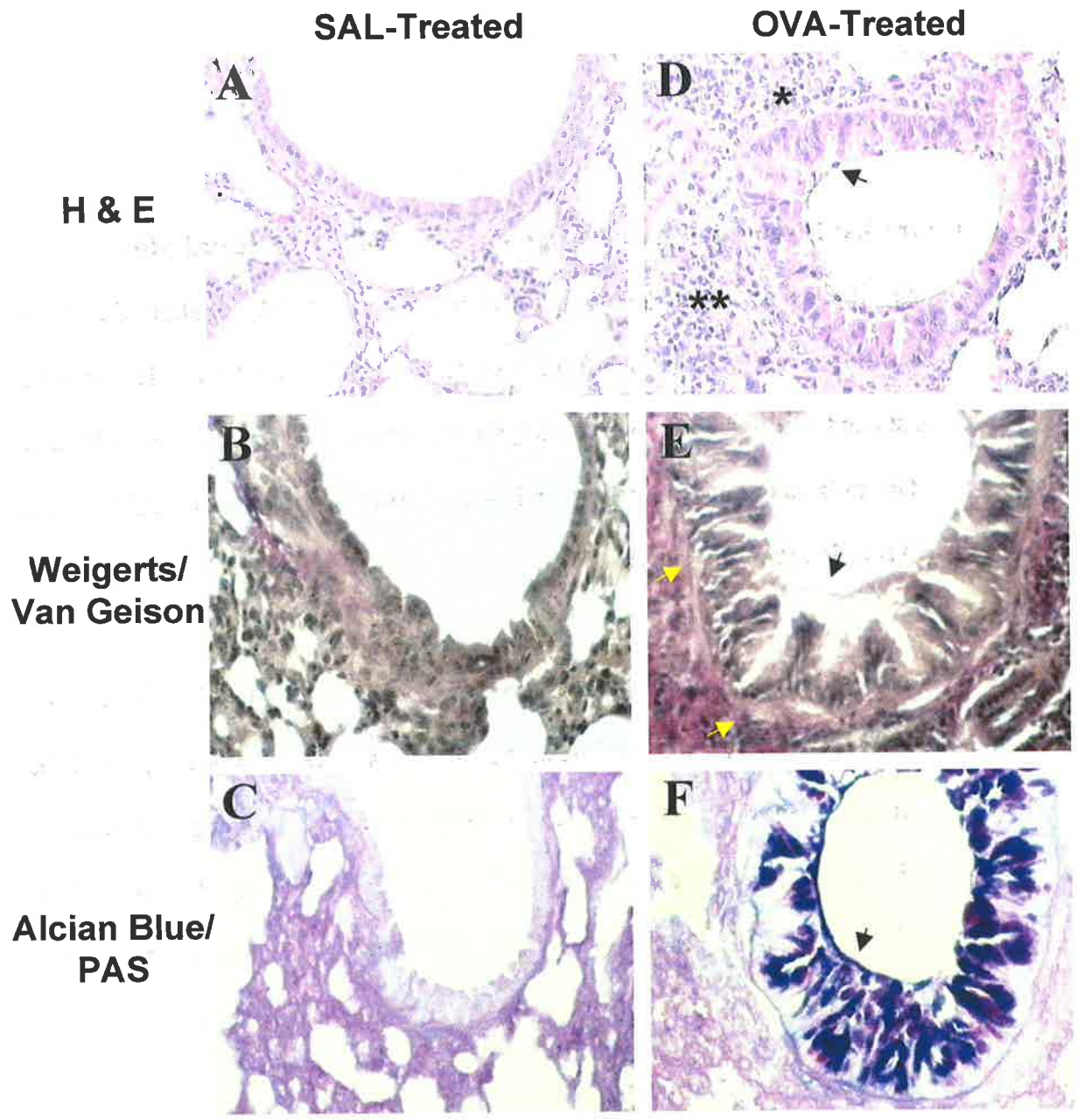
5.3.2 Allergic Airway Inflammation Enhances Blood, BALF and Tissue Eosinophil Numbers in BALB/c Mice

One major feature of allergic airway inflammation is the substantial increase in eosinophil numbers in a variety of tissues. As depicted in Figure 5.5, OVA-treated mice had increased eosinophils in blood (panel E), BALF (panel F) and lung tissue (panel G & H) when compared to the SAL-treated mice (panels A to D).

Figure 5.6 graphs the data quantified from blood, BALF and lung tissue of SAL and OVA-treated BALB/c mice. Firstly, as shown in Figure 5.6 panel A, OVA-treated mice had a significantly higher percentage of blood eosinophils at 13.8 ± 1.2 %, compared with the SAL-treated mice which had $3.0 \pm 0.4\%$ ($p < 0.005$). On the other hand, SAL mice had a higher percentage of neutrophils ($20.6 \pm 1.3\%$ vs $14.2 \pm 2.0\%$ in the OVA-treated mice, $p < 0.005$) and monocytes ($1.7 \pm 0.8\%$ vs $0.4 \pm 0.2\%$ in OVA-treated mice, $p < 0.005$) than the OVA-treated mice but no significant difference in lymphocyte percent ($74.0 \pm 1.6\%$ vs $71.6 \pm 2.3\%$).

Secondly, in panel B, BALF collected from the OVA-treated mice had a significantly higher number of inflammatory cells (327.5 ± 41.1 total cells/ 40x field of view, $p < 0.0005$) than the SAL-treated mice (17.40 ± 4.2 total cells/ 40x field of view). For the OVA-treated mice, $77.1 \pm 3.3\%$ of these cells were eosinophils, 12.25 ± 3.4 % were lymphocytes, 5.8 ± 0.9 % were macrophages and $4.9 \pm 0.9\%$ were neutrophils. BALF of the SAL-treated mice contained only epithelial cells (63.8 ± 18.6 %) and macrophages (36.2 ± 9.5 %) present as

Figure 5.5: Presence of Eosinophilia in OVA-Treated Mice

Eosinophilia is a distinct characteristic of allergic airway inflammation and can be detected in blood (panel E), BALF (panel F) and tissue (epithelial tissue; panel G and subepithelial; panel H) samples of OVA sensitized and challenged mice (RHS).

Panel A & E: Image of a typical blood smear from SAL (LHS) and OVA (RHS) treated mice. Blood smear from SAL-treated mice (panel A) contained mainly lymphocytes (blue arrow) and neutrophils (black arrow) while blood from OVA-treated mice (panel F) had increased numbers of eosinophils (red arrow). Note the distinct red granules found within the cytoplasm of the cells. 2500x initial magnification.

Panel B & F: Eosinophils were significantly increased in the BALF of OVA-treated mice and are depicted by the red arrows in panel F. BALF taken from SAL-treated mice contained mainly macrophages (green arrow, panel B). 2500x initial magnification.

Panel C, D, G & H: Increased numbers of infiltrating eosinophils were noted in the subepithelia (within red circles, panel G) and lamina propria (within red circles, panel H) of OVA-treated mice. Note the paucity of eosinophils in the airway tissue of SAL-treated mice (panel C & D). 2500x initial magnification.

SAL Treated
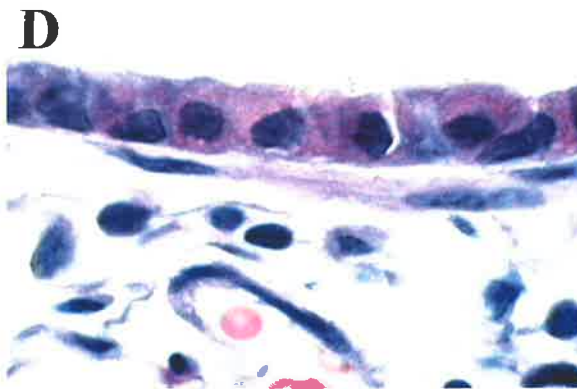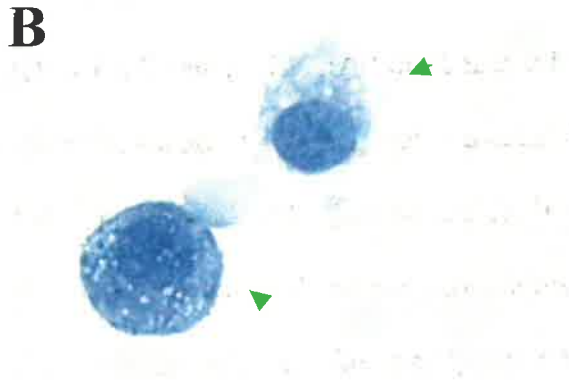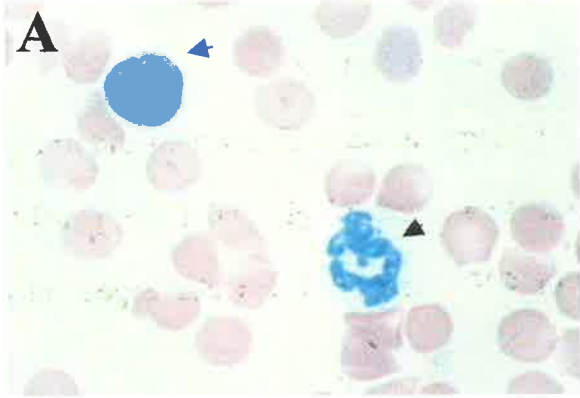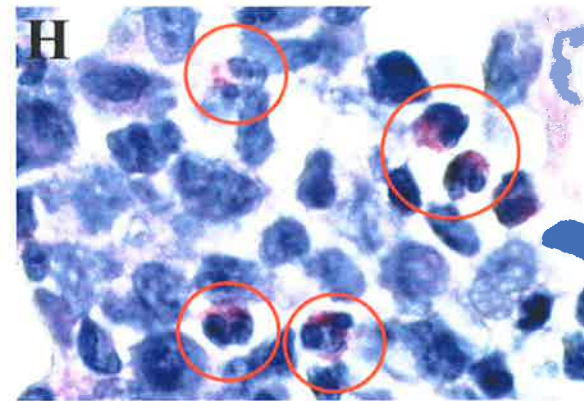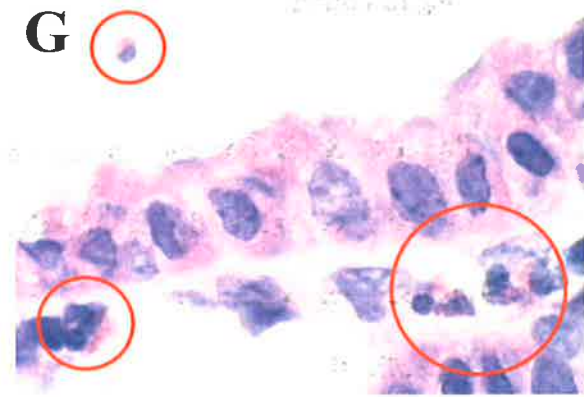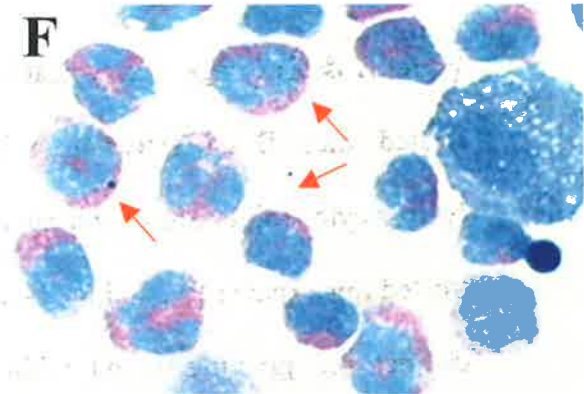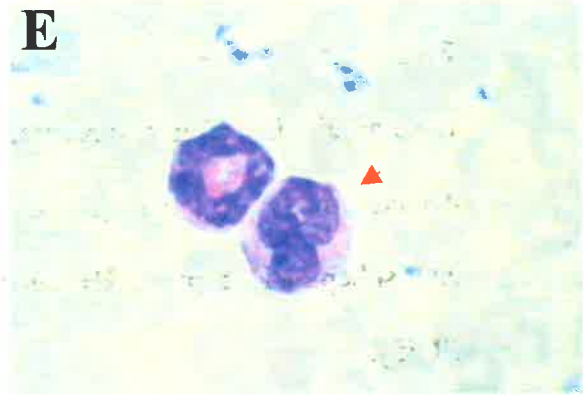
OVA Treated

Figure 5.6: Quantification of Eosinophil Numbers in Tissues of SAL and OVA-Treated Mice

Eosinophil numbers were quantified in blood (panel A), BALF (panel B) and airway tissue of SAL (light blue columns) and OVA (navy columns) treated BALB/c mice.

Panel A: Figure shows the blood differential leukocyte counts. Note the significant increase in eosinophil numbers in the OVA-treated mice. Data represent means ± SEM of 10 mice from 2 separate experiments. Significant differences refer to comparisons between SAL and OVA-treated mice: ** $p < 0.005$.

Panel B: BALF taken from SAL-treated mice had a lower leukocyte count than that of the OVA-treated mice. Data represent means ± SEM of 5 mice from 2 separate experiments. Significant differences refer to comparisons between SAL and OVA-treated mice: ** $p < 0.005$.

Panel C: BALF taken from OVA-treated mice had a substantial number of inflammatory cells, consisting mainly of eosinophils. Data represent means ± SEM of 5 mice from 2 separate experiments. Significant differences refer to comparisons between SAL and OVA-treated mice: ND; there were insufficient cells to determine the differential count in the SAL-treated mice.

Panel D: OVA-treated mice had increased numbers of eosinophils within the epithelium and subepithelial regions when compared with the SAL-treated mice. Data represent means ± SEM (n = 36 airways per group) 2 separate experiments. Significant differences refer to comparisons between SAL and OVA-treated mice: ** $p < 0.005$.

A Peripheral Blood

B BALF

C BALF

D Tissue Eosinophils
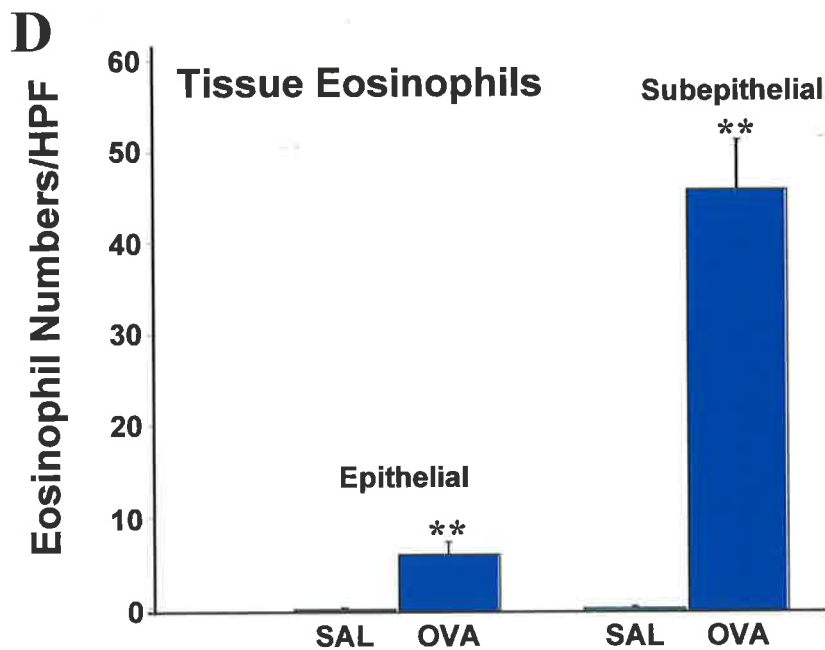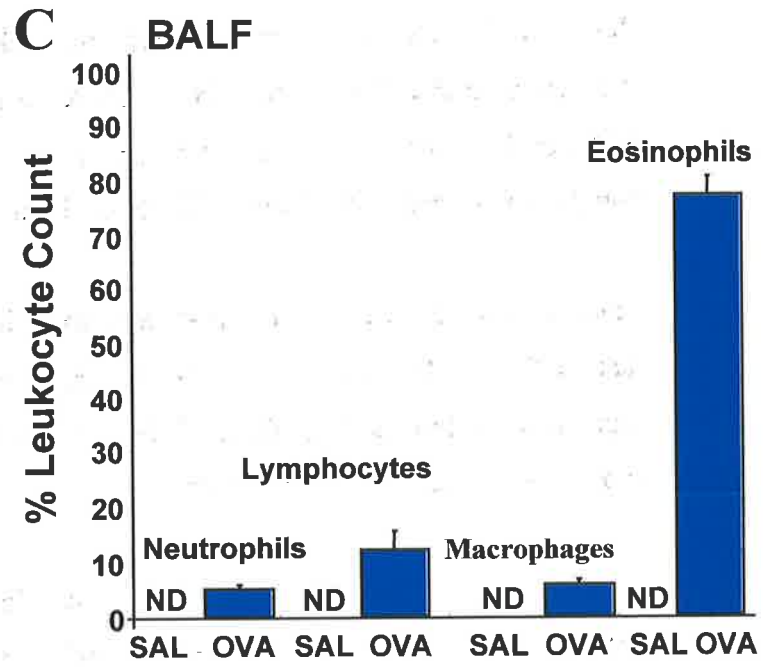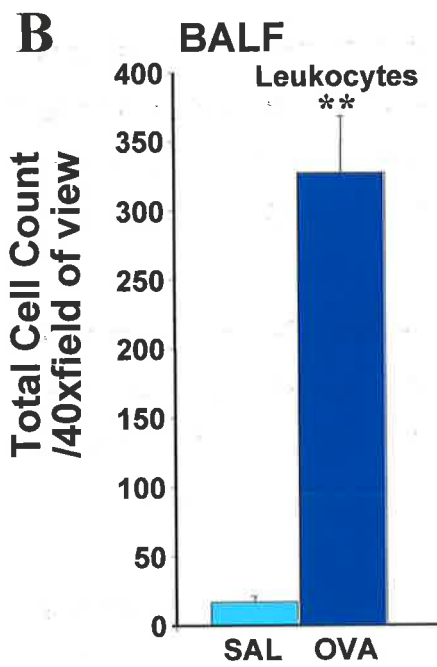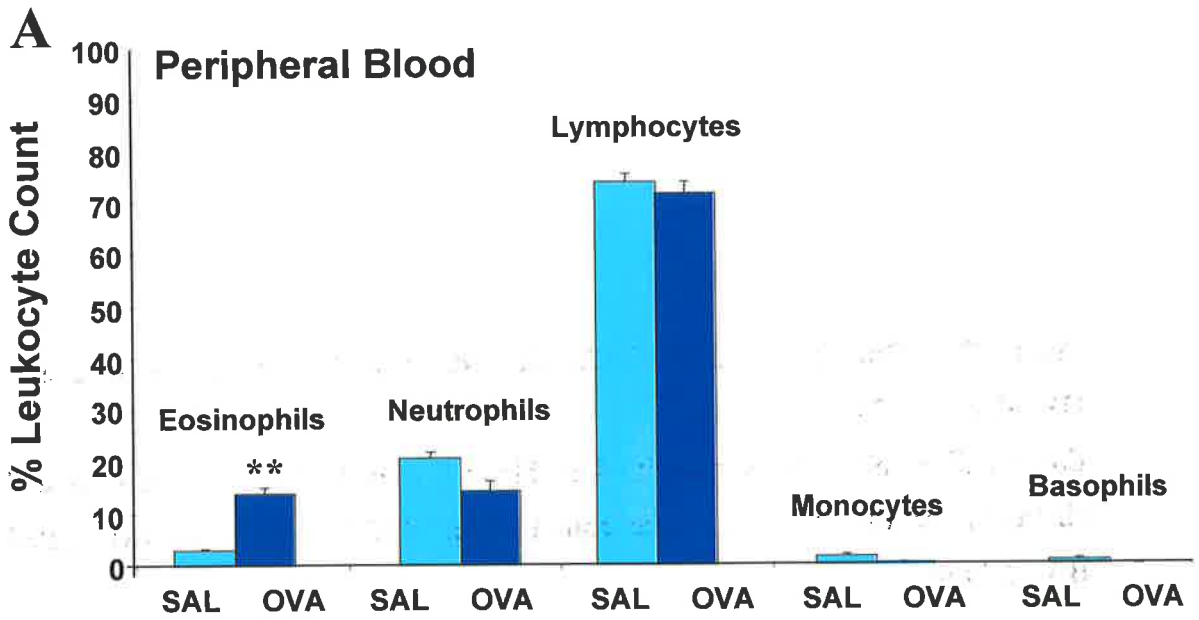
detected by morphological criteria. Since the number of inflammatory cells present was very low, a differential leukocyte cell count could not be determined.

Thirdly, consistent with an increase in blood eosinophils, there was a significant rise in the number of infiltrating tissue eosinophils around the airways of OVA-treated mice. These mice had an average of 6.1 ± 1.5 eosinophils/100xHPF within the epithelium and 46.2 ± 5.5 eosinophils/100xHPF in the subepithelial region when compared to the SAL mice which had an average of 0.17 ± 0.22 eosinophils/100xHPF ($p < 0.005$) within the epithelium and 0.28 ± 0.27 eosinophils/100xHPF in the subepithelial region ($p < 0.005$).

These results indicate that the induction of allergic airway inflammation by OVA treatment produced a significant eosinophilia which was widespread throughout the airway wall.

5.3.3 *Mucus Containing Cell Numbers are Increased in OVA Treated BALB/c Mice*

Increase in the numbers of mucus containing cells within the epithelium is a distinct feature of human asthma which results in the overproduction of mucus and the obstruction of the airways. Figure 5.7 shows the prominent presence of Alcian Blue/PAS positive mucus containing cells within the epithelium of the OVA-treated mice (panel B) compared with the paucity of mucus cells in the SAL-treated mice (panel A). In this model, OVA-treated mice had a mean mucus cell count of 137.6 ± 11.6 cells/HPF while the SAL-treated mice had 0.3 ± 0.3 cells/HPF (panel C, $p < 0.005$).

Figure 5.7: Quantification of Mucus cell numbers in Lung Tissue of SAL and OVA-Treated Mice

Mucus cell hyperplasia was detected in OVA sensitized and challenged BALB/c mice.

Panel A & B: Panels show typical images of lung tissue from SAL (A) and OVA (B) treated lung tissue stained with Alcian Blue/PAS. Note the prominence of PAS positive mucus cells within the airway epithelium of OVA-treated mice. 500x initial magnification.

Panel C: Mucus cells were counted within the airway epithelium of SAL (light blue column) and OVA-treated mice (navy column). OVA-treated mice had significantly increased numbers of mucus cells within the epithelium than the SAL-treated mice. Data represent means $\pm$ SEM (n = 36 airways per group). Significant differences refer to comparisons between SAL and OVA-treated mice: ** $p < 0.005$.

SAL-Treated

OVA-Treated

A

B

C

Mucus cells

Mucus Cell numbers/HPF

160

140

120

100

80

60

40

20

0

**

SAL

OVA
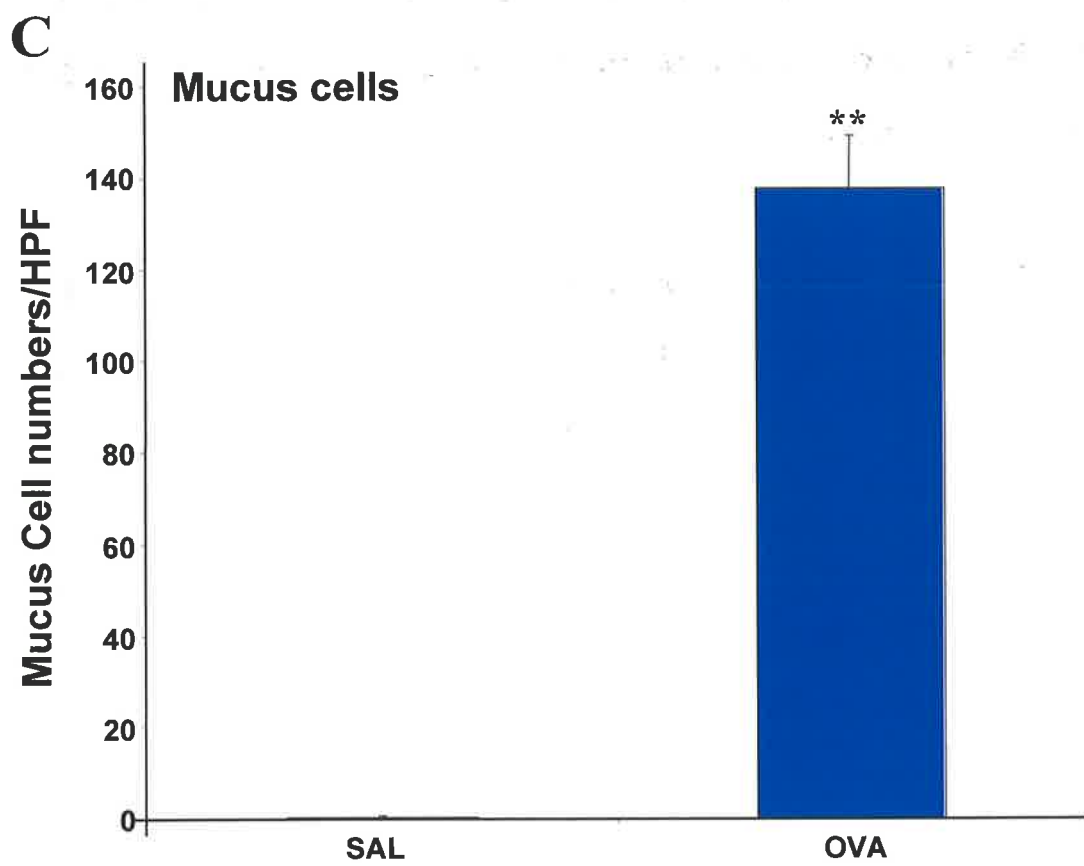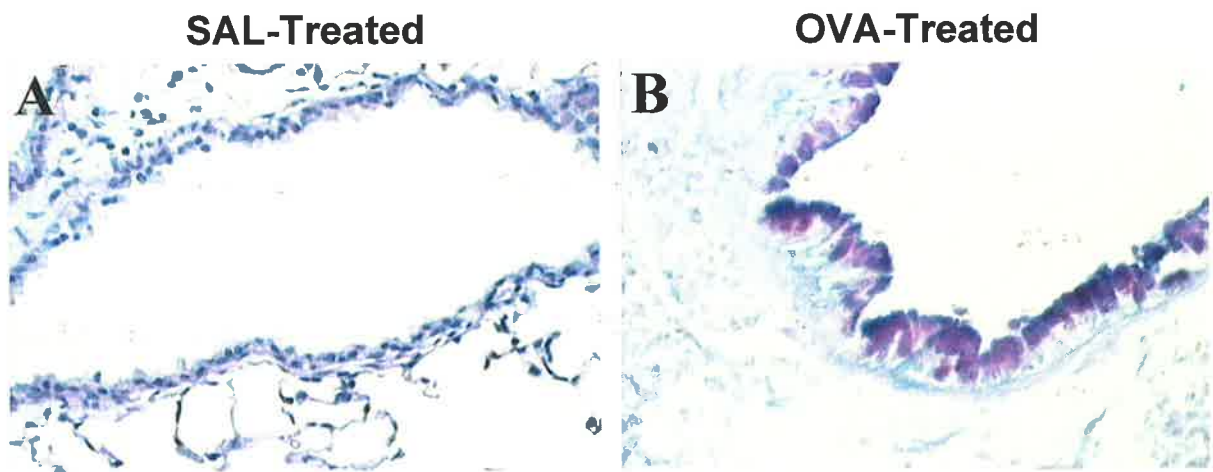
5.3.4 Levels of IL-5 and IgE are Increased in the Serum and BALF of OVA-Treated Mice

IL-5 and IgE levels were determined by ELISA in samples of BALF (n = 5 mice per group were lavaged) and serum (n = 10 mice per group) taken from SAL and OVA-treated mice. For IL-5 and IgE, linear standard curves were obtained (r^2 = 0.99 for ELISA's) and these were used to determine the concentration of IL-5 and IgE in each sample.

As expected, there were significant differences in IL-5 and IgE levels between the OVA and SAL-treated mice. OVA-treated mice had 32.3 ± 0.1 pg/ml of IL-5 in BALF samples, while the SAL-treated mice had 1.6 ± 0.005 pg/ml ($p <$ 0.005). There was however no difference in serum IL-5 levels between the two groups where OVA-treated mice had 439.7 ± 3.9 pg/ml while the SAL-treated mice had 441.8 ± 3.1 pg/ml.

IgE levels were also significantly increased in the OVA-treated mice for both the BALF and serum samples. BALF IgE levels were significantly higher at 10.1 ± 3.3 ng/ml for the OVA-treated mice ($p < 0.05$) compared to 3.3 ± 0.4 ng/ml for the SAL-treated mice. Secondly, serum IgE levels were 7 fold higher for the OVA-treated mice which had 374.2 ± 51.8 ng/ml IgE levels compared with 45.0 ± 2.8 ng/ml for the SAL-treated mice ($p < 0.005$).

5.4 DISCUSSION

Animal models of allergic airway inflammation were originally designed to exhibit major features of human asthma including bronchial eosinophilia and AHR. While acknowledging that these models do not fully reproduce human asthma, they do however provide rsearchers with a system which allows investigation into the pathogenesis of allergic pulmonary inflammation which can then be used to further understand these mechanisms in humans (Herz et al., 1996).

For the experiments described in this chapter a well established murine model of allergic airway inflammation was used (Xiong et al., 1999). Marked eosinophilia was detected in BALF, blood and airway tissues of the allergic OVA-treated mice. Eosinophils are thought to be the key effector leukocytes in human and animal asthma (Bousquet et al., 1990; Pauwels et al., 1997). When activated, eosinophils can release a range of mediators such as eosinophil peroxidase, eosinophil cationic protein, cytokines and chemokines which damage the airway epithelium enhancing the pathogenesis of asthma (reviewed in Reed, 1994). Other features similar to human asthma include a thickened epithelium due to mucus cell hyperplasia, collagen deposition within the basement membrane and marked levels of IL-5 and IgE in BALF and blood samples were also observed. These observations confirm the success of the allergy induction protocol and are similar to the findings reported by others using the same model (Foster et al., 1996; Hamelmann et al., 1997; Oshiba et al., 1996; Tomkinson et al., 2001). The lack of increase in serum IL-5 levels is not surprising since these levels are not normally increased in response to inflammation in these murine models (personal communications with Dr Dianne Webb, JCSMR, ACT).

As previously mentioned, despite the usefulness of these murine models, there are several limitations which also need to be taken into consideration when extrapolating results from this system to human asthma.

Firstly, one major disadvantage is that the pulmonary inflammation generated in these mice is not chronic (Bice et al., 2000). It has been suggested that this inflammation is easily resolved within two to eight weeks after challenge since production of IgE and the level of inflammatory cell infiltrate into the lungs can not be sustained any longer even with prolonged and repeated exposures of the animal to the antigen (Kung et al., 1994; Mathur et al., 1999; Temelkovski et al., 1998). This is very different to the human condition since asthma is an ongoing and chronic disease lasting many years (Bousquet et al., 1990). Furthermore, the increase in mucus containing cells within the epithelium becomes over exaggerated when compared to the human situation (Leong & Huston, 2001).

Secondly, while these models are able to induce some of the characteristics of human asthma e.g. increased levels of eosinophils, specific IgE immunoglobulin and Th_2 cytokines, true airway remodeling is difficult to produce in the tissues of these mice e.g. subepithelial fibrosis, increased mucus secretory glands within the lamina propria, increased vascularity of the airway wall and smooth muscle cell hypertrophy/hyperplasia. Furthermore, the inflammatory response observed is also coupled with a component of alveolitis which is not present in human asthma (Kumar & Foster, 2001). As a suggestion by Associate Professor Rakesh Kumar (UNSW, Australia), a sidestream nebuliser (Fisher and Paykel, Sydney, Australia). which produces smaller particles >3 μm (Fisher and Paykel, Sydney, Australia) was used for the experiments reported in Chapter 6 to minimise the level of

alveolitis present in this model. Similar findings of eosinophilia and increased mucus cells which were reported in this chapter, were also observed with the sidestream nebuliser in Chapter 6 but with a lesser degree of alveolitis.

Thirdly, to produce an allergic inflammatory response, mice are intraperitoneally immunised with antigen, a route of sensitisation which does not occur for humans. Furthermore, this sensitisation is always performed in the presence of the adjuvant alhydrogel (aluminium hydroxide) to ensure that the immune response generated is IgE and Th_2 mediated (Bice et al., 2000).

Finally, many laboratories use different strains of mice (e.g. BALB/c, C57BL/6 and A/J), varying doses of antigen given which can range between 1 µg to 8,000 µg and differing routes of antigen challenge (e.g. either by nebulisation or intranasally). The inconsistencies between protocols and genetic strains of mice all need to be considered when comparing the level of inflammation and AHR observed. Hence there is a need to establish a consistent and well accepted protocol for standardisation purposes and to use a better developed murine model of asthma which is representative of chronic airway inflammation, has less limitations and is more consistent with the desired characteristics of human asthma.

An improved murine model of chronic asthma has been developed by Temelkovski and colleagues (Temelkovski et al., 1998). This model involves systemic sensitisation of BALB/c mice with a lower dose of ovalbumin (10 µg/ml) and a subsequent chronic inhalation challenge protocol which uses low levels of aerosolised OVA (10-20 mg/m^3) but for an extended period of at least 6 to 8 weeks. The resultant effect is induction of a more chronic form of inflammation

which includes intraepithelial eosinophils, chronic inflammation in the lamina propria, epithelial hypertrophy, mucus cell hyperplasia/metaplasia and subepithelial fibrosis while lacking alveolitis. The authors attribute the control of the mass concentrations of antigen inhaled by the animals in a whole body inhalation exposure system to be the major factor in producing these observations (Kumar et al., 2000; Temelkovski et al., 1998). Use of this model has clarified the role of both IL-4 and IL-5 in directly regulating chronic inflammation rather than epithelial hypertrophy and subepithelial fibrosis (Kumar & Foster, 2001). Although this model has advantages over the other murine models of asthma, the one main disadvantage is that the whole body inhalation exposure system is expensive, difficult to construct and requires a dedicated room for its housing. Therefore, it was not used in the experiments described in this thesis. However it is still perhaps the most exciting of the animal models and may provide a more accurate representation of this complex disease.

In conclusion, the results described in this chapter confirm that certain features of allergic airway inflammation were successfully reproduced in the lungs of the OVA-treated mice. This model was subsequently used to investigate the role of Zn in regulating allergic airway inflammation described in Chapters 6 and 7.

CHAPTER 6

INVESTIGATION OF THE ROLE OF ZINC IN THE PATHOGENESIS OF ALLERGIC AIRWAY INFLAMMATION

CHAPTER 6 INVESTIGATION OF THE ROLE OF ZINC IN THE PATHOGENESIS OF ALLERGIC AIRWAY INFLAMMATION

6.1 INTRODUCTION

Chapter 5 reported the establishment of the murine model of allergic airway inflammation. This chapter reports modifications of the protocol to examine the influence of dietary Zn on airway hyperresponsiveness (AHR) and airway inflammation in SAL-treated and OVA-treated mice.

Zn is a major dietary antioxidant which has received limited attention in the asthma field, despite several studies reporting an association between asthma, wheezing and low Zn intake and hair/serum Zn levels (Di Toro et al., 1987; el-Kholy et al., 1990; Goldey et al., 1984; Kadrabova et al., 1996; Schwartz & Weiss, 1990; Vural et al., 2000; Wood et al., 2000). As such, further studies are now required to better understand the significance of the association between asthma symptoms, low serum Zn levels and low dietary Zn intake.

As discussed in Chapter 1, Zn is an essential cytoprotectant and anti-inflammatory agent for many biological systems. Therefore imbalances in dietary Zn intake can result in increased oxidative stress and inflammation since Zn deficiency produces a shift in the lymphocyte subset towards the pro-inflammatory Th$_2$ subset (Prasad, 2000). However, to date there is no data available on the role of Zn in regulating the pathogenesis of respiratory inflammatory diseases such as asthma.

The experiments reported in this chapter bring these two bodies of literature together by investigating the effects of Zn deficiency on allergic airway inflammation in a murine model. In this chapter, it was hypothesised that decreased Zn levels may contribute to increased oxidative stress, chronic inflammation and decreased protection of the airway epithelium.

Therefore the major aim of the experiments reported in this chapter was to determine whether alterations in Zn homeostasis are an influencing factor in the pathogenesis of asthma. In particular, this chapter examines 1) the effects of Zn deprivation alone on parameters of inflammation and AHR, 2) the interaction between Zn deprivation and allergic airway inflammation induced by sensitisation and challenge with OVA and 3) the effects of Zn repletion on these parameters.

6.2 METHODS

The data reported in this chapter relate to three separate experiments each with their own diet and experimental protocol. These will be called Egg White Diet with Allergy (Group 1), Casein Diet with Allergy (Group 2) and Casein Diet Alone (Group 3).

6.2.1 Egg White Diet with Allergy

Diet

In order to determine the optimal conditions for induction of allergic airway inflammation in Zn manipulated BALB/c mice, a pilot study using 4 mice per group was conducted. Induction of Zn deprivation was performed via the method of Coyle and colleagues (Coyle et al., 1999) which involves using an egg white

based diet. Four week old BALB/c mice were acclimatised for 7 days and given a Zn normal (ZN) egg white supplemented with $ZnCO_3$ to a final concentration of 50 mg of Zn per kg of diet (Table 6.1). Mice were then either fed this ZN diet (n = 4 mice) or given a Zn deprived (ZD, n = 4 mice) diet supplemented with $ZnCO_3$ to a final concentration of 5 mg of Zn per kg diet for the duration of the experiment. Care in minimising exogenous Zn contamination was crucial for these experiments; hence, stainless steel grids were used as the floor of mice cages and recycled paper bedding was preferred over the general sawdust bedding which is easily disturbed and contains a higher level of Zn (personal communications, Animal House Staff, The Queen Elizabeth Hospital). To further prevent Zn contamination, all stainless steel grids (Figure 6 panel A), mice cages (panel B) and water bottles were pre-washed (and further washed every 1-2 days) with milliQ water (Figure 6.1, panel C). Stainless steel grids were also constructed to fit the two tiered stage used during the aerochallenge of mice (Figure 6.1 panels E to H).

Experimental Protocol

After the 7 day acclimatisation period (designated as day 1 to 7), mice were put on their respective diets and given SAL or OVA treatments as described below. These were similar to those described in Chapter 5 with slight modifications. The two modifications were the timing of the protocol which had to fit in with the dietary time plan and the trip to Canberra for testing of AHR.

Mice were injected intraperitoneally (i.p) on days 7 and 19 and aerochallenged on days 24 and 26 with OVA 3 times a day for 30 min every second day as described in section 2.12.2. SAL-treated mice were nebulised with

Table 6.1 Composition of Diets

Ingredient	Egg White	Casein
	g/kg	g/kg
Egg White[a]	180	0
Casein[*]	0	200
Cellulose	30	50
Corn starch	430	430
Corn Oil[t]	100	0
Choline Bitartrate	2.0	2.5
L-Cysteine	0	3
Soybean Oil[t]	0	70
Sucrose	200	200
AIN 93M Mineral Mix[‡]	35	35
AIN 93VX Vitamin Mix[§]	10	10
$ZnCO_3$	0[a] or 0.009[b] or 0.086[c]	0 or 0.062[c]

[a]The egg white diet prior to addition of $ZnCO_3$ was Zn free (0 mg/kg) as determined by atomic absorption spectroscopy (AAS).

[b]The Zn content of the Zn Limited diet was 5 mg/kg as determined by AAS.

[c]The Zn content of the Zn normal diet was 50 mg/kg as determined by AAS.

[*]Zn content of the casein diet prior to addition of $ZnCO_3$ was 14 mg/kg as determined by atomic absorption spectroscopy (AAS). This is due to the Zn content of the casein used.

[t]Lion and Globe, Hop Hing Oil Factory, Kowloon, Hong Kong.

[‡] AIN 93M Mineral mix profile (g/kg diet): KH_2PO_4, 17.155; $CaCO_3$ 14.645; NaCl, 12.530; $MgSO_4 \cdot 7H_2O$, 4.99; $FeC_6H_5O_7 \cdot 5H_2O$, 0.296; $CaPO_4$, 0.170; $MnSO_4 \cdot 4H_2O$, 0.080; $CuSO_4 \cdot 5H_2O$, 0.123; KI, 0.00025; $(NH_4)_6Mo_7O_{24} \cdot 4H_2O$, 0.00125; Na_2SeO_3, 0.0005.

[¶] AIN 93VX vitamin mix profile (mg/kg diet): thiamine-HCl, 70; riboflavin, 30; nicotinic acid, 50; pantheric acid, 150; pyridoxal HCl, 15; hydroxocobalamin, 0.02; inositol, 400; P-aminobenzoic acid, 50; folic acid, 10; biotin, 0.4, cholecalciferol, 0.01; glucose, 225; and retinol palmitate, 2900 U/kg (ICN Biochemicals Australasia, Seven Hills, NSW, Australia).

Figure 6.1: Zn Deprivation and Allergic Airway Inflammation

Figure shows the equipment used for housing the mice, minimising exogenous Zn contamination and nebulisation.

Panel A to C: Stainless steel grids (A) were used as the floor of the cage (B) to restrict mice from eating the recycled paper bedding and their feces. This minimised Zn contamination in the experiments. The complete cage is shown in panel C.

Panel D: Mice were colour coded so that SAL and OVA-treated mice could be grouped according to diet and placed in the same cages.

Panel E to H: Stainless steel grids were also constructed for the two tiered stage used in the nebulisation chamber. The completed chamber is shown in panels G and H.
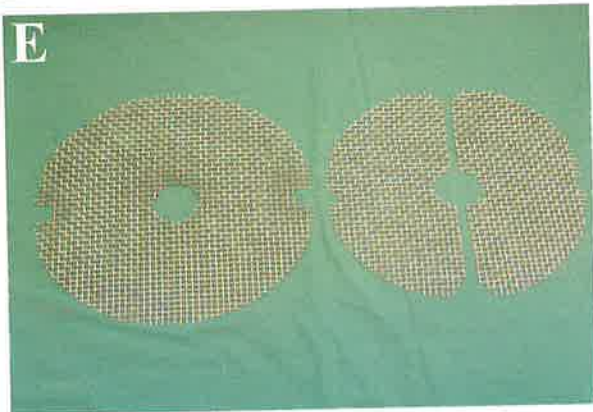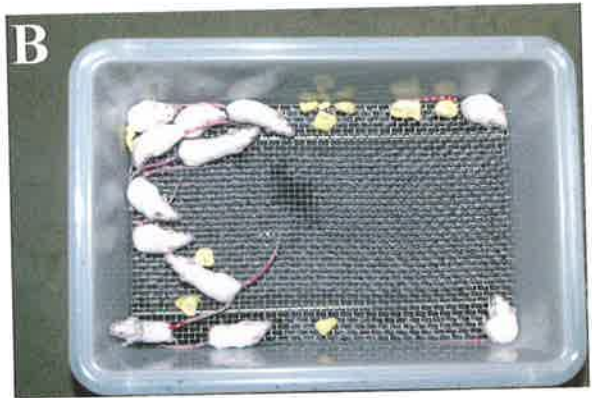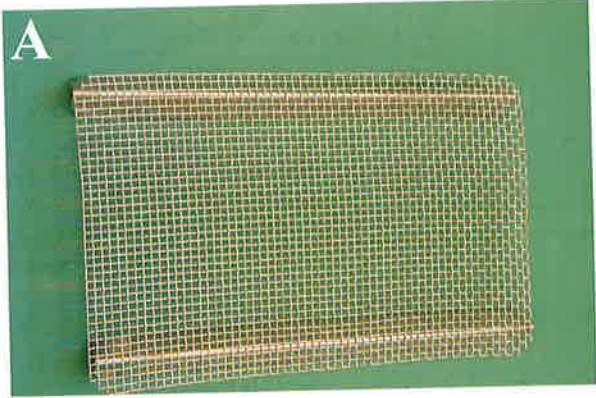
0.9% sterile saline alone. On day 27, mice were transported to Canberra by plane and housed in the laboratory of Dr. Paul Foster at the John Curtin School of Medical Research where they continued to receive two more nebulisations on days 28 and 30. AHR was performed (described below in section 6.2.3) on day 31 and animals sacrificed on day 32 for collection of tissues. Mice were bled by cardiac puncture and sacrificed by cervical dislocation and blood, BALF and lung tissues collected as outlined in section 2.12.3, 2.12.4, and 2.12.5, respectively.

6.2.2 Casein Diet with Allergy

Diet

A second method of induction of Zn deprivation was performed by substituting the egg white diet with casein protein. Since the casein protein used to make up the diet contains endogenous Zn, the complete non-Zn supplemented casein diet was found to contain 14 mg of Zn/kg diet. Therefore this was the lowest limit that could be used for the Zn limiting diet. The Zn normal diets were supplemented with $ZnCO_3$ to a final concentration of 50 mg Zn/kg diet (Table 6.1). These diets were chosen after discussion with Dr. Peter Coyle (Dept Clinical Biochemistry, IMVS) who has had extensive experience in creating varying levels of Zn deficiency in rodents. Four week old BALB/c mice were acclimatised for 7 days on the ZN diet. To prevent exogenous Zn contamination, the above housing procedure was used (as described for the egg white diet experiments). Mice were then either fed this ZN diet (n = 16 mice) or given the Zn limited (ZL, n = 32 mice) diet for the entire duration of the experiment. The reason for 32 mice in the ZL group is that 16 of these were then repleted with the ZN diet at day 37.

Experimental Protocol

Mice were i.p injected on days 7 and 19 and aerochallenged with OVA on days 26, 28, 30, 32, 34 and 36, 3 times a day for 30 min every second day as described in section 2.12.2. SAL-treated mice were nebulised with 0.9% sterile saline alone. On day 35, mice were transported to the Canberra as described in section 6.2.1. Mice were then tested for the first AHR reading (section 6.2.3) on day 37. At this time half of the mice receiving the ZL diet were then separated into a new cage and given the ZN diet (n = 8 mice). These mice are referred to as Zn repleted (ZR). Zn repletion was restricted to 7 days to minimise stress to the animals which also continued to receive nebulisations during this time (days 38, 40, 42 and 44). A second AHR reading was performed on day 45 and 24 h later, mice were bled by cardiac puncture and sacrificed by cervical dislocation for collection of tissues as described in section 6.2.1. A total of 8 mice were used per group.

Assessment of blood and BALF eosinophilia was determined as described in sections 5.2.3 and 5.2.4, respectively, while tissue eosinophilia and mucus cell numbers were counted as described in section 5.2.4. At the time of tissue collection, samples from the 8 mice per group were divided into 3 components for the following procedures; 1) lungs from 2 mice were formalin fixed for routine histological assessement, 2) lungs from 3 mice were frozen in OCT for immunohistochemistry (for experiments in Chapter 7) and 3) BALF samples were taken from 3 mice per group for assessment of infiltrating tissue eosinophilia.

Zn deficiency is commonly accompanied by a decrease in the growth rate, hence to monitor the effectiveness of the above mentioned diets, the weights of

these mice were recorded. Furthermore, serum and liver Zn levels of mice were also determined as previously described in section 2.6 but are reported in Chapter 7. To minimise stress, a set routine was established during the entire duration of these experiments whereby mice were weighed at 10 am every 2 to 3 days, mice cages were then cleaned and replaced with fresh bedding, food, MilliQ water and washed stainless steel grids.

6.2.3 Casein Diet Only

Diet

For this group the same induction of Zn deprivation by a casein diet was used as described for animals in section 6.2.2 where the Zn normal diets were supplemented with $ZnCO_3$ to a final concentration of 50 mg Zn/kg diet (Table 6.1), while the Zn limited diet contained 14 mg Zn/kg diet. To prevent exogenous Zn contamination, the above housing procedure was used (as described for the egg white diet experiments). Mice were then either fed this ZN diet (n = 16 mice) or given the Zn limited (ZL, n = 32 mice) diet for the entire duration of the experiment. The protocol for this experiment involved repletion of 16 mice within the ZL group with the ZN diet beginning at day 28 and 3 AHR readings performed on days 28, 33 and 40 to monitor the effect of Zn repletion on airway functions. No asthma was induced.

6.2.4 Assessment of AHR to Methacholine by a Barometric Whole Body Plethysmograph

In this thesis, airway response to a certain dosage of the bronchoconstrictor β-methacholine (Sigma-Aldrich, Sydney, Australia), is refered to as airway

hyperresponsiveness (AHR). AHR was assessed in conscious, unrestrained mice by barometric plethysmography using equipment and software from Buxco (Troy, NY). The system consists of a bias flow regulator (Figure 6.2, panel A), an ultrasonic nebuliser (panel A) and a preamplifier (panel B), and 4 cylindrical chambers (panel B & C). This system yields a dimensionless parameter known as enhanced pause (Penh) that reflects changes in waveform of the pressure signal from the plethysmography chamber combined with a timing comparison of early and late expiration. In OVA-treated mice, Penh is correlated with increased eosinophilia and other inflammatory indices and is used to empirically monitor airway function as described previously (Foster et al., 1996; Hamelmann et al., 1997). Mice were placed in a chamber (Figure 6.2 panel C & D) and exposed to an aerosol of water (baseline readings) and then cumulative doubling concentrations of methacholine (dissolved in water to produce final concentrations in solution of 0, 3.13, 6.25, 12.5 and 50 mg/ml). The aerosol was generated by an ultrasonic nebulizer (Figure 6.2 panel A & C) and drawn through the chamber for 2 min at a constant flow rate. The inlet was then closed, 5 Penh readings were taken for 3 min and averaged.

Data are expressed as means ± SEM. When suitable, results were interpreted using analysis of variance (ANOVA) with Tukey's post-hoc test using the General Linear Model on Minitab (Minitab, State College, PA). Otherwise, the student t test was performed. Differences were considered statistically significant at $p < 0.05$, unless otherwise stated.

Figure 6.2 BUXCO Whole Body Plethysmography for Measurement of AHR

AHR was determined by using the following apparatus.

Panel A: A bias flow regulator (B) and an ultrasonic nebuliser (N) were used to deliver a constant flow rate of aerosol to chambers containing mice.

Panel B: A preamplifier (P) was used to amplify and record the responses of mice to β-methacholine.

Panel C & D: Unrestrained mice were placed into individual cylindrical chambers (C) where their AHR was monitored.
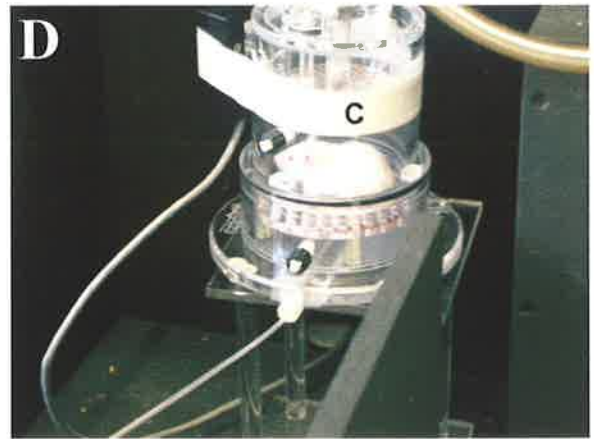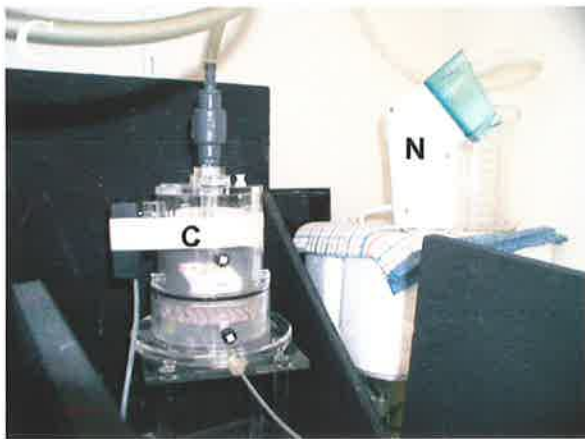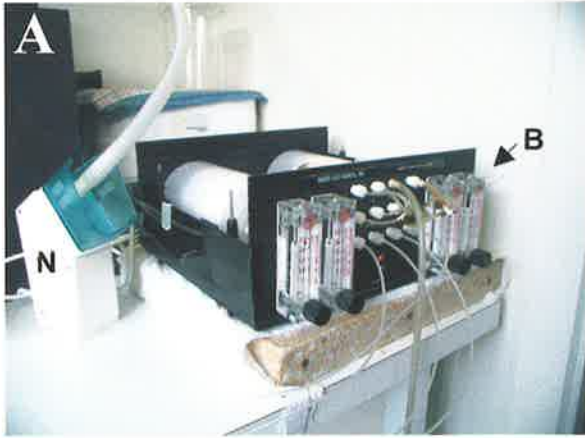
6.3 RESULTS

6.3.1 Preliminary Study

The first section of results refers to a pilot study with a small number of mice to determine whether manipulation of dietary Zn levels can influence one parameter of allergic airway inflammation, AHR. Mice received either a ZN (50mg of Zn/kg diet) or a ZL diet (5mg of Zn/kg diet) and allergy (OVA treated) induced using the protocol described in section 6.2.1. Non-allergic mice received SAL only.

6.3.1.1 Body Weights are Decreased in Zn Deprived BALB/c Mice

Figure 6.3 depicts the growth curves of these mice given the egg white diet. Note the distinct separation of weights between the ZN (blue lines) and ZL (red lines) SAL-treated mice (circles, panel A) and a smaller separation in the OVA-treated (triangles, panel B) mice from day 7 onwards. Significant differences ($p < 0.05$) in the weights of the mice were observed on days 14 and 16 in the SAL-treated mice.

Apart from the decrease in growth rate, mice fed the Zn limited diet did not display any other obvious signs consistent with Zn deficiency such as loss of fur or diarrhea.

6.3.1.2 AHR is Increased in Zn Deprivation

Of particular relevance, there was a trend towards increased AHR in mice given a Zn limited diet (red line) which was best illustrated in the SAL-treated

178

Figure 6.3: Growth Rate of BALB/C Mice Placed on an Egg White Diet and Receiving SAL or OVA Treatments

Four week old mice were given egg white based diets containing either a normal Zn content (50 mg Zn/kg, blue line) or a Zn deprived diet (5 mg Zn/kg, red line). Weights of mice (y-axis) were plotted against days on diet (x-axis) for SAL-treated (panel A) and OVA-treated (panel B) mice. Protocol for the sensitisation and nebulisation is shown in panel B. Figure shows the separation of weights, particularly for the SAL-treated mice between the different groups but only weakly for the OVA-treated mice. Data represent means $\pm$ SEM for 6 mice per group. Significant differences refer to comparisons between ZN and the ZL treated mice: * $p < 0.05$.

Key:

ZN Mice ▬▬▬

ZL Mice ▬▬▬

A

SAL-Treated

Weights (g) vs Days On Diet

* *

B

OVA-Treated

Weights (g) vs Days On Diet

Neb 1
(Day 24)

i.p 2
(Day 19)

i.p 1
(Day 7)

i.p 1
50μg/ml
OVA

i.p 2
50μg/ml
OVA

Nebulisations
1% OVA
3 x 30 min
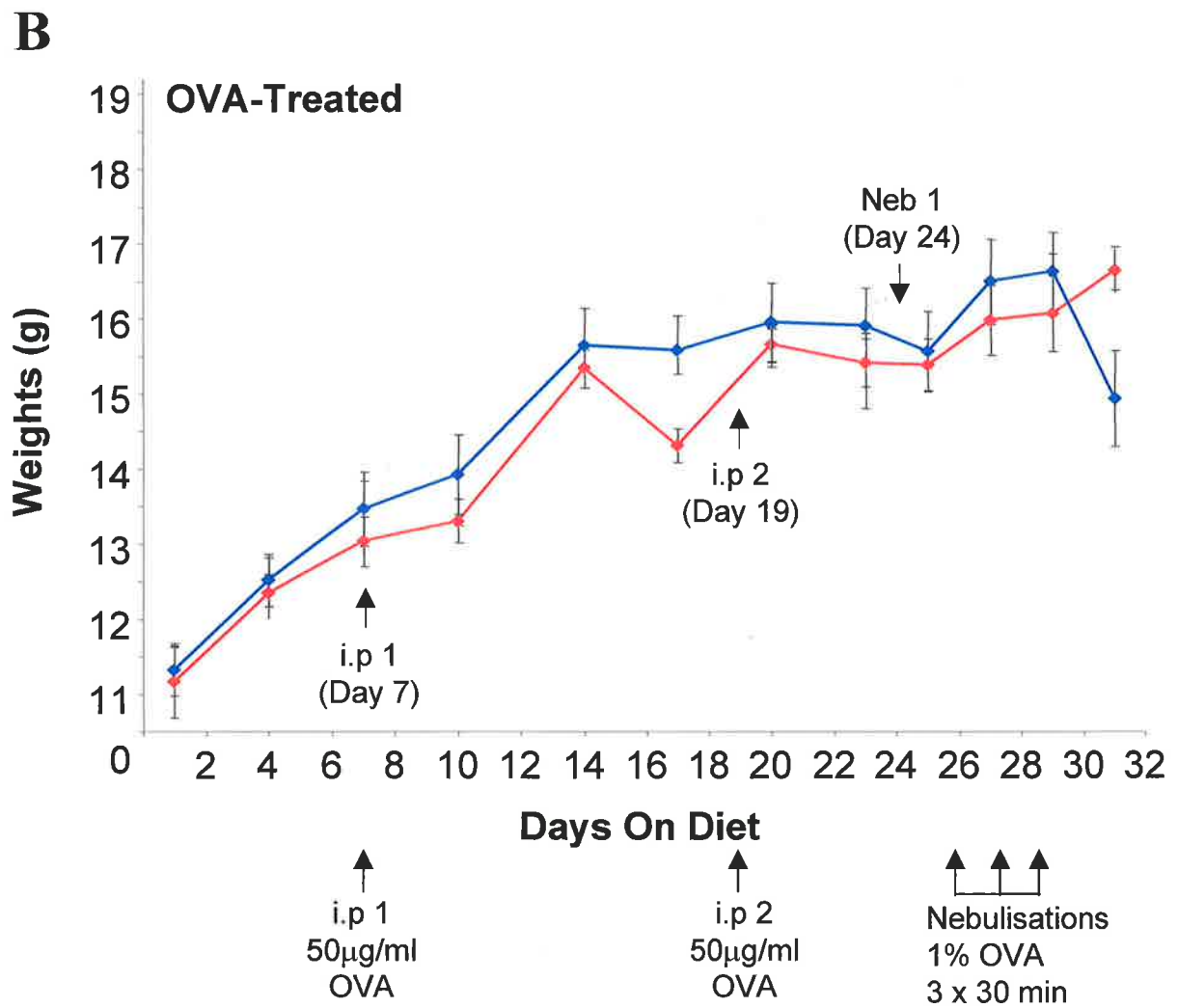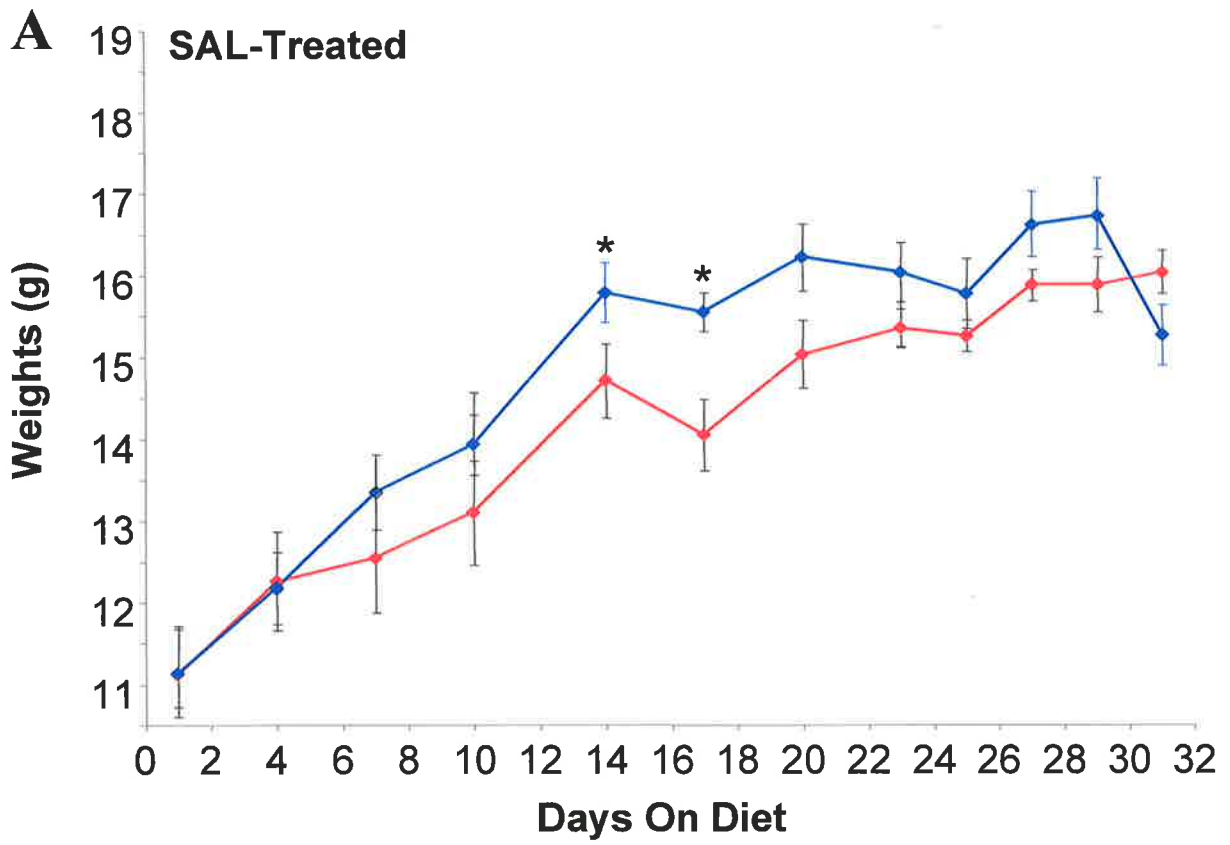
mice (Figure 6.4, panel A) where non-significant increases were seen at concentrations of β-methacholine $\geq$ 12.5 mg/ml. Significance was observed at 50 mg/ml β-methacholine where the AHR reading for the ZL SAL-treated mice was 2.3 $\pm$ 0.2 Penh units compared to 1.6 $\pm$ 0.3 Penh units in the ZN SAL-treated mice ($p < 0.05$).

Despite the higher Penh readings for the ZL OVA-treated mice when compared with the ZN OVA-treated groups, significance was not reached. Furthermore, the response to β-methacholine in the ZN and the ZL OVA treated mice was not at the levels normally expected (Penh > 3.0 Penh units or > 1000% increased over the baseline) for an allergic mouse (Foster et al., 2000; Hamelmann et al., 1997). For example, the ZN OVA-treated mice had a response of 2.3 $\pm$ 0.2 Penh while the ZL OVA-treated mice had a response of 2.1 $\pm$ 0.3 Penh units (Figure 6.4, panel B).

6.3.2 Effects of Zn Using Casein diet with Allergy

The main body of results in this chapter refer to 2 separate groups of mice given the casein diets. These mice will be refered to as group 2 and 3.

Group 2 mice consists of 6 subgroups of mice (n = 8 in each subgroup) on a protocol of dietary Zn manipulation via a casein based diet and allergic sensitization and challenge. For each parameter, two major comparisons were made between SAL-treated and OVA-treated mice (*Allery Type Comparisons*) and between diets for example the ZN versus ZL (*Diet Type Comparisons*). The groups are as follows: group 2A- ZN SAL-treated mice, group 2B-ZN OVA-treated mice,

Figure 6.4: AHR in SAL and OVA-Treated Mice Given an Egg White Diet

Figure depicts the AHR response to β-methacholine 24 h after the final nebulisation at day 31 for mice fed the Zn normal (50 mg Zn/kg, blue line, ZN) or a Zn limited diet (5 mg Zn/kg, red line, ZL). AHR Penh readings (y-axis) are plotted against β-methacholine concentrations (x-axis) for SAL-treated (panel A) and OVA-treated (panel B) mice. There is a trend towards elevated AHR in mice given the ZL diet, although significance was observed at only one point (*). Data represent means ± SEM for 4 mice per group. Significant differences refer to comparisons between ZN and the ZL treated mice: * $p < 0.05$.

Key:

    ZN Mice ▬▬
    ZL Mice ▬▬

A SAL-Treated Eggwhite Diet

B OVA-Treated Eggwhite Diet
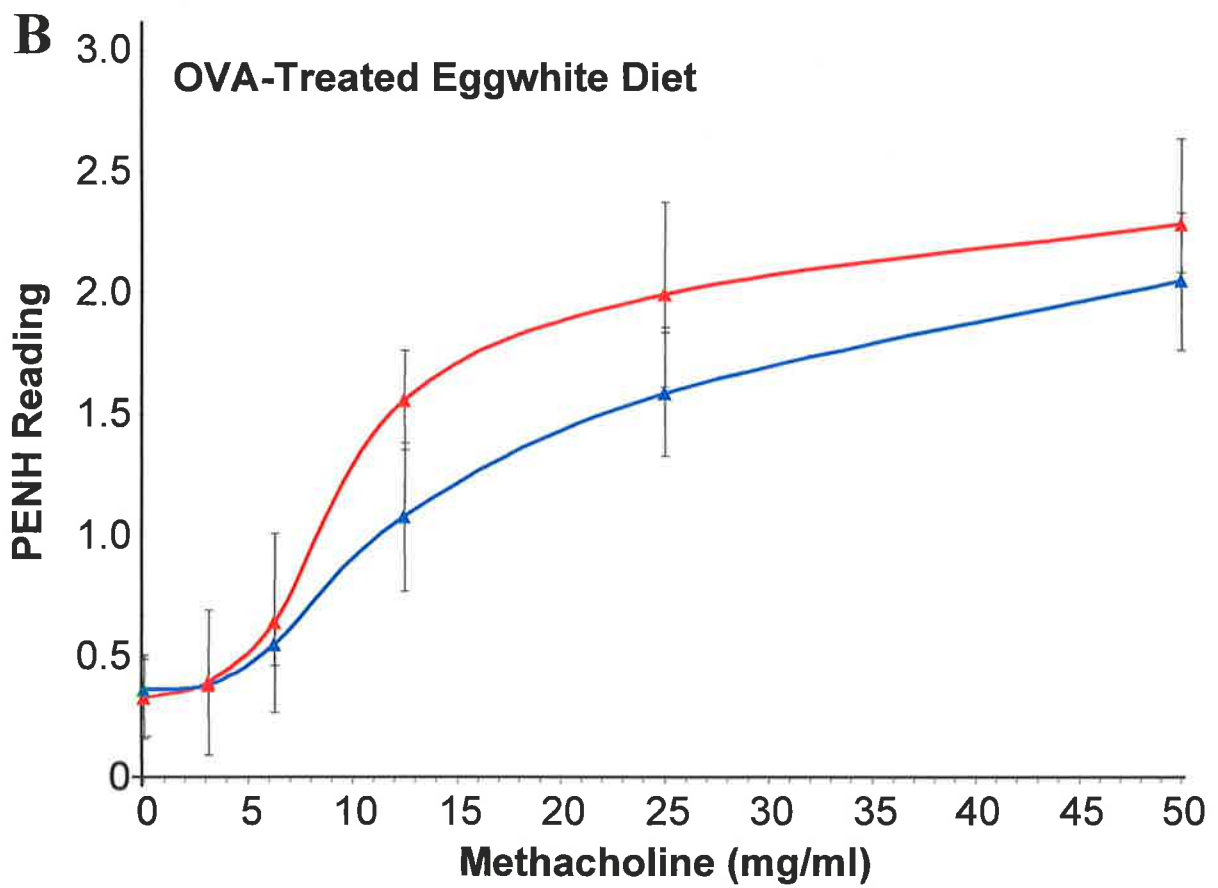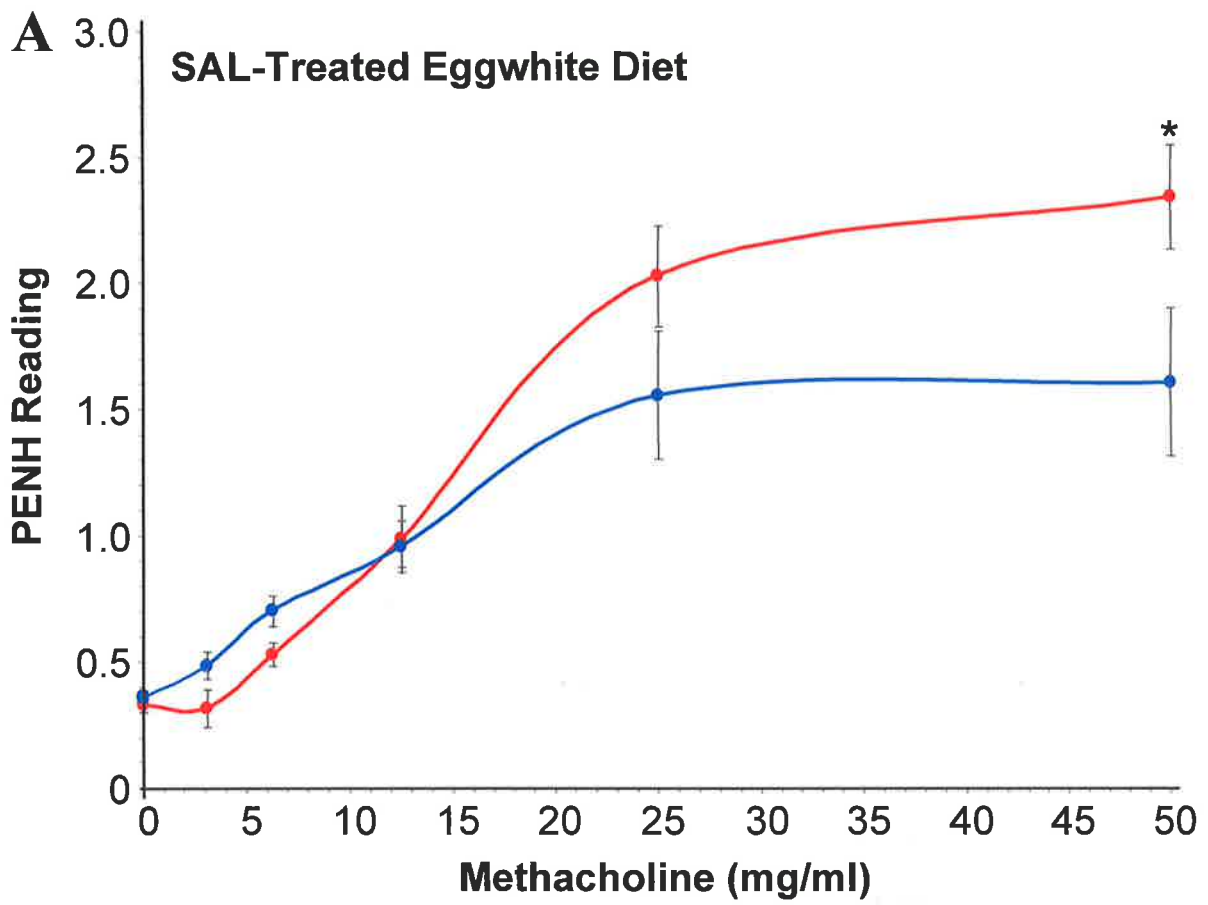
group 2C- ZL SAL-treated mice, group 2D-ZL OVA-treated mice, groups 2E-ZR SAL treated mice and finally group 2F-ZR OVA treated mice.

6.3.2.1 Body Weights are Decreased in Zn Deprived BALB/c Mice Given the Casein Diet

Body Weight

Allergy Type Comparisons

There was no effect of allergy on the weights of the ZN mice during the duration of the experiment. The curves for SAL-treated versus OVA-treated groups were similar, indicating that the sensitization and nebulization protocol has not affected growth (Figure 6.5) for both ZN (blue lines, panel A) and ZL (red lines, panel B) SAL (circle symbols) and OVA-treated mice (triangle symbols).

Diet Type Comparisons

There was a separation of weights ($p < 0.05$) between ZL mice and ZN mice where ZL mice had lower weights during the first 2 wks of dietary exposure, consistent with the known effects of Zn deficiency on growth (Figure 6.6). This separation was found for both SAL-treated (panel A) and OVA-treated (panel B) mice and occurred during the phase of maximal growth and at the time of sensitisation but prior to the nebulisations. At later time points, body weights plateaued and Zn deprivation had no further significant effect on the growth rates of these mice.

Mice designated as ZR were originally on a 14 mg/kg Zn diet from days 1 till 37 then switched to a 50mg/kg diet thereafter. The effects of Zn repletion on

Figure 6.5 Comparison of Weights Between SAL and OVA treated Mice on a Casein Diet

Four week old mice were given casein based diets containing either a normal Zn content in panel A (50 mg Zn/kg diet, ZN) or a Zn deprived diet in panel B (5 mg Zn/kg diet, ZD). Some of the ZL mice were switched to a ZN diet at day 37 (ZR group). Mice weights (y-axis) were plotted against days on diet (x-axis) for SAL-treated (circles) and OVA-treated (triangles) mice. Protocol for the sensitisation and nebulisation is shown in panel B. The figure illustrates that there was no significant separation of weights for the SAL and OVA treated mice receiving the same diets; although there was a trend towards increased weights in the OVA-treated mice between days 17 to 25 (ZN group) and days 15 and 23 (ZL group). Zn repletion for 7 days had no significant effect on weights of mice previously given the ZL diet. Airway hyperreactivity (AHR) was assessed twice on days 37 (AHR 1) and 45 (AHR 2). Data represent means $\pm$ SEM for 8 mice per group. Significant differences refer to comparisons between ZN and the ZL treated mice: * $p < 0.05$. No significant differences were observed between ZN and ZR mice.

Key:	SAL	OVA
ZN Mice	●	▲
ZL Mice	●	▲
ZR Mice	●	▲

A

ZN Diet

B

ZL Diet

Neb 1
(Day 26)

i.p 2
(Day 19)

AHR 1
+ Zn Repletion
(Day 37)

AHR 2
(Day 45)

i.p 1
(Day 7)

i.p 1
50μg/ml
OVA

i.p 2
50μg/ml
OVA

Nebulisations
1% OVA
3 x 30 min

A

SAL-Treated

B
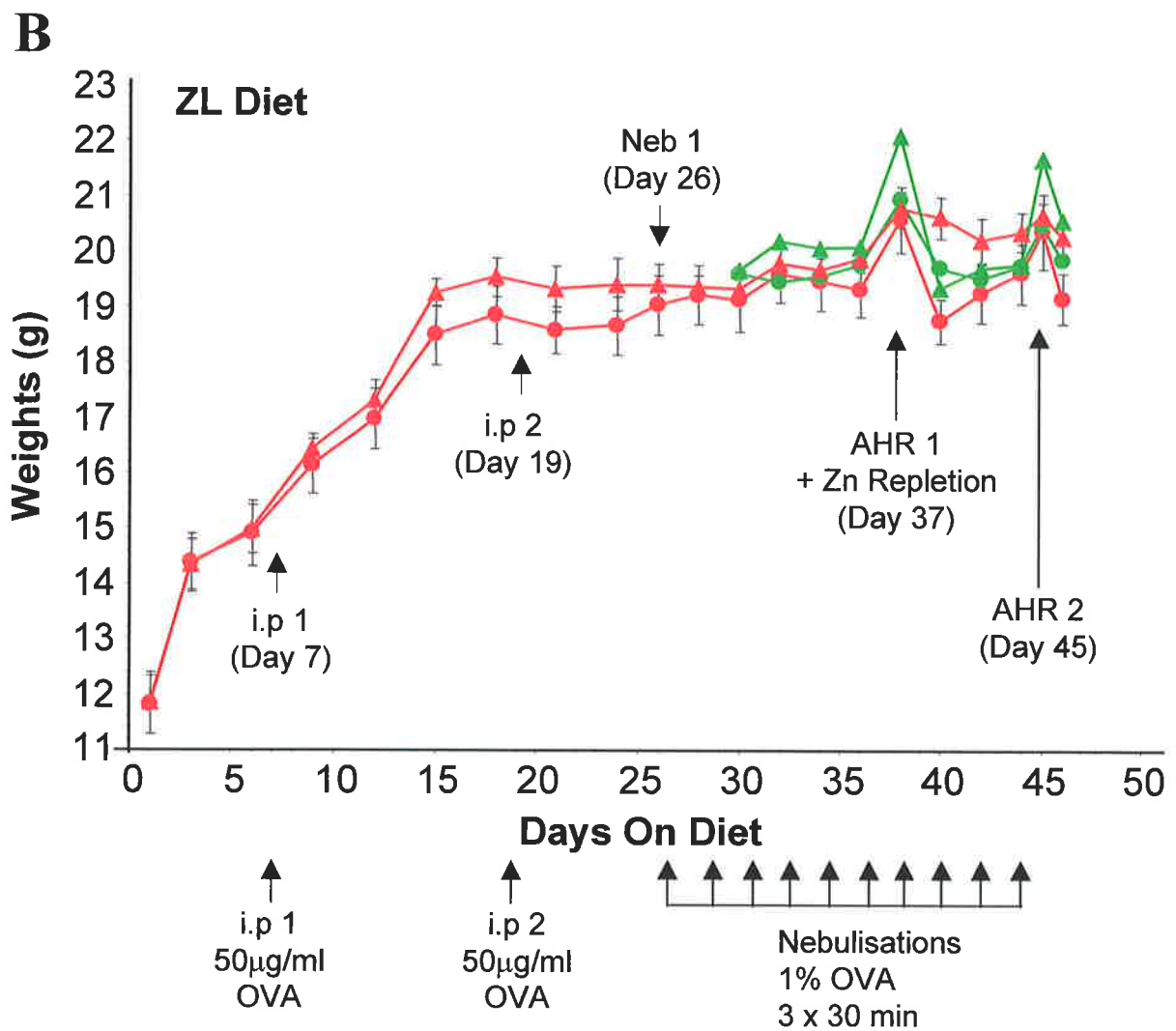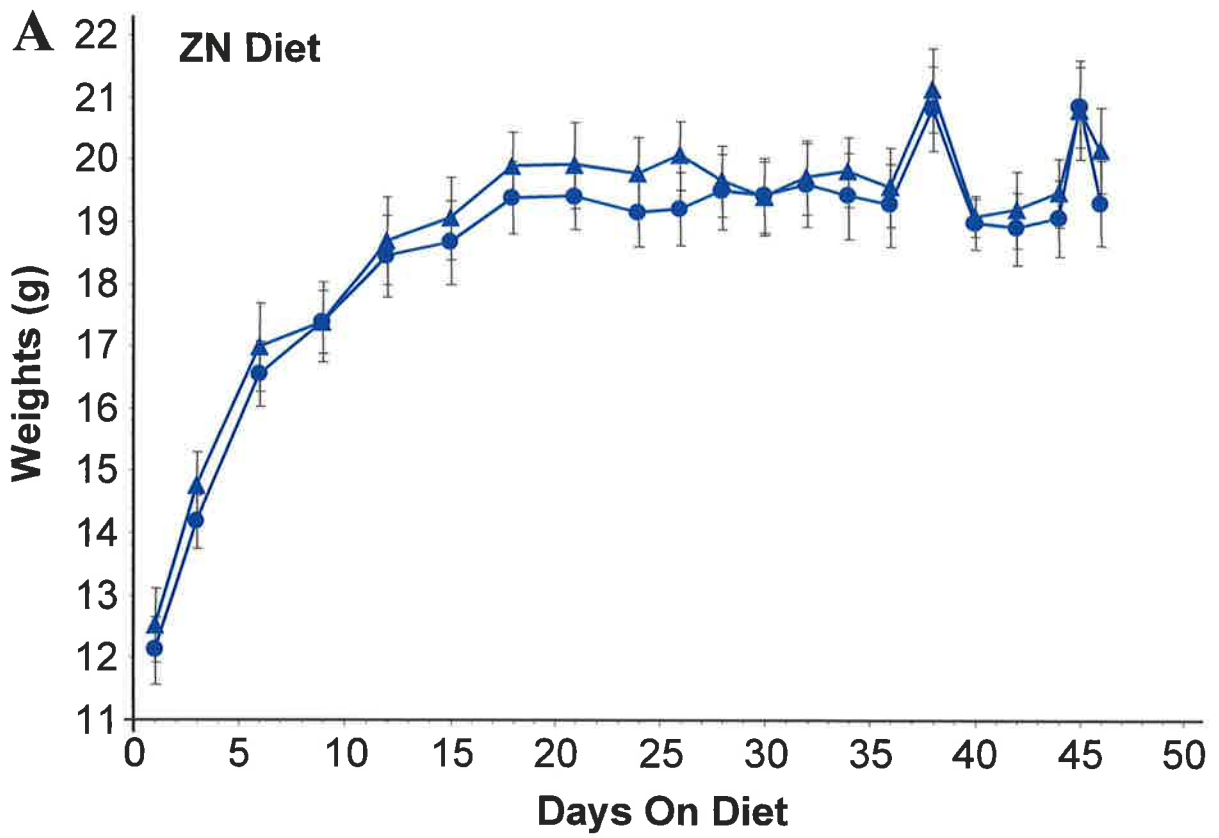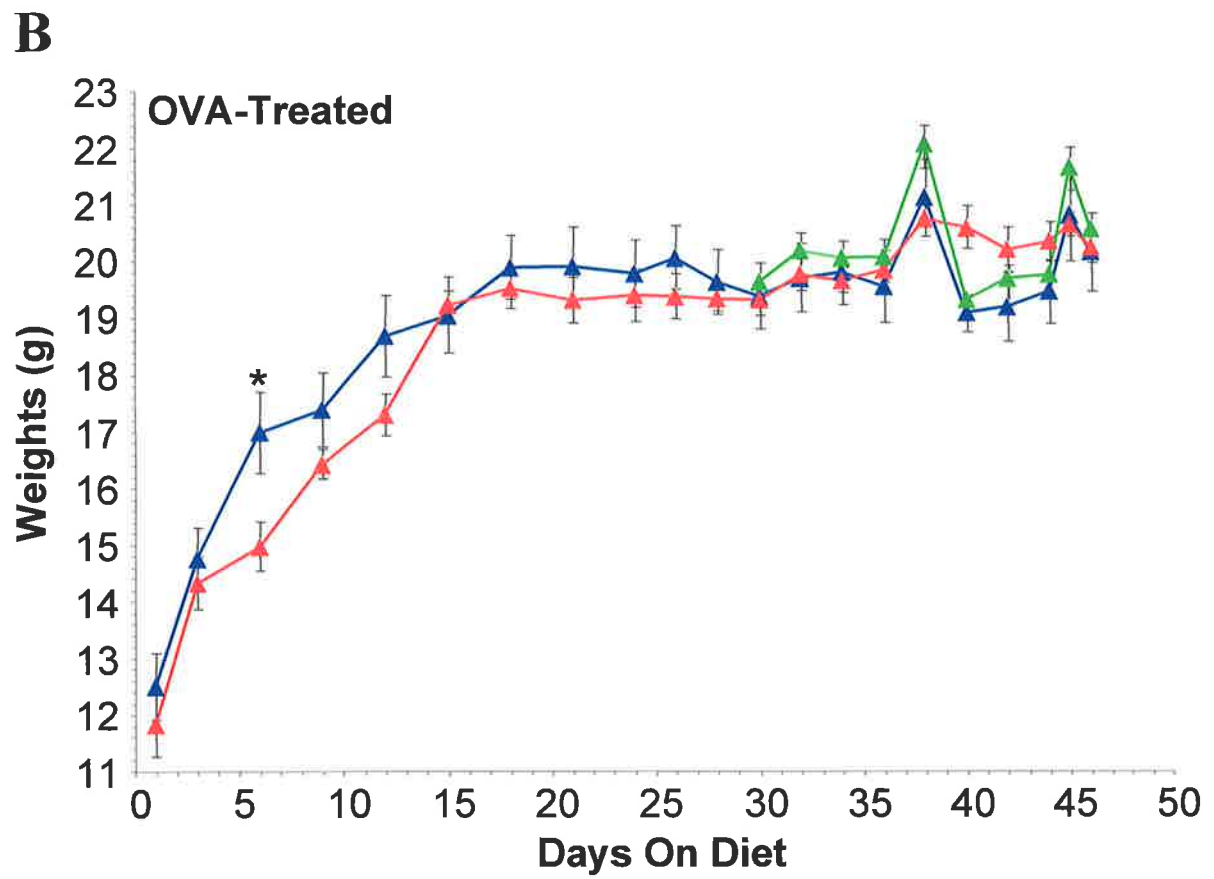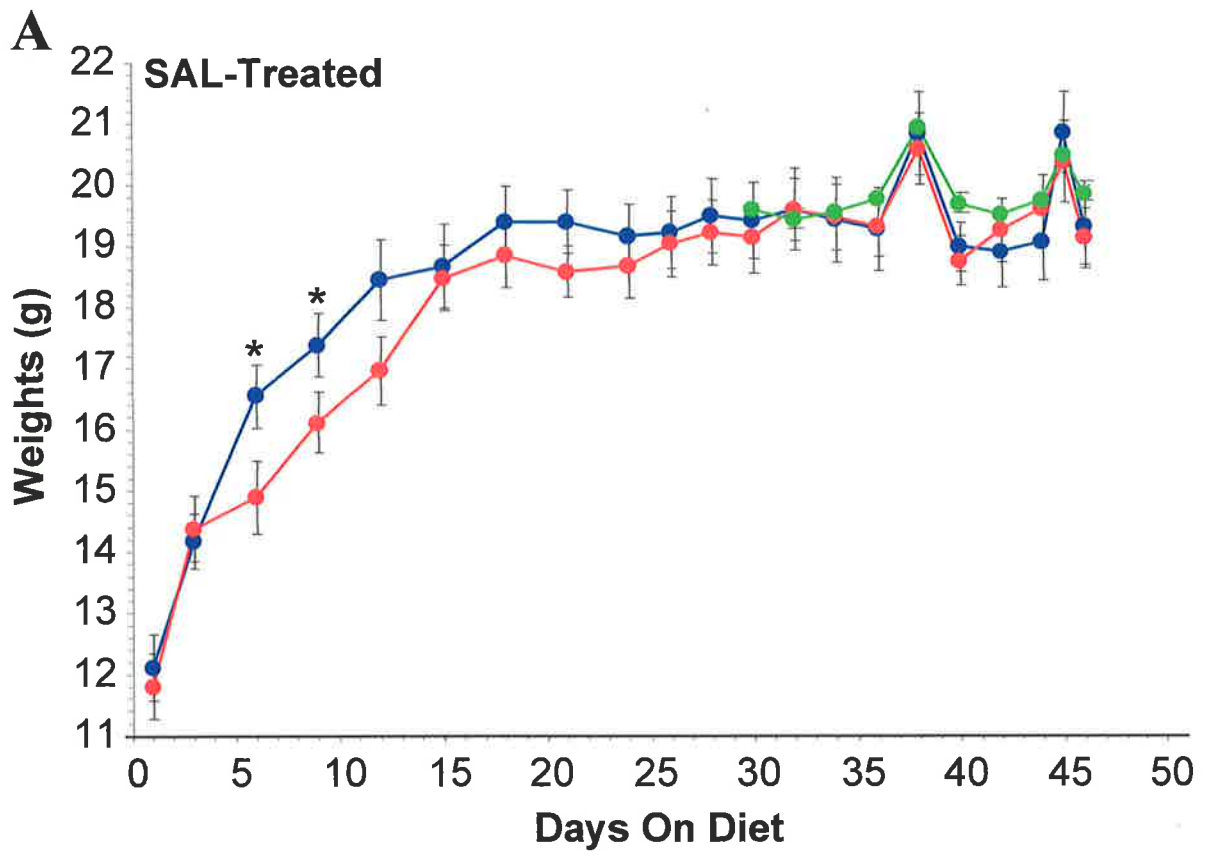
OVA-Treated

weight gain are difficult to interpret because these mice at the time of repletion were no longer actively growing. There were small increases in body weight over the ZL mice for both the SAL-treated and OVA-treated mice but these were not significant (Figure 6.5, green lines). These increases in weights occurred directly after the AHR testing on days 37 and 45 (Figure 6.5).

Apart from the decrease in growth rate, mice fed the Zn limited diet did not display any other obvious signs consistent with Zn deficiency such as loss of fur or diarrhea.

6.3.2.2 *Zn deprivation Enhances Eosinophil Numbers in Non-Allergic and Allergic Mice*

To determine whether Zn deprivation influences allergic airway inflammation, inflammatory indices of both SAL and OVA-treated mice were measured and are summarised in Table 6.2. Eosinophilia, was examined as described in Chapter 5.

BALF

Allergy Type Comparisons

All OVA-treated mice had highly significant increases in eosinophils in BALF, blood and lung tissue, compared to the SAL-treated mice, confirming the success of the allergy induction protocol (Table 6.2). Figure 6.7 shows that the BALF samples retrieved from OVA-treated (n = 3 mice per group, RHS panel) mice had a significantly higher number of cells than the SAL-treated mice (n = 3 mice per group, LHS panel). A cell count was determined on cytospins by enumerating leukocytes within 4 microscope fields of view using a 40x

181

Table 6.2 Inflammatory Parameters in SAL-Treated and OVA-Treated Mice on Different Zn Diets[1].

	SAL-Treated			OVA-Treated[2]			ANOVA[3]			
	ZN[4]	ZL	ZR	ZN	ZL	ZR	RMSE[5]	Allergy Type	Diet	Allergy x Diet
BALF	Percentage of Cells			Percentage of Cells						
Eosinophils	ND[6]	ND	ND	73.2	73.3	73.8	5.4	0.000	0.889	0.889
Neutrophils	ND	ND	ND	1.2	0.6	0.4	0.6	0.014	0.564	0.564
Lymphocytes	ND	ND	ND	17.4	19.1	19.9	7.3	0.000	0.679	0.679
Macropages	ND	ND	ND	8.3	7.0[a]	6.9	1.2	0.000	0.010	0.010
Peripheral Blood	Percentage of Cells			Percentage of Cells						
Eosinophils	1.3	1.5	1.0	5.0[b]	9.3[a,b]	7.5[b]	1.1	0.000	0.042	0.076
Neutrophils	19.5	22.0	16.0	17.0	14.3[b]	18.5	2.4	0.144	0.953	0.039
Lymphocytes	78.8	75.0	81.3	77.8	75.3	74.5	2.2	0.080	0.138	0.110
Monocytes	0.3	1.0	1.8	0.5	1.3	1.3	0.6	0.174	0.040	0.009
Lung Tissue	Cells/HPF[4]			Cells/HPF[4]						
Eosinophils	0.1	1.8[a]	0.6	41.4[b]	58.7[a,b]	52.4[b]	4.0	0.000	0.005	0.016
Mucus-secreting cells	0.1	1.1[a]	0.9	70.6[b]	132.3[a,b]	118.5[a,b]	7.1	0.000	0.000	0.000

[1] Values represent means, n = 3 mice per group. For the BALF and peripheral blood 800 leukocytes per mouse were analysed. For the lung tissues 6 airways per mouse were analysed.

[2] Mice were injected I.p with 50μg of OVA on days 7 & 19 followed by 9 nebulisations with 1% OVA.

[3] Two-way ANOVA using the factors Allergy (SAL-treated and OVA-treated, Diet (ZN, ZL, ZR).

[4] Abbreviations, SAL; saline, OVA; ovalbumin, ZN; normal Zn diet, ZL; Zn Limiting diet, ZR; Zn repleted diet, BALF; bronchoalveolar lavage fluid, HPF; high power field.

[5] RMSE, root mean square error, is an estimate of the overall standard deviation. It is the square root of the mean square error term from the ANOVA calculations.

[6] ND, not determined. For the BALF percentages in the non-allergic mice, too few cells were present and therefore an accurate percentage could not be determined.

[a] Significantly different from ZN mice of the same allergy group.

[b] Significantly different from SAL-Treated mice of the same diet group.

Figure 6.7: Increased BALF Eosinophil Percentages in SAL and OVA-Treated Mice

Airway tissue eosinophils were recovered from the lumen of SAL and OVA-treated mice by performing a bronchoalveolar lavage (BAL). Cells were centrifuged and resuspended in 1x HBBS and cytospun onto a glass slide. Figure shows an increase in the presence of eosinophils in the BALF of ZN (panel B), ZL (D) and ZR (F) OVA-treated mice. Note also the limited number of cells and the paucity of eosinophils in the BALF recovered from the ZN (A), ZL (C) and ZR (E) SAL-treated mice. 2500x initial magnification.

SAL-Treated | **OVA-Treated**

ZN — A, B

ZL — C, D

ZR — E, F
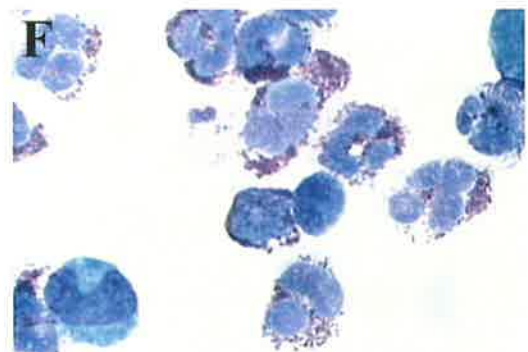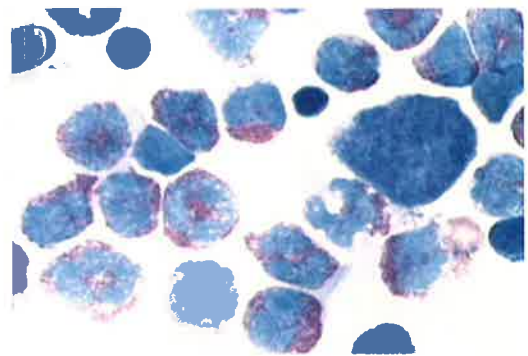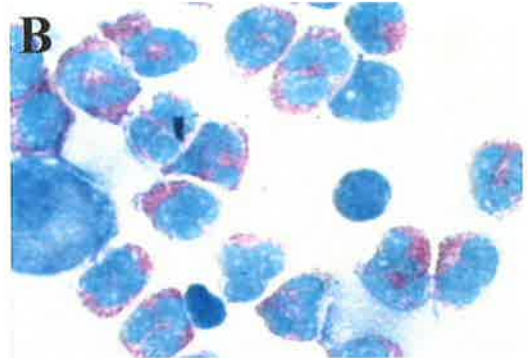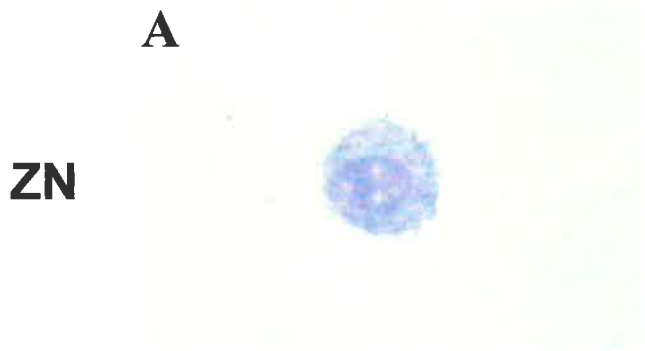
magnification lens. The ZN OVA-treated mice had a higher average total cell count of 393.3 ± 21.2 cells/40xHPF compared to ZN SAL-treated mice which had 22.1 ± 4.1 cells/40xHPF (p < 0.005).

Similar differences between SAL and OVA mice were observed for the ZL and ZR mice. For example, ZL OVA-treated mice had a total BALF cell count of 420.6 ± 23.2 cells/40xHPF compared to 18.3 ± 4.2 cells/40xHPF for the ZL SAL-treated mice, while the ZR OVA-treated mice had 405.4 ± 27.5 cells/40xHPF compared to their SAL-treated counterparts which had 22.0 ± 5.5 cells/40xHPF. As observed in Chapter 5, BALF samples from the ZN OVA-treated animals consisted mainly of eosinophils; the number of cells recovered in the BALF fluid of ZN SAL-treated mice was too low to obtain accurate percentages of cell types (Table 6.2).

Diet Type Comparisons

There was no difference in the percentage of BALF eosinophils when SAL-treated or OVA-treated mice were placed on Zn limited diets or were repleted (Table 6.2). There was also no significant change in neutrophils, lymphocytes or macrophages between the diet groups.

Cardiac Blood

Allergy Type Comparisons

As observed for Chapter 5, blood of ZN OVA-treated mice (n = 3 mice per group), had significantly increased percentages of eosinophils when compared to that from the ZN SAL-treated mice. Similar increases in eosinophil percentages were observed in the ZL OVA-treated mice when compared to the ZL SAL-treated

mice (p < 0.005). There were no significant differences in percentages of lymphocytes, monocytes or neutrophils between ZN OVA-treated and ZN SAL-treated animals (Table 6.2).

Diet Type Comparisons

In contrast to BALF findings, Zn deprivation significantly increased the percentage of eosinophils in the blood of OVA-treated mice from $5.0 \pm 0.6\%$ in the ZN OVA-treated mice to $9.3 \pm 0.5\%$ in the ZL OVA-treated mice (p < 0.005). ZR OVA-treated mice had $7.5 \pm 0.4\%$ of eosinophils which is not significantly different to the eosinophil percentages of the ZN or ZL OVA-treated mice (p > 0.05). In the SAL-treated mice, there was no effect of diet on blood eosinophil percentages (Table 6.2).

Lung Tissue

Figure 6.8 shows the normal lung tissue morphology and the lack of tissue eosinophils in typical images of paraffin tissue sections of ZN SAL-treated mice (panel A & B). ZL (panel C & D) and ZR (panel E & F) SAL-treated mice had an occasional eosinophil as depicted by the asterisk (*). Figure 6.9 illustrates the presence of inflammatory cell aggregates (arrowed) in OVA-treated ZN (panel A & B), ZL (C & D) and ZR (E & F) mice and increased numbers of eosinophils within the epithelium (panel B, D and E). Despite the significant increase in tissue eosinophila, there was little alveolitis observed in paraffin sections of the lung tissue of these mice (LHS panels).

Figure 6.8: Limited Numbers of Airway Tissue Eosinophils in SAL-Treated Mice

Figure shows the lack of tissue eosinophils in the lung of ZN (panel A & B) SAL-treated mice at low (250x initial) magnification and high (2500x initial) magnification. At high magnification, it was possible to see an occasional eosinophil (enclosed within red circles) within the subepithelial region of the airway in ZL (C & D) and ZR (E & F) SAL-treated mice.

SAL-Treated Mice
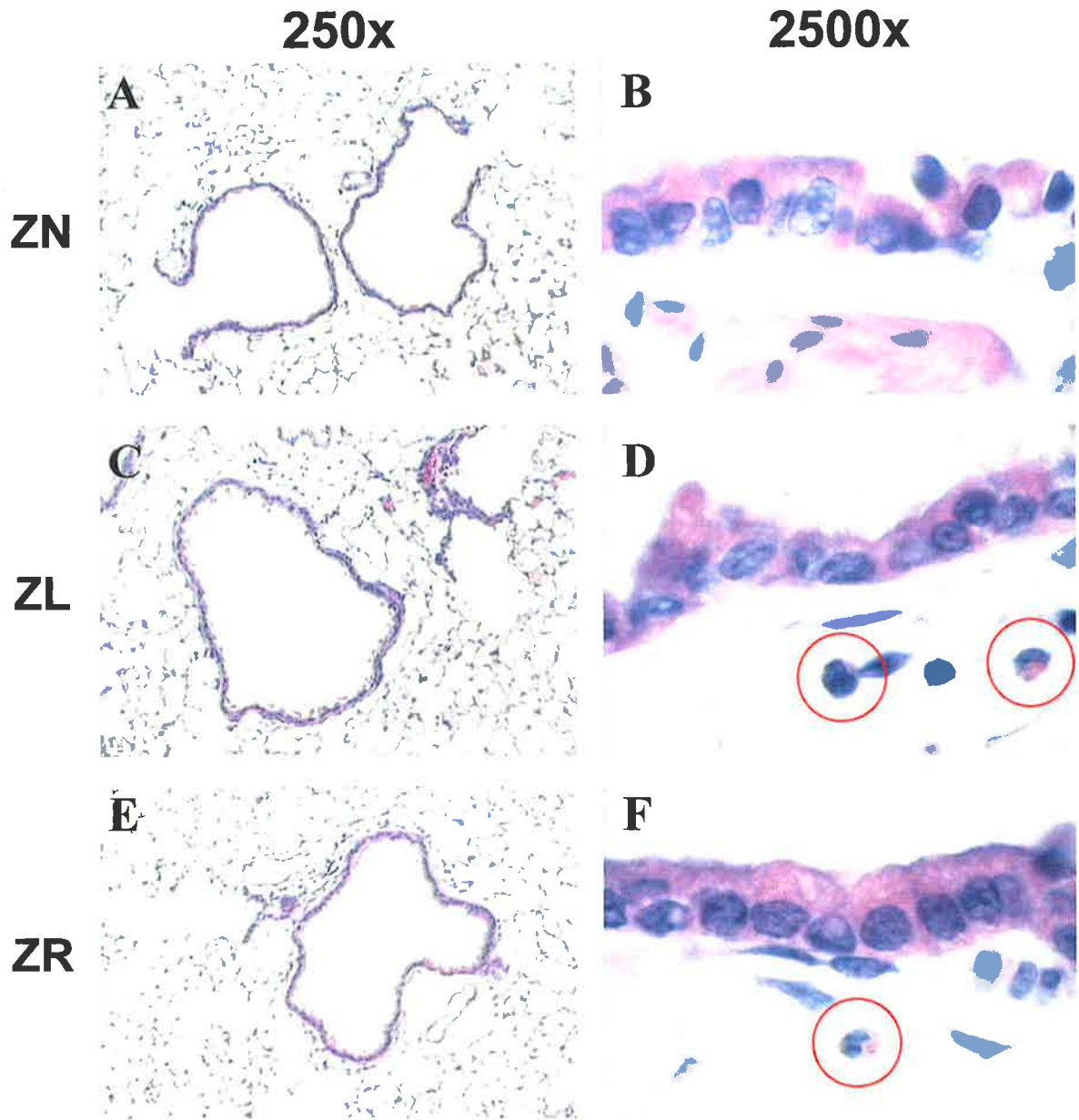
Figure 6.9: Elevated Numbers of Airway Tissue Eosinophils in OVA-Treated Mice

Figure shows the significant increase in the presence of inflammatory aggregates within the lamina propria and especially around the blood vessels (red arrow) of OVA-treated mice regardless of whether they were ZN (panel A & B), ZL (panel C & D) or ZR (panel E & F) OVA-treated mice (250x initial magnification). At high magnification (2500x), the majority of these cells were identified as eosinophils (enclosed within red circles) and were found within the subepithelial region (panel B & C) and the epithelium of these OVA-treated mice. Of particular interest, only a limited amount of alveolitis was observed in the OVA-treated mice (*, LHS panels).

OVA-Treated Mice

250x **2500x**
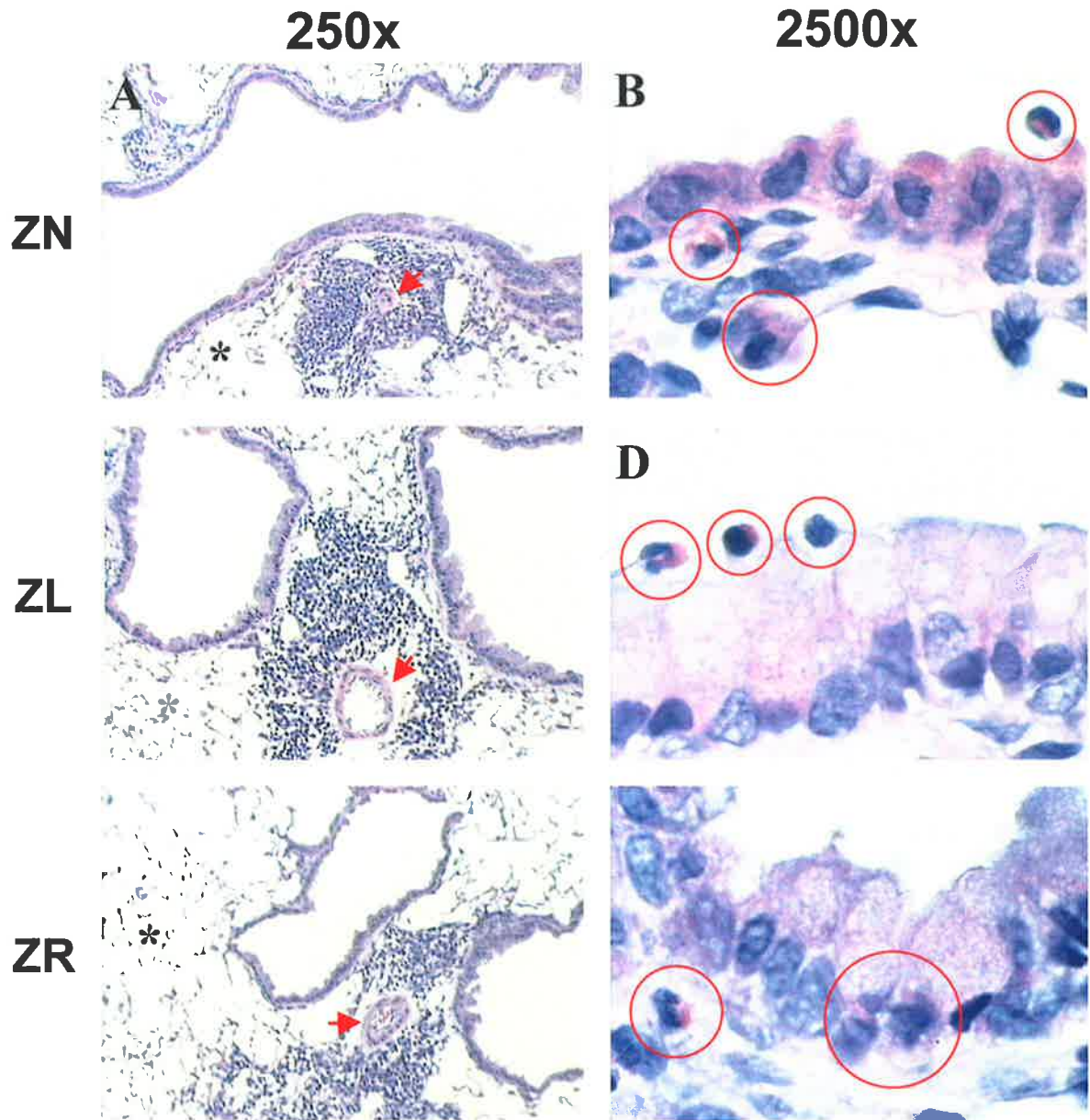
The number of tissue eosinophils were then assessed in at least 6 different airways of 3 different mice using a 100x objective lens and were expressed as mean number of eosinophils/100xHPF.

Allergy Type Comparisons

As shown in Chapter 5, ZN OVA-treated mice had a 400-fold increase in tissue eosinophils when compared to ZN SAL-treated mice. This trend was also present for the ZL mice (Table 6.2).

Diet Type Comparisons

This section compares the number of infiltrating tissue eosinophils in SAL and OVA-treated mice given the ZL diets to their ZN counterparts. Consistent with an increase in blood eosinophils, there was a small but significant rise in the number of infiltrating tissue eosinophils around the airways of both ZL SAL-treated and OVA-treated mice compared to the ZN SAL-treated and OVA-treated mice (Table 6.2). Firstly, in the SAL-treated groups, ZL mice had an 18 fold increase in eosinophils from 0.1 ± 0.1 cells/100xHPF in ZN mice to 1.8 ± 0.6 cells/100xHPF ($p < 0.05$). In addition, Zn deprivation further increased airway tissue eosinophil numbers in OVA-treated mice ($p < 0.05$). Thus, ZL OVA-treated mice (red column) had 58.7 ± 4.4 cells/HPF compared with 41.4 ± 4.9 cells/HPF (blue column) in the ZN OVA-treated mice ($p < 0.05$). Similarly, ZR SAL and OVA-treated mice had higher airway tissue eosinophil numbers than their ZN counterparts. ZR SAL-treated mice had 0.6 ± 0.1 cells/100xHPF while the ZR OVA-treated mice had 52.4 ± 1.9 cells/100xHPF, while the ZN SAL-treated mice had 0.1 ± 0.1 cells/100xHPF and ZN OVA-treated mice had 41.4 ± 4.9 cells/HPF. However this result was not statistically significant ($p > 0.05$).

184

6.3.2.3 Zn Deprivation Enhances Mucus-secreting Cell Numbers in Non-Allergic and Allergic Mice

Figure 6.10 shows the relative paucity of mucus cells in SAL-treated mice, while Figure 6.11 shows increased numbers of mucus cells in OVA-treated mice. Mucus cells were counted in at least 6 airways of 3 mice from both SAL-treated and OVA-treated groups and are expressed as mucus cells/40xHPF (Table 6.2).

Allergy Type Comparisons

As reported in Chapter 5, mucus cell numbers were significantly increased in all mice treated with OVA when compared to their SAL-treated counterparts ($p < 0.005$, Table 6.2)

Diet Type Comparisons

Zn deprivation increased mucus cell numbers in both SAL-treated and OVA-treated mice, while Zn repletion partially reversed these effects. There were increases in mucus cell numbers from 0.1 ± 0.1 cells/40xHPF in ZN SAL-treated mice to 1.1 ± 0.3 cells/40xHPF in ZL SAL-treated mice ($p < 0.05$) while ZR SAL-treated mice had 0.88 ± 0.2 cells/40xHPF. In the OVA-treated group, ZN mice had 70.6 ± 3.2 cells/40xHPF while the ZL mice had 132.3 ± 3.5 cells/HPF ($p < 0.005$) and the ZR OVA-treated mice had 118.5 ± 5.3 cells/40xHPF ($p = 0.06$, comparison with ZL mice).

Figure 6.10: Absence of Mucus Cells within the Airway Epithelium of SAL-Treated Mice

Paraffin sections were stained with Alcian Blue/PAS to identify mucus cells within the airway epithelium of SAL-treated mice. Figure shows the lack of tissue mucus cells in the airway epithelium of ZN (panel A & B), ZL (panel C & D) and ZR (panel E & F) SAL-treated mice at low (250x initial) and high (2500x initial) magnifications.

SAL-Treated Mice

250x   2500x
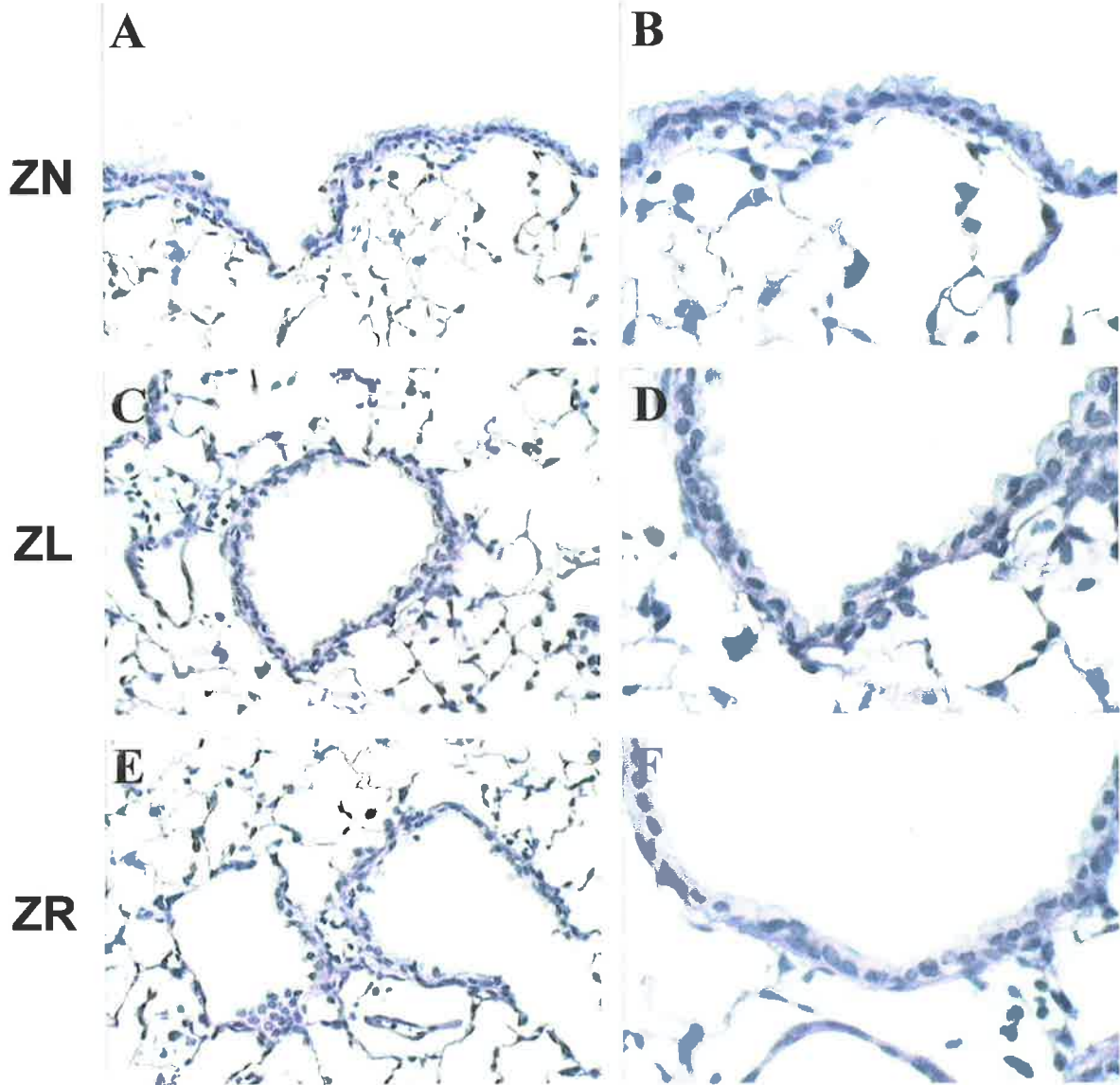
Figure 6.11: Increased Mucus Cell Numbers within the Airways of OVA-Treated Mice

Figure shows the significant increase of Alcian Blue/PAS positive mucus cells (blue staining) within the airway epithelium of ZN (panel A & B), ZL (panel C & D) and ZR (panel E & F) OVA-treated mice (250x initial magnification, RHS and 2500x magnification, *LHS*).

OVA-Treated Mice

250x   2500x
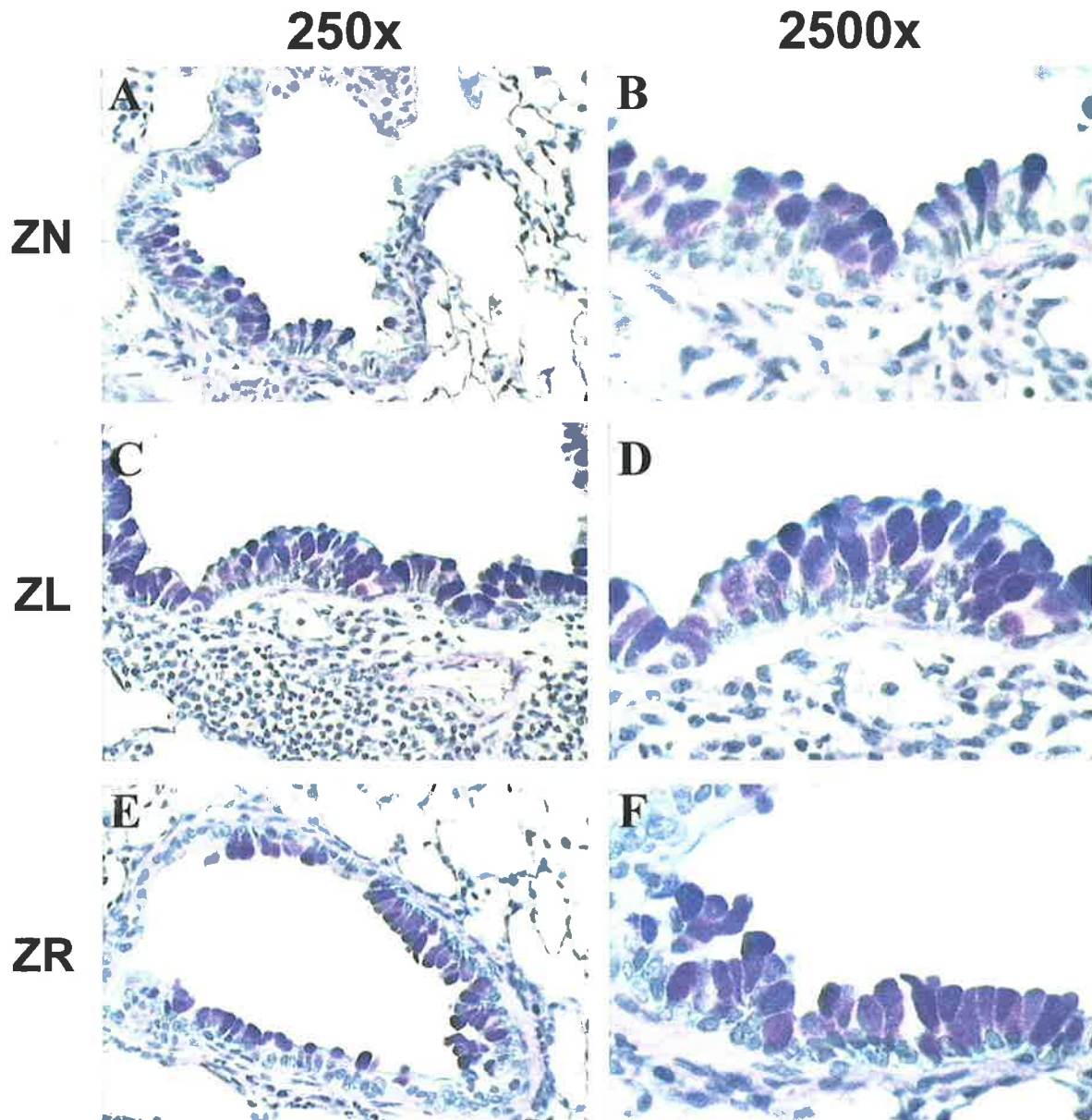
6.3.2.4 Zn Deprivation Increases AHR Response to β-Methacholine in BALB/c Mice

A part of the design of this experiment was to obtain two AHR readings, AHR 1, at the beginning of the repletion phase and AHR 2, 7 days after Zn repletion. Unfortunately, the BUXCO machine malfunctioned at the time of AHR 2. The machine was unable to accurately record the AHR responses to β-methacholine as the data collected was incomplete and artifactual readings of 0.000 Penh units were often obtained for all of the mice tested on that day. Therefore these data were disregarded. Since this experiment involved using facilities at the JCSMR and because this was one of the final experiments for this thesis, it was not possible to redo the experiment in full. However a second group of mice in Canberra were on a casein diet only regime (Group 3 mice) and it was possible to test in these mice the effects of Zn repletion on AHR after the BUXCO machine had been repaired (section 6.3.2.5).

The following results are expressed in Penh units (Figure 6.12) and as percentage increase over the baseline and data obtained from 8 mice per group (summarised in Table 6.3 and illustrated in Figure 6.12).

Allergy Type Comparisons

The ZN and ZL OVA-treated mice showed a typical response to increasing β-methacholine concentrations when compared to their SAL-treated counterparts (Figure 6.12 panel A). AHR was significantly increased in the OVA-treated mice at all concentrations of β-methacholine from 6.25 mg/ml to 50 mg/ml for ZN and ZL mice (Figure 6.12 for Penh units and Table 6.3 for percentage increase over baseline).

186

Figure 6.12: AHR in Mice Given Varying Zn Casein Diets

AHR was assessed in mice given varying Zn casein diets in the presence or absence of OVA.

Panel A: Figure depicts the AHR response to β-methacholine 24 h after the 6th nebulisation at day 37. AHR Penh readings (y-axis) are plotted against β-methacholine concentrations (x-axis) for ZN (blue lines) and ZL (red lines) SAL-treated (circles) and OVA-treated (triangles) mice. Figure shows a trend towards elevated AHR responses in mice given the ZL diet when compared to the ZN mice. Data represent means $\pm$ SEM for 8 mice per group. Significant differences refer to comparisons between ZN and the ZL treated mice: * $p < 0.05$.

Panel B: Figure depicts the AHR response to β-methacholine in mice given casein diets only. Figure shows a significant elevation in AHR responses in the ZL mice (red line) when compared to the ZN (blue line) and the ZR (green line) mice.

Inset: Inset depicts the growth curves obtained for these mice and show an early separation in weights between the ZL and the ZN mice. Zn repletion was able to increase weights of mice previously on the ZL diet. Data represent means $\pm$ SEM for 8 mice per group. Significant differences refer to comparisons between ZN and the ZL treated mice as depicted by the asterisk; * $p < 0.05$. A second comparison was performed between the ZL and ZR mice depicted by the symbol (*t*); $p < 0.05$.

A

Penh Reading (y-axis): 0, 1.0, 2.0, 3.0, 4.0, 5.0, 6.0, 7.0

β-Methacholine (mg/ml) (x-axis): 0, 5, 10, 15, 20, 25, 30, 35, 40, 45, 50

OVA
ZL
ZN
*
*
SAL
ZL *
ZN

B

Penh Reading (y-axis): 0, 0.5, 1.0, 1.5, 2.0, 2.5, 3.0, 3.5

β-Methacholine (mg/ml) (x-axis): 0, 5, 10, 15, 20, 25, 30, 35, 40, 45, 50

* * *
t

Inset:

Weight (g) (y-axis): 13.5, 14.5, 15.5, 16.5, 17.5, 18.5, 19.5

Days on Feed (x-axis): 0, 3, 6, 9, 12, 15, 18, 21, 24, 27, 30, 33, 36, 39, 42

ZR
ZN
ZD

*
*
*

AHR 1
+ Zn Repletion
(Day 28)

AHR 2
(Day 33)

AHR 3
(Day 40)
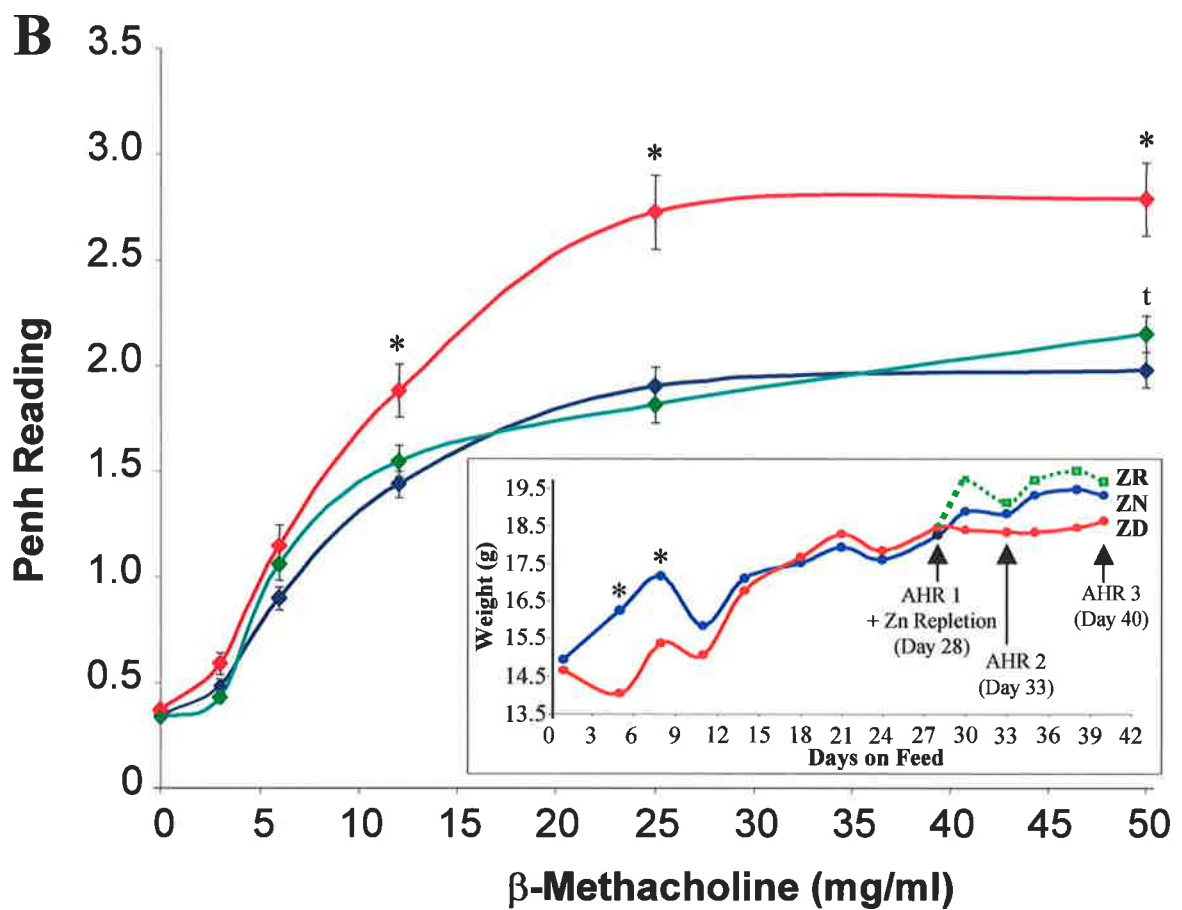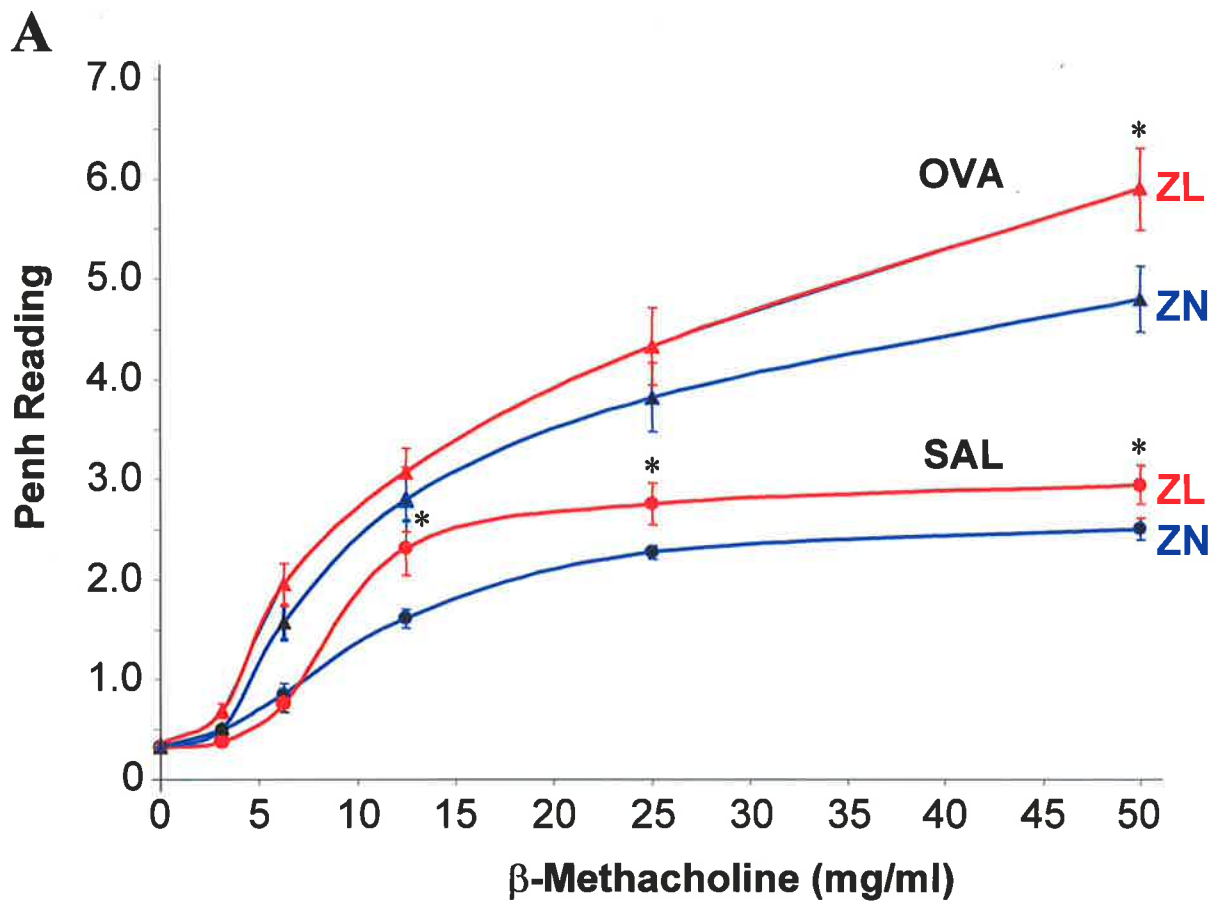
Table 6.3 AHR Responses to β-Methacholine for Egg White and Casein Fed Mice

	Egg White Diet[1]				Casein Diet[2]				Casein Diet[3]		
	Egg White Diet				Casein Diet				Casein Diet		
β-Methacholine	ZN SAL	ZL SAL	ZN OVA	ZL OVA	ZN SAL	ZL SAL	ZN OVA	ZL OVA	ZN only	ZL Only	ZR Only
(mg/ml)	(% increase over base line)[6]				(% increase over base line)				(% increase over base line)		
0	0.0	0.0	0.0	0.0	0.0	0.0	0.0	0.0	0.0	0.0	0.0
3	36.3	95.2	04.4	18.7	50.3	20.9	57.7	92.2	41.3	59.5	27.7
6	98.4	59.4	49.8	93.2	156.9	139.4	384.1	446.4	160.5	209.4	216.4
12	168.1	196.7	194.1	369.6	385.3	629.7[a]	763.7	656.2	317.3	407.1[a]	361.3
25	337.1	510.9	331.9	500.4	583.4	767.9[a]	1076.7	993.1	451.1	634.5[a]	440.2[c]
50	351.9	605.1[a]	459.1	587.4	652.6	827.8[a]	1377.6[b]	1443.0[a,b]	473.7	651.2[a]	539.9

[1] Mice on the egg white diet had 1 AHR reading performed. Values represent means, n = 4 mice.

[2] Mice on the casein diet (+ SAL or OVA treatment) had 1 AHR reading performed. Values represent means, n = 8 mice.

[3] Mice on the casein diet only had 3 AHR readings performed. Values represent means, n = 8 mice.

[4] Abbreviations, SAL; saline, OVA; ovalbumin, ZN; normal Zn diet, ZL; Zn Limiting diet, ZR; Zn repleted diet.

[5] AHR responses to β-methacholine expressed as penh units (*enhanced pause*) as generated by the BUXCO software.

[6] AHR responses to β-methacholine expressed as % increase over baseline.

[a] Significantly different from ZN mice of the same allergy group.

[b] Significantly different from SAL-Treated mice of the same diet group.

[c] Significantly different from ZL diet only mice.

Diet Type Comparisons

There was a significant increase ($p < 0.05$) in AHR of mice given a Zn limited diet. This was best seen in the SAL-treated mice where increases in AHR were seen at all concentrations of β-methacholine ≥ 12.5 mg/ml (Figure 6.12, panel A). For example, at 50 mg/ml of β-methacholine, AHR in the ZL SAL mice was 2.9 ± 0.2 Penh units compared to 2.5 ± 0.1 Penh units for the ZN SAL-treated mice ($p < 0.05$, Figure 6.16 panel A). With the ZL OVA-treated group, although all Penh readings were higher than the corresponding readings for the ZN OVA-treated groups, significance was only seen at 50 mg/ml β-methacholine ($p < 0.05$).

6.3.2.5 Zn Repletion Decreases AHR

To confirm these findings and investigate whether Zn repletion influences AHR, a separate experiment was conducted where mice were given the ZN and ZL casein diets in the absence of allergy for 40 days (diet only) and are referred to as group 3 mice. AHR was tested at one week intervals on days 28, 33 and 40 and Zn repletion of ZL mice occurred on day 28 after the first AHR reading.

Figure 6.12 panel B shows the average AHR responses observed for ZN, ZL and ZR mice. Significant increases ($p < 0.05$) in AHR were observed for ZL mice at β-methacholine concentrations of ≥ 12.5 mg/ml when compared to the ZN mice. At AHR responses at 12.5 mg/ml and 50 mg/ml of β-methacholine were 1.9 ± 0.1 Penh units for the ZL mice (red line) compared with 1.4 ± 0.1 for the ZN mice (blue line) and 2.8 ± 0.2 Penh units (ZL mice) compared with 2.0 ± 0.1 Penh units (ZN).

Of particular interest, this increase in AHR was decreased in ZL mice repleted with the ZN diet (50mg/kg Zn) for 14 days. AHR in ZR mice decreased by 15.8% at 12 mg/ml β-methacholine (1.6 ± 0.1 Penh units), 33.3% at 25 mg/ml β-methacholine (1.8 ± 0.1 Penh units, $p < 0.05$) and finally by 21.4% at 50 mg/ml β-methacholine (2.2 ± 0.8 Penh units, $p < 0.05$) bringing AHR responses down to that of the ZN mice (2.0 ± 0.1 Penh units).

The weights of these mice are depicted within the insert of Figure 6.12 panel B and there were significant differences in weight between the ZN and ZL mice at days 5 and 7 of the experiment with no significant difference observed thereafter. Surprisingly, there was a rapid increase in the weights of ZL mice after 2 days of Zn repletion with the ZN diet which lasted the entire duration of the experiment. This is different to the growth rate observed for the mice fed the same casein diets but were induced to have allergy.

6.4 DISCUSSION

This chapter focuses on whether Zn influences the key physiological (AHR) and histological features (tissue and blood eosinophilia and mucus-secreting cell numbers) associated with asthma. The major findings were significant increases in 1) the presence of eosinophils in blood and airway tissue, 2) mucus cell numbers and 3) AHR in Zn limited SAL-treated and ZL OVA-treated mice, compared with their Zn normal counterparts.

One of the main features of this study was the manipulation of Zn status via the diet to induce a mild Zn deficiency. In this thesis, mild Zn deficiency is defined

as causing a small transient reduction in weight with no other obvious signs consistent with Zn deficiency such as loss of fur or diarrhea. The mild Zn deficiency was achieved firstly using an egg white diet. This diet is more commonly used to create a severe level of Zn deficiency in rodents since it contains less than 1mg/kg of Zn (Coyle et al., 1999; Luecke & Fraker, 1979; Simon & Taylor, 2001). Since one of the aims of the current study was to create a mild to moderate Zn deficiency, this diet was supplemented with $ZnCO_3$ to give a Zn limited diet with a final concentration of 5 mg Zn/kg diet. A separation in the weights between the ZN and ZL SAL-treated mice was observed after 7 days on their respective diets and achieving significance at days 14 and 16. This suggests that the Zn limited diet was successful in partially limiting the growth of these mice. A similar trend was also noted for the ZL OVA-treated mice but with smaller differences in the weight when compared to the ZN OVA-treated mice. The reason for this is not clear and may be related to the level of inflammation present in these mice which may have influenced their ability to thrive. Consistent with this speculation, mice fed the ZL casein diets only and not induced to have allergy did experience an increase in growth rate when repleted with the ZN diet for 14 days (section 6.3.2.5). Further studies will assess the amount of diet consumed by these mice and compare this to their growth rates.

An increase in AHR was observed in mice given the ZL diet (for both SAL and OVA-treated groups) when compared to their ZN counterparts for the mice receiving the casein diets suggesting that Zn deprivation had adverse effects on airway function. However a lack of AHR was noted in both the ZN and the ZL OVA-treated mice which were fed the egg white diets. The poor AHR response of mice on the egg white diet is unlikely to be due to the batch of OVA used since

these were within the specified expiry date but rather because the egg white diet contained ovalbumin. This diet may have down regulated the specific immune responses to this antigen and therefore suppress the sensitisation of these mice. This could be tested by using an *in vitro* cell culture of splenocytes taken from OVA treated mice and measuring cytokine release in response to soluble OVA. These results could then be compared to the response given by the splenocytes obtained from mice on a different diet. The results reported in this chapter may be similar to the suppressed response observed by Dr. Dianne Webb (personal communication, JCSMR) when she used a batch of mouse food contaminated with chicken meat which also contains OVA. Therefore, a non-egg white diet was chosen for the second part of these studies and it was observed that this diet did not interfere with the level of inflammation created.

To overcome the above mentioned problem, it was possible to use a casein-based diet to study effects of mild Zn deficiency on allergic responses. This diet contained 14mg/kg Zn due to the Zn bound to casein. As a result for the ZL group, no further Zn was added to this diet. Zn deficiency was demonstrated by reduction in growth rates between days 6 and day 12, which was during the first period of OVA sensitisation. Growth inhibition is a sensitive marker of Zn deficiency (Prasad, 2001) and the growth curves for the ZL and ZN mice clearly show that Zn was the only limiting factor to weight gain in these mice. The effects of the Zn limiting diet on systemic and airway epithelial Zn levels is described in Chapter 7. The rationale behind inducing a mild, rather than a more severe Zn deficiency in these mice is that this more adequately reflects the suboptimal levels found in asthmatics (Di Toro et al., 1987; el-Kholy et al., 1990; Goldey et al., 1984; Kadrabova et al., 1996; Vural et al., 2000; Wood et al., 2000).

The mild Zn deficiency created in these experiments was able to produce significant differences in several inflammatory indices such as eosinophilia and mucus cell hyperplasia in the murine model used. Zn is a known anti-inflammatory agent acting both on the immune system and inflammatory cells. The immune system is partially dependent on the availability of Zn for its homeostasis since Zn regulates the balance between Th_1 and Th_2 lymphocyte subsets (Shankar & Prasad, 1998; Wellinghausen & Rink, 1998). Inflammatory diseases can cause an increase in the demand for Zn hence decreasing circulating Zn levels. This is detrimental since Zn deficiency enhances the activation of natural killer cells, phagocytic cells and granulocytes, including mast cells (Marone et al., 1986) and eosinophils (Winqvist et al., 1985), hence creating a continuous cycle of oxidative damage. The study by Winqvist and colleagues found that Zn ions were able to inhibit the release of eosinophilic cationic protein, a protein crucial for facilitating eosinophilic inflammation, by interacting with the eosinophils plasma membrane functions (Winqvist et al., 1985). The data described in this chapter reporting increased peripheral blood and tissue esosinophil percentages in the ZL mice may support these observations. Increased eosinophil numbers in the ZL SAL-treated mice may suggest an enhancement in the susceptibity of these mice to an inflammatory response or tissue damage. Significant increases noted in the ZL OVA-treated mice also support the hypothesis that Zn deprivation worsens the inflammatory response by enhancing eosinophil chemotaxis which ultimately exacerbates the damage to the airway epithelium. It was interesting to note that while Zn deprivation did significantly increase tissue eosinophil numbers, these changes were small in magnitude and did not influence the number of eosinophils recovered in the BALF and may be related to the severity of the level of Zn deprivation created. A more chronic state of Zn deficiency for two to three months

may have increased the numbers of eosinophils in the tissue to a greater extent, resulting in greater recovery in the BALF of these mice. However, to date no existing model will enable this type of experiment to be performed. The cytokine profile of the ZL non-allergic and allergic mice now needs to be investigated to determine if levels of IL-4, IL-5 and IgE in serum and lavage fluid are elevated.

The significant increase in mucus-secreting cell numbers noted in the ZL mice (SAL and OVA-treated) further supports the hypothesis that Zn deprivation has adverse effects on the pathogenesis of airway inflammation. Increased mucus cell numbers would ultimately contribute to the pathogenesis of allergic airway inflammation since mucus cell hyperplasia and metaplasia are distinct features of airway remodelling (reviewed in Holgate, 2000; Kumar, 2001). The mechanisms responsible for regulating the formation of mucus-secreting cells in allergic airway inflammation are unclear and will require further investigations. Future studies should focus on determining whether Zn deprivation can directly influence mucus cell secretion in the absence and or presence of IL-13 *in vivo* and *in vitro* since it has been reported that IL-13 induces airway mucus hypersecretion and goblet cell hyperplasia (Zhu et al., 1999).

As discussed in Chapter 5, one of the limitations of using an acute murine model of allergic airway inflammation is the presence of alveolitis. This has been minimised by using a sidestream jet nebuliser which delivers smaller particles when compared with the RapidFlo nebuliser. However, this observation is somewhat paradoxical in that smaller particles have been reported to penetrate further down the respiratory tract depositing in the alveolar tissue and hence should increase the risk of creating alveolitis (Ruffin et al., 1978).

The findings of increased AHR in ZL mice and the reversal of this response by 14 days of Zn repletion (diet only experiment) suggests that changes in dietary Zn levels can directly influence airway function. Hence, even mild Zn deficiency and a short period of Zn repletion is able to significantly regulate airway physiology. It is possible that the lesser effects of Zn deprivation on AHR in OVA-treated mice are due to the high level of inflammation already present in these mice.

The mechanisms controlling the increased AHR in the ZL mice now need to be further investigated to determine whether this is an effect primarily on the smooth muscle or rather an effect on the airway epithelium. One possible mechanism of action is via inhibitory effects of Zn on muscarinic and nicotinic receptors (Palma et al., 1998; Taylor & Peers, 2000). Recently, Taylor and Peers, using PC12 cells, reported that Zn^{2+} ions were able to prevent the activation of acetylcholine receptors by blocking Ca^{2+} ion influx across the plasma membrane (Taylor & Peers, 2000). One scenario is that Zn deprivation facilitates activation of muscarinic or β_2-adrenergic receptors, calcium channels and calcium influx in either smooth muscle or airway epithelium resulting in enhanced bronchoconstriction and similar effects on AEC may influence other factors. The suggestion that Zn deprivation enhances receptor activation is further supported by two recent biochemical studies. It was reported that physiological concentrations of Zn ions were able to inhibit the activation of β_2-adrenergic receptors and therefore stimulation of G proteins by binding to histidines within the receptor (Sheikh et al., 1999; Swaminath et al., 2002). Although these studies were not conducted within airway related cells, the mechanism by which Zn inhibits these receptors can be applied to the airways, since muscarinic and β_2-adrenergic receptors are present

within both the airway epithelium and the surrounding smooth muscle. Alternatively, increased AHR in ZL mice may be due to the increase in the numbers of mucus-secreting cells noted in the ZL mice. Future studies will determine whether creating a more severe Zn deficiency in these mice further exacerbates AHR and whether incubation of airway smooth muscle cells with an exogenous Zn salt blocks β-methacholine-induced activation of muscarinic or β_2-adrenergic receptors *in vitro*. Other effects of Zn deficiency on AHR may include enhanced inflammation due to shifts in the balance of lymphocyte subsets towards the pro-inflammatory Th_2 subset (Shankar & Prasad, 1998; Wellinghausen & Rink, 1998), increases in activation of mast cells and eosinophils (Marone et al., 1986; Winqvist et al., 1985) and increases in pro-inflammatory cytokines (Marone et al., 1986; Prasad, 2000; Winqvist et al., 1985).

There are two possible experiments which now need to be conducted. In order to further address some of the findings reported in this chapter. One of the limitations of this study is the restricted range of Zn deprivation and repletion studies performed. Hence it is therefore suggested that a broader range of Zn diets (inducing different levels of Zn deficiency) are used. In these experiments, repletion was for 7 days only to minimise stress caused by extra nebulisations. As such, the second suggestion would be to prolong this repletion period and possibly conduct this with a higher Zn content. This could be achieved by repleting the ZL mice at an earlier time point e.g. after the 4th nebulisation (day 32) at a time when an allergic response is ensured, (reviewed in Leong & Huston, 2001). By repleting at this time point, Zn repletion is extended to 14 days. The full kinetics of these changes needs to be thoroughly investigated. However, the key point is that effects

of Zn depletion on AHR can be reversed. This is an important finding in the context of extension to human disease.

One other major limitation of this study is the inability to draw direct conclusions between the animal studies and the human disease. For example, the amount of Zn administered to mice can not be directly compared to that of the RDI levels of Zn for humans. This is because mice consume 1/5th of their body weight per day while humans are thought to consume approximately $1/70^{th}$ of their body weight per day (personal communications Dr. Peter Coyle, Dept Clinical Biochemistry, IMVS). Hence the requirement of nutrient intake for rodents may be significantly increased. Furthermore the diet administered is carefully controlled and is casein based, however this is different for humans who obtain their Zn from a wider range of foods. Hence the results reported in this chapter describe a trend rather than creating a direct correlation between the animal model and the human situation.

In conclusion, this study has provided new data which may lead to a greater understanding of the interaction between Zn deficiency and airway disease. To further investigate the significance of Zn in allergic airway inflammation, levels of Zn and the Zn sensitive enzyme caspase-3, were analysed in the tissues of these mice in experiments described in Chapter 7.

Some of the results reported in this chapter are in the following manuscript:

1. Altered Zinc Homeostasis and Caspase-3 Activity in a Murine Model of Allergic Airway Inflammation. Truong-Tran AQ, Ruffin RE, Foster PS,

Koskinen AM, Coyle P, Philcox JC, Rofe AM and Zalewski PD. AMJRCMB (*in press*).

CHAPTER 7
ALTERED ZINC HOMEOSTASIS AND
CASPASE-3 ACTIVITY IN MURINE ALLERGIC
AIRWAY INFLAMMATION

CHAPTER 7 ALTERED ZINC HOMEOSTASIS AND CASPASE-3 ACTIVITY IN MURINE ALLERGIC AIRWAY INFLAMMATION

7.1 INTRODUCTION

One major pathological feature of asthma is the shedding and desquamation of the respiratory epithelium. Bronchial biopsies taken from asthmatic patients not being treated with inhaled steroids commonly demonstrate loss of the mucosal epithelium, and the swelling of ciliated columnar cells, giving the epithelium a "fragile appearance" (Laitinen et al., 1985) It has been suggested that increased release of serine proteases from neutrophils recruited during airway inflammation may be responsible for the detachment of human epithelial cells from their basement membrane (Venaille et al., 1995). However, the mechanism of cell death associated with the shedding of this epithelium remains unclear. Since apoptotic pathways can be targeted by specific inhibitors (Cursio et al., 2000; Lee et al., 2000) it is important to determine whether AEC in asthmatics die by apoptosis, resulting in shedding.

Although apoptosis is a normal process, the regulation of apoptosis becomes altered in some chronic diseases such as HIV and diabetes (Kumar, 1999). Recently, it has been shown that active caspase-3 (AC3) protein was increased in the epithelium and submucosa of human bronchial biopsies from asthmatics, both steroid treated and untreated, when compared with non-asthmatic subjects (Benayoun et al., 2001). This sudy is the first to report increases in AC3 protein within AEC of human bronchial biospies taken from human asthmatics.

In Chapter 3 of this thesis, intracellular labile Zn was found to be localised within the apical region of AEC as detected by the novel Zn specific fluorophore Zinquin. This cytoplasmic distribution of Zn was similar to that of the zymogen form of caspase-3 (Krajewska et al., 1997; Truong-Tran et al., 2001) and as described in Chapter 4, was also reported to be an essential regulator of caspase-mediated REC apoptosis. Thus the experiments reported in this chapter attempt to further these studies by investigating the effects of Zn deficiency on caspase activation in an *in vivo* model and to determine whether an alteration in systemic Zn levels exist.

In this chapter, it was hypothesised that low systemic Zn levels and AEC Zn levels may facilitate the development of airway disease or the clinical expression of airway diseases by enhancing caspase mediated apoptosis of AEC.

The aim of the experiments described in this chapter was therefore to examine the influence of allergic inflammation *per se* on levels of serum and liver Zn, intracellular AEC Zn, pro-caspase-3 (PC3), AC3 protein and apoptosis in AEC using tissues obtained from the experiments previously described in Chapters 5 and 6.

7.2 METHODS

7.2.1 Determination of Serum and Liver Zn levels by Atomic Absorption Spectroscopy

Serum and liver Zn levels were determined as previously described in section 2.6 using graphite atomic absorption spectroscopy for serum Zn analysis and flame atomic absorption spectroscopy for liver Zn analysis.

7.2.2 Detection of the PC3 Protein and AC3 Protein Levels by Immunohistochemistry.

PC3 protein and AC3 protein expression were determined by immunohistochemistry as described in section 2.11.3 using the primary rabbit anti-human precursor 32kDa caspase-3 antibody and a primary rabbit anti-human active 17kDa caspase-3 antibody, both of which were cross-reactive with mouse caspase proteins. Negative controls lacked the primary antibody.

7.2.3 Co-localisation of PC3 Protein and Zn

In some experiments, dual staining was performed as described in section 2.11.4. After the PC3 protein immunostaining procedure was completed, sections were treated with Zinquin and permanently mounted with fluorescent mounting medium.

7.2.4 Detection of a Caspase Cleavage Product of Cytokeratin 18 (CK18) by Immunohistochemistry.

To confirm apoptosis, the M30 Cytodeath Kit (Roche Diagnostics, Mannheim, Germany) was used to detect apoptotic cells in cryostat sections of mice lung tissue. This was performed as described in section 2.11.5. The M30 Cytodeath kit uses a mouse IgG_{2b} monoclonal antibody which detects an epitope formed during the cleavage of CK18 by caspases in the early stages of apoptosis. Negative controls lacked the primary antibody.

7.2.5 Confocal Image Analysis

All slides were examined using standard light microscopy and UV laser confocal microscopy as described in section 2.11.6 A Bio-Rad MRC-1000 UV Laser Scanning Confocal Microscope System, equipped with a UV-Argon laser, was used in combination with a Nikon Diaphot 300 inverted microscope in fluorescence mode. Before the capturing of images, the laser settings of the confocal microscope were adjusted to a level which excluded background fluorescence. The laser strength for Zinquin fluorescence was 3% and for FITC fluorescence, the laser was 10%. Where dual staining was performed, fluorescence images were merged to demonstrate both Zinquin and PC3 protein staining using the Confocal Assistant (Version 4.02) software package. For each image, 5 randomly positioned profiles lines were drawn at 90° to the epithelial surface so that they spanned the entire epithelium. The mean fluorescence intensity was calculated for each of 15 evenly spaced intervals across the epithelium, the first beginning at the luminal surface and the last terminating at the basement membrane. Apical region is defined as intervals from 1 to 5 and the basal region as intervals from 6 and 15. Fluorescence was quantified using the

CoMOS software package (Bio-Rad, Hemel Hempstead, UK) and results expressed as GSU between 0-255 units. The mean fluorescence intensity was collated from at least 2 different mice per group, each having 5 to 6 airways assessed (n = 60 profiles were obtained per group).

The data reported in this chapter are expressed as means ± standard error of the mean (SEM). Where appropriate, the student t test was performed. Differences were considered statistically significant at $p < 0.05$, unless otherwise stated.

7.3 RESULTS

The results described in this chapter refer to experiments conducted on serum, liver and lung tissue samples collected from the SAL and OVA-treated mice (Group 1 mice) described in Chapter 5 and the ZN and ZL SAL and OVA-treated mice (Group 2 mice) described in Chapter 6. Because of the small effects of the 7 days of Zn repletion on inflammatory indices and the limited time and availability of reagents, it was decided only to assay the ZN and ZL mouse tissues. A more extensive look at the effects of Zn repletion will form the basis for future experiments in this laboratory.

7.3.1 Serum and Liver Zn levels are Not Altered in Allergic Airway inflammation

To determine whether Zn status was altered in OVA-treated mice, total serum (n = 4-10 mice per group) and liver Zn levels (n = 8-10 mice per group) were determined by atomic absorption spectroscopy.

Group 1- SAL and OVA Only

Both serum and liver total Zn levels were significantly increased in the OVA-treated mice. OVA-treated mice had a 2 fold increase in serum Zn levels at 17.8 ± 0.9 μM when compared to the SAL-treated mice which had 9.0 ± 1.1 μM (n =10 mice per group, $p < 0.005$). Similarly, total liver Zn levels were significantly increased by 1.2 fold from 442.2 ± 22.4 nmol/gram liver in the SAL-treated mice to 525.6 ± 33.0 nmol/gram liver in the OVA-treated mice (n = 10 mice per group, $p < 0.05$).

Group 2- Casein Diet plus SAL and OVA

A trend towards decreased serum Zn levels but not liver Zn levels was noted in the ZN OVA-treated mice when compared to their ZN SAL-treated counterparts. Firstly, analysis of serum Zn showed a non-significant 25% decrease from 17.6 ± 5.1 μM in the ZN SAL-treated mice (n = 4 mice) to 13.2 ± 3.4 μM in the ZN OVA-treated mice (n = 6 mice). A similar decrease in serum Zn levels was noted in the ZL SAL-treated mice (n = 8 mice) which had 13.5 ± 1.5 μM when compared to the ZN SAL-treated mice. A decrease in serum Zn levels did not however occur when ZL mice were treated with OVA (15.8 ± 1.7 μM, n = 8 mice). The discrepancies noted in these serum Zn levels for group 1 and 2 mice will be discussed in section 7.4.

Liver Zn levels were not significantly decreased when mice were given the ZL diet (n = 8 mice per group). ZL SAL-treated mice had a liver Zn concentration of 445.3 ± 15.4 nmol/gram liver while the ZL OVA-treated mice had 458.0 ± 10.0 nmol/gram liver compared to the ZN SAL and OVA-treated mice which had 488.2 ± 6.1 nmol/gram liver and 465.0 ± 12.3 nmol/gram liver, respectively ($p > 0.05$).

203

7.3.2 AEC Intracellular Zn Levels are Decreased in Allergic Airway Inflammation

There was a significant decrease in AEC Zn levels as detected by Zinquin fluorescence and quantified by image analysis in the OVA-treated mice from both group 1 and 2 mice.

Group 1-SAL and OVA Only

For group 1 mice (n = 60 profile lines), total Zinquin fluorescence decreased by 1.5 fold falling from 132.4 ± 5.6 GSU in the SAL-treated mice to 86.3 ± 1.4 GSU in the OVA-treated mice ($p < 0.005$). Figure 7.1 illustrates the distribution of Zinquin fluorescence quantified along a profile line in the airway epithelium of SAL (panel A) and OVA-treated (panel B) mice. The distribution of Zinquin was found to be mainly apical in the airway epithelium of the SAL-treated mice and was contained between intervals 1 and 6 (panel A). However there was a distinct shift in the localisation of this fluorescence to a more evenly distributed and homogenous pattern in the OVA-treated mice (panel B). Table 7.1 reports the significant ($p < 0.005$) decreases in epithelial Zn levels for the OVA-treated mice which occurred in both the apical and basal compartments of the epithelium. For example, SAL-treated mice had an apical fluorescence of 157.16 ± 2.13 GSU and a basal fluorescence of 120.0 ± 0.85 GSU compared to the OVA-treated mice which had an apical fluorescence of 91.1 ± 3.5 GSU and a basal fluorescence of 83.84 ± 1.17 GSU ($p < 0.005$). Hence Zinquin fluorescence decreased 1.7 fold (apical) and 1.4 fold (basal) in the OVA-treated mice.

Figure 7.1: Quantification of Zinquin Fluorescence Across Respiratory Epithelium of Group 1 SAL and OVA-Treated Mice

Figure shows the quantification of Zinquin fluorescence across the entire airway epithelium in SAL (panel A, light purple) and OVA-treated (panel B, dark purple) mice. Zinquin fluorescence, expressed as mean GSU, is plotted on the y-axis against the distance from the lumen to the basement membrane of the airway epithelium. Fifteen evenly-spaced intervals were quantified at 1 μm distances which span the entire epithelia from the apical luminal surface (intervals 1 to 5) to the basal surface (intervals 6 to 15). OVA-treated mice had a marked decrease in Zn resulting in a shift in the distribution of fluorescence from an apical to a more homogenous pattern. The mean fluorescence intensity was collated from at least 2 different mice per group, each having 5 to 6 airways assessed (n = 60 profiles were obtained per group).

A

SAL Only

132.4 ± 5.6

Zinquin Fluorescence (GSU)

Distance from Lumen to the BM Across The Epithelium (μm)

B

OVA Only

86.3 ± 1.3

Zinquin Fluorescence (GSU)

Distance from Lumen to the BM Across The Epithelium (μm)

Table 7.1 Alterations in Zinquin Fluorescence and PC-3 Levels in SAL-Treated and OVA-Treated Mice on Different Zn Diets[1].

	Zinquin Fluorescence (GSU)		PC-3 FITC Fluorescence (GSU)	
	Apical	Basal	Apical	Basal
Group-1				
SAL[2]	157.16 ± 2.13	120.0 ± 0.85	177.68 ± 4.59	113.11 ± 5.80
OVA	91.10 ± 3.51^a	83.84 ± 1.17^a	195.40 ± 2.00^a	176.40 ± 1.80^a
Group-2				
ZN SAL-Treated	107.0 ± 1.80	97.80 ± 1.70	207.80 ± 5.20	164.00 ± 5.30
ZN OVA-Treated	47.10 ± 1.60^c	34.80 ± 1.20^c	240.50 ± 2.20^c	219.90 ± 3.40^c
ZL SAL-Treated	95.30 ± 90.40^b	90.40 ± 2.30^b	190.00 ± 4.60^b	160.00 ± 4.90
ZL OVA-Treated	47.30 ± 2.91^c	$47.70 \pm 1.60^{b,c}$	$213.40 \pm 4.40^{b,c}$	160.00 ± 4.60^b

[1] Values represent means $\pm$ SEM, n = 60 profiles per group.

[2] Abbreviations, SAL; saline, OVA; ovalbumin, ZN; normal Zn diet, ZL; Zn Limiting diet.

[a] Significantly different from SAL-Treated mice (Group 1 mice).

[b] Significantly different from ZN mice of the same allergy group (Group 2 mice).

[c] Significantly different from SAL-Treated mice of the same diet group (Group 2 mice).

Group 2-Casein Diet plus SAL and OVA

Figure 7.2 illustrates the distribution of Zinquin fluorescence quantified along profile lines in the airway epithelium of group 2- ZN (top panel), ZL (bottom panel) SAL (LHS panels) and OVA-treated (RHS panels) mice (n = 60 profile lines). Once again, there were significant decreases in epithelial Zn levels in the ZN and ZL OVA-treated mice (panels B & D). ZN SAL-treated mice had an average total Zinquin fluorescence of 100.9 ± 3.2 GSU which significantly decreased to 38.9 ± 1.9 GSU (p < 0.005) in the ZN OVA-treated mice. Similarly, ZL SAL treated mice had 92.1 ± 3.3 GSU while the ZL OVA-treated mice had 47.5 ± 0.8 GSU (panel B, p < 0.005). Both the ZN and ZL OVA-treated mice had a pattern of Zinquin fluorescence which was homogenous.

Mice given the Zn deprived diets had significantly decreased Zinquin fluorescence in the airway epithelium when compared to their ZN counterparts, but the magnitude of this decrease was much less than that due to allergy alone. For example, ZN SAL-treated mice had 100.9 ± 3.2 GSU compared to 92.05 ± 3.3 GSU in the ZL SAL-treated mice (Figure 7.2, panels A & C, p < 0.05). Zn deprivation did not however further decrease Zinquin fluorescence in the ZL OVA-treated group which had 47.6 ± 0.8 GSU when compared to its ZN OVA-treated counterpart which had 38.9 ± 1.9 GSU (Figure 7.2, panels B & D).

Table 7.1 reports the significant (p < 0.005) decreases in epithelial Zn levels for these mice which occurred in both the apical and basal compartments of the epithelium when compared to their SAL-treated counterparts. As with effects of allergy alone, Zn deprivation also decreased Zinquin fluorescence in both the apical and basal compartments.

205

Figure 7.2: Quantification of Zinquin Fluorescence Across Respiratory Epithelium of Group 2 SAL and OVA-Treated Mice

Figure shows the quantification of Zinquin fluorescence across the entire airway epithelium for the SAL (ZN-light blue panel A and ZL-pink panel C) and OVA-treated (ZN-navy panel B and ZL-red panel D) mice. Zinquin fluorescence values expressed as mean GSU are plotted on the y-axis against the distance from the lumen to the basement membrane (BM) of the airway epithelium A marked decrease in labile Zn was observed in the ZN (panel B) and ZL (panel D) OVA-treated mice. Apical and basal regions are defined as for Figure 7.1. The mean fluorescence intensity was collated from at least 2 different mice per group, each having 5 to 6 airways assessed (n = 60 profiles were obtained per group).

A ZN SAL — 100.9 ± 3.2

B ZN OVA — 38.9 ± 1.9

C ZL SAL — 92.1 ± 3.3

D ZL OVA — 47.5 ± 0.8

Zinquin Fluorescence (GSU)

Distance from Lumen to the BM Across The Epithelium (μm)
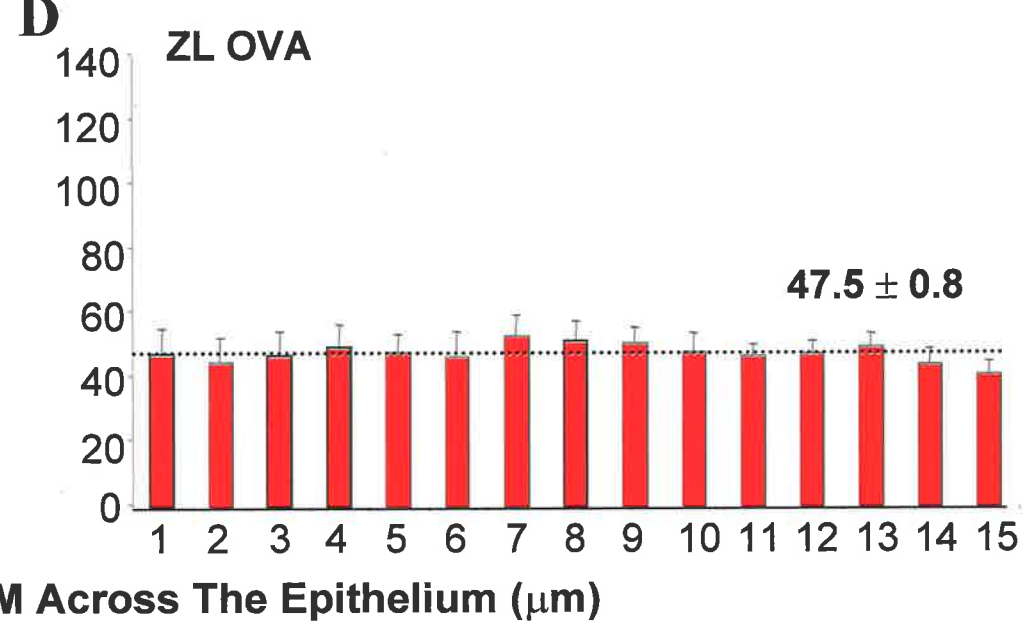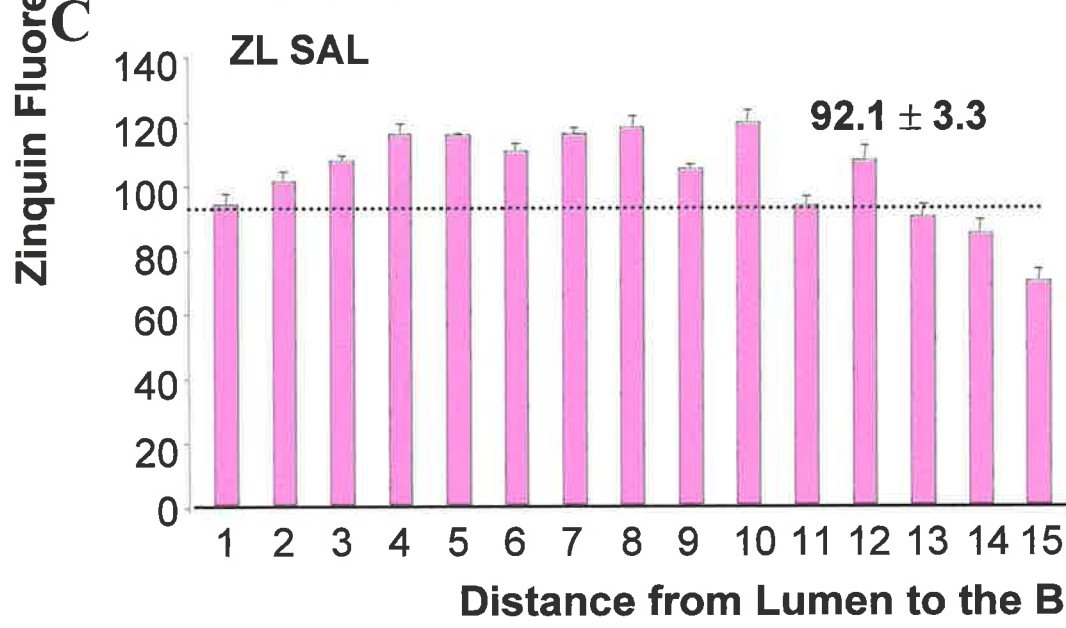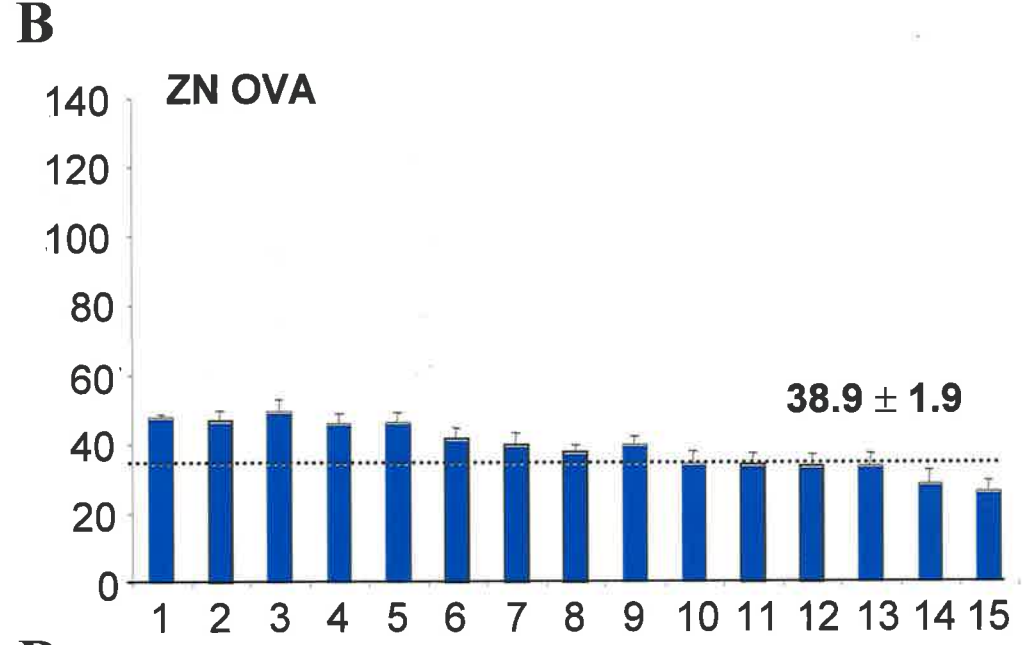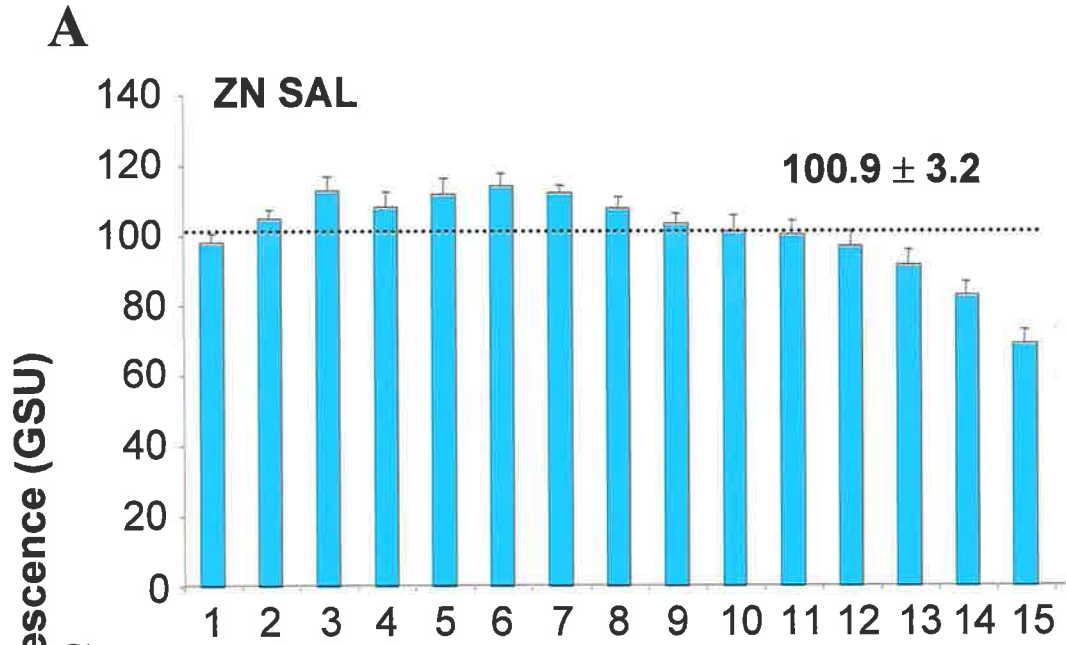
The variability in baseline Zinquin fluorescence for group 1 and 2 mice may be due to experiments being conducted at different time points. These discrepancies are discussed in detail in section 7.4.

7.3.3 PC3 Protein Levels are Increased in Allergic Airway Inflammation

Since labile intracellular Zn levels were disturbed in OVA-treated ZN and ZL mice and Zn is a known regulator of caspase-3 activation, it was important to determine whether alterations in PC3 protein had also occurred. Firstly, there was a significant increase in the levels of PC3 protein as determined by immunohistochemistry and quantified by image analysis in the OVA-treated mice from both group 1 (n = 60 profile lines) and 2 mice (n = 60 profile lines).

Group 1-SAL and OVA Only

For group 1 mice, PC3 protein levels were increased by 1.4 fold rising from 131.2 ± 10.1 GSU in the SAL-treated mice to 182.0 ± 3.1 GSU in the OVA-treated mice (p < 0.005). Figure 7.3 illustrates the distribution of PC3 protein quantified along a profile line in the airway epithelium of SAL (panel A) and OVA-treated (panel B) mice and depicts a change from an apical to a more homogenous pattern. As reported in Table 7.1 increases in PC3 protein occurred both in the apical and basal compartments of the airway epithelium of the OVA-treated mice.

Group 2-Casein Diet plus SAL and OVA

Figure 7.4 illustrates the increase in epithelial PC3 protein levels noted in the group 2 OVA-treated mice. ZN SAL-treated mice had an average total PC3-FITC fluorescence of 178.6 ± 6.9 GSU (panel A) while, in the ZN OVA-treated

Figure 7.3: Quantification Of Pro-Caspase-3 FITC (PC3-FITC) Fluorescence Across Respiratory Epithelium of Group 1 SAL and OVA-Treated Mice

Figure shows the quantification of PC3-FITC fluorescence across the entire airway epithelium in SAL (panel A, light purple) and OVA-treated (panel B, dark purple) mice. PC3-FITC fluorescence values expressed as mean GSU are plotted on the y-axis against the distance from the lumen to the basement membrane of the airway epithelium Apical and basal regions are defined as for Figure 7.1. OVA-treated mice had a marked increase in PC3 protein levels resulting in a shift in the distribution of fluorescence from an apical to a more homogenous appearance. The mean fluorescence intensity was collated from at least 2 different mice per group, each having 5 to 6 airways assessed (n = 60 profiles were obtained per group).

A SAL Only

PC3-FITC Fluorescence (GSU)

131.2 ± 10.1

Distance from Lumen to the BM Across The Epithelium (μm)

B OVA Only

PC3-FITC Fluorescence (GSU)

182.0 ± 3.1

Distance from Lumen to the BM Across The Epithelium (μm)
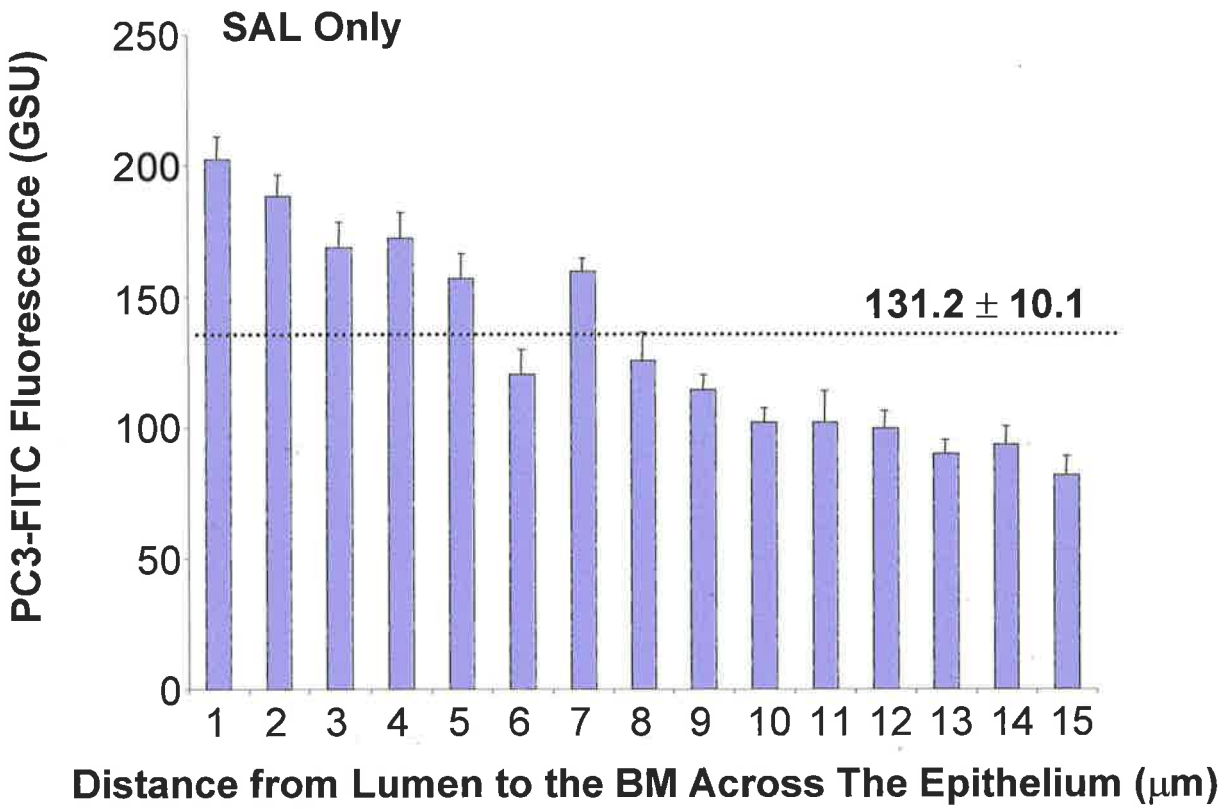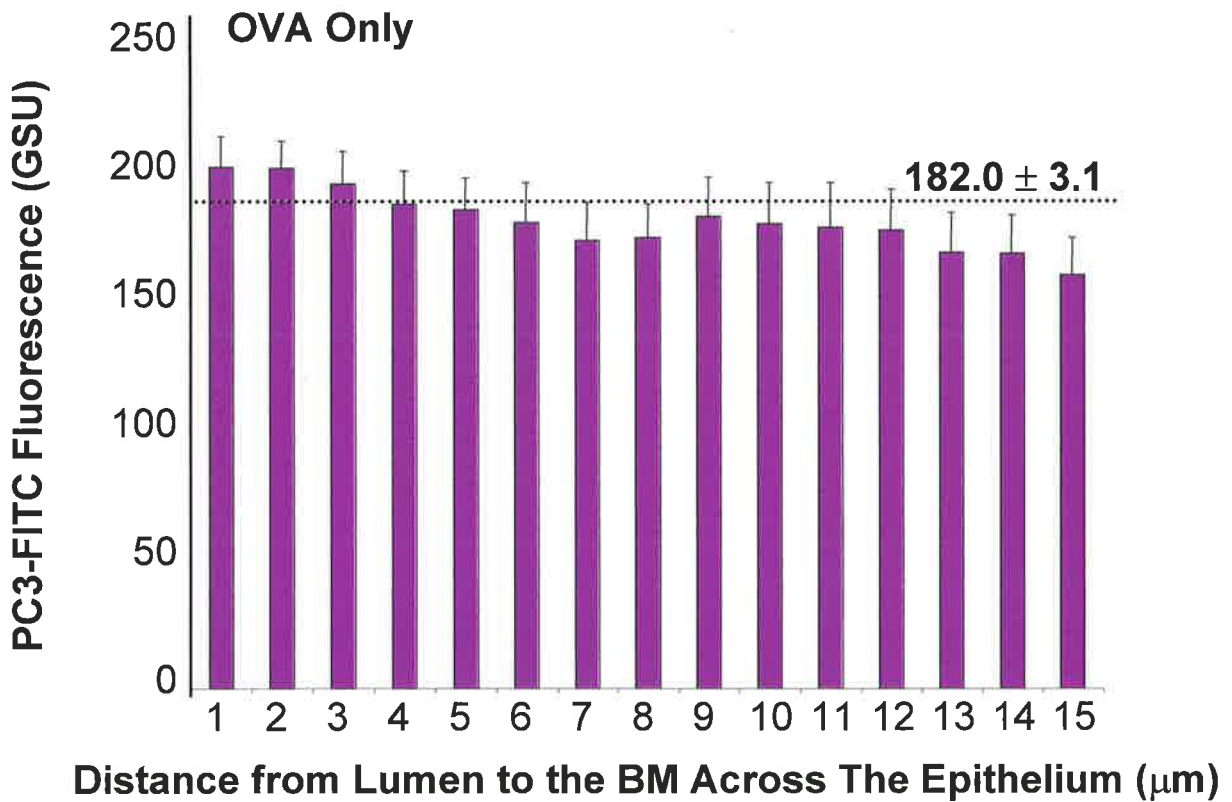
Figure 7.4: Quantification of Pro-Caspase-3 (PC3-FITC) Fluorescence Across Respiratory Epithelium of Group 2 SAL and OVA-Treated Mice

Figure shows the quantification of PC3-FITC fluorescence across the entire epithelium of the airway epithelium for the SAL (ZN-light blue panel A and ZL-pink panel C) and OVA-treated (ZN-navy panel B and ZL-red panel D) mice. PC3-FITC fluorescence expressed as mean GSU was plotted on the y-axis against the distance from the lumen to the basement membrane of the airway epithelium. Apical and basal regions are defined as for Figure 7.1. Note that the majority of the changes in PC3 protein affects both the apical and basal compartments. A marked increase in PC3 protein levels was observed in the ZN (panel B) and ZL (panel D) OVA-treated mice occurring in a homogenous pattern. Note the lower fluorescence in PC3 protein levels of ZL OVA-treated mice compared with their ZN counterparts. The mean fluorescence intensity was collated from at least 2 different mice per group, each having 5 to 6 air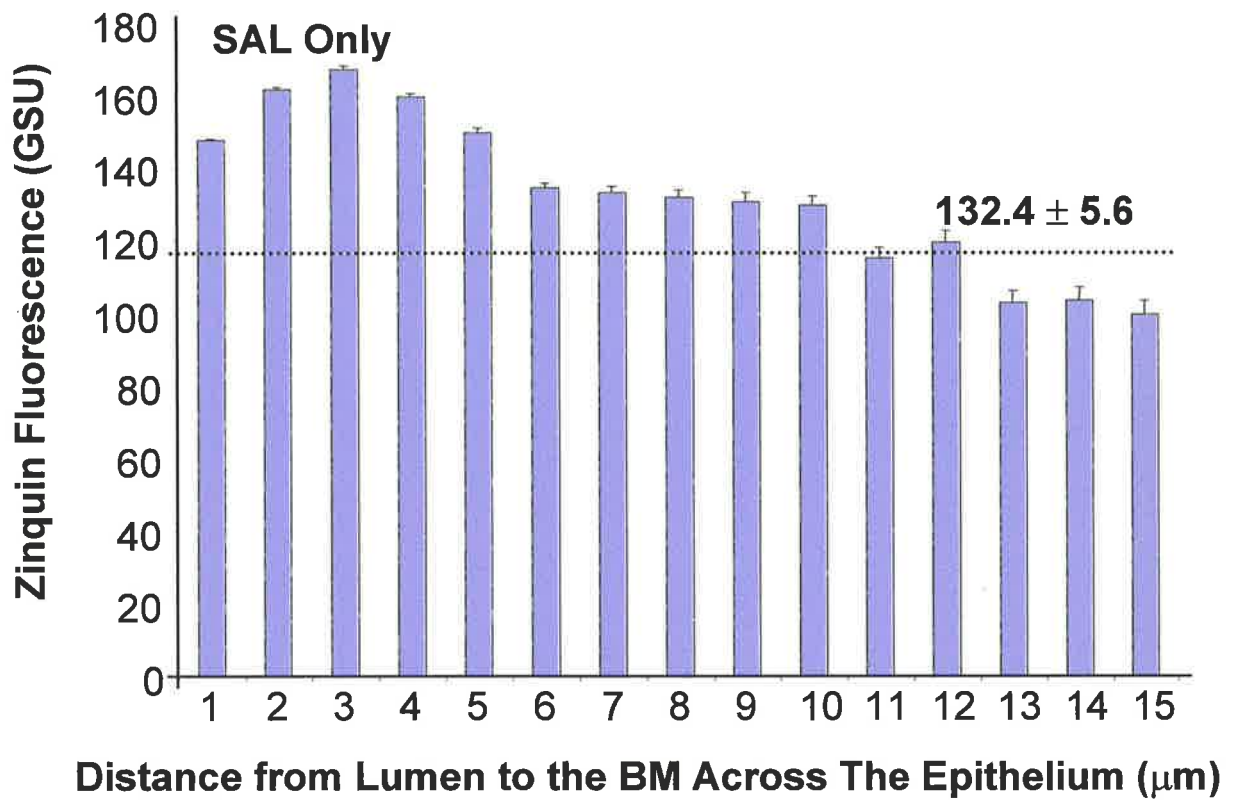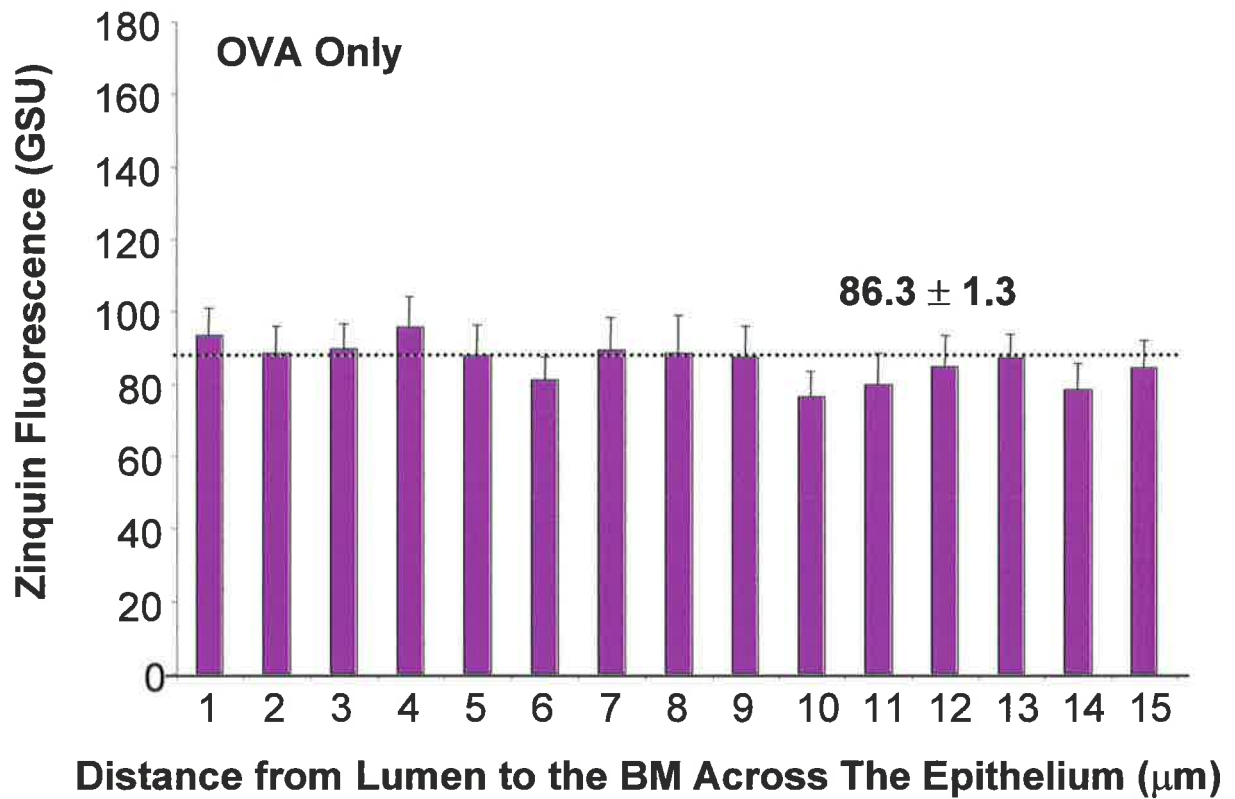ways assessed (n = 60 profiles were obtained per group). Significant differences between groups are denoted by the p values stated.

A ZN SAL — 178.6 ± 6.9

B ZN OVA — 226.8 ± 5.4

C ZL SAL — 168.4 ± 6.0

D ZL OVA — 177.8 ± 9.1

Y-axis: PC3-FITC Fluorescence (GSU)

X-axis: Distance from Lumen to the BM Across The Epithelium (μm)
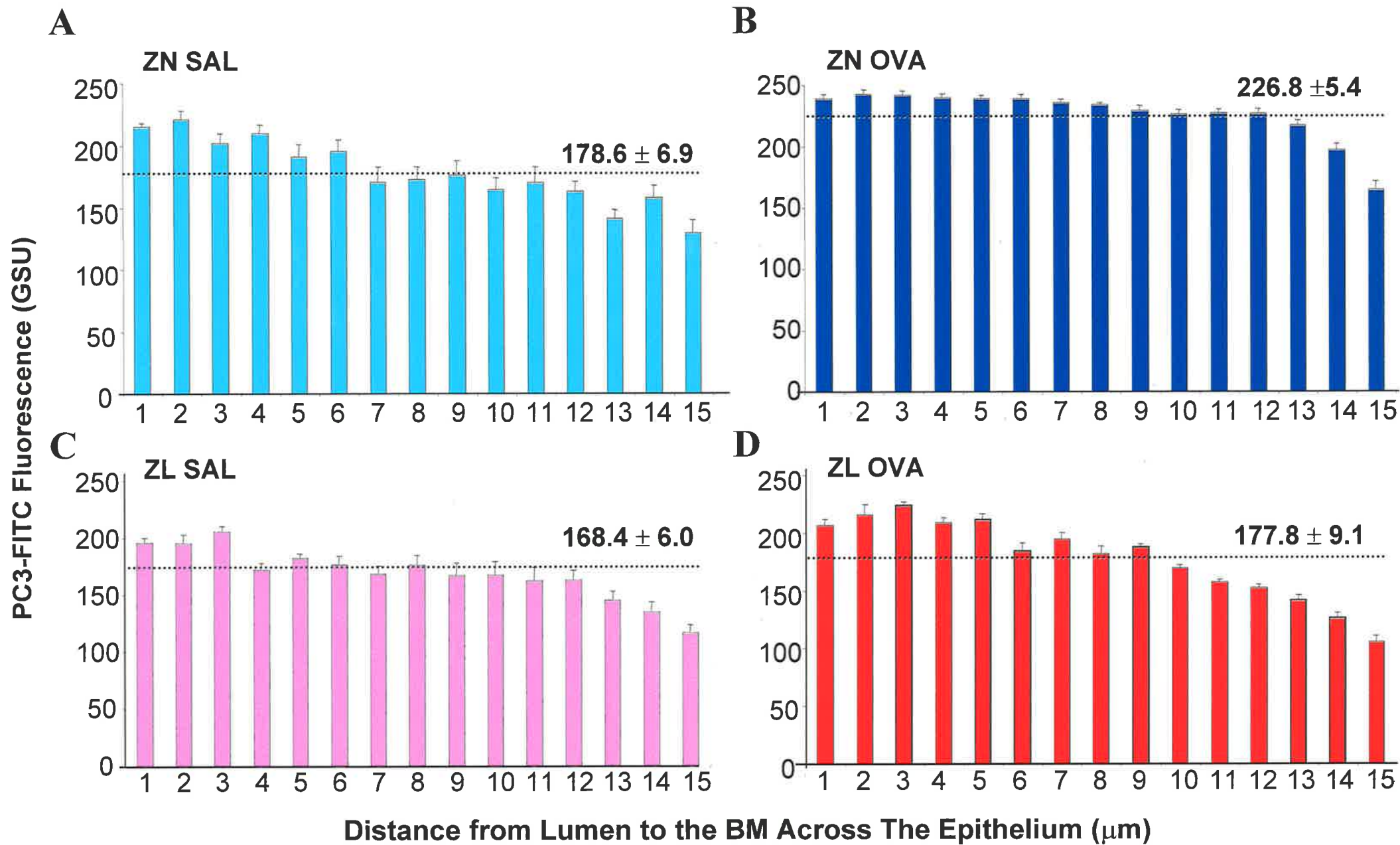
mice, this was significantly increased to 226.8 ± 5.4 GSU (panel B, p < 0.001). Similarly, ZL SAL treated mice had 168.4 ± 6.0 GSU (panel C) compared to the ZL OVA-treated mice which had 177.8 ± 9.1 GSU (panel D), however this was found to be not significant.

Increases in epithelial PC3 protein levels occurred in both the apical and basal compartments for the ZN OVA-treated mice (Table 7.1). Of particular interest, dietary Zn related changes were greatest in the ZL OVA-treated mice, occurring in both the apical and basal compartments of the airway epithelium. ZN OVA-treated mice had an apical level of 240.5 ± 2.2 GSU compared with the ZL OVA which had 213.4 ± 4.4 GSU (p < 0.005), while, the basal PC3 protein levels were 219.9 ± 3.4 GSU and 160 ± 4.6 GSU, respectively (p < 0.005).

As observed for the Zinquin fluorescence, the variability in baseline PC3-FITC fluorescence for group 1 and 2 mice may be due to experiments being conducted at different time points. These discrepancies are discussed in detail in section 7.4.

Figure 7.5, shows a montage of typical images of Zinquin and PC3 protein labelling in the airway epithelium of group 1 (panels A to F) and group 2 (panels G to R) mice. To determine whether Zn and PC3 protein were co-localised in the airway epithelium, Zinquin fluorescent images were merged with that of PC3 images (panels E & F for group 1 and panels O to R for group 2 mice).

Firstly, both Zn and PC3 protein were concentrated in the apical region of the epithelium of SAL-treated ZL mice (Zinquin-panels A, G & H and PC3-panels

207

Figure 7.5: Effects of Allergy and Zn Status on Available Airway Epithelial Zn and Pro-Caspase-3 Levels

Figure shows a montage of typical images of Zinquin and pro-caspase-3 FITC fluorescence in group 1 (panels A to F) and group 2 (panels G to R) mice. Confocal images were taken with a 40x objective lens and samples were labelled with Zinquin (A, B, G, H, I & J) or with primary anti-pro-caspase protein detected with a secondary FITC conjugated antibody (C, D, K, L, M, & N). Panels E, F, O, P, Q & R show the co-localisation of available Zn (blue) and PC3 (green) in dual labelled sections of airway epithelium of mice. Typical images are shown; arrows indicate the lumen of airways.

Figure shows a pronounced decrease in available Zn levels in the airway epithelium of group 1 OVA-treated (panel B) mice and group 2 ZN OVA-treated (I) and ZL OVA-treated (J) compared to the SAL-treated counterparts (A, G and H, respectively). A decrease in the available Zn was found in the epithelium of ZL SAL-treated (H) when compared to ZN SAL-treated mice (G). However, there was no further decrease in available Zn levels in mice rendered both Zn limited and OVA-treated (J), compared with just ZN OVA-treated alone (I). Conversely, there was a significant increase in PC3 protein levels in airway epithelium of group 1 OVA-treated (panel D) and group 2 ZN OVA-treated (M) compared to their SAL-treated counterparts (C & K, respectively). Similarly, ZL OVA-treated mice (N) also had an increase in PC3 protein levels compared with ZL SAL-treated mice (L).

| Zn (Pseudocoloured) | Pro-caspase-3 (Pseudocoloured) | Zn + Pro-caspase-3 (Pseudocoloured) |
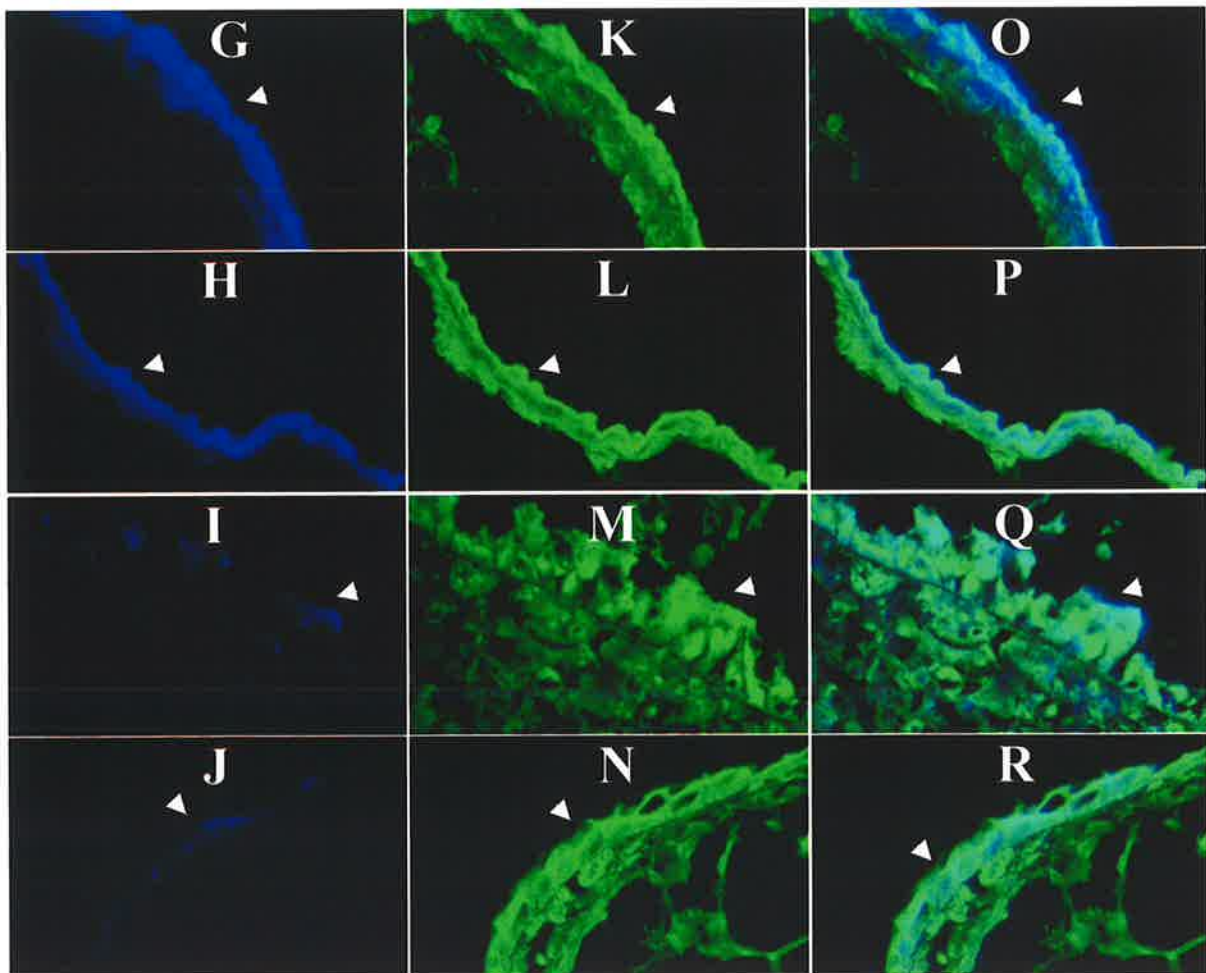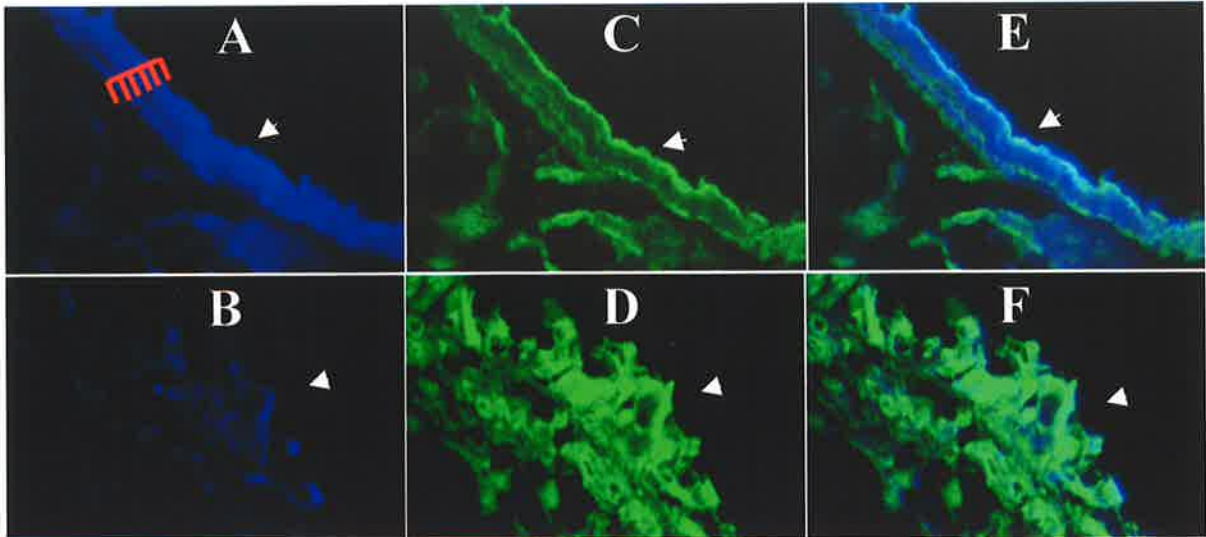
C, K & L). However, the OVA-treated mice had a more homogenous and disperse distribution (Zinquin fluorescence-panels B, I & J and PC3-panels D, M and N). Figure depicts the significant decrease in Zn levels in all of the OVA treated mice (panels B, I & J) when compared to their SAL-treated counterparts (panels A, G and H). As previously mentioned, Zn deprivation decreased Zinquin fluorescence in SAL-treated (panel H) but not in the OVA-treated mice (panel J).

Decreases in Zn levels in the OVA-treated mice were also accompanied by a significant increase in PC3 protein levels (panels D, M & N) compared to the SAL treated mice (C, K & L). In the OVA-treated mice the remaining Zn was found to be co-localised with PC3 protein although the distribution of both was more homogenous (panels F, Q and R).

As observed for the Zinquin fluorescence, differences in baseline FITC fluorescence for group 1 and 2 mice may be due to experiments being conducted at different time points. These discrepancies are discussed in detail in section 7.4.

7.3.4 Early Markers of Apoptosis are Increased in Allergic Airway Inflammation

Figure 7.6 shows images of two early markers of apoptosis, AC3 protein (with anti-17kDa caspase-3 antibody, panels A to D) and cleaved CK18 fluorescence labelling (with mouse anti-cleaved CK18, panels E to H) in the lung tissue of the group 2 ZN and ZL SAL and OVA-treated mice. The images presented were merged from a collection of a z-series of optical confocal sections through individual tissue sections at 1 μm intervals. Figure 7.6 panels A and E are typical images showing very little labelling of either AC3 protein or its cleaved substrate in ZN SAL-treated mouse airway epithelium. Similar results were seen

Figure 7.6: Comparison of Activated Caspase-3 (AC3) Protein and Cleaved Substrate Cytokeratin 18 (CK18) in Airway Epithelium

Figure shows the labeling patterns for two early markers of apoptosis, the active form of caspase-3 (A to D) and the cleaved form of CK18, a caspase-3 substrate (E to H). For morphological comparisons, the corresponding differential interference images of panels E to H are shown in panels I to L. ZN SAL-treated mice (A & E) had negligible apoptosis. There was a slight enhancement of AC3 protein in the ZL SAL-treated mice (B) but no cleavage of CK18 was seen in the epithelium (F). A moderate increase in AC3 protein labeling and cleaved CK18 was seen in the epithelium of ZN OVA-treated mice (C & G). However there were marked increases in both AC3 protein and cleaved CK18 in the epithelium of ZL OVA-treated mice (arrowed, D & H). Note also the positive staining within the subepithelial region and lamina propria (*). All images were taken with a 40x objective lens and 3x zoom. Each image is a merge of 12-16 optical slices of a z-series through the section. Typical images are shown and scale bar represents 20 µm.
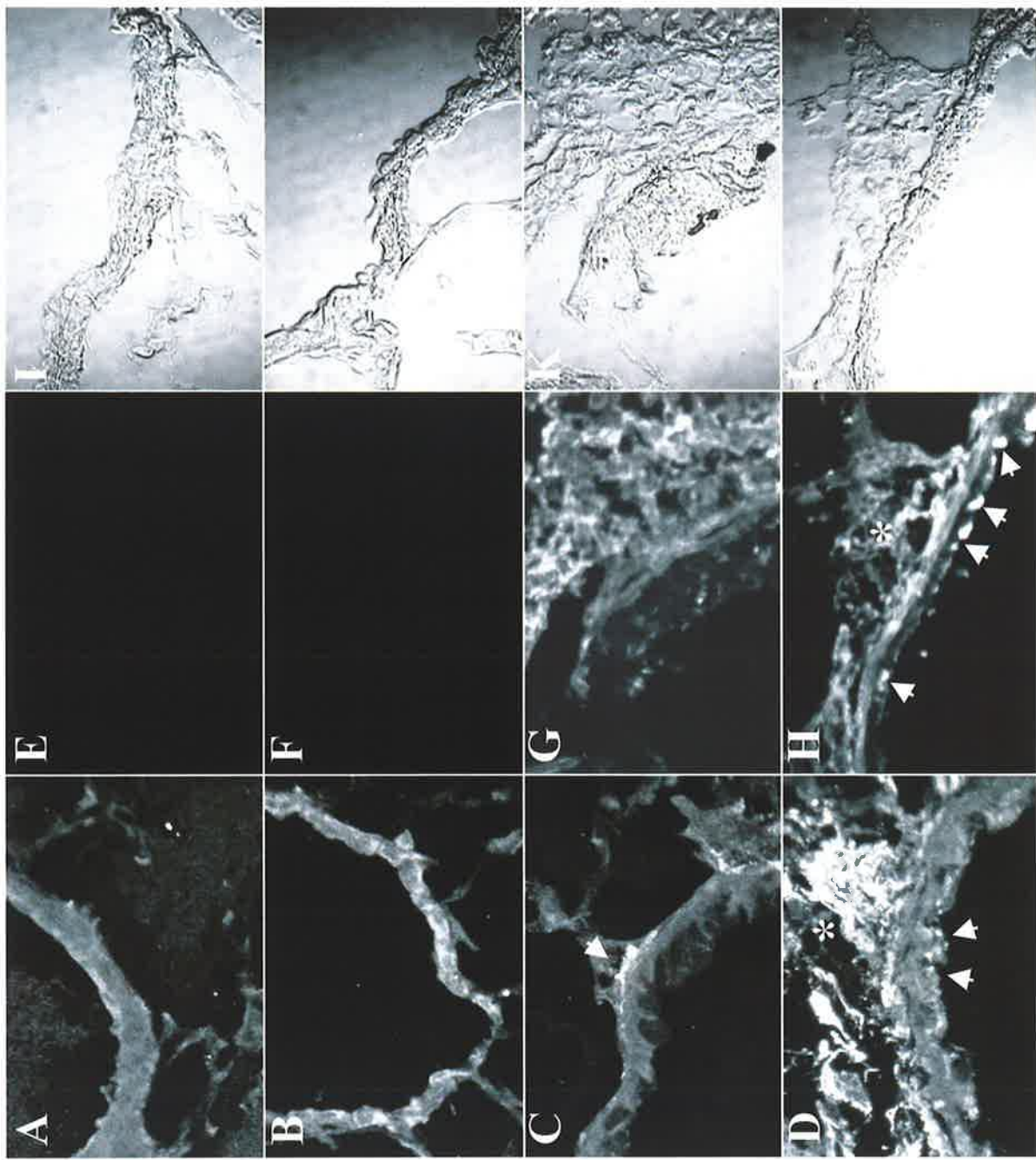
for the ZL SAL-treated mice (panels B & F). This suggests little or no apoptosis in these tissues. By contrast, there was increased AC3 protein and cleaved CK18, particularly along the basement membrane of the ZN OVA-treated mice (panel C & G), indicating enhanced apoptosis. There was also some positive labelling in the subepithelial region and lamina propria (Panels C and G). The significance of this labelling is unclear but may represent either eosinophil or fibroblast apoptosis.

In the ZL OVA-treated mice, substantial amounts of AC3 protein and its cleaved substrate were seen in a localised pattern particularly along the basement membrane (panel D & H) and also within the subepithelial region and lamina propria (*). Note also a high frequency of apoptotic bodies at the apical surface of the epithelium (arrowed) and in the lumen (panel H).

Apoptotic bodies in the airway epithelium were enumerated under high magnification (2500x) in 20 fields from duplicate slides stained for cleaved CK18 from the different groups of mice. The mean number ($\pm$ SD) of apoptotic bodies per high power field were 0.1 $\pm$ 0.4 for ZN SAL-treated mice and 0.3 $\pm$ 0.7 for ZL SAL-treated mice (not significant). However there were significant increases in the number of apoptotic bodies in OVA treated mice ($p < 0.005$) where ZN OVA treated mice had 2.2 $\pm$ 1.7 apoptotic bodies and the ZL OVA-treated mice had 7.0 $\pm$ 3.3. The value for ZL OVA-treated mice was also significantly different from the ZN OVA-treated mice ($p < 0.005$) suggesting that restriction of dietary Zn further enhances AEC apoptosis over that due to the allergen treatment alone.

7.3.5 Airway Epithelial Thickness

Increased epithelial thickness due to epithelial cell and mucus-secreting cell hyperplasia and metaplasia is a common feature of allergic asthma. Epithelial thickness in these mice was quantified by image analysis firstly on cryostat sections by using the CoMOS confocal software package and secondly on paraffin sections using the Image analysis program Video Pro. As expected, significant ($p < 0.005$) increases in the thickness of the epithelium were observed in all OVA-treated mice when compared to the SAL-treated mice.

For the group 1 mice, cryostat lung tissue sections from the OVA-treated mice had an epithelial thickness which was 2-fold greater than that of the SAL-treated mice. The epithelial thickness was found to be $17.8 \pm 0.9 \mu m$ for the OVA-treated mice and $9.03 \pm 1.1 \mu m$ for the SAL-treated mice ($p < 0.005$). Similarly, this increase in airway epithelial thickness in the OVA-treated mice was reproduced when using paraffin embedded lung sections. OVA-treated mice had an epithelial thickness of $27.5 \pm 1.1 \mu m$ which is 3.4 fold greater than the SAL-treated mice ($8.2 \pm 1.1 \mu m$, $p < 0.005$).

For the group 2 mice, ZN OVA-treated mice had an average epithelial thickness of $17.3 \pm 0.9 \mu m$ while the ZN SAL-treated mice had an average epithelial thickness of $11.4 \pm 0.7 \mu m$ when quantified using cryostat sections. Similarly, ZL OVA-treated mice had a thickness of $14.9 \pm 0.8 \mu m$ compared to $9.4 \pm 0.5 \mu m$ in the ZL SAL-treated mice. When airway epithelial thickness was quantified on paraffin sections, ZN OVA-treated mice had an epithelium which was 2.3 fold greater than that of the ZN SAL-treated mice at $26.3 \pm 2.5 \mu m$ and

11.3 ± 1.2 µm, respectively (p < 0.005). Likewise, there was a 2.6 fold increase in the thickness of the epithelium in ZL OVA-treated mice. ZL OVA-treated mice treated had epithelium which were 29.9 ± 3.1 µM thick compared to 11.6 ± 1.2 µM in the SAL-treated mice (p < 0.005).

7.4 DISCUSSION

These studies are the first to investigate whether Zn status and levels of apoptosis are altered in allergic airway inflammation. The major findings include a reduction of Zinquin fluorescence which was associated with an increase in PC3 protein labelling in the respiratory epithelium of OVA-treated mice and an increase in AC3 protein labelling in the basal region of the airway epithelium of OVA-treated mice, especially those which were Zn deprived.

The majority of these experiments were conducted on lung tissues collected from two separate groups of mice. Group 1 mice were obtained from experiments described in Chapter 5 which involved treating mice with either SAL or OVA only, while the second group were obtained from mice given either the ZN or ZL diets and treated with SAL or OVA as described in Chapter 6. It should also be noted that these experiments were conducted at different times during this Ph.D candidature, in December 2000 for mice from Chapter 5 and in May 2001 for mice in Chapter 6. Hence, this also resulted in the use of different batches of both Zinquin solution and PC3 protein antibody and may explain the different basal levels of Zn and PC3 protein observed between the SAL and OVA treated mice and the ZN SAL and ZN OVA-treated mice. Furthermore, it is very difficult to obtain the same strength of laser output. For example, conducting experiments on

differing days and especially in this case, several weeks to months, will ultimately result in a change in the strength of the laser output even if the same laser settings are kept constant. However, it important to note that all comparisons within a group were made in the same session on the microscope.

One of the aims of the experiments in this chapter was to determine whether Zn homeostasis was altered in allergic airway inflammation by analysing a variety of different tissues. Total Zn concentrations were quantified in the serum and liver samples of group 1 and 2 mice by using AAS. Serum Zn levels were analysed using graphite AAS rather than flame AAS since this method allows smaller volumes of sample to be assayed (i.e 10 μl) when compared to the flame method (200 μl) which was used for quantifying liver Zn levels. The results obtained provided conflicting data since the Zn levels were elevated in some of the OVA-treated mice (group 1-OVA treated and group 2-ZL OVA) while decreased in others (group 2-ZN OVA) when compared to their SAL-treated counterparts. Some of the reasons for this variability in serum Zn include a limited number of serum samples for the mice ranging between 4 and 8 samples and haemolysis in some of the samples which constitutes a significant source of Zn contamination from red blood cells. With regards to the liver Zn values, it is not clear why there were no differences between the SAL and OVA treated mice in group 2. This could be further investigated by having a more sensitive technique to measure Zn levels and a larger sample size within each group.

Although the serum Zn changes observed in the ZL group-2 mice (casein diet plus allergy) are small, they are typical of changes induced by a diet which aims to produce a mild level of Zn deficiency. Growth rate, as reported in Chapter

6, a more sensitive functional physiological marker of Zn status, was significantly lower in the ZL mice during the sensitisation period. Based on the variability of these results no conclusion can be reached regarding circulating and liver Zn levels in allergic airway inflammation in mice.

This study has provided the first information on lung epithelial Zn levels in allergic airway inflammation using Zinquin. One of the major findings of this study was the substantial loss of airway epithelial Zn in the lungs of the OVA-treated mice, both in Group 1 and 2. The reduction in available Zn was homogenous and occurred in both the apical and basal compartments of the epithelium suggesting that there is an overall loss of Zn perhaps also in the other cell types (basal and mucus cells) found within the epithelium rather than from one cell type (i.e. AEC). However, it must be formally determined whether this loss is predominantly in the ciliated cells, in the mucus cells or in both, since as reported in Chapter 6, in the OVA-treated mice the majority of the airway epithelium consists of mucus-secreting cells. It is technically difficult to address this issue since Zinquin fluorescence can only be done on frozen tissues and not in conjunction with Alcian Blue/PAS staining. One possible solution would be to double label tissues with Zinquin in conjunction with antibodies to specific epithelial mucus cell markers such as muc5b.

The mechanism behind the marked decrease in available Zn in the airway epithelium of OVA-treated mice is not known. This decrease in Zinquin fluorescence may represent a net reduction in epithelial Zn concentration and/or an incorporation of a greater proportion of Zn into metallothionein, which attenuates Zinquin fluorescence (Coyle et al., 1994). For example, labile Zn may have been

213

transferred to metallothionein within the AEC, removing it from Zn regulated enzymes such as caspase-3 (Maret et al., 1999). If Zn has indeed been lost from the airway epithelium, several factors may play a part. Firstly, losses of cellular Zn are associated with enhanced cell turnover (Solomons, 1988) a feature which is also found in asthmatics, in whom there is shedding of Zn rich AEC and eosinophils into the airway lumen. Secondly, Zn may be lost from the AEC by secretion into the epithelial lining fluid or by binding to the negatively charged muco-polysaccharides in the mucin layer. Thirdly, the low Zinquin fluorescence observed in the OVA-treated mice may suggest decreased recruitment or transport of Zn back into AEC during inflammation.

One of the implications of Zn loss in the OVA-treated airway epithelium is the potential for enhanced apoptosis since Zn is a potent suppressor of this mechanism of cell death. Zn is thought to act by blocking the activation of caspase-3 (Perry et al., 1997; Prasad, 2000; Solomons, 1988). Of particular interest, labile Zn was co-localised with PC3 protein in the airway epithelium of SAL and OVA-treated mice suggesting that Zn may play a functional role in stabilizing the activation of this protein. In light of this, the increase in PC3 protein levels in the OVA-treated tissues is very interesting. It is however not yet clear how PC3 protein is upregulated in the OVA-treated mice. Hence the mechanisms regulating this increase now need to be further investigated by determining whether this is due to an upregulation of gene expression at the transcriptional level, an increase in the translation of the protein, an alteration in the levels of protein turnover or an increase in the availability of the protein epitope which was detected by the primary antibody. Nevertheless, the increase in PC3 protein may have important implications for the survival of the airway epithelium. Increased PC3 protein may

enhance the susceptibility of AEC to apoptosis, thereby increasing the fragility of the epithelium in asthma. Apoptosis of bronchial epithelial cells in human asthmatics has recently been suggested by Benayoun and colleagues who showed increased peroxisome proliferator-activated receptor gamma levels and AC3 in the lamina propria and the basement membrane (Benayoun et al., 2001). The studies described in this chapter, using an antibody against AC3 protein and its cleaved substrate cytokeratin 18 (CK18) supports these findings in a murine model of allergic airway inflammation. The results show increased labelling at the basement membrane which may indicate that this is the first site of damage in the airway epithelium. AC3 protein was also increased in the lamina propria within regions where there is an accumulation of eosinophils. Whether this reflects direct apoptosis of eosinophils or damage to surrounding tissue fibroblasts by factors released from eosinophils is not known. This could be tested by dual staining also for eosinophils using an antibody directed to myelin basic protein.

The mechanisms that trigger apoptosis in the airway epithelium of the OVA-treated mice are not fully understood and Zn depletion is likely to be only one of the factors. Other possible triggers for apoptosis include damage from oxyradicals and cytokines released from inflammatory cells. There was enhanced AC3 protein and cleavage of CK18 in the ZL OVA-treated mice suggesting that an interaction may be occurring between Zn deficiency and the enhanced inflammatory response in the airways of the allergic mice. The further increase in apoptosis in the epithelium of ZL OVA-treated mice is consistent with other studies showing enhanced rates of apoptosis in various tissues of Zn deficient animals and humans (Cui et al., 2000; Mori et al., 1996).

A paradox exists in the data relating to the ZN and ZL OVA-treated mice in that the labile Zn levels in the airway epithelium were similar but there was an apparent substantial increase in AC3 protein and cleavage of CK18 in the ZL OVA-treated mice. One possible explanation may be that as described in Chapter 6, nutritional Zn deprivation enhanced eosinophilia and mucus cell numbers and this may have been due to an increase in the level of inflammation present in these mice thereby further enhancing the susceptibility of the airway epithelium to tissue damage and subsequent apoptosis. A second explanation is that the pools of Zn depleted in the ZN OVA-treated mice are not the pools responsible for regulating caspase-3 activation. However, dietary Zn deprivation may target the pools of Zn which are crucial for regulating caspase-3 activation. This speculation may explain the increase in apoptosis observed in the ZL OVA-treated mice.

Airway remodelling is an important feature in asthma and is accompanied not only by increased mucus numbers and size but also by an increase in epithelial thickness since the AEC themselves swell and become phamacologically active (Holgate et al., 2000). As expected, the airway epithelial thickness was significantly increased in the ZN and ZL OVA-treated mice when compared to their SAL-treated counterparts. It was also expected that Zn deprivation would increase epithelial thickness due to mucus hyperplasia and increased inflammation. This was observed in the paraffin sections of the ZL OVA treated mice when compared to those of the ZN OVA mice. However, in cryostat sections not only was this not seen but the epithelial thickness of the ZL OVA mice was significantly less than in the ZN mice. These differing observations may be due to the different processing techniques of the tissues. Formalin fixation of sections may have preserved the ultrastructure of the epithelium in these mice more

adequately than the rapid freezing of the same tissues in liquid nitrogen. The fragility of the airway epithelium in the OVA-treated mice would have remained constant at the time of sacrifice. However the fixation and embedding of these tissues would influence the morphology of the epithelial tissue at the time of sectioning. However, Zn is important for maintaining the cytoskeleton of the cell, hence Zn deprivation may have an adverse effect by compromising the integrity of this organelle (Bettger & O'Dell, 1981). This may ultimately increase the fragility, permeability and ultrastructure of the epithelium in the ZL mice and result in increased damage to these cells which would be more easily seen in the cryostat sections. Another factor which may have increased the fragility of this epithelium is the increased levels of inflammation in ZL OVA-treated mice as reported in Chapter 6.

There are two main limitations encountered in the experiments described in this chapter. The first is the variability in baseline fluorescence levels for the Zinquin and PC3 protein staining. This is unavoidable since there are variations in the laser power of the confocal microscope and the batches of antibody and Zinquin used between experiments. The second limitation is that it is unclear which cell types for example, ciliated AEC, mucus-secreting or basal cells experience the alterations in labile Zn and PC3 protein levels. This could be overcome by isolating the individual cells from the allergic mice using protease treatment.

The experiments in this chapter have extended the findings reported in Chapter 6 concerning interactions between nutritional Zn deprivation and allergen treatment on parameters of inflammation, by now showing a significant decrease in

airway epithelial Zn levels and increased PC3 protein and early markers of apoptosis in the OVA-treated mice.

Some of the results reported in this chapter are in the following manuscript:

Altered Zinc Homeostasis and Caspase-3 Activity in a Murine Model of Allergic Airway Inflammation. Truong-Tran AQ, Ruffin RE, Foster PS, Koskinen AM, Coyle P, Philcox JC, Rofe AM and Zalewski PD. AMJRCMB (in press).

CHAPTER 8

DISCUSSION AND CONCLUSION

CHAPTER 8 DISCUSSION AND CONCLUSION

8.1 MAJOR FINDINGS OF THIS THESIS

A number of novel findings have been presented in this thesis. These were: 1) AEC contained a high level of labile intracellular Zn within the apical cytoplasm, 2) induction of allergic airway inflammation in mice substantially decreased labile intracellular pools of Zn within AEC and 3) there was a positive interaction between nutritional Zn deprivation and allergic airway inflammation which resulted in increased inflammation, AHR, and AEC apoptosis. These findings have attempted to address the three major hypotheses of this thesis; that 1) labile intracellular Zn plays an important role in protecting REC from oxidative damage and apoptosis, 2) decreased Zn levels may contribute to increased oxidative stress, chronic inflammation and decreased protection of the airway epithelium and 3) low AEC Zn levels may facilitate the development of airway disease or the clinical expression of airway diseases.

8.1.1 AEC Contain High Levels of Intracellular Labile Pools of Zinc within the Apical Cytoplasm

The first major aim of this thesis was to determine the localisation of labile intracellular pools of Zn in airway epithelium. The finding that Zn is highly concentrated in the apical cytoplasm, both around the mitochondria and within the microtubular-derived basal bodies and cilia of sheep, pig and human primary AEC has a number of potential implications.

Firstly, since Zn is an anti-oxidant, the pools of labile Zn observed within this apical region of AEC may protect against oxidative damage to plasma membrane and other organelles thereby enhancing the integrity of the epithelium. A similar role for Zn has previously been reported for erythrocytes and neurons (Chapter 3 discussion). Therefore, if labile Zn is crucial for the maintenance of AEC plasma membrane integrity then depletion of this crucial Zn may increase the permeability of the epithelium. It would be possible to test this hypothesis, by measuring AEC barrier functions in Zn depleted AEC monolayers with transepithelial electrical resistance or mannitol transport from the apical surface of the epithelium to the basolateral side. The lower levels of labile Zn observed in alveolar cells may be due to the differences in capacities for Zn uptake or metabolic requirements for Zn. Zn has been shown to be crucial for the survival of these cells since Zn deficiency exacerbated hyperoxia-induced lung damage while Zn supplementation had a protective effect (Taylor & Bray, 1991). One interesting experiment would be to investigate the extent of damage present in the upper AEC of Zn deficient mice which have been exposed to hyperoxia.

Secondly, the finding that Zn within the apical region of AEC is co-localised within PC3 protein (as reported by (Krajewska et al., 1997; Truong-Tran et al., 2001) suggests that Zn performs an anti-apoptotic function by stabilising this protein, hence preventing its activation. This fnding achieves part of the second aim of this thesis which was to investigate the functionality of this labile Zn within REC. The results reported indicate that Zn is likely to have a protective effect since depletion of these stores by the Zn chelator TPEN increased caspase-3 activity and morphological features of apoptosis. Depletion of Zn further enhanced caspase-3 activity levels in REC during oxyradical-induced apoptosis, since cells treated with

H_2O_2 in combination with TPEN had greater caspase-3 levels than achieved by the additive effects of the individual agents. Furthermore, supplementation of REC with exogenous $ZnSO_4$ suppressed caspase-3 activation and morphological features of apoptosis, even in the presence of H_2O_2. These results support the hypothesis that intracellular Zn levels are essential for regulating caspase-3-activated apoptosis in REC, and, are also consistent with other findings relating to Zn in a variety cells types (Aiuchi et al., 1998; Jankowski-Hennig et al., 2000; Oteiza et al., 2000). At the time when these experiments were conducted there were limited studies investigating caspase activity and apoptosis in REC (Goldkorn et al., 1998; Scavo et al., 1998). The precise mechanism by which Zn regulates caspase activation now needs to be further investigated.

Thirdly, the finding of localisation of labile Zn within the basal bodies and the cilia of AEC may suggest that this Zn is important for ciliary function. The role of intracellular Zn in ciliary function could be assessed by measuring ciliary beat frequency in AEC which have been treated with TPEN or NaPYR to alter intracellular Zn levels.

To further understand the functionality of labile Zn, it will be important to determine how Zn is acquired and transported within AEC and what the controlling mechanisms are. Zn has to originate from the capillaries at the basal membranes of these cells or be reabsorbed from previously secreted Zn in the periciliary fluid. The mechanisms involved and the transporters (ZnT and the hZIP families) utilised in the uptake and compartmentalization of this Zn now need to be determined. These studies are planned in our laboratory using specific antibodies to ZnT-4 in collaboration with Dr. Chiara Murgia (Rome).

The present finding suggests that the unique distribution and high levels of labile Zn observed within AEC may contribute to the protection and survival of these cells.

8.1.2 Induction of Allergic Airway Inflammation in Mice Substantially Decreased AEC Zn Levels

A major finding of this thesis is the marked loss of labile pools of Zn from the airway epithelium of OVA-treated mice. This was observed for the mice given both the ZN and the ZL diets and raises important questions: 1) how is this Zn lost from the epithelium? 2) when does this loss occur? and 3) does this occur in humans.

How is this Zn lost?

There are several possible mechanisms by which Zn can be lost from the AEC in allergic inflammation. One plausible process is by AEC secretion. During airway inflammation, the epithelium becomes pharmacologically active increasing its secretion of pro-inflammatory mediators and cytokines. Hence labile pools of Zn may also be released from AEC in association with these proteins during this secretory phase. To what extent this Zn may be secreted in conjunction with the AEC derived cytokines needs further investigation. Alternatively, Zn secretion may occur independently from release of cytokines. The hypothesis that AEC lose their Zn by secretion into the airway lumen can be investigated by culturing cells with IL-13, a cytokine not only increased in allergic inflammation but also reported to induce a secretory phenotype in human AEC (Danahay et al., 2002). Alternatively it can also be measured in the sputum samples of asthmatic patients by examining the periciliary fluid.

A second mechanism, which may be involved, is an alteration in the chemical state of this Zn, hence shifting it from a labile form to a more tightly bound form which now can not be detected by Zinquin. This hypothesis would suggest that labile pools of Zn in the OVA-treated mice have now become incorporated into metalloproteins such as the anti-oxidant metallothionein as a response to the inflammation present. This speculation is plausible since metallothionein is a known regulator of Zn homeostasis, is able to sequester free Zn ions from plasma and the liver and may have similar influences in the AEC of the OVA-treated mice. At present there are limited studies reporting the role of metallothionein in the lung although, a recent paper reported that this protein was increased in the lungs of mice exposed to hyperoxia during the acute phase response (Levy et al., 2001). Possible experiments which investigate the levels and localisation of metallothionein in AEC may provide insights into whether metallothionein is able to sequester labile pools of Zn in the epithelium of OVA-treated mice. To investigate this, dual staining of the airway epithelium using Zinquin and a specific antibody directed towards metallothionein and also measurement of lung metallothionein levels using biochemical assays should prove informative. To determine whether metallothionein can directly alter labile pools of Zn *in vitro*, AEC cells can be treated with dexamethasone, a known inducer of methallothione and cultured in the presence of Zinquin which could then be used to monitor labile Zn levels within cells. Alternatively, repeating these experiments using metallothionein knockout mice may also be informative.

A third reason why the AEC Zn in the OVA-treated mice was depleted may be related to a defect in the ability of the AEC to recruit labile Zn back into the airway epithelium. Determining the mechanisms regulating Zn acquisition and

transport within AEC should have important implications. To study these mechanisms it may be beneficial to firstly, determine the levels and localisations of different Zn transporters within the lungs of these mice and secondly, to monitor the rate at which ^{65}Zn radioisotopes are transported and absorbed across the respiratory system in mice with varying levels of allergy.

The results reported in this thesis do not support one mechanism over the other for the loss of Zn from the respiratory epithelium of OVA-treated mice. However, the secretory mechanism is preferred since numerous studies have reported high labile Zn content within epithelial cells which have a secretory function (Frederickson et al., 1987b). Furthermore, these cells release this Zn in association with other substances such as insulin (pancreatic islets), neurotransmitters (neurons), histamine (mast cells) and citrate (prostate) (Danscher et al., 1980; Frederickson, 2001; Huang & Arvan, 1995; Sorensen et al., 1997; Zalewski et al., 1994b).

When does this loss of labile Zn occur?

The answer to this question requires an experiment which investigates the kinetics of Zn redistribution within allergic airway inflammation. For example, intracellular Zn measurements could be made at several time points during the induction of allergic airway inflammation. The labile Zn that is lost from the AEC is likely to be secondary to the inflammation present since dietary Zn deprivation was able to significantly lower labile AEC levels in SAL-treated mice but unable to further deplete labile Zn levels within the AEC of ZN OVA-treated mice. However, it is currently unclear whether replenishment of Zn, either systemically or locally, will influence the structural changes of the airways if implemented

either before or after allergen challenge. Hence, future studies are required to understand the significance of these findings in both the murine model used and also in humans.

Does this loss of Zn occur in Humans?

At present it is not known whether this decrease in AEC labile Zn pools also occurs in human asthma. Determining this will enable clinicians to monitor patients who may become at risk of Zn deficiency. Furthermore, if the clinical symptoms of asthma are improved using oral Zn supplementation, then this may become a cost-effective therapeutic measure which could also be used in conjunction to the current asthma medication. Studies are currently being conducted at the Basil Hetzel Institute by obtaining nasal AEC via brushing of the nasal cavities, and bronchial AEC during a routine bronchoscopy procedure from a population of people who have atopy and asthma. The AEC collected from bronchial brushings are being labeled for Zn by Zinquin and also used to measure levels of different Zn transporters. Zn supplementation of people with asthma who have low AEC labile Zn and measuring their clinical responses should prove interesting.

8.1.3 A Positive Interaction Exists between Zn deprivation and Allergic Airway Inflammation

A third major aim of this thesis was to determine whether nutritional Zn deficiency could influence the pathogenesis of allergic airway inflammation. The finding that the Zn deprivation (maintained before and after induction of allergy) significantly (albeit modestly) increased eosinophilia, mucus cell hyperplasia and

AHR and increased AEC apoptosis has implications for allergic airway inflammation in humans.

One implication is that the presence of dietary Zn deficiency early in the development of human asthma may exacerbate the symptoms of this disease by increasing the inflammation, AHR and damage to the airway epithelium. For example, a child with mild Zn deficiency and the genetic susceptibility for asthma may be more likely to develop asthma than a child with normal Zn and the same level of genetic susceptibility. There may be a need to monitor Zn levels within asthmatics and supplement with Zn where necessary. The animal data reported in this thesis suggests that it is not clear whether such monitoring requires AEC or plasma Zn levels.

The first observation that mild dietary Zn deprivation exacerbated the level of inflammation already present in asthma implies that Zn is an important factor able to influence the immune response in airway inflammation. It is known that Zn deficiency results in an imbalance between Th_1 and Th_2 cytokine profiles (Prasad, 2000) and this milieu is also present in human asthma (Mosmann & Coffman, 1989; Robinson, 2000). Therefore, the Zn deprivation created in these mice may have increased levels of Th_2 cytokines released from either the Th_2 lymphocytes, eosinophils or the AEC thereby further enhancing eosinophil and mucus cell numbers. This could be investigated by measuring the Th_2 cytokine profiles (such as IL-4, 5, 6 and 13) of the SAL-treated and OVA-treated mice given the Zn normal and the Zn deprived diets in the serum and the secretion of bone marrow cells, blood eosinophils, lymphocytes and splenocytes. The increase in eosinophil

226

and mucus cell numbers in the Zn deprived SAL-treated mice suggests that there may be an enhanced susceptibility of these mice to airway inflammation.

The second observation that Zn deprivation increased levels of AHR, in both SAL-treated and OVA-treated mice, was unexpected and implies that dietary Zn can directly influence airway function regardless of allergic status. A possible mechanism of action is that Zn deprivation affects acetylcholine or β_2-adrenoreceptors within the airways. Zn deprivation may stimulate cytokine release from AEC, increased smooth muscle reactivity, activation of the cell membrane or changes in receptor levels and functions. Determining whether this occurs within the AEC or smooth muscle cells should be informative and can be investigated by measuring functional levels of these receptors within tissues obtained from mice fed varying Zn diets. The mechanism proposed is plausible, since Zn ions have been reported to prevent the activation of muscarinic receptors by blocking Ca^{2+} ion influx across the plasma membrane (Taylor & Peers, 2000) and by inhibiting the activation of β_2-adrenergic receptors by binding to histidines within the receptor (Sheikh et al., 1999). The observations reported by these authors have significant relevance to the results reported in this thesis, despite the fact that they were derived from non-airway cells. Similar experiments now need to be conducted in AEC and smooth muscle cells obtained from the airways of mice or humans which have varying levels of allergic airway inflammation and Zn homeostasis. Other possible mechanisms which may be involved in the Zn mediated AHR could include increased secretion of mucus or IL-13, a cytokine implicated in enhancing AHR (Venkayya et al., 2002).

Zn deprived OVA-treated mice had only a slightly higher level of AHR than the Zn normal OVA-treated mice. One explanation is that the AHR response in the OVA-treated mice has reached its maximal level due to the high level of inflammation already present, hence Zn deprivation could not further influence the activation of acetylcholine receptors. In a separate experiment using mice given the diet only, repletion of Zn deprived mice with the Zn normal diet for 14 days significantly decreased AHR levels to those that were observed in their Zn normal counterparts. This observation is consistent with the hypothesis that Zn inhibits the activation of acetylcholine receptors and should have implications for human disease.

The third observation was the marked increase in levels of AEC PC3 protein in the Zn normal OVA-treated mice. This increase was accompanied by moderate increases in AC3 protein and cleavage of cytokeratin 18, a substrate of caspase-3. The observation of increased PC3 protein suggests that the airway epithelium in the OVA-treated mice may be primed for apoptosis since PC3 protein is one of the major executioner pro-apoptotic proteins and cells which contain higher levels of this protein also have a faster turn over rate (Krajewska et al., 1997).

The results reported in this thesis do not provide data on the mechanism by which this protein is increased. It is possible that this increase is a response to the airway epithelial damage present in allergic airway inflammation. The upregulation of this protein is likely to have occurred at the gene transcription level and therefore measurement of PC3 mRNA in the allergic airway epithelium, either by in situ hybridisation or analysis of laser micro-dissected tissue should prove

informative. Alternatively, the high levels of PC3 present may be due to a decreased turn over of this protein since AEC may require it for triggering apoptosis. This could be confirmed by quantitatively measuring PC3 protein levels.

One of the most interesting findings reported in this thesis is the large increase in AC3 protein and cleaved CK18 in the Zn deprived OVA-treated mice above that of the Zn normal OVA-treated mice. As discussed above, allergic airway inflammation alone was able to considerably deplete labile Zn pools from AEC while Zn deprivation was also able to decrease Zn, but the magnitude of this decrease was much less than that due to allergy. There are at least two possible explanations. Dietary Zn deprivation may deplete a separate pool of labile Zn which is required for regulating the activation of caspase-3, while the pools depleted by allergic airway inflammation alone do not interact with this pro-apoptotic protein. If this were true then one would expect increased rates of apoptosis in the Zn deprived SAL-treated mice also. This was not observed suggesting that the level of Zn removed from the AEC of the SAL-treated mice was not substantial enough to activate caspase-3 since the dietary Zn deprivation created was a mild to moderate one. One implication of these results may be that there are two signals which act synergistically to induce apoptosis: signal one occurs in response to the allergic inflammation, increasing PC3 protein levels and susceptibility to apoptosis while signal two is provided by nutritional Zn deprivation and results in the activation of this caspase. This observation may explain the results reported in chapter 4 but in an *in vivo* environment where TPEN is replaced by the dietary Zn deprivation and H_2O_2 is replaced by the increase in ROS generated from the level of inflammation present within the OVA-treated mice. It can be speculated that the Zn deprived OVA-treated mice resembles the

combined state of Zn deficiency and chronic inflammation observed in long term asthma as discussed in section 1.5.3. The deprivation of dietary Zn may have hastened the natural course of inflammatory events if the loss of Zn from the airway epithelium over a long period of time leads to a secondary Zn deficiency. Theoretically, if the Zn normal OVA-treated mice were kept alive longer (say for 3 months) then one would predict that they would become Zn deficient due to the ongoing loss of Zn from AEC and the increased usage of Zn to drive the inflammation. For example, Zn is required for the activation of inflammatory cells and is a major component of the secretory granules of mast cells and eosinophils (section 1.1.3.8). However, there are currently no murine models designed which will accommodate such an experiment. How much Zn is lost from the airway epithelium compared to the levels used up in inflammation is not known. Zn supplementation is likely to have a beneficial effect since it may maintain healthy Zn levels within the epithelium. Figure 8.1 shows a schema of possible interactions between allergy and Zn deprivation.

8.2 LIMITATIONS OF THIS STUDY

There are a number of limitations in this thesis. Firstly, with regard to the *in vitro* experiments involving manipulation of intracellular Zn levels, it is unclear as to how much Zn is being altered by a given concentration of TPEN or NaPYR and whether the levels of Zn achieved are within the physiological or pathological range. While this limitation is true the decreases induced by TPEN in REC are of the same order of magnitude as those that occur in the OVA-treated animals. For example, 6.25 μM TPEN decreased labile intracellular Zn levels by approximately 40-45% in primary ciliated AEC, while allergy decreased labile Zn levels in mouse AEC by 35-40%. At present it is difficult to determine an accurate concentration of

Figure 8.1: Speculative Model of the Interaction between Allergy and Zn Deficiency

1) The airway epithelium contains an abundance of intracellular Zn within the apical cytoplasm and the basal bodies of the AEC. 2) Some of this Zn is co-localized with pro-caspase-3 (PC3) protein and acts by stabilizing this protein. This is the situation in the ZN SAL mice. In the ZN OVA-treated mice, 3) the majority of labile Zn in AEC is lost through secretion or efflux. 4) This loss of Zn does not result in activation of PC3 protein but increases the fragility of these cells to oxidative stress. A direct consequence of the loss of Zn is the increase in PC3 protein in the cytoplasm by an unknown mechanism. This may prime the cells for apoptosis induced by oxyradicals and other toxins. At this stage apoptosis is only modest as the pools of Zn which are depleted by allergy, are different to those responsible for suppression of PC3 protein activation. In the ZL OVA-treated mice, there are two separate signals; the first being the increase in PC3 protein levels in response to the inflammation and the second being the nutritional Zn deprivation. These signals act in a synergistic manner to increase apoptosis as detected by enhanced levels of 5) AC3 protein, cleavage of CK18 and the presence of apoptotic bodies (black circles). This may resemble the situation in humans with chronic airway inflammation where there is a generalized Zn deficiency that may be caused by continual loss of AEC Zn and consumption of Zn during the inflammatory process. Therefore the nutritional Zn deprivation may speed up the natural process by creating a rapid Zn deficiency. This has implications for trends towards decreased intake of dietary Zn and other anti-oxidants over the last 3 decades.

1 Zn

2 PC3

Allergen → IgE
            IL-5
            GM-CSF

3 Zn   Zn   Zn   Zn

4 ↑PC3   CD

6 Chronic airway inflammation
   leading to secondary Zn deficiency

5 ↑AC3   Zn   Zn   Zn
   ↑AHR
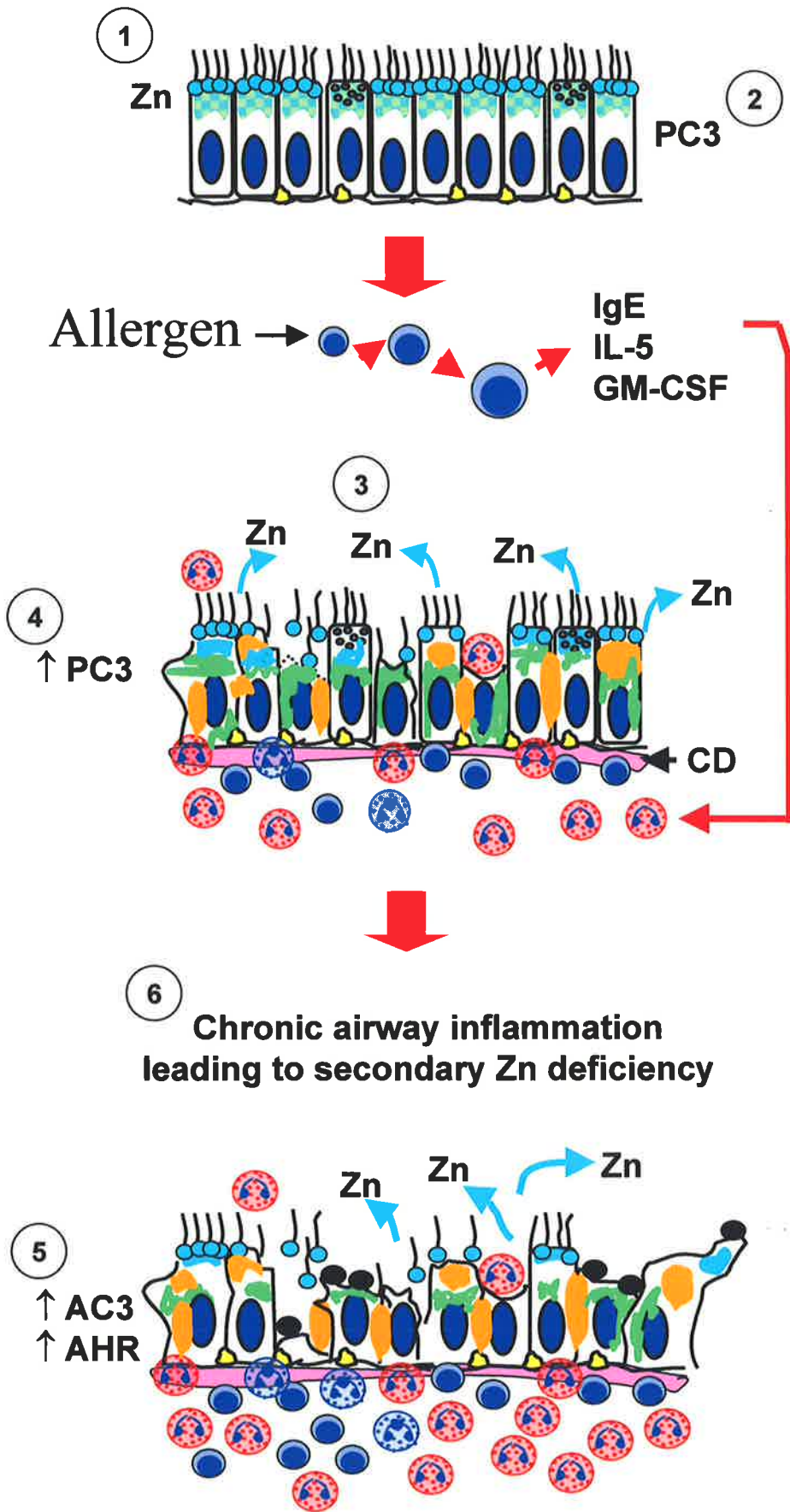
labile Zn within cells based on fluorescence intensity. The construction of a standard curve within splenocytes in Chapter 3 has attempted to address this issue although it cannot give an accurate indication of how much Zn is within a given compartment of the cell and as such was not used for subsequent experiments.

Another limitation is the method by which circulating Zn levels were measured. The serum samples which were obtained from the mice were small in volume and therefore at the dilution used, were at the lower levels of sensitivity of the machine. Furthermore, there was some haemolysis which is a source of Zn contamination and was difficult to avoid.

The murine model of allergic airway inflammation has a number of inherent limitations which have been discussed in chapter 5. Principally these are the model cannot replicate all of the features of human asthma and there is the presence of alveolitis. Furthermore, human asthma is an ongoing disease lasting many years and clearly no animal model can replicate this level of chronic inflammation. This limits the period in which Zn deprivation and/or repletion can be induced since one must also take into account the life span and the response of these mice to the inflammation generated. The Zn repletion did not cause significant changes over a period of 7 days, however Zn did have a significant effect on AHR in mice repleted for 14 days. Longer periods of Zn repletion greater than the time points used in this thesis and/or diets higher in Zn content are now required to be tested.

Other limitations include the total number of mice which can be used per group (8 to 10) during any one experiment. Each experiment involved 6 groups of

animals with multiple tests performed, AHR readings and the sacrificing of mice 24 H after the last Buxco in Canberra. Future studies may allow measurements to be conducted at more than a single time point enabling the full kinetics of the responses to be determined. The transport of mice to Canberra for the final parts of the experiments by plane may have added extra stress to the mice. This was allowed for by testing for AHR 48 h after arrival. This limitation can be overcome by forming a collaborative project with Dr Paul Foster whereby experiments are initiated and maintained in Canberra.

Finally, it was not possible to distinguish which cell types were responsible for the Zn and PC3 protein staining in the intact epithelium because these are performed on unstained cryostat sections where it is difficult to determine the morphology of the cells. Therefore this thesis contains no information on the comparative levels of Zn in ciliated AEC, mucus cells and basal cells within the epithelium. This is even more of a problem in the OVA-treated mice where there is mucus cell hyperplasia and epithelial damage. One possible method which could overcome this limitation is the isolation of AEC from the OVA-treated mice by protease treatment.

8.3 CONCLUSION

In conclusion, this thesis reports the localisation of Zn in AEC, its loss in murine allergic inflammation and the effects of Zn deprivation and allergic airway inflammation on Zn homeostasis and its role in apoptosis. These findings provide the first data for adverse effects of Zn deficiency on the respiratory epithelium and support a role for altered Zn homeostasis and caspase up-regulation in allergic airway inflammation. These studies, which now need to be further pursued in

232

additional animal experiments and confirmed in human respiratory cells and human asthma, provide an impetus for understanding the physiological influence of Zn in the normal respiratory system and its influences on the pathological changes in airway diseases.

REFERENCES

- Abou-Mohamed, G., Papapetropoulos, A., Catravas, J.D. & Caldwell, R.W. (1998). Zn2+ inhibits nitric oxide formation in response to lipopolysaccharides: implication in its anti-inflammatory activity. *Eur J Pharmacol*, 341, 265-72.

- Ackland, M.L. & Mercer, J.F. (1992). The murine mutation, lethal milk, results in production of zinc-deficient milk. *Journal of Nutrition*, 122, 1214-8.

- Adams, J.M. & Cory, S. (1998). The Bcl-2 protein family: arbiters of cell survival. *Science*, 281, 1322-6.

- Adams, R., Ruffin, R., Wakefield, M., Campbell, D. & Smith, B. (1997). Asthma prevalence, morbidity and management practices in South Australia, 1992-1995. *Aust N Z J Med*, 27, 672-9.

- Adrain, C. & Martin, S.J. (2001). The mitochondrial apoptosome: a killer unleashed by the cytochrome seas. *Trends in Biochemical Sciences*, 26, 390-7.

- Aggett, P.J. & Comerford, J.G. (1995). Zinc and human health. *Nutrition Reviews*, 53, S16-22.

- Aggett, P.J., Delves, H.T., Harries, J.T. & Bangham, A.D. (1979). The possible role of diodoquin as a zinc ionophore in the treatment of acrodermatitis enteropathica. *Biochemical & Biophysical Research Communications*, 87, 513-7.

- Agren, M.S. (1990). Percutaneous absorption of zinc from zinc oxide applied topically to intact skin in man. *Dermatologica*, 180, 36-9.

- Agren, M.S. (1991). Collagen synthesis in connective tissue of wounded rat mesentery: effect of dietary zinc deficiency. *European Journal of Surgery*, 157, 453-5.

- Ahmed, T., Ungo, J., Zhou, M. & Campo, C. (2000). Inhibition of allergic late airway responses by inhaled heparin-derived oligosaccharides. *Journal of Applied Physiology*, 88, 1721-9.

- Aiuchi, T., Mihara, S., Nakaya, M., Masuda, Y., Nakajo, S. & Nakaya, K. (1998). Zinc ions prevent processing of caspase-3 during apoptosis induced by geranylgeraniol in HL-60 cells. *J Biochem (Tokyo)*, 124, 300-3.

- Allan, D.J., Howell, A., Roberts, S.A., Williams, G.T., Watson, R.J., Coyne, J.D., Clarke, R.B., Laidlaw, I.J. & Potten, C.S. (1992). Reduction in apoptosis relative to mitosis in histologically normal epithelium accompanies fibrocystic change and carcinoma of the premenopausal human breast. *Journal of Pathology.*, 167, 25-32.

- Andersson, P. (1980). Antigen-induced bronchial anaphylaxis in actively sensitized guinea-pigs. Pattern of response in relation to immunization regimen. *Allergy*, 35, 65-71.

- Anonymous. (1995). Asthma--United States, 1982-1992. *MMWR - Morbidity & Mortality Weekly Report*, 43, 952-5.

- Antonucci, A., Di Baldassarre, A., Di Giacomo, F., Stuppia, L. & Palka, G. (1997). Detection of apoptosis in peripheral blood cells of 31 subjects affected by Down syndrome before and after zinc therapy. *Ultrastructural Pathology*, 21, 449-52.

- Baer, M.T. & King, J.C. (1984). Tissue zinc levels and zinc excretion during experimental zinc depletion in young men. *American Journal of Clinical Nutrition*, 39, 556-70.

- Bartholomew, M., Tupper, R. & Wormall, A. (1959). Incorporation of 65ZN in the sub-cellular fractions of the liver and spontaneously occurring mammary

tumours of mice of the injection of zinc-glycine containing 65Zn. *Biochem J*, 73, 256-261.

- Beach, R.S., Gershwin, M.E. & Hurley, L.S. (1980). Growth and development in postnatally zinc-deprived mice. *Journal of Nutrition*, 110, 201-11.

- Benayoun, L., Letuve, S., Druilhe, A., Boczkowski, J., Dombret, M.-C., Mechighel, P., Megret, J., Leseche, G., Aubier, M. & Pretolani, M. (2001). Regulation of Peroxisome Proliferator-activated Receptor gamma Expression in Human Asthmatic Airways . Relationship with Proliferation, Apoptosis, and Airway Remodeling. *Am. J. Respir. Crit. Care Med.*, 164, 1487-1494.

- Benedict, M.A., Hu, Y., Inohara, N. & Nunez, G. (2000). Expression and functional analysis of Apaf-1 isoforms. Extra Wd-40 repeat is required for cytochrome c binding and regulated activation of procaspase-9. *Journal of Biological Chemistry*, 275, 8461-8.

- Bertholf, R.L. (1988). Zinc. In *Handbook on toxicity of inorganic compounds*, Sigel, H.G. (ed) pp. 788-800. Dekker: New York.

- Bettger, W.J. & O'Dell, B.L. (1981). A critical physiological role of zinc in the structure and function of biomembranes. *Life Sciences*, 28, 1425-38.

- Beyer, P. & Zawislak, R. (1978). Acrodermatitis enteropathica: mode of action of diiodohydroxyquinolin. *Nouvelle Presse Medicale*, 7, 117.

- Bhan, M.K., Sommerfelt, H. & Strand, T. (2001). Micronutrient deficiency in children. *British Journal of Nutrition*, 85, S199-203.

- Bhandari, N., Bahl, R., Taneja, S., Strand, T., Molbak, K., Ulvik, R.J., Sommerfelt, H. & Bhan, M.K. (2002). Effect of routine zinc supplementation on pneumonia in children aged 6 months to 3 years: randomised controlled trial in an urban slum. *Bmj.*, 324, 1358.

- Bice, D.E., Seagrave, J. & Green, F.H. (2000). Animal models of asthma: potential usefulness for studying health effects of inhaled particles. *Inhalation Toxicology*, 12, 829-62.

- Birinyi, A., Parker, D., Antal, M. & Shupliakov, O. (2001). Zinc co-localizes with GABA and glycine in synapses in the lamprey spinal cord. *Journal of Comparative Neurology*, 433, 208-21.

- Black, R.A., Kronheim, S.R., Merriam, J.E., March, C.J. & Hopp, T.P. (1989). A pre-aspartate-specific protease from human leukocytes that cleaves pro-interleukin-1 beta. *Journal of Biological Chemistry*, 264, 5323-6.

- Black, R.E. (1998). Therapeutic and preventive effects of zinc on serious childhood infectious diseases in developing countries. *American Journal of Clinical Nutrition*, 68, 476S-479S.

- Bloxam, D.L., Tan, J.C. & Parkinson, C.E. (1984). Non-protein bound zinc concentration in human plasma and amniotic fluid measured by ultrafiltration. *Clinica Chimica Acta*, 144, 81-93.

- Bodey, K.J., Semper, A.E., Redington, A.E., Madden, J., Teran, L.M., Holgate, S.T. & Frew, A.J. (1999). Cytokine profiles of BAL T cells and T-cell clones obtained from human asthmatic airways after local allergen challenge. *Allergy.*, 54, 1083-93.

- Boers, J.E., Ambergen, A.W. & Thunnissen, F.B. (1998). Number and proliferation of basal and parabasal cells in normal human airway epithelium. *Am J Respir Crit Care Med*, 157, 2000-6.

- Bousquet, J., Chanez, P., Lacoste, J.Y., Barneon, G., Ghavanian, N., Enander, I., Venge, P., Ahlstedt, S., Simony-Lafontaine, J. & Godard, P. (1990). Eosinophilic inflammation in asthma. *New England Journal of Medicine*, 323, 1033-9.

- Brown, R.S., Sander, C. & Argos, P. (1985). The primary structure of transcription factor TFIIIA has 12 consecutive repeats. *FEBS Letters*, 186, 271-4.

- Buisson, A.C., Zahm, J.M., Polette, M., Pierrot, D., Bellon, G., Puchelle, E., Birembaut, P. & Tournier, J.M. (1996). Gelatinase B is involved in the in vitro wound repair of human respiratory epithelium. *Journal of Cellular Physiology.*, 166, 413-26.

- Burkitt, G.H., Stevens, A., Lowe, J.S. & Young, B. (1996). *Wheater's Basic Histopathology: A Colour Atlas and Text*: Melbourne.

- Burkitt, G.H., Young, B., J.W., H. & Wheater, P. (1993). *Wheater's Functional Histology: A Text And Colour Atlas*. Churchill Livingstone: Melbourne.

- Burlacu, A., Jinga, V., Gafencu, A.V. & Simionescu, M. (2001). Severity of oxidative stress generates different mechanisms of endothelial cell death. *Cell & Tissue Research.*, 306, 409-16.

- Burr, J.S., Kimzey, S.L., Randolph, D.R. & Green, J.M. (2001). CD28 and CTLA4 coordinately regulate airway inflammatory cell recruitment and T-helper cell differentiation after inhaled allergen. *American Journal of Respiratory Cell & Molecular Biology*, 24, 563-8.

- Busse, W.W. & Lemanske, R.F. (2001). Asthma. *N Engl J Med*, 344, 350-362.

- Cai, J., Yang, J. & Jones, D.P. (1998). Mitochondrial control of apoptosis: the role of cytochrome c. *Biochimica et Biophysica Acta*, 1366, 139-49.

- Cain, K., Bratton, S.B., Langlais, C., Walker, G., Brown, D.G., Sun, X.M. & Cohen, G.M. (2000). Apaf-1 oligomerizes into biologically active approximately 700-kDa and inactive approximately 1.4-MDa apoptosome complexes. *Journal of Biological Chemistry*, 275, 6067-70.

- Cotran, R.S., Kumar, V., Collins, T. & Robbins, S.L. (1999). *Robbin's Pathologic Basis of Disease*. Saunders: Philadelphia.

- Cantin, A.M. (2001). Biology of respiratory epithelial cells: role in defense against infections. *Pediatric Pulmonology*, Suppl, 167-9.

- Canzoniero, L.M., Sensi, S.L. & Choi, D.W. (1997). Measurement of intracellular free zinc in living neurons. *Neurobiology of Disease*, 4, 275-9.

- Cao, J., Bobo, J.A., Liuzzi, J.P. & Cousins, R.J. (2001). Effects of intracellular zinc depletion on metallothionein and ZIP2 transporter expression and apoptosis. *Journal of Leukocyte Biology*, 70, 559-66.

- Cario, E., Jung, S., Harder D'Heureuse, J., Schulte, C., Sturm, A., Wiedenmann, B., Goebell, H. & Dignass, A.U. (2000). Effects of exogenous zinc supplementation on intestinal epithelial repair in vitro. *Eur J Clin Invest*, 30, 419-28.

- Castillo-Duran, C. & Uauy, R. (2001). Zinc supplementation saves the lives of children living in poverty. *Pediatrics*, 108, 1366.

- Chai, F., Truong-Tran, A.Q., Evdokiou, A., Young, G.P. & Zalewski, P.D. (2000). Intracellular zinc depletion induces caspase activation and p21 Waf1/Cip1 cleavage in human epithelial cell lines. *J Infect Dis*, 182 Suppl 1, S85-92.

- Chan, C. & Goldkorn, T. (2000). Ceramide path in human lung cell death. *American Journal of Respiratory Cell & Molecular Biology*, 22, 460-8.

- Chanez, P., Vignola, A.M., Vic, P., Guddo, F., Bonsignore, G., Godard, P. & Bousquet, J. (1999). Comparison between nasal and bronchial inflammation in asthmatic and control subjects. *American Journal of Respiratory & Critical Care Medicine*, 159, 588-95.

- Chang, H.Y. & Yang, X. (2000). Proteases for Cell Suicide: Functions and Regulation of Caspases. *Microbiol. Mol. Biol. Rev.*, 64, 821-846.

- Cheek, D.B., Smith, R.M., Spargo, R.M. & Francis, N. (1981). Zinc, copper and environmental factors in the aboriginal peoples of the North West. *Australian & New Zealand Journal of Medicine*, 11, 508-12.

- Cheng, J.B. & Townley, R.G. (1982). Effects of chronic histamine and ovalbumin aerosols on pulmonary beta adrenergic receptors in sensitized guinea pigs. *Research Communications in Chemical Pathology & Pharmacology*, 36, 507-10.

- Chevion, M. (1991). Protection Against Free Radical-Induced and Transition Metal-Mediated Damage: The Use of "Pull" and "Push" Mechanisms. *Free Radical Research Communications*, 12-13, 691.

- Chimienti, F., Seve, M., Richard, S., Mathieu, J. & Favier, A. (2001). Role of cellular zinc in programmed cell death: temporal relationship between zinc depletion, activation of caspases, and cleavage of Sp family transcription factors. *Biochemical Pharmacology.*, 62, 51-62.

- Cho, C.H., Dai, S. & Ogle, C.W. (1977). The effect of zinc on anaphylaxis in vivo in the guinea-pig. *Br J Pharmacol*, 60, 607-8.

- Cohen, G.M. (1997). Caspases: the executioners of apoptosis. *Biochemical Journal*, 326, 1-16.

- Cohen, J.J. & Duke, R.C. (1984). Glucocorticoid activation of a calcium-dependent endonuclease in thymocyte nuclei leads to cell death. *J Immunol*, 132, 38-42.

- Corry, D.B., Folkesson, H.G., Warnock, M.L., Erle, D.J., Matthay, M.A., Wiener-Kronish, J.P. & Locksley, R.M. (1996). Interleukin 4, but not

interleukin 5 or eosinophils, is required in a murine model of acute airway hyperreactivity. *Journal of Experimental Medicine*, 183, 109-17.

- Cousins, R.J. (1985). Absorption, transport, and hepatic metabolism of copper and zinc: special reference to metallothionein and ceruloplasmin. *Physiological Reviews*, 65, 238-309.

- Cousins, R.J. (1989). Theoretical and practical aspects of zinc uptake and absorption. *Advances in Experimental Medicine & Biology*, 249, 3-12.

- Coyle, P., Philcox, J.C., Carey, L.C. & Rofe, A.M. (2002). Metallothionein: the multipurpose protein. *Cellular & Molecular Life Sciences.*, 59, 627-47.

- Coyle, P., Philcox, J.C. & Rofe, A.M. (1999). Metallothionein-null mice absorb less Zn from an egg-white diet, but a similar amount from solutions, although with altered intertissue Zn distribution. *Journal of Nutrition*, 129, 372-9.

- Coyle, P., Zalewski, P.D., Philcox, J.C., Forbes, I.J., Ward, A.D., Lincoln, S.F., Mahadevan, I. & Rofe, A.M. (1994). Measurement of zinc in hepatocytes by using a fluorescent probe, zinquin: relationship to metallothionein and intracellular zinc. *Biochemical Journal*, 303, 781-6.

- Crapo, J.D., Harmsen, A.G., Sherman, M.P. & Musson, R.A. (2000). Pulmonary immunobiology and inflammation in pulmonary diseases. *American Journal of Respiratory & Critical Care Medicine*, 162, 1983-6.

- Crook, N.E., Clem, R.J. & Miller, L.K. (1993). An apoptosis-inhibiting baculovirus gene with a zinc finger-like motif. *Journal of Virology.*, 67, 2168-74.

- Cui, L., Takagi, Y., Sando, K., Wasa, M. & Okada, A. (2000). Nitric oxide synthase inhibitor attenuates inflammatory lesions in the skin of zinc-deficient rats. *Nutrition*, 16, 34-41.

- Cursio, R., Gugenheim, J., Ricci, J.E., Crenesse, D., Rostagno, P., Maulon, L., Saint-Paul, M.C., Ferrua, B., Mouiel, J. & Auberger, P. (2000). Caspase inhibition protects from liver injury following ischemia and reperfusion in rats. *Transplant International*, 13, S568-72.

- Da Silva, J.J., and Williams R.J. (1991). Zinc: Lewis acid catalysis and regulation. In *The Biological Chemistry of the Elements*, Williams, R.J. (ed) pp. 299-318. Clarendon: Oxford, UK.

- Danahay, H., Atherton, H., Jones, G., Bridges, R.J. & Poll, C.T. (2002). Interleukin-13 induces a hypersecretory ion transport phenotype in human bronchial epithelial cells. *Am J Physiol Lung Cell Mol Physiol*, 282, L226-236.

- Danscher, G. & Andreasen, A. (1997). Demonstration of vessels in CNS and other organs by AMG silver enhancement of colloidal gold particles dispersed in gelatine. *Journal of Neuroscience Methods*, 77, 175-81.

- Danscher, G., Obel, J. & Thorlacius-Ussing, O. (1980). Electron microscopic demonstration of metals in rat mast cells. A cytochemical study based on an improved sulphide silver method. *Histochemistry*, 66, 293-300.

- Davis, S.R. & Cousins, R.J. (2000). Metallothionein expression in animals: a physiological perspective on function. *Journal of Nutrition*, 130, 1085-8.

- Davis, S.R., McMahon, R.J. & Cousins, R.J. (1998). Metallothionein knockout and transgenic mice exhibit altered intestinal processing of zinc with uniform zinc-dependent zinc transporter-1 expression. *Journal of Nutrition*, 128, 825-31.

- De Raeve, H.R., Thunnissen, F.B., Kaneko, F.T., Guo, F.H., Lewis, M., Kavuru, M.S., Secic, M., Thomassen, M.J. & Erzurum, S.C. (1997). Decreased Cu,Zn-SOD activity in asthmatic airway epithelium: correction by inhaled corticosteroid in vivo. *Am J Physiol*, 272, L148-54.

- Di Toro, R., Galdo Capotorti, G., Gialanella, G., Miraglia del Giudice, M., Moro, R. & Perrone, L. (1987). Zinc and copper status of allergic children. *Acta Paediatr Scand*, 76, 612-7.

- Dimmeler, S., Haendeler, J., Nehls, M. & Zeiher, A.M. (1997). Suppression of apoptosis by nitric oxide via inhibition of interleukin-1beta-converting enzyme (ICE)-like and cysteine protease protein (CPP)-32-like proteases. *Journal of Experimental Medicine*, 185, 601-7.

- Downs, S.H., Marks, G.B., Sporik, R., Belosouva, E.G., Car, N.G. & Peat, J.K. (2001). Continued increase in the prevalence of asthma and atopy. *Archives of Disease in Childhood*, 84, 20-23.

- Dreosti, I.E. (1993). Recommended dietary intakes of iron, zinc, and other inorganic nutrients and their chemical form and bioavailability. *Nutrition*, 9, 542-5.

- Duke, R.C., Chervenak, R. & Cohen, J.J. (1983). Endogenous endonuclease-induced DNA fragmentation: an early event in cell-mediated cytolysis. *Proceedings of the National Academy of Sciences of the United States of America*, 80, 6361-5.

- Dvorak, A.M. (2002). Ultrastructure of human mast cells. *International Archives of Allergy & Immunology*, 127, 100-5.

- Earnshaw, W.C., Martins, L.M. & Kaufmann, S.H. (1999). Mammalian caspases: structure, activation, substrates, and functions during apoptosis. *Annu Rev Biochem*, 68, 383-424.

- El-Hashim, A.Z., Banner, K.H., Paul, W. & Page, C.P. (1999). Effects of dexamethasone on airway hyper-responsiveness to the adenosine A1 receptor agonist cyclo-pentyl adenosine in an allergic rabbit model. *British Journal of Pharmacology*, 126, 1513-21.

- el-Kholy, M.S., Gas Allah, M.A., el-Shimi, S., el-Baz, F., el-Tayeb, H. & Abdel-Hamid, M.S. (1990). Zinc and copper status in children with bronchial asthma and atopic dermatitis. *J Egypt Public Health Assoc*, 65, 657-68.

- Ellis, H.M. & Horvitz, H.R. (1986). Genetic control of programmed cell death in the nematode C. elegans. *Cell*, 44, 817-29.

- Ellul-Micallef, R., Galdes, A. & Fenech, F.F. (1976). Serum zinc levels in corticosteroid-treated asthmatic patients. *Postgrad Med J*, 52, 148-50.

- Elmes, M.E. (1977). Apoptosis in the small intestine of zinc-deficient and fasted rats. *Journal of Pathology*, 123, 219-23.

- Enari, M., Sakahira, H., Yokoyama, H., Okawa, K., Iwamatsu, A. & Nagata, S. (1998). A caspase-activated DNase that degrades DNA during apoptosis, and its inhibitor ICAD. *Nature*, 391, 43-50.

- Evans, P. & Halliwell, B. (2001). Micronutrients: oxidant/antioxidant status. *British Journal of Nutrition*, 85, S67-74.

- Floersheim, G.L., Christ, A., Koenig, R., Racine, C. & Gudat, F. (1992). Radiation-induced lymphoid tumors and radiation lethality are inhibited by combined treatment with small doses of zinc aspartate and WR 2721. *International Journal of Cancer*, 52, 604-8.

- Fogarty, A. & Britton, J. (2000a). Nutritional issues and asthma. *Current Opinion in Pulmonary Medicine*, 6, 86-9.

- Fogarty, A. & Britton, J. (2000b). The role of diet in the aetiology of asthma. *Clinical & Experimental Allergy*, 30, 615-27.

- Foster, P.S., Hogan, S.P., Ramsay, A.J., Matthaei, K.I. & Young, I.G. (1996). Interleukin 5 deficiency abolishes eosinophilia, airways hyperreactivity, and lung damage in a mouse asthma model. *Journal of Experimental Medicine*, 183, 195-201.

- Foster, P.S., Ming, Y., Matthei, K.I., Young, I.G., Temelkovski, J. & Kumar, R.K. (2000). Dissociation of inflammatory and epithelial responses in a murine model of chronic asthma. *Lab Invest*, 80, 655-62.

- Frade, J.M. & Michaelidis, T.M. (1997). Origin of eukaryotic programmed cell death: a consequence of aerobic metabolism? *Bioessays*, 19, 827-32.

- Fraker, P.J. & Telford, W.G. (1997). A reappraisal of the role of zinc in life and death decisions of cells. *Proc Soc Exp Biol Med*, 215, 229-36.

- Frederickson, C.J., Kasarskis, E.J., Ringo, D. & Frederickson, R.E. (1987a). A quinoline fluorescence method for visualizing and assaying the histochemically reactive zinc (bouton zinc) in the brain. *Journal of Neuroscience Methods*, 20, 91-103.

- Frederickson, C.J., Perez-Clausell, J. & Danscher, G. (1987b). Zinc-containing 7S-NGF complex. Evidence from zinc histochemistry for localization in salivary secretory granules. *Journal of Histochemistry & Cytochemistry*, 35, 579-83.

- Frederickson, C.J., Rampy, B.A., Reamy-Rampy, S. & Howell, G.A. (1992). Distribution of histochemically reactive zinc in the forebrain of the rat. *Journal of Chemical Neuroanatomy*, 5, 521-30.

- Frederickson, C.J.B.A.I. (2001). Synaptically released zinc: physiological functions and pathological effects. *Biometals*, 14, 353-66.

- Freeland-Graves, J.H., Bodzy, P.W. & Eppright, M.A. (1980). Zinc status of vegetarians. *Journal of the American Dietetic Association*, 77, 655-61.

- Fujisawa, T., Kato, Y., Nagase, H., Atsuta, J., Terada, A., Iguchi, K., Kamiya, H., Morita, Y., Kitaura, M., Kawasaki, H., Yoshie, O. & Hirai, K. (2000). Chemokines induce eosinophil degranulation through CCR-3. *Journal of Allergy & Clinical Immunology*, 106, 507-13.

- Fukamachi, Y., Karasaki, Y., Sugiura, T., Itoh, H., Abe, T., Yamamura, K. & Higashi, K. (1998). Zinc suppresses apoptosis of U937 cells induced by hydrogen peroxide through an increase of the Bcl-2/Bax ratio. *Biochem Biophys Res Commun*, 246, 364-9.

- Fuortes, L. & Schenck, D. (2000). Marked elevation of urinary zinc levels and pleural-friction rub in metal fume fever. *Vet Hum Toxicol*, 42, 164-5.

- Gaither, L.A. & Eide, D.J. (2000). Functional expression of the human hZIP2 zinc transporter. *Journal of Biological Chemistry*, 275, 5560-4.

- Gajewska, B.U., Swirski, F.K., Alvarez, D., Ritz, S.A., Goncharova, S., Cundall, M., Snider, D.P., Coyle, A.J., Gutierrez-Ramos, J.C., Stampfli, M.R. & Jordana, M. (2001). Temporal-spatial analysis of the immune response in a murine model of ovalbumin-induced airways inflammation. *American Journal of Respiratory Cell & Molecular Biology*, 25, 326-34.

- Gallaher, B.W., Hille, R., Raile, K. & Kiess, W. (2001). Apoptosis: live or die--hard work either way! *Hormone & Metabolic Research*, 33, 511-9.

- Galli, S.J., Dvorak, A.M. & Dvorak, H.F. (1984). Basophils and mast cells: morphologic insights into their biology, secretory patterns, and function. *Progress in Allergy*, 34, 1-141.

- Gavett, S.H., O'Hearn, D.J., Karp, C.L., Patel, E.A., Schofield, B.H., Finkelman, F.D. & Wills-Karp, M. (1997). Interleukin-4 receptor blockade prevents airway responses induced by antigen challenge in mice. *American Journal of Physiology*, 272, L253-61.

- Gergen, P.J., Mullally, D.I. & Evans, R., 3rd. (1988). National survey of prevalence of asthma among children in the United States, 1976 to 1980. *Pediatrics*, 81, 1-7.

- Gilks, C.B., Price, K., Wright, J.L. & Churg, A. (1998). Antioxidant gene expression in rat lung after exposure to cigarette smoke. *American Journal of Pathology*, 152, 269-78.

- Gillardon, F., Bottiger, B., Schmitz, B., Zimmermann, M. & Hossmann, K.A. (1997). Activation of CPP-32 protease in hippocampal neurons following ischemia and epilepsy. *Brain Research. Molecular Brain Research*, 50, 16-22.

- Goldey, D.H., Mansmann, H.C., Jr. & Rasmussen, A.I. (1984). Zinc status of asthmatic, prednisone-treated asthmatic, and non- asthmatic children. *J Am Diet Assoc*, 84, 157-63.

- Goldkorn, T., Balaban, N., Shannon, M., Chea, V., Matsukuma, K., Gilchrist, D., Wang, H. & Chan, C. (1998). H2O2 acts on cellular membranes to generate ceramide signaling and initiate apoptosis in tracheobronchial epithelial cells. *Journal of Cell Science*, 111, 3209-20.

- Gompertz, S. & Stockley, R.A. (2000). Inflammation--role of the neutrophil and the eosinophil. *Seminars in Respiratory Infections*, 15, 14-23.

- Gray, T., Koo, J.S. & Nettesheim, P. (2001). Regulation of mucous differentiation and mucin gene expression in the tracheobronchial epithelium. *Toxicology.*, 160, 35-46.

- Graziano, F., Haley, C., Gundersen, L. & Askenase, P.W. (1981). IgE antibody production in guinea pigs treated with cyclophosphamide. *Journal of Immunology*, 127, 1067-70.

- Greene, L.S. (1999). Asthma, oxidant stress, and diet. *Nutrition*, 15, 899-907.

- Greenfeder, S., Umland, S.P., Cuss, F.M., Chapman, R.W. & Egan, R.W. (2001). Th2 cytokines and asthma. The role of interleukin-5 in allergic eosinophilic disease. *Respiratory Research*, 2, 71-9.

- Guerinot, M.L. & Eide, D. (1999). Zeroing in on zinc uptake in yeast and plants. *Current Opinion in Plant Biology*, 2, 244-9.

- Gunshin, H., Mackenzie, B., Berger, U.V., Gunshin, Y., Romero, M.F., Boron, W.F., Nussberger, S., Gollan, J.L. & Hediger, M.A. (1997). Cloning and characterization of a mammalian proton-coupled metal-ion transporter. *Nature*, 388, 482-8.

- Guo, Y., Srinivasula, S.M., Druilhe, A., Fernandes-Alnemri, T. & Alnemri, E.S. (2002). Caspase-2 Induces Apoptosis by Releasing Proapoptotic Proteins from Mitochondria. *J. Biol. Chem.*, 277, 13430-13437.

- Gustafson, G.T. (1967). Heavy metals in rat mast cell granules. *Laboratory Investigation*, 17, 588-98.

- Haczku, A., Macary, P., Haddad, E.B., Huang, T.J., Kemeny, D.M., Moqbel, R. & Chung, K.F. (1996). Expression of Th-2 cytokines interleukin-4 and -5 and of Th-1 cytokine interferon-gamma in ovalbumin-exposed sensitized Brown-Norway rats. *Immunology*, 88, 247-51.

- Hallbook, T. & Lanner, E. (1972). Serum-zinc and healing of venous leg ulcers. *Lancet*, 2, 780-2.

- Halliwell, B. (1991). Reactive oxygen species in living systems: source, biochemistry, and role in human disease. *Am J Med*, 91, 14S-22S.

- Halliwell, B., Gutteridge, J.M. & Cross, C.E. (1992). Free radicals, antioxidants, and human disease: where are we now? *Journal of Laboratory & Clinical Medicine*, 119, 598-620.

- Hambidge, M. (2000). Human zinc deficiency. *Journal of Nutrition*, 130, 1344S-9S.

- Hamelmann, E. & Gelfand, E.W. (2001). IL-5-induced airway eosinophilia-- the key to asthma? *Immunological Reviews*, 179, 182-91.

- Hamelmann, E., Schwarze, J., Takeda, K., Oshiba, A., Larsen, G.L., Irvin, C.G. & Gelfand, E.W. (1997). Noninvasive measurement of airway responsiveness in allergic mice using barometric plethysmography. *American Journal of Respiratory & Critical Care Medicine*, 156, 766-75.

- Hamelmann, E., Tadeda, K., Oshiba, A. & Gelfand, E.W. (1999). Role of IgE in the development of allergic airway inflammation and airway hyperresponsiveness--a murine model. *Allergy*, 54, 297-305.

- Hampton, M.B. & Orrenius, S. (1997). Dual regulation of caspase activity by hydrogen peroxide: implications for apoptosis. *FEBS Letters*, 414, 552-6.

- Hanas, J.S., Hazuda, D.J., Bogenhagen, D.F., Wu, F.Y. & Wu, C.W. (1983). Xenopus transcription factor A requires zinc for binding to the 5 S RNA gene. *Journal of Biological Chemistry*, 258, 14120-5.

- Hengartner, M.O. & Horvitz, H.R. (1994). Programmed cell death in Caenorhabditis elegans. *Current Opinion in Genetics & Development*, 4, 581-6.

- Henkin, R.I. (1976). Trace metals in endocrinology. *Medical Clinics of North America*, 60, 779-97.

- Hennig, B., McClain, C.J. & Diana, J.N. (1993). Function of vitamin E and zinc in maintaining endothelial integrity. Implications in atherosclerosis. *Ann N Y Acad Sci*, 686, 99-109; discussion 109-11.

- Hennig, B., Meerarani, P., Ramadass, P., Toborek, M., Malecki, A., Slim, R. & McClain, C.J. (1999). Zinc nutrition and apoptosis of vascular endothelial cells: implications in atherosclerosis. *Nutrition*, 15, 744-8.

- Hennig, B., Wang, Y., Ramasamy, S. & McClain, C.J. (1992). Zinc deficiency alters barrier function of cultured porcine endothelial cells. *J Nutr*, 122, 1242-7.

- Henricks, P.A.N.F.P. (2001). Reactive oxygen species as mediators in asthma. *Pulmonary Pharmacology & Therapeutics*, 14, 409-20.

- Herz, U., Lumpp, U., Da Palma, J.C., Enssle, K., Takatsu, K., Schnoy, N., Daser, A., Kottgen, E., Wahn, U. & Renz, H. (1996). The relevance of murine animal models to study the development of allergic bronchial asthma. *Immunol Cell Biol*, 74, 209-17.

- Hesketh, J.E. (1982). Zinc-stimulated microtubule assembly and evidence for zinc binding to tubulin. *Int J Biochem*, 14, 983-90.

- Hickey, M.J., Granger, D.N. & Kubes, P. (1999). Molecular mechanisms underlying IL-4-induced leukocyte recruitment in vivo: a critical role for the alpha 4 integrin. *Journal of Immunology.*, 163, 3441-8.

- Ho, L.H., Ratnaike, R.N. & Zalewski, P.D. (2000). Involvement of intracellular labile zinc in suppression of DEVD-caspase activity in human neuroblastoma cells. *Biochemical & Biophysical Research Communications*, 268, 148-54.

- Hodge, L., Salome, C.M., Hughes, J.M., Liu-Brennan, D., Rimmer, J., Allman, M., Pang, D., Armour, C. & Woolcock, A.J. (1998). Effect of dietary intake of omega-3 and omega-6 fatty acids on severity of asthma in children. *European Respiratory Journal*, 11, 361-5.

- Holcik, M. & Korneluk, R.G. (2001). XIAP, the guardian angel. *Nature Reviews Molecular Cell Biology.*, 2, 550-6.

- Holgate, S.T. (2000). Inflammatory and structural changes in the airways of patients with asthma. *Respiratory Medicine*, 94, S3-6.

- Holgate, S.T., Lackie, P., Wilson, S., Roche, W. & Davies, D. (2000). Bronchial epithelium as a key regulator of airway allergen sensitization and remodeling in asthma. *American Journal of Respiratory & Critical Care Medicine*, 162, S113-7.

- Holme, G. & Piechuta, H. (1981). The derivation of an inbred line of rats which develop asthma-like symptoms following challenge with aerosolized antigen. *Immunology*, 42, 19-24.

- Huang, E.P. (1997). Metal ions and synaptic transmission: think zinc. *Proceedings of the National Academy of Sciences of the United States of America*, 94, 13386-7.

- Huang, L. & Gitschier, J. (1997). A novel gene involved in zinc transport is deficient in the lethal milk mouse. *Nature Genetics*, 17, 292-7.

- Huang, S.K., Xiao, H.Q., Kleine-Tebbe, J., Paciotti, G., Marsh, D.G., Lichtenstein, L.M. & Liu, M.C. (1995). IL-13 expression at the sites of allergen challenge in patients with asthma. *Journal of Immunology.*, 155, 2688-94.

- Huang, X.F. & Arvan, P. (1995). Intracellular transport of proinsulin in pancreatic beta-cells. Structural maturation probed by disulfide accessibility. *Journal of Biological Chemistry*, 270, 20417-23.

- Inayama, Y., Hook, G.E., Brody, A.R., Cameron, G.S., Jetten, A.M., Gilmore, L.B., Gray, T. & Nettesheim, P. (1988). The differentiation potential of tracheal basal cells. *Laboratory Investigation*, 58, 706-17.

- Ito, A., Uehara, T., Tokumitsu, A., Okuma, Y. & Nomura, Y. (1999). Possible involvement of cytochrome c release and sequential activation of caspases in ceramide-induced apoptosis in SK-N-MC cells. *Biochimica et Biophysica Acta.*, 1452, 263-74.

- Jackson, M.J. (1989). Physiology of Zinc:General Aspects. In *Zinc in human biology*, Mills, C.F. (ed) pp. 1-14. Springer-Verlag.: London.

- Jackson, M.J., Jones, D.A., Edwards, R.H., Swainbank, I.G. & Coleman, M.L. (1984). Zinc homeostasis in man: studies using a new stable isotope-dilution technique. *British Journal of Nutrition.*, 51, 199-208.

- Jankowski-Hennig, M.A., Clegg, M.S., Daston, G.P., Rogers, J.M. & Keen, C.L. (2000). Zinc-deficient rat embryos have increased caspase 3-like activity and apoptosis. *Biochemical & Biophysical Research Communications*, 271, 250-6.

- Janson, C., Anto, J., Burney, P., Chinn, S., de Marco, R., Heinrich, J., Jarvis, D., Kuenzli, N., Leynaert, B., Luczynska, C., Neukirch, F., Svanes, C., Sunyer, J., Wjst, M. & European Community Respiratory Health, S., II. (2001). The European Community Respiratory Health Survey: what are the main results so far? European Community Respiratory Health Survey II. *European Respiratory Journal.*, 18, 598-611.

- Janssen, Y.M., Matalon, S. & Mossman, B.T. (1997). Differential induction of c-fos, c-jun, and apoptosis in lung epithelial cells exposed to ROS or RNS. *American Journal of Physiology*, 273, L789-96.

- Jeon, K.-I., Jeong, J.-Y. & Jue, D.-M. (2000). Thiol-Reactive Metal Compounds Inhibit NF-{kappa}B Activation by Blocking I{kappa}B Kinase. *J Immunol*, 164, 5981-5989.

- Jiang, L.J., Maret, W. & Vallee, B.L. (1998). The glutathione redox couple modulates zinc transfer from metallothionein to zinc-depleted sorbitol dehydrogenase. *Proc Natl Acad Sci U S A*, 95, 3483-8.

- Jiang, X. & Wang, X. (2000). Cytochrome c promotes caspase-9 activation by inducing nucleotide binding to Apaf-1. *Journal of Biological Chemistry*, 275, 31199-203.

- Kadrabova, J., Mad'aric, A., Podivinsky, F., Gazdik, F. & Ginter, F. (1996). Plasma zinc, copper and copper/zinc ratio in intrinsic asthma. *J Trace Elem Med Biol*, 10, 50-3.

- Kambe, T., Narita, H., Yamaguchi-Iwai, Y., Hirose, J., Amano, T., Sugiura, N., Sasaki, R., Mori, K., Iwanaga, T. & Nagao, M. (2002). Cloning and characterization of a novel mammalian zinc transporter, zinc transporter 5, abundantly expressed in pancreatic beta cells. *Journal of Biological Chemistry*, 277, 19049-55.

- Kappus, H. (1995). Lipid peroxidation: Mechanisms, analysis, enzymology and biological relevance. In *Oxidative Stress*, H, S. (ed) pp. 273-310. Academic Press: New York.

- Kelsen, S.G., Johnson, R.A., Mest, S., Stauber, Z., Zhou, S., Aksoy, M. & Hilfer, S.R. (1993). Explant culture of rabbit tracheobronchial epithelium: structure and prostaglandin metabolism. *American Journal of Respiratory Cell & Molecular Biology*, 8, 472-9.

- Kerr, J.F. (1997). Definition of Apoptosis And Overview of its Incidence. In *Programmed cell Death: The Cellular and Molecular Biology of Apoptosis.* pp. 2-3. Harwood Acedemic Publishers: Switzerland.

- Kerr, J.F., Wyllie, A.H. & Currie, A.R. (1972). Apoptosis: a basic biological phenomenon with wide-ranging implications in tissue kinetics. *British Journal of Cancer*, 26, 239-57.

- Kilic, I., Ozalp, I., Coskun, T., Tokatli, A., Emre, S., Saldamli, I., Koksel, H. & Ozboy, O. (1998). The effect of zinc-supplemented bread consumption on school children with asymptomatic zinc deficiency. *Journal of Pediatric Gastroenterology & Nutrition*, 26, 167-71.

- King, J.C., Shames, D.M. & Woodhouse, L.R. (2000). Zinc homeostasis in humans. *Journal of Nutrition*, 130, 1360S-6S.

- Kinlaw, W.B., Levine, A.S., Morley, J.E., Silvis, S.E. & McClain, C.J. (1983). Abnormal zinc metabolism in type II diabetes mellitus. *American Journal of Medicine*, 75, 273-7.

- Kischkel, F.C., Hellbardt, S., Behrmann, I., Germer, M., Pawlita, M., Krammer, P.H. & Peter, M.E. (1995). Cytotoxicity-dependent APO-1 (Fas/CD95)-associated proteins form a death-inducing signaling complex (DISC) with the receptor. *EMBO Journal*, 14, 5579-88.

- Kitamura, Y. & Fujita, J. (1989). Regulation of mast cell differentiation. *Bioessays*, 10, 193-6.

- Kopf, M., Le Gros, G., Bachmann, M., Lamers, M.C., Bluethmann, H. & Kohler, G. (1993). Disruption of the murine IL-4 gene blocks Th2 cytokine responses. *Nature.*, 362, 245-8.

- Korsmeyer, S.J., Shutter, J.R., Veis, D.J., Merry, D.E. & Oltvai, Z.N. (1993). Bcl-2/Bax: a rheostat that regulates an anti-oxidant pathway and cell death. *Semin Cancer Biol*, 4, 327-32.

- Kown, M.H., Van der Steenhoven, T., Blankenberg, F.G., Hoyt, G., Berry, G.J., Tait, J.F., Strauss, H.W. & Robbins, R.C. (2000). Zinc-mediated reduction of apoptosis in cardiac allografts. *Circulation*, 102, III228-32.

- Krajewska, M., Wang, H.G., Krajewski, S., Zapata, J.M., Shabaik, A., Gascoyne, R. & Reed, J.C. (1997). Immunohistochemical analysis of in vivo patterns of expression of CPP32 (Caspase-3), a cell death protease. *Cancer Res*, 57, 1605-13.

- Krebs, N.F. (2000). Overview of zinc absorption and excretion in the human gastrointestinal tract. *Journal of Nutrition*, 130, 1374S-7S.

- Kroegel, C., Julius, P., Matthys, H., Virchow, J.C., Jr. & Luttmann, W. (1996). Endobronchial secretion of interleukin-13 following local allergen challenge in

atopic asthma: relationship to interleukin-4 and eosinophil counts. *European Respiratory Journal.*, 9, 899-904.

- Kroemer, G., Petit, P., Zamzami, N., Vayssiere, J.L. & Mignotte, B. (1995). The biochemistry of programmed cell death. *Faseb J*, 9, 1277-87.

- Kruczynski, D., Passia, D., Haider, S.G. & Glassmeyer, M. (1985). Zinc transport through residual bodies in the rat testis; a histochemical study. *Andrologia*, 17, 98-103.

- Kumar, R.K. (2001). Understanding airway wall remodeling in asthma: A basis for improvements in therapy. *Pharmacology and Therapeutics*, 91, 93-104.

- Kumar, R.K. & Foster, P.S. (2001). Murine model of chronic human asthma. *Immunol Cell Biol*, 79, 141-4.

- Kumar, R.K., Temelkovski, J., McNeil, H.P. & Hunter, N. (2000). Airway inflammation in a murine model of chronic asthma: evidence for a local humoral immune response. *Clin Exp Allergy*, 30, 1486-92.

- Kumar, S. (1999). Regulation of caspase activation in apoptosis: implications in pathogenesis and treatment of disease. *Clin Exp Pharmacol Physiol*, 26, 295-303.

- Kung, T.T., Jones, H., Adams, G.K., 3rd, Umland, S.P., Kreutner, W., Egan, R.W., Chapman, R.W. & Watnick, A.S. (1994). Characterization of a murine model of allergic pulmonary inflammation. *International Archives of Allergy & Immunology*, 105, 83-90.

- Laitinen, L.A., Heino, M., Laitinen, A., Kava, T. & Haahtela, T. (1985). Damage of the airway epithelium and bronchial reactivity in patients with asthma. *American Review of Respiratory Disease*, 131, 599-606.

- Lambrecht, B.N., Hoogsteden, H.C. & Pauwels, R.A. (2001). Dendritic cells as regulators of the immune response to inhaled allergen: recent findings in

animal models of asthma. *International Archives of Allergy & Immunology*, 124, 432-46.

- Lansdown, A.B., Sampson, B. & Rowe, A. (1999). Sequential changes in trace metal, metallothionein and calmodulin concentrations in healing skin wounds. *Journal of Anatomy*, 195, 375-86.

- Larsen, G.L., White, C.W., Takeda, K., Loader, J.E., Nguyen, D.D., Joetham, A., Groner, Y. & Gelfand, E.W. (2000). Mice that overexpress Cu/Zn superoxide dismutase are resistant to allergen-induced changes in airway control. *American Journal of Physiology - Lung Cellular & Molecular Physiology*, 279, L350-9.

- Lavrentiadou, S.N., Chan, C., Kawcak, T., Ravid, T., Tsaba, A., van der Vliet, A., Rasooly, R. & Goldkorn, T. (2001). Ceramide-mediated apoptosis in lung epithelial cells is regulated by glutathione. *American Journal of Respiratory Cell & Molecular Biology*, 25, 676-84.

- Le Souef, P.N. (2001). Growth and development of the lung. *Current Opinion in Allergy & Clinical Immunology*, 1, 127-31.

- Lee, D., Long, S.A., Adams, J.L., Chan, G., Vaidya, K.S., Francis, T.A., Kikly, K., Winkler, J.D., Sung, C.M., Debouck, C., Richardson, S., Levy, M.A., DeWolf, W.E., Jr., Keller, P.M., Tomaszek, T., Head, M.S., Ryan, M.D., Haltiwanger, R.C., Liang, P.H., Janson, C.A., McDevitt, P.J., Johanson, K., Concha, N.O., Chan, W., Abdel-Meguid, S.S., Badger, A.M., Lark, M.W., Nadeau, D.P., Suva, L.J., Gowen, M. & Nuttall, M.E. (2000). Potent and selective nonpeptide inhibitors of caspases 3 and 7 inhibit apoptosis and maintain cell functionality. *Journal of Biological Chemistry*, 275, 16007-14.

- Lee, H.H., Prasad, A.S., Brewer, G.J. & Owyang, C. (1989). Zinc absorption in human small intestine. *American Journal of Physiology*, 256, G87-91.

- Lee, Y.J. & Shacter, E. (2000). Hydrogen peroxide inhibits activation, not activity, of cellular caspase-3 in vivo. *Free Radical Biology & Medicine.*, 29, 684-92.

- Lefort, S., Vita, N., Reeb, R., Caput, D. & Ferrara, P. (1995). IL-13 and IL-4 share signal transduction elements as well as receptor components in TF-1 cells. *FEBS Letters.*, 366, 122-6.

- Leong, K.P. & Huston, D.P. (2001). Understanding the pathogenesis of allergic asthma using mouse models. *Annals of Allergy, Asthma, & Immunology*, 87, 96-109; quiz 110.

- Levy, M.A., Tsai, Y.-H., Reaume, A. & Bray, T.M. (2001). Cellular response of antioxidant metalloproteins in Cu/Zn SOD transgenic mice exposed to hyperoxia. *Am J Physiol Lung Cell Mol Physiol*, 281, L172-82.

- Lewis, D.J. & Jakins, P.R. (1981). Effect of tobacco smoke exposure on rat tracheal submucosal glands: an ultrastructural study. *Thorax*, 36, 622-4.

- Licastro, F., Mariani, R.A., Faldella, G., Carpene, E., Guidicini, G., Rangoni, A., Grilli, T. & Bazzocchi, G. (2001). Immune-endocrine status and coeliac disease in children with Down's syndrome: relationships with zinc and cognitive efficiency. *Brain Research Bulletin*, 55, 313-7.

- Lopez, A.F., Sanderson, C.J., Gamble, J.R., Campbell, H.D., Young, I.G. & Vadas, M.A. (1988). Recombinant human interleukin 5 is a selective activator of human eosinophil function. *Journal of Experimental Medicine*, 167, 219-24.

- Luecke, R.W. & Fraker, P.J. (1979). The effect of varying dietary zinc levels on growth and antibody-mediated response in two strains of mice. *Journal of Nutrition*, 109, 1373-6.

- Lukowiak, B., Vandewalle, B., Riachy, R., Kerr-Conte, J., Gmyr, V., Belaich, S., Lefebvre, J. & Pattou, F. (2001). Identification and purification of

functional human beta-cells by a new specific zinc-fluorescent probe. *Journal of Histochemistry & Cytochemistry*, 49, 519-28.

- MacDonald, R.S. (2000). The role of zinc in growth and cell proliferation. *Journal of Nutrition*, 130, 1500S-8S.

- MacKenzie, J.R., Mattes, J., Dent, L.A. & Foster, P.S. (2001). Eosinophils promote allergic disease of the lung by regulating CD4(+) Th2 lymphocyte function. *Journal of Immunology*, 167, 3146-55.

- Mahadevan, I., M.C. Kimber., S.F. Lincoln., E.R. Tiekink., A.D. Ward., W.H. Betts., I.J. Forbes., and P.D Zalewski. (1996). The Synthesis of Zinquin ester and Zinquin acid, Zn (II)-specific fluorescing agents for use in the study of biological Zn (II). *Australian Journal of Chemistry*, 49, 561-568.

- Maret, W. (2000). The function of zinc metallothionein: a link between cellular zinc and redox state. *Journal of Nutrition*, 130, 1455S-8S.

- Maret, W., Jacob, C., Vallee, B.L. & Fischer, E.H. (1999). Inhibitory sites in enzymes: zinc removal and reactivation by thionein. *Proc Natl Acad Sci U S A*, 96, 1936-40.

- Marini, M., Vittori, E., Hollemborg, J. & Mattoli, S. (1992). Expression of the potent inflammatory cytokines, granulocyte-macrophage-colony-stimulating factor and interleukin-6 and interleukin-8, in bronchial epithelial cells of patients with asthma. *Journal of Allergy & Clinical Immunology*, 89, 1001-9.

- Marone, G., Columbo, M., de Paulis, A., Cirillo, R., Giugliano, R. & Condorelli, M. (1986). Physiological concentrations of zinc inhibit the release of histamine from human basophils and lung mast cells. *Agents Actions*, 18, 103-6.

- Martin, S.J., Mazdai, G., Strain, J.J., Cotter, T.G. & Hannigan, B.M. (1991). Programmed cell death (apoptosis) in lymphoid and myeloid cell lines during zinc deficiency. *Clin Exp Immunol*, 83, 338-43.

- Mathur, M., Herrmann, K., Li, X., Qin, Y., Weinstock, J., Elliot, D., MONAHAN, J. & Padrid, P. (1999). TRFK-5 Reverses Established Airway Eosinophilia But Not Established Hyperresponsiveness in a Murine Model of Chronic Asthma. *Am. J. Respir. Crit. Care Med.*, 159, 580-587.

- Matsui, T. & Yamaguchi, M. (1995). Zinc modulation of insulin-like growth factor's effect in osteoblastic MC3T3-E1 cells. *Peptides*, 16, 1063-8.

- McClain, C.J., Kasarskis, E.J., Jr. & Allen, J.J. (1985). Functional consequences of zinc deficiency. *Progress in Food & Nutrition Science*, 9, 185-226.

- McCormick, C.C., Menard, M.P. & Cousins, R.J. (1981). Induction of hepatic metallothionein by feeding zinc to rats of depleted zinc status. *American Journal of Physiology*, 240, E414-21.

- McMahon, R.J. & Cousins, R.J. (1998). Mammalian zinc transporters. *Journal of Nutrition*, 128, 667-70.

- Medina, V., Edmonds, B., Young, G.P., James, R., Appleton, S. & Zalewski, P.D. (1997). Induction of caspase-3 protease activity and apoptosis by butyrate and trichostatin A (inhibitors of histone deacetylase): dependence on protein synthesis and synergy with a mitochondrial/cytochrome c-dependent pathway. *Cancer Research*, 57, 3697-707.

- Michalczyk, A.A., Allen, J., Blomeley, R.C. & Ackland, M.L. (2002). Constitutive expression of hZnT4 zinc transporter in human breast epithelial cells. *Biochemical Journal*, 364, 105-13.

- Miles, A.T., Hawksworth, G.M., Beattie, J.H. & Rodilla, V. (2000). Induction, regulation, degradation, and biological significance of mammalian metallothioneins. *Critical Reviews in Biochemistry & Molecular Biology*, 35, 35-70.

- Milman, N., Hvid-Jacobsen, K., Hegnhoj, J. & Sorensen, S.S. (1983). Zinc absorption in patients with compensated alcoholic cirrhosis. *Scandinavian Journal of Gastroenterology*, 18, 871-5.

- Minshall, E., Spina, D. & Page, C.P. (1996). Effects of neonatal immunization and repeated allergen exposure on airway responsiveness in the rabbit. *Journal of Applied Physiology*, 80, 2108-19.

- Mocchegiani, E. & Muzzioli, M. (2000). Therapeutic application of zinc in human immunodeficiency virus against opportunistic infections. *Journal of Nutrition*, 130, 1424S-31S.

- Mocchegiani, E., Muzzioli, M. & Giacconi, R. (2000). Zinc, metallothioneins, immune responses, survival and ageing. *Biogerontology*, 1, 133-43.

- Mori, H., Matsumoto, Y., Tamada, Y. & Ohashi, M. (1996). Apoptotic cell death in formation of vesicular skin lesions in patients with acquired zinc deficiency. *J Cutan Pathol*, 23, 359-63.

- Mosmann, T.R. & Coffman, R.L. (1989). TH1 and TH2 cells: different patterns of lymphokine secretion lead to different functional properties. *Annual Review of Immunology*, 7, 145-73.

- Murgia, C., Vespignani, I., Cerase, J., Nobili, F. & Perozzi, G. (1999). Cloning, expression, and vesicular localization of zinc transporter Dri 27/ZnT4 in intestinal tissue and cells. *American Journal of Physiology*, 277, G1231-9.

- Nagakura, T., Matsuda, S., Shichijyo, K., Sugimoto, H. & Hata, K. (2000). Dietary supplementation with fish oil rich in omega-3 polyunsaturated fatty

acids in children with bronchial asthma. *European Respiratory Journal*, 16, 861-5.

- Nakajima, H., Iwamoto, I., Tomoe, S., Matsumura, R., Tomioka, H., Takatsu, K. & Yoshida, S. (1992). CD4+ T-lymphocytes and interleukin-5 mediate antigen-induced eosinophil infiltration into the mouse trachea. *American Review of Respiratory Disease.*, 146, 374-7.

- Nasir, M.S., Fahrni, C.J., Suhy, D.A., Kolodsick, K.J., Singer, C.P. & O'Halloran, T.V. (1999). The chemical cell biology of zinc: structure and intracellular fluorescence of a zinc-quinolinesulfonamide complex. *Journal of Biological Inorganic Chemistry*, 4, 775-83.

- Naveh, Y., Schapira, D., Ravel, Y., Geller, E. & Scharf, Y. (1997). Zinc metabolism in rheumatoid arthritis: plasma and urinary zinc and relationship to disease activity. *Journal of Rheumatology*, 24, 643-6.

- Netter, F.H. (1995). *Respiratory System*. Vol. 7. The Ciba Collection of Medical Illlustrations. Library of Congress: USA.

- Nguyen, M., Millar, D.G., Yong, V.W., Korsmeyer, S.J. & Shore, G.C. (1993). Targeting of Bcl-2 to the mitochondrial outer membrane by a COOH-terminal signal anchor sequence. *Journal of Biological Chemistry*, 268, 25265-8.

- Nicholson, D.W., Ali, A., Thornberry, N.A., Vaillancourt, J.P., Ding, C.K., Gallant, M., Gareau, Y., Griffin, P.R., Labelle, M., Lazebnik, Y.A. & et al. (1995). Identification and inhibition of the ICE/CED-3 protease necessary for mammalian apoptosis. *Nature*, 376, 37-43.

- Nodera, M., Yanagisawa, H. & Wada, O. (2001). Increased apoptosis in a variety of tissues of zinc-deficient rats. *Life Sciences.*, 69, 1639-49.

- Novick, S.G., Godfrey, J.C., Pollack, R.L. & Wilder, H.R. (1997). Zinc-induced suppression of inflammation in the respiratory tract, caused by

infection with human rhinovirus and other irritants. *Med Hypotheses*, 49, 347-57.

- Novoselov, S.V., Peshenko, I.V., Popov, V.I., Novoselov, V.I., Bystrova, M.F., Evdokimov, V.J., Kamzalov, S.S., Merkulova, M.I., Shuvaeva, T.M., Lipkin, V.M. & Fesenko, E.E. (1999). Localization of 28-kDa peroxiredoxin in rat epithelial tissues and its antioxidant properties. *Cell & Tissue Research.*, 298, 471-80.

- O'Dell, B.L. (2000). Role of zinc in plasma membrane function. *J Nutr*, 130, 1432S-6S.

- O'Dell, B.L., Browning, J.D. & Reeves, P.G. (1987). Zinc deficiency increases the osmotic fragility of rat erythrocytes. *Journal of Nutrition*, 117, 1883-9.

- Ohno, Y., Fukuda, K., Takemura, G., Toyota, M., Watanabe, M., Yasuda, N., Xinbin, Q., Maruyama, R., Akao, S., Gotou, K., Fujiwara, T. & Fujiwara, H. (1999). Induction of apoptosis by gallic acid in lung cancer cells. *Anti-Cancer Drugs*, 10, 845-51.

- Oshiba, A., Hamelmann, E., Takeda, K., Bradley, K.L., Loader, J.E., Larsen, G.L. & Gelfand, E.W. (1996). Passive transfer of immediate hypersensitivity and airway hyperresponsiveness by allergen-specific immunoglobulin (Ig) E and IgG1 in mice. *Journal of Clinical Investigation*, 97, 1398-408.

- Oteiza, P.I., Clegg, M.S., Zago, M.P. & Keen, C.L. (2000). Zinc deficiency induces oxidative stress and AP-1 activation in 3T3 cells. *Free Radic Biol Med*, 28, 1091-9.

- Oteiza, P.I., Hurley, L.S., Lonnerdal, B. & Keen, C.L. (1990). Effects of marginal zinc deficiency on microtubule polymerization in the developing rat brain. *Biological Trace Element Research*, 24, 13-23.

- Oteiza, P.L., Olin, K.L., Fraga, C.G. & Keen, C.L. (1996). Oxidant defense systems in testes from zinc-deficient rats. *Proc Soc Exp Biol Med*, 213, 85-91.

- Padrid, P., Snook, S., Finucane, T., Shiue, P., Cozzi, P., Solway, J. & Leff, A.R. (1995). Persistent airway hyperresponsiveness and histologic alterations after chronic antigen challenge in cats. *American Journal of Respiratory & Critical Care Medicine*, 151, 184-93.

- Palma, E., Maggi, L., Miledi, R. & Eusebi, F. (1998). Effects of Zn2+ on wild and mutant neuronal alpha7 nicotinic receptors. *Proceedings of the National Academy of Sciences of the United States of America*, 95, 10246-50.

- Palmiter, R.D., Cole, T.B. & Findley, S.D. (1996a). ZnT-2, a mammalian protein that confers resistance to zinc by facilitating vesicular sequestration. *EMBO Journal*, 15, 1784-91.

- Palmiter, R.D., Cole, T.B., Quaife, C.J. & Findley, S.D. (1996b). ZnT-3, a putative transporter of zinc into synaptic vesicles. *Proceedings of the National Academy of Sciences of the United States of America*, 93, 14934-9.

- Palmiter, R.D. & Findley, S.D. (1995). Cloning and functional characterization of a mammalian zinc transporter that confers resistance to zinc. *EMBO Journal*, 14, 639-49.

- Parsons, S.E. & DiSilvestro, R.A. (1994). Effects of mild zinc deficiency, plus or minus an acute-phase response, on galactosamine-induced hepatitis in rats. *British Journal of Nutrition*, 72, 611-8.

- Patterson, R. & Kelly, J.F. (1974). Animal models of the asthmatic state. *Annual Review of Medicine*, 25, 53-68.

- Pauwels, R.A., Brusselle, G.J. & Kips, J.C. (1997). Cytokine manipulation in animal models of asthma. *American Journal of Respiratory & Critical Care Medicine*, 156, S78-81.

- Pawankar, R. (2001). Mast cells as orchestrators of the allergic reaction: the IgE-IgE receptor mast cell network. *Current Opinion in Allergy & Clinical Immunology*, 1, 3-6.

- Pearce, N., Sunyer, J., Cheng, S., Chinn, S., Bjorksten, B., Burr, M., Keil, U., Anderson, H.R. & Burney, P. (2000). Comparison of asthma prevalence in the ISAAC and the ECRHS. ISAAC Steering Committee and the European Community Respiratory Health Survey. International Study of Asthma and Allergies in Childhood. *European Respiratory Journal.*, 16, 420-6.

- Peat, J.K. (1998). Can asthma be prevented? Evidence from epidemiological studies of children in Australia and New Zealand in the last decade. *Clinical & Experimental Allergy*, 28, 261-5.

- Peat, J.K., Van Den Berg, R.H., Green, W.F., Mellis, G.M., Leeder, S.R. & Woolcock, A.J. (1994). Changing Prevalence of Asthma in Australian Children. *B.M.J*, 308, 1591-1596.

- Perry, D.K., Smyth, M.J., Stennicke, H.R., Salvesen, G.S., Duriez, P., Poirier, G.G. & Hannun, Y.A. (1997). Zinc is a potent inhibitor of the apoptotic protease, caspase-3. A novel target for zinc in the inhibition of apoptosis. *J Biol Chem*, 272, 18530-3.

- Picado, C., Deulofeu, R., Lleonart, R., Agusti, M., Mullol, J., Quinto, L. & Torra, M. (2001). Dietary micronutrients/antioxidants and their relationship with bronchial asthma severity. *Allergy.*, 56, 43-9.

- Ploysangam, A., Falciglia, G.A. & Brehm, B.J. (1997). Effect of marginal zinc deficiency on human growth and development. *Journal of Tropical Pediatrics*, 43, 192-8.

- Pope, S.M., Brandt, E.B., Mishra, A., Hogan, S.P., Zimmermann, N., Matthaei, K.I., Foster, P.S. & Rothenberg, M.E. (2001). IL-13 induces eosinophil

recruitment into the lung by an IL-5- and eotaxin-dependent mechanism. *Journal of Allergy & Clinical Immunology*, 108, 594-601.

- Popkin, B.M. (2001). Nutrition in transition: the changing global nutrition challenge. *Asia Pacific Journal of Clinical Nutrition*, 10, S13-8.

- Pories, W.J., Henzel, J.H., Rob, C.G. & Strain, W.H. (1967). Acceleration of healing with zinc sulfate. *Ann Surg*, 165, 432-6.

- Powell, S.R. (2000). The antioxidant properties of zinc. *J Nutr*, 130, 1447S-54S.

- Prasad, A.S. (1991). Discovery of human zinc deficiency and studies in an experimental human model. *American Journal of Clinical Nutrition*, 53, 403-12.

- Prasad, A.S. (2000). Effects of zinc deficiency on Th1 and Th2 cytokine shifts. *Journal of Infectious Diseases*, 182, S62-8.

- Prasad, A.S. (2001). Recognition of zinc-deficiency syndrome. *Nutrition*, 17, 67-9.

- Prasad, A.S., Fitzgerald, J.T., Bao, B., Beck, F.W. & Chandrasekar, P.H. (2000). Duration of symptoms and plasma cytokine levels in patients with the common cold treated with zinc acetate. A randomized, double-blind, placebo-controlled trial. *Ann Intern Med*, 133, 245-52.

- Pretolani, M. & Vargaftig, B.B. (1993). From lung hypersensitivity to bronchial hyperreactivity. What can we learn from studies on animal models? *Biochemical Pharmacology*, 45, 791-800.

- Qian, W.J., Aspinwall, C.A., Battiste, M.A. & Kennedy, R.T. (2000). Detection of secretion from single pancreatic beta-cells using extracellular fluorogenic reactions and confocal fluorescence microscopy. *Analytical Chemistry*, 72, 711-7.

- Rahman, I. & MacNee, W. (1999). Lung glutathione and oxidative stress: implications in cigarette smoke-induced airway disease. *American Journal of Physiology*, 277, L1067-88.

- Rajcan-Separovic, E., Liston, P., Lefebvre, C. & Korneluk, R.G. (1996). Assignment of human inhibitor of apoptosis protein (IAP) genes xiap, hiap-1, and hiap-2 to chromosomes Xq25 and 11q22-q23 by fluorescence in situ hybridization. *Genomics.*, 37, 404-6.

- Ramachandran, A., Moellering, D., Go, Y.M., Shiva, S., Levonen, A.L., Jo, H., Patel, R.P., Parthasarathy, S. & Darley-Usmar, V.M. (2002). Activation of c-Jun N-terminal kinase and apoptosis in endothelial cells mediated by endogenous generation of hydrogen peroxide. *Biological Chemistry*, 383, 693-701.

- Ravanti, L. & Kahari, V.M. (2000). Matrix metalloproteinases in wound repair (review). *Int J Mol Med*, 6, 391-407.

- Record, I.R., Tulsi, R.S., Dreosti, I.E. & Fraser, F.J. (1985). Cellular necrosis in zinc-deficient rat embryos. *Teratology*, 32, 397-405.

- Reed, B.R. & Clark, R.A. (1985). Cutaneous tissue repair: practical implications of current knowledge. II. *Journal of the American Academy of Dermatology*, 13, 919-41.

- Reed, C.E. (1994). The importance of eosinophils in the immunology of asthma and allergic disease. *Annals of Allergy*, 72, 376-80.

- Reyes, J.G. (1996). Zinc transport in mammalian cells. *American Journal of Physiology*, 270, C401-10.

- Robertson, C.F., Dalton, M.F., Peat, J.K., Haby, M.M., Bauman, A., Kennedy, J.D. & Landau, L.I. (1998). Asthma and other atopic diseases in Australian

children. Australian arm of the International Study of Asthma and Allergy in Childhood. *Medical Journal of Australia.*, 168, 434-8.

- Robinson, D.S. (2000). Th-2 cytokines in allergic disease. *British Medical Bulletin*, 56, 956-68.

- Rolfs, A. & Hediger, M.A. (1999). Metal ion transporters in mammals: structure, function and pathological implications. *Journal of Physiology*, 518, 1-12.

- Romagnani, S. (2002). Cytokines and chemoattractants in allergic inflammation. *Molecular Immunology.*, 38, 881-5.

- Rosenstreich, D.L., Eggleston, P., Kattan, M., Baker, D., Slavin, R.G., Gergen, P., Mitchell, H., McNiff-Mortimer, K., Lynn, H., Ownby, D. & Malveaux, F. (1997). The role of cockroach allergy and exposure to cockroach allergen in causing morbidity among inner-city children with asthma. *N Engl J Med*, 336, 1356-63.

- Roth, H. & Kirchgessner, M. (1997). Course of concentration changes of growth hormone igf-1, insulin and c-peptide in serum, pituitary and liver of zinc- deficient rats. *J. Anim. Phys. Anim. Nutr.*, 77, 91-101.

- Rowe, D.J. & Bobilya, D.J. (2000). Albumin facilitates zinc acquisition by endothelial cells. *Proceedings of the Society for Experimental Biology & Medicine*, 224, 178-86.

- Ruffin, R.E., Dolovich, M.B., Wolff, R.K. & Newhouse, M.T. (1978). The effects of preferential deposition of histamine in the human airway. *American Review of Respiratory Disease*, 117, 485-92.

- Rutten van-Molken, M.P. & Feenstra, T.L. (2001). The burden of asthma and chronic obstructive pulmonary disease: data from The Netherlands. *Pharmacoeconomics*, 19, 1-6.

- Salgueiro, M.J., Zubillaga, M., Lysionek, A., Cremaschi, G., Goldman, C.G., Caro, R., De Paoli, T., Hager, A., Weill, R. & Boccio, J. (2000). Zinc status and immune system relationship: a review. *Biological Trace Element Research*, 76, 193-205.

- Sandstead, H.H. (1991). Zinc deficiency. A public health problem? *American Journal of Diseases of Children*, 145, 853-9.

- Sandstead, H.H. (1995). Is zinc deficiency a public health problem? *Nutrition*, 11, 87-92.

- Sandstead, H.H., Fosmire, G.J., McKenzie, J.M. & Halas, E.S. (1975). Zinc deficiency and brain development in the rat. *Federation Proceedings*, 34, 86-8.

- Santing, R.E., Schraa, E.O., Wachters, A., Olymulder, C.G., Zaagsma, J. & Meurs, H. (1994). Role of histamine in allergen-induced asthmatic reactions, bronchial hyperreactivity and inflammation in unrestrained guinea pigs. *European Journal of Pharmacology*, 254, 49-57.

- Savage, D.D., Montano, C.Y. & Kasarskis, E.J. (1989). Quantitative histofluorescence of hippocampal mossy fiber zinc. *Brain Research*, 496, 257-67.

- Sazawal, S., Bentley, M., Black, R.E., Dhingra, P., George, S. & Bhan, M.K. (1996). Effect of zinc supplementation on observed activity in low socioeconomic Indian preschool children. *Pediatrics*, 98, 1132-7.

- Sazawal, S., Black, R.E., Bhan, M.K., Bhandari, N., Sinha, A. & Jalla, S. (1995). Zinc supplementation in young children with acute diarrhea in India. *New England Journal of Medicine*, 333, 839-44.

- Sazawal, S., Black, R.E., Bhan, M.K., Jalla, S., Sinha, A. & Bhandari, N. (1997). Efficacy of zinc supplementation in reducing the incidence and

prevalence of acute diarrhea--a community-based, double-blind, controlled trial. *American Journal of Clinical Nutrition*, 66, 413-8.

- Sazawal, S., Black, R.E., Jalla, S., Mazumdar, S., Sinha, A. & Bhan, M.K. (1998). Zinc supplementation reduces the incidence of acute lower respiratory infections in infants and preschool children: a double-blind, controlled trial. *Pediatrics*, 102, 1-5.

- Scavo, L.M., Ertsey, R., Chapin, C.J., Allen, L. & Kitterman, J.A. (1998). Apoptosis in the Development of Rat and Human Fetal Lungs. *Am. J. Respir. Cell Mol. Biol.*, 18, 21-31.

- Schwartz, J. & Weiss, S.T. (1990). Dietary factors and their relation to respiratory symptoms. The Second National Health and Nutrition Examination Survey. *Am J Epidemiol*, 132, 67-76.

- Schwartz, J. & Weiss, S.T. (1994). Relationship between dietary vitamin C intake and pulmonary function in the First National Health and Nutrition Examination Survey (NHANES I). *American Journal of Clinical Nutrition*, 59, 110-4.

- Seiler, W.O. (2001). Clinical pictures of malnutrition in ill elderly subjects. *Nutrition.*, 17, 496-8.

- Semrad, C.E. (1999). Zinc and intestinal function. *Current Gastroenterology Reports*, 1, 398-403.

- Shampain, M.P., Behrens, B.L., Larsen, G.L. & Henson, P.M. (1982). An animal model of late pulmonary responses to Alternaria challenge. *American Review of Respiratory Disease*, 126, 493-8.

- Shankar, A.H. & Prasad, A.S. (1998). Zinc and immune function: the biological basis of altered resistance to infection. *Am J Clin Nutr*, 68, 447S-463S.

- Shapiro, G.I., Koestner, D.A., Matranga, C.B. & Rollins, B.J. (1999). Flavopiridol induces cell cycle arrest and p53-independent apoptosis in non-small cell lung cancer cell lines. *Clinical Cancer Research*, 5, 2925-38.

- Shaw, R.J., Djukanovic, R., Tashkin, D.P., Millar, A.B., du Bois, R.M. & Orr, P.A. (2002). The role of small airways in lung disease. *Respiratory Medicine*, 96, 67-80.

- Sheikh, S.P., Vilardarga, J.-P., Baranski, T.J., Lichtarge, O., Iiri, T., Meng, E.C., Nissenson, R.A. & Bourne, H.R. (1999). Similar Structures and Shared Switch Mechanisms of the beta 2-Adrenoceptor and the Parathyroid Hormone Receptor. Zn(II) BRIDGES BETWEEN HELICES III AND VI BLOCK ACTIVATION. *J. Biol. Chem.*, 274, 17033-17041.

- Shi, Y. (2002). Mechanisms of caspase activation and inhibition during apoptosis. *Molecular Cell.*, 9, 459-70.

- Simon, S.F. & Taylor, C.G. (2001). Dietary zinc supplementation attenuates hyperglycemia in db/db mice. *Experimental Biology & Medicine (Maywood, N.J.)*, 226, 43-51.

- Singh, K. & Nath, R. (1973). Distribution of cadmium and zinc among protein fractions of rat testis. *Indian Journal of Experimental Biology*, 11, 498-9.

- Solomons, N.W. (1988). Zinc and copper. In *MODERN NUTRITION IN HEALTH AND DISEASE*, Shils, M.E.a.Y., V.R (ed) pp. 238-262. Lea Febiger: Philadelphia.

- Sorensen, J.A., Andersen, O. & Nielsen, J.B. (1998). An in vivo study of the gastrointestinal absorption site for zinc chloride in mice. *Journal of Trace Elements in Medicine & Biology*, 12, 16-22.

- Sorensen, M.B., Stoltenberg, M., Juhl, S., Danscher, G. & Ernst, E. (1997). Ultrastructural localization of zinc ions in the rat prostate: an autometallographic study. *Prostate*, 31, 125-30.

- Soutar, A., Seaton, A. & Brown, K. (1997). Bronchial reactivity and dietary antioxidants. *Thorax*, 52, 166-70.

- Sporik, R., Ingram, J.M., Price, W., Sussman, J.H., Honsinger, R.W. & Platts-Mills, T.A. (1995). Association of asthma with serum IgE and skin test reactivity to allergens among children living at high altitude. Tickling the dragon's breath. *Am J Respir Crit Care Med*, 151, 1388-92.

- Sprietsma, J.E. (1999). Modern diets and diseases: NO-zinc balance. Under Th1, zinc and nitrogen monoxide (NO) collectively protect against viruses, AIDS, autoimmunity, diabetes, allergies, asthma, infectious diseases, atherosclerosis and cancer. *Med Hypotheses*, 53, 6-16.

- Squillace, S.P., Sporik, R.B., Rakes, G., Couture, N., Lawrence, A., Merriam, S., Zhang, J. & Platts-Mills, A.E. (1997). Sensitization to dust mites as a dominant risk factor for asthma among adolescents living in central Virginia. Multiple regression analysis of a population-based study. *Am J Respir Crit Care Med*, 156, 1760-4.

- Srinivasula, S.M., Fernandes-Alnemri, T., Zangrilli, J., Robertson, N., Armstrong, R.C., Wang, L., Trapani, J.A., Tomaselli, K.J., Litwack, G. & Alnemri, E.S. (1996). The Ced-3/Interleukin 1beta Converting Enzyme-like Homolog Mch6 and the Lamin-cleaving Enzyme Mch2alpha Are Substrates for the Apoptotic Mediator CPP32. *J. Biol. Chem.*, 271, 27099-27106.

- Sriramarao, P., von Andrian, U.H., Butcher, E.C., Bourdon, M.A. & Broide, D.H. (1994). L-selectin and very late antigen-4 integrin promote eosinophil

rolling at physiological shear rates in vivo. *Journal of Immunology*, 153, 4238-46.

- St Croix, C.M., Wasserloos, K.J., Dineley, K.E., Reynolds, I.J., Levitan, E.S. & Pitt, B.R. (2002). Nitric oxide-induced changes in intracellular zinc homeostasis are mediated by metallothionein/thionein. *American Journal of Physiology - Lung Cellular & Molecular Physiology*, 282, L185-92.

- Stennicke, H.R. & Salvesen, G.S. (1997). Biochemical characteristics of caspases-3, -6, -7, and -8. *J Biol Chem*, 272, 25719-23.

- Strachan, D.P. (1989). Hay fever, hygiene, and household size. *Bmj*, 299, 1259-60.

- Strachan, D.P. (2000). Family size, infection and atopy: the first decade of the "hygiene hypothesis". *Thorax*, 55 Suppl 1, S2-10.

- Strasser, A., O'Connor, L. & Dixit, V.M. (2000). Apoptosis signaling. *Annu Rev Biochem*, 69, 217-45.

- Stridh, H., Kimland, M., Jones, D.P., Orrenius, S. & Hampton, M.B. (1998). Cytochrome c release and caspase activation in hydrogen peroxide- and tributyltin-induced apoptosis. *FEBS Letters.*, 429, 351-5.

- Suhy, D.A. & O'Halloran, T.V. (1996). Metal-responsive gene regulation and the zinc metalloregulatory model. *Metal Ions in Biological Systems*, 32, 557-78.

- Sunderman, F.W., Jr. (1995). The influence of zinc on apoptosis. *Ann Clin Lab Sci*, 25, 134-42.

- Swaminath, G., Steenhuis, J., Kobilka, B. & Lee, T.W. (2002). Allosteric Modulation of beta 2-Adrenergic Receptor by Zn2+. *Mol Pharmacol*, 61, 65-72.

- Szelenyi, I. (2000). Animal models of bronchial asthma. *Inflamm Res*, 49, 639-54.

- Takagi, H., Nagamine, T., Abe, T., Takayama, H., Sato, K., Otsuka, T., Kakizaki, S., Hashimoto, Y., Matsumoto, T., Kojima, A., Takezawa, J., Suzuki, K., Sato, S. & Mori, M. (2001). Zinc supplementation enhances the response to interferon therapy in patients with chronic hepatitis C. *Journal of Viral Hepatitis*, 8, 367-71.

- Takahashi, A., Alnemri, E.S., Lazebnik, Y.A., Fernandes-Alnemri, T., Litwack, G., Moir, R.D., Goldman, R.D., Poirier, G.G., Kaufmann, S.H. & Earnshaw, W.C. (1996). Cleavage of lamin A by Mch2 alpha but not CPP32: multiple interleukin 1 beta-converting enzyme-related proteases with distinct substrate recognition properties are active in apoptosis. *Proc Natl Acad Sci U S A*, 93, 8395-400.

- Takeda, A., Ohnuma, M., Sawashita, J. & Okada, S. (1997). Zinc transport in the rat olfactory system. *Neuroscience Letters*, 225, 69-71.

- Takizawa, H., Romberger, D., Beckmann, J.D., Matsuda, T., Eccleston-Joyner, C., Shoji, S., Rickard, K.A., Claassen, L.R., Ertl, R.F. & Linder, J. (1990). Separation of bovine bronchial epithelial cell subpopulations by density centrifugation: a method to isolate ciliated and nonciliated cell fractions. *American Journal of Respiratory Cell & Molecular Biology*, 3, 553-62.

- Tang, C., Inman, M.D., van Rooijen, N., Yang, P., Shen, H., Matsumoto, K. & O'Byrne, P.M. (2001). Th type 1-stimulating activity of lung macrophages inhibits Th2-mediated allergic airway inflammation by an IFN-gamma-dependent mechanism. *Journal of Immunology*, 166, 1471-81.

- Taylor, C.G. & Bray, T.M. (1991). Effect of hyperoxia on oxygen free radical defense enzymes in the lung of zinc-deficient rats. *Journal of Nutrition*, 121, 460-6.

- Taylor, S.C. & Peers, C. (2000). Three distinct Ca(2+) influx pathways couple acetylcholine receptor activation to catecholamine secretion from PC12 cells. *Journal of Neurochemistry*, 75, 1583-9.

- Tekin, D., Sin, B.A., Mungan, D., Misirligil, Z. & Yavuzer, S. (2000). The antioxidative defense in asthma. *Journal of Asthma*, 37, 59-63.

- Temelkovski, J., Hogan, S.P., Shepherd, D.P., Foster, P.S. & Kumar, R.K. (1998). An improved murine model of asthma: selective airway inflammation, epithelial lesions and increased methacholine responsiveness following chronic exposure to aerosolised allergen. *Thorax*, 53, 849-56.

- Teramoto, S., Tomita, T., Matsui, H., Ohga, E., Matsuse, T. & Ouchi, Y. (1999). Hydrogen peroxide-induced apoptosis and necrosis in human lung fibroblasts: protective roles of glutathione. *Japanese Journal of Pharmacology.*, 79, 33-40.

- Tewari, M., Quan, L.T., O'Rourke, K., Desnoyers, S., Zeng, Z., Beidler, D.R., Poirier, G.G., Salvesen, G.S. & Dixit, V.M. (1995). Yama/CPP32 beta, a mammalian homolog of CED-3, is a CrmA-inhibitable protease that cleaves the death substrate poly(ADP-ribose) polymerase. *Cell*, 81, 801-9.

- Theodorou, A., Weger, N., Kunke, K., Rhee, K., Bice, D., Muggenberg, B. & Lemen, R. (1997). Ragweed sensitization alters pulmonary vascular responses to bronchoprovocation in beagle dogs. *Journal of Applied Physiology*, 83, 912-7.

- Thompson, P.J. (1998). Unique role of allergens and the epithelium in asthma. *Clinical & Experimental Allergy*, 28, 110-6; discussion 117-8.

- Thornberry, N.A. & Lazebnik, Y. (1998). Caspases: enemies within. *Science*, 281, 1312-6.

- Tomkinson, A., Duez, C., Cieslewicz, G., Pratt, J.C., Joetham, A., Shanafelt, M.C., Gundel, R. & Gelfand, E.W. (2001). A murine IL-4 receptor antagonist that inhibits IL-4- and IL-13-induced responses prevents antigen-induced airway eosinophilia and airway hyperresponsiveness. *Journal of Immunology*, 166, 5792-800.

- Tran, C.D., Butler, R.N., Howarth, G.S., Philcox, J.C., Rofe, A.M. & Coyle, P. (1999). Regional distribution and localization of zinc and metallothionein in the intestine of rats fed diets differing in zinc content. *Scandinavian Journal of Gastroenterology*, 34, 689-95.

- Treves, S., Trentini, P.L., Ascanelli, M., Bucci, G. & Di Virgilio, F. (1994). Apoptosis is dependent on intracellular zinc and independent of intracellular calcium in lymphocytes. *Experimental Cell Research*, 211, 339-43.

- Truong-Tran, A.Q., Ruffin, R.E. & Zalewski, P.D. (2000). Visualization of labile zinc and its role in apoptosis of primary airway epithelial cells and cell lines. *American Journal of Physiology - Lung Cellular & Molecular Physiology*, 279, L1172-83.

- Truong-Tran, A.Q., Ruffin, R.E. & Zalewski, P.D. (2001). The role of zinc in caspase activation and apoptotic cell death. *Biometals*, 14, 315-330.

- Turner, R.B. & Cetnarowski, W.E. (2000). Effect of treatment with zinc gluconate or zinc acetate on experimental and natural colds. *Clinical Infectious Diseases*, 31, 1202-8.

- Underwood, S., Foster, M., Raeburn, D., Bottoms, S. & Karlsson, J.A. (1995). Time-course of antigen-induced airway inflammation in the guinea-pig and its

relationship to airway hyperresponsiveness. *European Respiratory Journal*, 8, 2104-13.

- Uvnas, B., Aborg, C.H. & Bergqvist, U. (1975). No role for zinc in the storage of histamine in rat peritoneal mast cells. *Acta Physiologica Scandinavica*, 93, 401-8.

- Vallee, B.L. (1988). Zinc: biochemistry, physiology, toxicology and clinical pathology. *Biofactors*, 1, 31-6.

- Vallee, B.L. & Auld, D.S. (1990). Active-site zinc ligands and activated H_2O of zinc enzymes. *Proceedings of the National Academy of Sciences of the United States of America*, 87, 220-4.

- Vallee, B.L. & Auld, D.S. (1993). Cocatalytic zinc motifs in enzyme catalysis. *Proceedings of the National Academy of Sciences of the United States of America*, 90, 2715-8.

- Vallee, B.L. & Falchuk, K.H. (1993). The biochemical basis of zinc physiology. *Physiol Rev*, 73, 79-118.

- Van de Craen, M., Van Loo, G., Pype, S., Van Criekinge, W., Van den brande, I., Molemans, F., Fiers, W., Declercq, W. & Vandenabeele, P. (1998). Identification of a new caspase homologue: caspase-14. *Cell Death & Differentiation*, 5, 838-46.

- Varea, E.P.X.M.A.D.G.L.-G.C. (2001). Imaging synaptic zinc release in living nervous tissue. *Journal of Neuroscience Methods*, 110, 57-63.

- Vargaftig, B.B. (1999). What can we learn from murine models of asthma? *Clinical & Experimental Allergy*, 29, 9-13.

- Venaille, T.J., Mendis, A.H., Phillips, M.J., Thompson, P.J. & Robinson, B.W. (1995). Role of neutrophils in mediating human epithelial cell detachment from

native basement membrane. *Journal of Allergy & Clinical Immunology*, 95, 597-606.

- Venkayya, R., Lam, M., Willkom, M., Grunig, G., Corry, D.B. & Erle, D.J. (2002). The Th2 Lymphocyte Products IL-4 and IL-13 Rapidly Induce Airway Hyperresponsiveness Through Direct Effects on Resident Airway Cells. *Am. J. Respir. Cell Mol. Biol.*, 26, 202-208.

- von Mutius, E., Martinez, F., Fritzsch, C., Nicolai, T., Roell, G. & Thiemann, H. (1994). Prevalence of asthma and atopy in two areas of West and East Germany. *Am. J. Respir. Crit. Care Med.*, 149, 358-364.

- Vural, H., Uzun, K., Uz, E., Kocyigit, A., Cigli, A. & Akyol, O. (2000). Concentrations of copper, zinc and various elements in serum of patients with bronchial asthma. *Journal of Trace Elements in Medicine & Biology*, 14, 88-91.

- Wang, X., Fosmire, G.J., Gay, C.V. & Leach, R.M., Jr. (2002). Short-term zinc deficiency inhibits chondrocyte proliferation and induces cell apoptosis in the epiphyseal growth plate of young chickens. *Journal of Nutrition.*, 132, 665-73.

- Waring, P., Egan, M., Braithwaite, A., Mullbacher, A. & Sjaarda, A. (1990). Apoptosis induced in macrophages and T blasts by the mycotoxin sporidesmin and protection by Zn2+ salts. *International Journal of Immunopharmacology*, 12, 445-57.

- Wastney, M.E., House, W.A., Barnes, R.M. & Subramanian, K.N. (2000). Kinetics of zinc metabolism: variation with diet, genetics and disease. *Journal of Nutrition*, 130, 1355S-9S.

- Weiland, S.K., von Mutius, E., Hirsch, T., Duhme, H., Fritzsch, C., Werner, B., Husing, A., Stender, M., Renz, H., Leupold, W. & Keil, U. (1999). Prevalence

of respiratory and atopic disorders among children in the East and West of Germany five years after unification. *Eur Respir J*, 14, 862-70.

- Wellinghausen, N. & Rink, L. (1998). The significance of zinc for leukocyte biology. *Journal of Leukocyte Biology*, 64, 571-7.

- Williams, R.J.P. (1987). The biochemistry of zinc. *Polyhedron*, 6, 61-9.

- Winqvist, I., Olofsson, T. & Persson, E. (1985). Effect of zinc and other cations on the release of the eosinophil cationic protein. *Scand J Clin Lab Invest*, 45, 671-7.

- Wolf, C.M. & Eastman, A. (1999). The temporal relationship between protein phosphatase, mitochondrial cytochrome c release, and caspase activation in apoptosis. *Experimental Cell Research*, 247, 505-13.

- Wood, L.G., Fitzgerald, D.A., Gibson, P.G., Cooper, D.M. & Garg, M.L. (2000). Lipid peroxidation as determined by plasma isoprostanes is related to disease severity in mild asthma. *Lipids*, 35, 967-74.

- Woolcock, A.J., Bastiampillai, S.A., Marks, G.B. & Keena, V.A. (2001). The burden of asthma in Australia. *Medical Journal of Australia*, 175, 141-5.

- Wyllie, A.H. (1987). Apoptosis: cell death in tissue regulation. *Journal of Pathology*, 153, 313-6.

- Wyllie, A.H. (1997). Apoptosis: an overview. *British Medical Bulletin*, 53, 451-65.

- Xiong, Y., Karupiah, G., Hogan, S.P., Foster, P.S. & Ramsay, A.J. (1999). Inhibition of Allergic Airway Inflammation in Mice Lacking Nitric Oxide Synthase 2. *J Immunol*, 162, 445-452.

- Yuan, J., Shaham, S., Ledoux, S., Ellis, H.M. & Horvitz, H.R. (1993). The C. elegans cell death gene ced-3 encodes a protein similar to mammalian interleukin-1 beta-converting enzyme. *Cell*, 75, 641-52.

- Zalewski, P.D., Forbes, I.J. & Betts, W.H. (1993). Correlation of apoptosis with change in intracellular labile Zn(II) using zinquin [(2-methyl-8-p-toluenesulphonamido-6-quinolyloxy)acetic acid], a new specific fluorescent probe for Zn(II). *Biochemical Journal*, 296, 403-8.

- Zalewski, P.D., Forbes, I.J. & Giannakis, C. (1991). Physiological role for zinc in prevention of apoptosis (gene-directed death). *Biochemistry International*, 24, 1093-101.

- Zalewski, P.D., Forbes, I.J., Seamark, R.F., Borlinghaus, R., Betts, W.H., Lincoln, S.F. & Ward, A.D. (1994a). Flux of intracellular labile zinc during apoptosis (gene-directed cell death) revealed by a specific chemical probe, Zinquin. *Chemistry & Biology*, 1, 153-61.

- Zalewski, P.D., Jian, X., Soon, L.L., Breed, W.G., Seamark, R.F., Lincoln, S.F., Ward, A.D. & Sun, F.Z. (1996). Changes in distribution of labile zinc in mouse spermatozoa during maturation in the epididymis assessed by the fluorophore Zinquin. *Reproduction, Fertility, & Development*, 8, 1097-105.

- Zalewski, P.D., Millard, S.H., Forbes, I.J., Kapaniris, O., Slavotinek, A., Betts, W.H., Ward, A.D., Lincoln, S.F. & Mahadevan, I. (1994b). Video image analysis of labile zinc in viable pancreatic islet cells using a specific fluorescent probe for zinc. *J Histochem Cytochem*, 42, 877-84.

- Zemel, B.S., Kawchak, D.A., Fung, E.B., Ohene-Frempong, K. & Stallings, V.A. (2002). Effect of zinc supplementation on growth and body composition in children with sickle cell disease. *American Journal of Clinical Nutrition*, 75, 300-7.

- Zhang, Y., Fujita, N. & Tsuruo, T. (1999). p21Waf1/Cip1 acts in synergy with bcl-2 to confer multidrug resistance in a camptothecin-selected human lung-cancer cell line. *International Journal of Cancer*, 83, 790-7.

- Zhao, H., Butler, E., Rodgers, J., Spizzo, T., Duesterhoeft, S. & Eide, D. (1998). Regulation of zinc homeostasis in yeast by binding of the ZAP1 transcriptional activator to zinc-responsive promoter elements. *Journal of Biological Chemistry*, 273, 28713-20.

- Zhu, Z., Homer, R.J., Wang, Z., Chen, Q., Geba, G.P., Wang, J., Zhang, Y. & Elias, J.A. (1999). Pulmonary expression of interleukin-13 causes inflammation, mucus hypersecretion, subepithelial fibrosis, physiologic abnormalities, and eotaxin production. *Journal of Clinical Investigation*, 103, 779-88.

- Zou, H., Li, Y., Liu, X. & Wang, X. (1999). An APAF-1·Cytochrome c Multimeric Complex Is a Functional Apoptosome That Activates Procaspase-9. *J. Biol. Chem.*, 274, 11549-11556.

- Zuhdi Alimam, M., Piazza, F.M., Selby, D.M., Letwin, N., Huang, L. & Rose, M.C. (2000). Muc-5/5ac mucin messenger RNA and protein expression is a marker of goblet cell metaplasia in murine airways. *American Journal of Respiratory Cell & Molecular Biology*, 22, 253-60.

APPENDIX 1

REAGENTS AND MANUFACTUERS

APPENDIX 1 REAGENTS AND MANUFACTURERS

1.1 ANIMAL MODEL OF ALLERGIC AIRWAY INFLAMMATION

Ovalbumin	Sigma-Aldrich, Sydney, Australia
Alhydrogel	CSL, Parkville, Australia
0.9% Saline	Sigma-Aldrich, Sydney, Australia
β-methacholine	Sigma-Aldrich, Sydney, Australia

1.2 APOPTOSIS STUDIES

Reagents	**Manufacturers**
Inducers of Apoptosis	
Dimethyl sulphoxide (DMSO)	Promega Corp., Sydney, NSW, Australia
Hydrogen Peroxide (30% W/V)	Merck Pty Ltd, Kilsyth, Vic., Australia
Sodium Butyrate	BDH Chemicals, Kilsyth, Vic., Australia
TPEN (Zinc chelator)	Sigma Chemical Co., St Louis, MO, USA
Caspase Assays	
CHAPS	Sigma Chemical Co., St Louis, USA
Disposable half-sized cuvettes	Greiner Labortechnik, Austria
Dithiothreitol (DTT)	Sigma Chemical Co., St Louis, USA
HEPES	Sigma Chemical Co., St Louis, USA
Sucrose	Sigma Chemical Co., St Louis, USA
DEVD-AFC	Kamiya Biomedical Co., Tukwila, WA
YVAD-AFC	Kamiya Biomedical Co., Tukwila, WA
VDVAD-AFC	Calbiochem, NSW, Australia
VEID-AFC	Calbiochem, NSW, Australia
LEVD-AFC	Calbiochem, NSW, Australia

WEHD-AFC	Calbiochem, NSW, Australia
LEHD-AFC	Calbiochem, NSW, Australia

1.3 CELL LINES

The A549 and NCI H929 were a gift from Dr. P. Thompson (University of Western Australia).

1.4 CELL CULTURE

Reagents Used	**Manufacturers**
Amphotericin B	Sigma Chemical Co., St Louis, MO, USA
Epidermal Growth Factor	Sigma Chemical Co., St Louis, MO, USA
Foetal Bovine Serum	Biosciences Pty Ltd, Sydney, NSW, Australia
Gentamicin	David Bull Labs, Melbourne, Vic, Australia
HEPES	Sigma Chemical Co., St Louis, MO, USA
Insulin	Sigma Chemical Co., St Louis, MO, USA
L-glutamine	Sigma Chemical Co., St Louis, MO, USA
LHC-9 Basal Epithelial Medium	BioWhittaker, Verviers, Belgium
Penicillin/Streptomycin (2x)	ICN Biomedicals inc., Aurora, OH, USA
RPMI 1640 (with glutamine)	ICN Biomedicals inc., Aurora, OH, USA
Retinoic acid.	Sigma Chemical Co., St Louis, MO, USA
Streptomyces.griseus protease	Sigma Chemical Co., St Louis, MO, USA
Sodium bicarbonate	BDH Chemicals, Kilsyth, Vic., Australia
Tissue Culture Flasks	Iwaki Glass, Japan
Transferrin	Sigma Chemical Co., St Louis, MO, USA
Trypsin/EDTA (%)	ICN Biomedicals Inc., Aurora, OH, USA

1.5 DC PROTEIN ASSAY

Reagents	Manufactures
Bovine Serum Albumin	Sigma Chemical Co., St Louis, MO, USA
DC Protein Assay Kit	BIO-RAD Laboratories, California, USA
Bio-Rad 1940 disposable Cuvettes	BIO-RAD Laboratories, California, USA

1.6 IMMUNOHISTOCHEMISTRY

Rabbit anti-human active caspase-3 (17/19kDa protein)	New England BioLabs, Beverly MA., USA
Rabbit anti-human pro-caspase-3 (CP332 32kDa protein)	Pharmingen, Becton-Dickinson, CA, USA
MD30 cytodeath kit (mouse anti-CK18 epitope)	Roche Diagnostics, USA
Goat Anti-rabbit FITC Secondary antibody	Santa Cruz, USA
Anti-mouse FITC	Kind gift from Dr Chiara Murgia, Rome, Italy

1.7 KITS USED FOR THE DETERMINATION OF IL-5 AND IgE

Endogen Mouse IL-5 Elisa Kit	Endogen, Maryland, USA
Murine OptIEA™ IgE ELISA kit	PharMingen, CA, USA

1.8 PREPARATION OF CELL LYSATES

Reagents	Manufacturers
EDTA	Sigma Chemical Co., St Louis, MO, USA
Hanks Balanced Salt Solution (10x)	Life Technologies Pty Ltd, Victoria,

Australia

Nonidet P-40	Sigma Chemical Co., St Louis, MO, USA
Sucrose	Sigma Chemical Co., St Louis, MO, USA
Tris-HCl	Sigma Chemical Co., St Louis, MO, USA

1.9 TISSUE PREPARATION AND MORPHOLOGICAL ASSESSMENT

Reagents	Manufactures
Acetone	Merck Pty Ltd, Kilsyth, Vic., Australia
Alcian Blue	Merck Pty Ltd, Kilsyth, Vic., Australia
Basic Fuchsin	Merck Pty Ltd, Kilsyth, Vic., Australia
Cryoembedding Moulds	Tissue-Tek, Tokyo, Japan
Chloroform	BDH Chemicals, Kilsyth, Vic., Australia
Eosin	Merck Pty Ltd, Kilsyth, Vic., Australia
Ethanol	Merck Pty Ltd, Kilsyth, Vic., Australia
Geimsa staining	Merck Pty Ltd, Kilsyth, Vic., Australia
Erhlich's Haematoxylin	Merck Pty Ltd, Kilsyth, Vic., Australia
Hoechst dye # 334442	Sigma-Aldhrich, NSW, Australia
Isopentane	BDH Chemicals, Kilsyth, Vic., Australia
Lendrums Carbolchromotrope	Merck Pty Ltd, Kilsyth, Vic., Australia
Neutral Buffered Formalin	Histopathology Lab, The Queen Elizabeth Hospital, Australia
May Grunwald	Merck Pty Ltd, Kilsyth, Vic., Australia
Optimum Cooling Tissue Medium	Tissue-Tek, Tokyo, Japan
Periodic Acid	Histopathology Lab, The Queen Elizabeth Hospital, Australia
Trypan Blue	Merck Pty Ltd, Kilsyth, Vic., Australia

Weigert's Haematoxylin   University of South Australia

Van Geison Stain   University of South Australia

2.0 Zn MANIPULATED DIETS

Eggwhite Diet   ICN Biochemicals, NSW, Australia

Casein Casein Protein Diet   Bonlac Foods, Victoria, Australia

Soya Bean Oil   Lion and Globe, Hop Hing Oil Factory,

          Kowloon, Hong Kong.

AIN 93M Mineral mix   ICN Biochemicals, NSW, Australia

AIN 93VX vitamin mix   ICN Biochemicals, NSW, Australia

Recycled Paper Bedding   Fibercycle, South Australia, Australia

2.1 TOTAL Zn CONCENTRATION DETERMINATION

Zn Free Diluent

Butan-1-ol   Sigma-Aldhrich, NSW, Australia

30% Bridge 35   Kind gift from Dr Peter Coyle, IMVS

Hydrochloric Acid   BDH Chemicals, Kilsyth, Vic., Australia

2.2   ZINQUIN STUDIES

Reagents   **Manufacturers**

Dimethyl sulphoxide (DMSO)   Promega Corp., NSW, Australia

Zinquin   University of Adelaide, Australia

Anti-Fade Fluorescence

Mounting Medium   DAKO Corporations, CA

APPENDIX 2

COMPOSITION OF MEDIA, BUFFERS AND

SOLUTIONS

APPENDIX 2 COMPOSITION OF MEDIA, BUFFERS AND

SOLUTIONS

2.1 CASPASE SUBSTRATE BUFFER

Ingredients

2.4 g HEPES (50mM)

20 g Sucrose (10%)

0.2 g CHAPS (0.1%)

195.4 ml MilliQ filtered water (200ml solution)

1. Place all ingredients into a 500ml beaker.

2. Dissolve in 195.4ml of MilliQ filtered water, mixing the solution well with a magnetic stirring rod.

3. Adjust the media, using 1M of HCl and 1M NaOH, to pH 7.4.

4. Pour this solution into a sterilised 500ml Schotts bottle and refrigerate when unused.

2.2 CASPASE PROTEASE BUFFER

Ingredients

75 mg Dithiothreitol (DTT)

50 µl of 2.5mM zDEVD-AFC substrate

50 ml of caspase substrate buffer (50ml solution)

1. The volume of DTT required was determined by the equation:

$$V_{DTT} = \frac{\text{Total Vol solution} \times 15}{10}$$

2. For 50ml of protease solution, 75mg of DTT and 50μl of 2.5mM zDEVD-AFC substrate was placed into a sterile 50ml centrifuge tube and dissolved into 50ml of Caspase substrate buffer.

3. The protease buffer must be used immediately.

2.3 MAY GRUNWALD AND GEIMSA STAINING

May Grunwald Stock Solution

Ingredients

1. Dissolve 1.5g May Grunwald powder in 500ml Methanol.

2. Heat to 50°C x 2 hrs, mix occasionally.

3. Cool it and swirl several times during the day dissolving for 24 h.

4. Filter before use.

Giemsa Stock solution

Ingredients

1. Dissolve 3.0g Giemsa powder in 198ml glycerol.

2. Mix the solution well and heat at 56°C for 90-120mins, and swirl to mix it well.

3. Add 198ml methanol and stand this solution at room temp for 7 days

4. Filter before use.

2.4 OVALBUMIN FOR SENSITISATION AND NEBULISATION OF BALB/C MICE

Ingredients

Ovalbumin

Aluminium Hydroxide

0.9% Sterile Saline

This procedure requires a 50 µg/ml of OVA dissolved in 0.9% saline and aluminium hydroxide (refer to the following page for the preparation of OVA).

Proportions of OVA/Alum/Saline Required for i.p Injection of Mice to get 50 µg/ml of OVA

# Mice to inject	Vol of OVA (stock- 10mg/ml)	Vol of ALUM	Vol of Saline	Total Vol Produced
5	25µl	100µl	875µl	1ml
10	50µl	200µl	1.750ml	2ml
15	75µl	300µl	2.625ml	3ml
20	100µl	400µl	3.500ml	4ml
25	125µl	500µl	4.375ml	5ml
30	150µl	600µl	5.250ml	6ml
35	175µl	700µl	6.125ml	7ml
40	200µl	800µl	7.000ml	8ml
45	225µl	900µl	7.875ml	9ml
50	250µl	1.000ml	8.750ml	10ml
55	275µl	1.100ml	9.625ml	11ml
60	300µl	1.200ml	10.500ml	12ml
65	325µl	1.300ml	11.375ml	13ml
70	350µl	1.400ml	12.250ml	14ml
75	375µl	1.500ml	13.125ml	15ml

2.5 PERCOLL SEPARATION SOLUTION

Ingredients

Percoll

10x HBSS

1x HBSS

1. Place 9 mls of sterile fresh percoll into 1ml of 10x HBSS making the solution isotonic.

2. The percoll has an original density of 2.141. To make the percoll reach a density of 1.045, 2.796 ml of isotonic percoll is mixed with 0.204ml of 1x HBSS.

3. This gives a total volume of 3 mls of a percoll solution which has the correct density.

2.6 RPMI 1640 MEDIUM

Ingredients

1 packet of RPMI 1640 media

2 vials of gentamycin

5 ml of penicillin/streptomycin

6 g HEPES

2 g NaHCO$_3$

1 L of filtered MilliQ water

1. Place all ingredients into a glass beaker and dissolve in 1 L of the filtered MilliQ water. The powder must be mixed well with a magnetic stiring rod.

2. Adjust the media to pH 7.4 using 1M HCl and 1M NaOH.

3. Using aseptic techniques and pre-sterilised equipment, dispense this solution into a vacuum filtering system containing a sterilised disc of Millipore filter paper of 0.22 μm pore sizes.

4. Pour the flitered media into autoclaved Schotts bottles and refrigerate at 4°C.

5. The working medium is made up with a 10% FBS concentrate.

2.7 NP-40 LYSIS BUFFER

Ingredients

2.5 ml 10% NP-40

0.25 ml Tris HCl, pH 7.5

0.25 ml 1M EDTA, pH 9.4

47 ml MilliQ water

1. Place all ingredients into a sterile 50ml centrifuge tube and shake gently for adequate mixing.

2. Use this solution immediately, otherwise store at 4°C in the refrigerator for the day.

2.8 PHOSPHATE BUFFERED SALINE SOLUTION

Ingredients

0.2 g KCl (MW 74.56)

0.24 g KH_2PO_4 (MW 136.09)

1.44 g Na_2HPO_4 (MW 141.96)

8 g NaCl (MW 58.4)

1. Place all ingredients into a 1L glass beaker and dissolve content with 1L of filtered MilliQ water.

2. Mix solution well with a magnetic stirrer and adjust pH to pH 7.4 using 1M HCl and 1M NaOH.

3. Place the buffer into sterilised Schotts bottles and sterilise via autoclaving.

2.9 Zn DILUENT FOR ATOMIC ABSORPTION SPECTROSCOPY

Ingredients

50 ml Butan-1-ol

1.5 ml 30% bridge 35

8.9 ml concentrated HCL

Make to 1 L using pure Zn free milli Q water

1. Place all ingredients into a clean Zn free schotts bottle and mix well.

2. Store Zn diluent at 4 °C.

2.10 Zn Diets

Ingredients

Please refer to Table 6.1 for the Eggwhite and Casein Zn diet compositions

Zn free MilliQ water

1. Place the cellulose and starch into an electric food processor and mix for 20 min.

2. Add all remaining dry ingredients and mix for a further 30 min.

3. Add the oil and mix for 30 min.

4. Add 300 ml of Zn free H_2O per Kg of diet and mix well for 30 min.

APPENDIX 3
EQUIPMENT USED

APPENDIX 3 EQUIPMENT USED

Instruments/equipment	Manufacturers
Bio-Rad MRC-1000 UV Laser Scanning	
Centrifuge (IEC-Centra-7R)	International Equipment Co., USA
Confocal Microscope System	Bio-Rad, Hemel Hempstead, UK
CoMOS software package	Bio-Rad, Hemel Hempstead, UK)
Disposable Sidestream Nebulisers	Fisher and Paykel, Sydney, Australia
Flame Atomic Absorption	
Spectrophotometer	Perkin-Elmer, Uberlinger, Germany
Graphite Atomic Absorption	
Spectrophotometer	Perkin-Elmer, Uberlinger, Germany
Microcentrifuge (5414s)	Eppendorf, Hamburg, Germany
Phase-Contrast Microscope	Olympus, Tokyo, Japan
Potter-Elvehjem Homogeniser	Wheaton, NJ, USA
RapidFlo Nebuliser Bowl	Allersearch, Victoria, Australia
Sidestream Nebuliser Bowl	Niche Medical Supplies, South Australia, Australia
Spectrofluorimeter (LS-50)	Perkin Elmer Corp., NSW, Australia
Spectrophotometer (DMS 200)	Varian Techron Pty Ltd, VIC, Australia
Titertek® MC Microplate Reader	Titertek, Alabama, U.S.A.
Video Pro Image Analysis System	Leading Edge Pty Ltd, South Australia
Ultracentrifuge (Optima™ TLX)	Beckman Instruments Inc., CA USA
UV Fluorescence microscope (BH-2)	Olympus, Tokyo, Japan

APPENDIX 4

JOURNAL PAPERS